PhD

3rd CYCLE

FCUP
UA
FCT NOVA
2024

Occurrence, distribution and effects of micro-, nanoplastics and other contaminants in soil

Diana Sofia Gouveia Mendes Rede

Occurrence, distribution and effects of micro-, nanoplastics and other contaminants in soil

Diana Sofia Gouveia Mendes Rede
Doctoral Programme in Sustainable Chemistry
Faculty of Sciences of the University of Porto
Department of Chemistry and Biochemistry
2024

Occurrence, distribution and effects of micro-, nanoplastics and other contaminants in soil

Diana Sofia Gouveia Mendes Rede
Doctoral Programme in Sustainable Chemistry
Faculty of Sciences of the University of Porto
Department of Chemistry and Biochemistry
2024

Supervisor
Cristina Maria Fernandes Delerue Alvim de Matos, Professora Coordenadora Principal, Instituto Superior de Engenharia do Porto

Co-supervisor
Virgínia Maria Monteiro da Cruz Fernandes, Investigadora e Professora Adjunta Convidada, Instituto Superior de Engenharia do Porto

LAQV requimte
LABORATÓRIO ASSOCIADO PARA A QUÍMICA VERDE

GRAQ GRUPO DE REAÇÃO E ANÁLISES QUÍMICAS

Dedicated to all the women in my life

Reproduction of any part of this thesis is authorized solely for the purpose of scientific research and requires a written statement from the involved party. This is subject to prior authorization by the publishers of the respective scientific papers and book chapter.

This work was financially supported by national funds through Fundação para a Ciência Tecnologia/Ministério da Ciência, Tecnologia e Ensino Superior (FCT/MCTES) and the European Social Fund (ESF) under NORTE 2020 (Programa Operacional Região Norte) through a PhD grant reference SFRH/BD/147404/2019, as well as by projects UIDB/50006/2020, UIDP/50006/2020, and LA/P/0008/2020. This work also received financial support from FCT/MCTES through project MTS/SAS/0077/2020 titled "Honey+: New reasons to care for honey from the Natural Park of Montesinho: A bioindicator of environmental quality & its therapeutic potential". Further support was also received from FCT and Campus France for the PLASTOXIC project (2022.15094.CBM), which enabled bilateral cooperation between France and Portugal under the PHC-Pessoa Program for the 2023–2024 period.











The present study was conducted within the Grupo de Reação e Análises Químicas (GRAQ), which is part of the Laboratório Associado para a Química Verde | Associated Laboratory for Green Chemistry (LAQV) of the Network of Chemistry and Technology (REQUIMTE). GRAQ is based at the Instituto Superior de Engenharia do Porto (ISEP), Instituto Politécnico do Porto.

Acknowledgements

First and foremost, I would like to express my deepest gratitude to the Fundação para a Ciência e a Tecnologia for their financial support of this thesis.

I would like to express my sincere gratitude to my PhD supervisors, Professor Cristina Delerue Matos and Professor Virginia Cruz Fernandes. Their unshakable support and guidance have been instrumental throughout this journey. Professor Cristina Delerue-Matos, who selected me for a scientific initiation project in 2009, has been a driving force behind the growth of our team and has fostered a vibrant and inspiring research environment through her openness to new ideas. Equally, Professor Virginia Cruz Fernandes has provided invaluable mentorship, continuously challenging me to broaden my horizons and offering committed encouragement. Her dedication has been crucial in helping me explore new avenues and advance my research beyond my initial expectations.

I am also grateful to Professor Laurence Poirier and the *Institut des Substances et Organismes de la Mer* (ISOMer) at the University of Nantes, France, for their warm welcome and for sharing their expertise during my stay.

My gratitude extends to the students with whom I had the pleasure of collaborating on supervising their projects. Working with them has been a valuable learning experience, and their contributions have greatly enriched my own work

To my teammates, especially Maria Freitas, Maria João Fernandes, Sílvia Martinho, Sara Sousa, Luísa Correia de Sá, and Paula Paíga, I extend my heartfelt thanks. Your encouraging words, gentle nudges to keep writing, engaging discussions, coffee breaks, and shared moments of humor about the challenges of the PhD journey have been invaluable.

Lastly, to my family and friends, for their constant support and understanding of my absences, even when I am physically present but mentally elsewhere, my deepest gratitude.

To all of you, thank you very much.

Resumo

Os padrões atuais de consumo não estão alinhados com os recursos limitados do planeta, o que resultará na depleção de recursos, na degradação ambiental e em desequilíbrios ecológicos. Além disso, o crescimento populacional estimado pode intensificar a pressão sobre os recursos, tornando ainda mais crucial que o desenvolvimento seja abordado de uma forma abrangente. É necessário considerar a interdependência entre o meio ambiente, a economia e os direitos humanos para garantir um futuro equilibrado e equitativo, onde o progresso não comprometa a saúde do planeta nem os direitos das pessoas.

O plástico tornou-se um material essencial na sociedade moderna, com mais de 400 milhões de toneladas produzidas anualmente. As elevadas taxas de produção, juntamente com a gestão e a eliminação inadequadas dos resíduos, exercem uma pressão significativa nos ecossistemas. A maior parte dos resíduos de plástico é depositada em aterros sanitários ou não é recolhida pelos sistemas formais de gestão de resíduos, degradando-se em partículas microscópicas conhecidas como microplásticos (MPs). Estas pequenas partículas infiltram-se nos ambientes marinhos e de água doce, solo, ar, alimentos e em diversas espécies, incluindo os seres humanos. O seu potencial para acumulação no ambiente e o papel que desempenham como vetores no transporte de produtos químicos associados ao plástico destacam a interconexão entre a saúde ambiental, animal e humana. Nesse sentido, o conceito de Uma Só Saúde pode oferecer uma abordagem integrada que promova a colaboração entre diferentes disciplinas para enfrentar de forma eficaz e holística desafios como o impacto ambiental dos MPs, os efeitos sobre a vida selvagem e os ecossistemas, e os potenciais riscos para a saúde humana através da contaminação de alimentos, água e ar.

Apesar da sua presença generalizada no ambiente, ainda há uma lacuna significativa no conhecimento sobre as fontes de poluição, as concentrações ambientais, as interações entre os poluentes, os impactos ecológicos e os efeitos potenciais dos MPs e dos compostos químicos associados na saúde. Deste modo, é urgente desenvolver protocolos padronizados que permitam compreender a extensão da contaminação ambiental por plásticos e avaliar os efeitos tóxicos associados. Esta tese aborda estas lacunas ao avaliar a presença de MPs e de compostos químicos associados aos plásticos no solo, concentrando-se nas fontes de poluição, em estudos de coexistência e no desenvolvimento de métodos para extração e identificação de MPs nos solos.

As lamas produzidas nas Estações de Tratamento de Águas Residuais (ETAR), amplamente utilizadas como fertilizante, emergem como uma fonte significativa de micropoluentes emergentes e prioritários, que podem contribuir para o transporte e acumulação de poluentes no solo. Para abordar este problema, foi desenvolvido um método otimizado de extração *Quick, Easy, Cheap, Effective, Rugged, and Safe* (QuEChERS), associado a técnicas de cromatografia gasosa e líquida. Este método detetou 42 compostos orgânicos, incluindo pesticidas, bifenilos policlorados, retardadores de chama e hidrocarbonetos aromáticos policíclicos, em amostras de lamas de sete ETAR Portuguesas. Foram identificados poluentes orgânicos persistentes, como o α-endossulfão, e retardadores de chama organofosforados não regulamentados, como o fosfato de trifenilo (TPhP). A análise também incluiu parâmetros agronómicos e o teor de metais pesados, demonstrando conformidade com os limites estabelecidos pela Diretiva do Conselho 86/278/EEC de 12 de junho de 1986.

O estudo também se debruçou sobre a coexistência e as interações entre poluente, analisando a dinâmica de adsorção de TPhP no solo na presença de MPs sob condições ambientais simuladas. Estas condições incluíram variações na radiação (fluorescente e ultravioleta) e nos níveis de pH (4,0, 5,5 e 7,0). Os resultados destacaram a influência significativa desses fatores ambientais na adsorção do TPhP. Além disso, análises espectroscópicas, como a microscopia Raman e a espectroscopia de infravermelho por transformada de Fourier com reflectância total atenuada, juntamente com testes de ângulo de contato com água, revelaram processos de fotooxidação e alterações nas propriedades de superfície dos MPs.

Por último, para abordar lacunas metodológicas, foi desenvolvida uma abordagem analítica verde baseada nos princípios do QuEChERS para detetar MPs em solos agrícolas, com foco na minimização do consumo de reagentes e na produção de resíduos, enquanto se mantém a eficiência na extração e análise. Os testes de recuperação realizados com solos certificados e MPs virgens demonstraram maior eficiência na extração de partículas de 3-5 mm em comparação com partículas de 15-300 µm. A análise de amostras de solo agrícola apresentou desafios, como interferências espectrais de frações minerais, cores de polímeros e níveis variados de envelhecimento dos polímeros. O polipropileno e o polietileno (PE) foram os mesoplásticos mais frequentemente identificados, com o PE destacando-se como o polímero predominante entre os MPs identificados. A sustentabilidade do método foi avaliada utilizando a Escala Ecológica Analítica e a Métrica de Sustentabilidade

Analítica (métricas AGREE), o que destacou o seu potencial como uma abordagem ecológica para a análise de MPs em solos.

Identificar fontes de poluição do solo, como as lamas de ETAR e a agricultura intensiva, é crucial para prevenir vias de contaminação e implementar estratégias direcionadas de mitigação. Compreender a origem destes poluentes permite o desenvolvimento de testes padronizados para quantificar MPs, avaliar a sua presença no solo e entender como interagem com as matrizes do solo, compostos químicos associados aos plásticos e os impactos sobre a biota do solo. Esta tese integra pesquisa científica com aplicações práticas, sublinhando a urgência de abordar a poluição por MPs no solo. Também fornece conhecimentos essenciais para moldar políticas ambientais alinhadas com os Objetivos de Desenvolvimento Sustentável, particularmente o Objetivo 15 (Proteger a Vida Terrestre) e o Objetivo 3 (Saúde e Bem-Estar).

Palavras-chave: poluição, solo, microplásticos, PP, PS, EVA, LDPE, PA6, TWP, produtos químicos associados ao plástico, POP, PCB, PAH, PBDE, OPE, TPhP, lamas de ETAR, QuEChERS, estudos de coexistência, espectroscopia Raman, ATR-FTIR, Química Verde

Abstract

Current consumption patterns do not align with the Earth's limited resources, leading to resource depletion, environmental degradation, and ecological imbalances. Furthermore, the estimated population growth may increase pressure on resources, making it even more crucial for development to be approached comprehensively. It is essential to consider the critical interdependence between the environment, the economy, and human rights to ensure a balanced and equitable future, where progress does not compromise the health of the planet or the rights of individuals.

Plastic has become an essential material in modern society, with more than 400 million tons produced annually. The high production rates, coupled with insufficient waste management and disposal place significant strain on ecosystems. Most of the plastic waste is either landfilled or leaks from formal waste collection systems, degrading into micro-sized particles known as microplastics (MPs). These small particles infiltrate marine and freshwater environments, soil, air, food, and various species, including humans. Their potential for accumulation in the environment and their role as vectors for transporting plastic-related chemicals highlight the interconnection between environmental, animal, and human health. In this context, the One Health concept offers an integrated approach that fosters collaboration among different disciplines to effectively and holistically address challenges such as the environmental impact of MPs, their effects on wildlife and ecosystems, and their potential health risks to humans through food and water contamination.

Despite their pervasive presence, there remains a lack of knowledge about pollution sources, environmental concentrations, pollutant interactions, ecological impacts, and potential health effects of MPs and their related chemicals. Therefore, urgent action is needed to develop standardized protocols for understanding the extent of environmental contamination by plastics and assessing associated toxic effects. This thesis addresses these gaps by evaluating the presence of MPs and plastic-related chemicals in soil, focusing on pollution sources, coexistence studies, and developing extraction and identification methods for MPs in soils.

Sewage sludge (SS), which is widely used as fertilizer, emerges as a significant source of emerging and priority micropollutants that can contribute to the transport and accumulation of pollutants in the soil. To address this issue, an optimized Quick, Easy, Cheap, Effective, Rugged, and Safe (QuEChERS) extraction method was developed, combined with gas and liquid chromatography techniques. This method detected 42

organic compounds, including pesticides, polychlorinated biphenyls, flame retardants, and polycyclic aromatic hydrocarbons, in SS samples from seven Portuguese wastewater treatment plants. Persistent organic pollutants like α-endosulfan and non-legislated organophosphate esters such as triphenyl phosphate (TPhP) were detected. The analysis also covered agronomic parameters and heavy metal content, demonstrating compliance with legal limits (Council directive 86/278/EEC of 12 June 1986).

The study also focused on the coexistence and interactions between pollutants by analyzing the adsorption dynamics of TPhP in soil in the presence of MPs under simulated environmental conditions. These conditions included variations in radiation (fluorescent and ultraviolet) and pH levels (4.0, 5.5, and 7.0). Results underscored the significant influence of these environmental factors on TPhP adsorption. Additionally, spectroscopic analyses (Raman microscopy and Attenuated Total Reflectance Fourier Transform Infrared spectroscopy) and water contact angle tests revealed photooxidation processes and changes in the surface properties of MPs.

Lastly, addressing methodological gaps, a green analytical approach grounded in QuEChERS principles was developed to screen MPs in agricultural soils, focusing on minimizing reagent consumption and waste production while maintaining extraction and analysis efficiency. Recovery tests conducted with certified soils and virgin MPs demonstrated higher efficiency in extracting particles of 3-5 mm compared to particles of 15-300 µm. Analysing agricultural soil samples presented challenges such as spectral interferences from mineral fractions, polymer colors, and varying levels of polymer aging. Polypropylene (PP) and polyethylene (PE) were the most commonly identified mesoplastics, with PE emerging as the predominant polymer among the MPs identified. The sustainability of the method was assessed using the Analytical Eco-Scale and the Analytical GREEnness Metric Approach (AGREE metrics), which highlighted its potential as an eco-friendly approach for MP analysis in soils.

Identifying sources of soil pollution, such as SS and intensive farming, is crucial for preventing contamination pathways and implementing targeted mitigation strategies. Understanding the origin of pollutants allows for the development of standardized tests to quantify MPs, assess their presence in the soil, and understand how they interact with soil matrices, plastic-related chemicals, and their impacts on soil biota. This thesis integrates scientific research with practical applications, emphasizing the urgency of addressing MP pollution in soil. It provides essential knowledge to shape environmental

policies aligned with the Sustainable Development Goals, particularly Goal 15 (Life on Land) and Goal 3 (Good Health and Well-Being).

Keywords: pollution, soil, microplastics, PP, PS, EVA, LDPE, PA6, TWP, plastic-related chemicals, POPs, PCBs, PAHs, PBDEs, OPEs, TPhP, sewage sludge, QuEChERS, coexistence studies, Raman spectroscopy, ATR-FTIR, Green Analytical Chemistry

List of Publications

The majority of the contents included in this thesis, derived from both experimental work and review studies, have either been published or are currently under review for publication. This thesis includes three scientific papers published in international peer-reviewed journals and one additional paper that is currently under review. These papers are referenced as follows:

1. Rede, D., Vilarinho, R., Moreira, J.A., Delerue-Matos, C., & Cruz Fernandes, V. (2024) 'Investigating the impact of microplastics on triphenyl phosphate adsorption in soil: Insights into environmental factors and soil properties', Science of the Total Environment, 944, p. 173745. Available at: https://doi.org/10.1016/j.scitotenv.2024.173745. (Q1, Impact Factor 8.2)
2. Rede, D., Teixeira, I., Delerue-Matos, C., & Cruz Fernandes, V. (2023) 'Assessing emerging and priority micropollutants in sewage sludge: environmental insights and analytical approaches', Environmental Science and Pollution Research, 31, pp. 3152–3168. Available at: https://doi.org/10.1007/s11356-023-30963-1. (Q1 Impact Factor 5.8)
3. Rede, D., Delerue-Matos, C., & Cruz Fernandes, V. (2023) 'The Microplastics Iceberg: Filling Gaps in Our Understanding', Polymers, 15(16), p. 3356. Available at: https://doi.org/10.3390/polym15163356. (Q1, Impact Factor 4.7)
4. Rede, D., Vilarinho, R., Moreira, J.A., Nizzetto, L., Delerue-Matos, C., & Cruz Fernandes, V. (2024) 'Screening for microplastics in agricultural soils: Applying Green Chemistry Principles in extraction and analysis', Environmental Pollution. (Q1, Under review, Manuscript No. ENVPOL-D-24-06001)

Additionally, the thesis includes a chapter from a book. This chapter is referenced as:

Rede, D., Delerue-Matos, C., & Cruz Fernandes, V. (2024) 'Plastic-Related Chemicals: Occurrence in Environment and Ecotoxicological Impacts', in Inamuddin, Altalhi, T., & Cruz Fernandes, V. (eds) Toxic Effects of Micro- and Nanoplastics: Environment, Food and Human Health. Beverly, MA: Scrivener Publishing LLC, pp. 347-374. Available at: https://doi.org/10.1002/9781394238163.ch16.

Moreover, the research findings have been disseminated through various international and national scientific meetings, including oral and poster communications. The details of these presentations are as follows:

Oral communications

1. Rede, D., Delerue-Matos, C. & Cruz Fernandes, V., 2023. Tracking Emerging and Priority Micropollutants in Sewage Sludge. Plastoxic Meeting, ISOmer, Nantes University, 5 December, Nantes, France. *Invited speaker*.
2. Rede, D., Vilarinho, R., Moreira, J.A., Delerue-Matos, C. & Cruz Fernandes, V., 2023. UV Light and pH Effects on Microplastic Aging in Soil. XXVII Encontro Luso-Galego de Química, 22-24 November, Porto, Portugal.
3. Rede, D., Pereira, A., Delerue-Matos, C. & Cruz Fernandes, V., 2023. Plastic-Related Chemicals in the Soil from the Natural Park of Montesinho. 18th International Conference on Chemistry and the Environment (ICCE 2023), 11-15 June, Venice, Italy.
4. Rede, D., Delerue-Matos, C. & Cruz Fernandes, V., 2022. Sewage Sludge Application on Agricultural Soils: Friend or Foe?. LAQV-Webinar, 26 October, online event. *Invited speaker*.
5. Pereira, A., Rede, D., Delerue-Matos, C. & Cruz Fernandes, V., 2022. Plastic-Related Chemicals in Terrestrial Environments: An Emerging Challenge. IJUP 16th Meeting of Young Researchers, 4-6 May, online event. ISBN 978-989-746-329-7.
6. Rede, D., Delerue-Matos, C. & Cruz Fernandes, V., 2021. Plastic-Related Chemicals on Sludge: A Chromatography Challenge. Chromatography Helps in Times of Crisis, 17 December, online event organized by the Portuguese Society of Chemistry.
7. Rede, D., Teixeira, P., Oliveira, M., Delerue-Matos, C. & Cruz Fernandes, V., 2021. Monitoring of Emerging Pollutants in Sewage Sludge. International Conference on Management and Rehabilitation of Contaminated Areas - CIGRAC 2020+1, 11-14 May, online event. ISBN 978-989-33-1802-7, pp. 80-81.
8. Teixeira, I., Rede, D., Delerue-Matos, C. & Cruz Fernandes, V., 2021. Physico-Chemical Characteristics of Sewage Sludge Produced in Portuguese Wastewater Treatment Plants. IJUP 14th Meeting of Young Researchers, 5-7 May, online event. ISBN 978-989-746-295-5.

Poster communications

1. Rede, D., Vilarinho, R., Moreira, J.A., Delerue-Matos, C. & Cruz Fernandes, V., 2024. Microplastics Influence on Triphenyl Phosphate Sorption in Soil. Encontro Ciência 2024, 3-5 July, Porto, Portugal.

2. Rede, D., Vilarinho, R., Moreira, J.A., Delerue-Matos, C. & Cruz Fernandes, V., 2023. Raman Spectroscopy: A Tool for Investigating Microplastic Aging in the Environment. XXVII Encontro Luso-Galego de Química, 22-24 November, Porto, Portugal.
3. Rede, D., Pereira, A., Delerue-Matos, C. & Cruz Fernandes, V., 2023. Plastic-Related Chemicals in the Soil from the Natural Park of Montesinho. 18th International Conference on Chemistry and the Environment (ICCE 2023), 11-15 June, Venice, Italy.
4. Rede, D., Mbene, F., Vilarinho, R., Moreira, J.A., Delerue-Matos, C. & Cruz Fernandes, V., 2023. Extraction Efficiency of Several Microplastics from Soil and Identification by Raman Spectroscopy. 7th Green and Sustainable Chemistry Conference, 21-24 May, Dresden, Germany.
5. Rede, D., Pereira, A., Delerue-Matos, C. & Cruz Fernandes, V., 2022. Occurrence of Plastic-Related Chemicals in Soil Samples from the Natural Park of Montesinho. 12th National Chromatography Meeting - XIV WARPA, 6-8 December, Aveiro, Portugal.
6. Rede, D., Mbene, F., Vilarinho, R., Moreira, J.A., Delerue-Matos, C. & Cruz Fernandes, V., 2022. Microplastics in Portuguese Agricultural Soil: Identification by Raman Spectroscopy. XXVI Encontro Galego-Portugués de Química, 16-18 November, Santiago de Compostela, Spain.
7. Rede, D., Teixeira, P., Oliveira, M., Delerue-Matos, C. & Cruz Fernandes, V., 2022. Is Sewage Sludge a Source of Priority Emerging Micropollutants for Agricultural Soils?. 58th North American Chemical Residue Workshop (NACRW2022), 25-29 July, online event.
8. Rede, D., Teixeira, P., Oliveira, M., Delerue-Matos, C. & Cruz Fernandes, V., 2021. Development and Optimization of QuEChERS Method for the Analysis of Organic Pollutants in Sewage Sludge. 57th North American Chemical Residue Workshop (NACRW2021), 26-30 July, online event.

Related Publication not included in the thesis:

1. Selonen, S., Dolar, A., Jemec Kokalj, A., Sackey, L.N.A., Skalar, T., Cruz Fernandes, V., Rede, D., Delerue-Matos, C., Hurley, R., Nizzetto, L., & van Gestel, C.A.M. (2021) 'Exploring the impacts of microplastics and associated chemicals in the terrestrial environment – Exposure of soil invertebrates to tire particles', Environmental Research, 201, p. 111495. Available at: https://doi.org/10.1016/j.envres.2021.111495. (Q1, Impact Factor 8.3)

2. Garzón-Vidueira, R., Rede, D., Rial-Otero, R., Vilarinho, R., Moreira, J., Jorge, S., André, M., Barbosa, R., & Delerue-Matos, C. (2024) 'Investigating multiple vegetable oils and recycled variant for microplastics extraction from water, integrated with Raman spectroscopy', Science of the Total Environment, 955, p. 177112. Available at: https://doi.org/10.1016/j.scitotenv.2024.177112. (Q1, Impact Factor 8.2)
3. Rede, D., Cruz Fernandes, V., Pereira, A. Delerue-Matos, C. 'Assessment of the presence of plastic-related chemicals in plants and soil from the Natural Park of Montesinho'. (In preparation for submission)
4. de Chatillon, C.C., Rede, D., Guinle, C., Zalouk-Vergnoux, A., François, Y., Delerue-Matos, C., Fernandes, V. F., & Poirier, L. 'Mussel Mytilus edulis response to the exposure to elutriates of wastewater treatment plant sludges and to microplastics'. (In preparation for submission)

Table of Contents

List of Tables xviiii

List of Figures xxi

List of Abbreviations xxviiii

Introduction 1

Contextualization and Thesis Outline 3

1.State of the Art 11

1.1. The Microplastics Iceberg: Filling Gaps in Our Understanding 13

1.2. Plastic-Related Chemicals: Occurrence in Environment and Ecotoxicological Impact.. 42

2.Sewage Sludge as a Potential Source of Soil Contamination 71

2.1. Assessing Emerging and Priority Micropollutants in Sewage Sludge: Environmental Insights and Analytical Approaches 73

3.Coexistence of Microplastics and Plastic-related Chemicals in Soil 105

3.1. Investigating the Impact of Microplastics on Triphenyl Phosphate Adsorption in Soil: Insights into Environmental Factors and Soil Properties 107

4.Extracting Microplastics from Soil 129

4.1. Screening for Microplastics in Agricultural Soils: Applying Green Chemistry Principles in Extraction and Analysis 131

Conclusions and Final Remarks 173

List of Tables

1. State of the Art

1.1. The Microplastics Iceberg: Filling Gaps in Our Understanding

Table 1. Summary of MPs' concentrations in the environment covering a range of compartments. The selected studies had methodological details. (dw: dry weight; WTP: water treatment plant; KWS: Korona–Walzen–Scheider; Py-GC-MS: pyrolysis gas chromatography–mass spectrometry; DSC: differential scanning calorimetry; FTIR: Fourier transform infrared spectroscopy; µ-FTIR: micro-FTIR; ATR-FTIR: attenuated total reflection FTIR; FE-SEM: field-emission scanning electron microscopy; SM-EDX: SEM energy electron microscopy; X-ray CT: X-ray computed tomography; HS-SPME-GC-MS: headspace solid-phase microextraction coupled with gas chromatography and mass spectrometry; LC-UV: liquid chromatography with UV detection; TED-GC-MS: thermal desorption gas chromatography–mass spectrometry; TGA-MS: thermogravimetry–mass spectrometry;. EGA-MS: evolved gas analysis–mass spectrometry). 22

Table 2. Illustrative toxicological effects observed in diverse organisms, including fishes, crustaceans, nematodes, arthropods, and annelids, and plants, caused by MPs of varying shapes, types, and sizes. 32

1.2. Plastic-Related Chemicals: Occurrence in Environment and Ecotoxicological Impact

Table 1. Occurrence of plasticizers in the environment, concentration ranges, and matrixsources (time span: 2017–2023).. 46

Table 2. Occurrence of NBFRs and OPEs in the environment, concentration ranges, and matrix sources (time span: 2017–2023). N.D., not detected; MDL, method detection limit; LOD, limit of detection; dw, dry weight; lw, lipid weight..... 58

2. Sewage Sludge as a Potential Source of Soil Contamination

2.1. Assessing Emerging and Priority Micropollutants in Sewage Sludge: Environmental Insights and Analytical Approaches

Table 1. Composition of the d-SPE mixtures tested in the two sets……..79

Table 2. Coefficient of determination (R^2), limit of detection (LOD) and quantification (LOQ), recovery (RE), matrix effect (ME), repeatability, and reproducibility (%RSD, n = 2) of the developed method for the studied compounds. 81

Table 3. Concentrations (µg g^{-1} dw) of OPPs, OPEs, PBDEs, PCBs, OCPs, PYRs, and PAHs in sewage sludge collected from municipal wastewater treatment plants located in the north of Portugal (n = 6; ND – not detected; < LOQ – below method quantification limit). 83

Table S1. SIM program used to confirm the OPPs, OPEs, PCBs, PBDEs, OCPs, and PYRs detected in the SS samples. 94

Table S2. Physicochemical properties, heavy metals, and other trace elements content of SS samples (n=2) (mean ± SD) (ND = Not detected). 94

Table S3. Concentrations (µg g^{-1} dw) of OPPs, OPEs, PBDEs, PCBs, OCPs, PYRs, and PAHs in sewage sludge collected from municipal wastewater treatment plants located in the north of Portugal (mean values, n=6; ND: not detected; <LOQ: below method quantification limit).. 95

Table S4. Literature-reported concentrations for OPPs, OPEs, PBDEs, PCBs, OCPs, PYRs, and PAHs in sewage sludge. 97

3. Coexistence of Microplastics and Plastic-related Chemicals in Soil

3.1. Investigating the Impact of Microplastics on Triphenyl Phosphate Adsorption in Soil: Insights into Environmental Factors and Soil Properties

Table 1. Water contact angles (θ, in degrees) of pristine and aged microplastics of polypropylene (PP-MPs), polystyrene (PS-MPs), and ethylene-vinyl acetate (EVA-MPS) in MP-only systems under various pH and UV exposure conditions. (n = 8)…. 114

Table 2. Water contact angles (θ, in degrees) of pristine and aged microplastics of polypropylene (PP-MPs), polystyrene (PS-MPs), and ethylene-vinyl acetate (EVA-MPS) in soil-MP systems under various pH and UV exposure conditions. (*n* = 8). 117

Table S1. Manufacturer-provided characteristics of pristine microplastics used in the study (GoodFellow 2024a, b, c). N.a. – not available on the technical sheets. 120

Table S2. Concentration of TPhP over time in MP-only systems subjected to pH 5.5 with UV radiation. 122

4. Extracting Microplastics from Soil

4.1. Screening for Microplastics in Agricultural Soils: Applying Green Chemistry Principles in Extraction and Analysis

Table 1. Cumulative recovery percentages of TWP, LDPE, and PA 6 in sandy soil and Lufa 2.2 soil at various polymer concentrations 144

Table 2. Fractions, soil samples, and methods of polymer identification. 145

Table 3. Analysis of microparticles in soil Samples C, D, and E, showing characteristics and polymer compositions, including number of particles, shape, colour, polymer type, and distribution in 5 g of subsamples. 147

Table 1S. Analysis of mesoplastics extracted from samples D and E, showing characteristics and polymer compositions, including number of particles, shape, color, polymer type, and images obtained with a microscope and µ-Raman. 168

List of Figures

1. State of the Art

1.1. The Microplastics Iceberg: Filling Gaps in Our Understanding

Figure 1. Types of plastic debris found on a beach in Northern Portugal. The plastic materials include: (a) a plastiglomerate, (b) mesoplastic fragments, (c,d) microplastics. 16

Figure 2. Sources and routes of microplastics and plastic-related chemical pollution in soil environment..... 17

Figure 3. The main steps involved in analysing microplastics in environmental samples: pretreatment, extraction, and identification. 20

Figure 4. Factors that lead to the ingestion or absorption of microplastics causing potential ecotoxicological and toxicological impacts. 29

1.2. Plastic-Related Chemicals: Occurrence in Environment and Ecotoxicological Impact

Figure 1. Four main categories of additives are used to maximize the performance and versatility of everyday plastics. 44

2. Sewage Sludge as a Potential Source of Soil Contamination

2.1. Assessing Emerging and Priority Micropollutants in Sewage Sludge: Environmental Insights and Analytical Approaches

Figure 1. Color removal with different d-SPE mixtures applied to samples A and B in the first set of clean-ups. The d-SPE tube contained a typical mixture of 150 mg of $MgSO_4$, 50 mg of PSA, and 50 mg of C18 with A-I — 3 mg of CB; A-II —10 mg of CB; A-III — 20 mg of CB; A-IV — 20 mg of CB and 10 mg of Z-Sep; A-V — 50 mg of CB; B-I — 3 mg of CB; B-II — 6 mg of CB; B-III — 10 mg of CB; B-IV — 10 mg of CB and 10 mg of Z-Sep; B-V — 50 mg of CB. 79

Figure 2. RE (%) (a) and ME (b) obtained with the different formulations of d-SPE sorbents (VI–IX) used in the clean-up of the *sludge mixture*. The d-SPE tube contained a typical mixture of 150 mg of $MgSO_4$, 50 mg of PSA, and 50 mg of C18 combined with VI – 10 mg of CB and 10 mg of Z-Sep; VII – 5 mg of CB and 15 mg of Z-Sep; VIII– 5 mg of CB and 20 mg of Z-Sep; IX – 5 mg of CB and 25 mg of Z-Sep. 80

Figure 1S. Map of the sampling sites located in Continental Portugal - Sampling sites (A to F) across the Porto, Viseu and Aveiro regions (1 to 3). 91

Figure 2S. Chromatographic data for OPPs and OPEs obtained by GC-FPD. a) Chromatogram of a matrix-matched standard solution; b) chromatogram of a reagent-only standard solution; and c) chromatogram of sample F……99

Figure 3S. Chromatographic information of TPhP in sample E: a) chromatogram of sample E obtained by GC-FPD, b) chromatogram of sample E obtained by GC-MS, and c) mass spectrum of TPhP in sample E. 100

Figure 4S. Chromatographic data for PCBs PBDEs, OCPs, and PYRs obtained using GC-ECD. a) Chromatogram of a matrix-matched standard solution, b) chromatogram of a reagent-only standard solution, and c) chromatogram of sample A. 101

Figure 5S. Chromatographic data for PAHs obtained using LC-PDA-FLD. a) Chromatogram of a reagent-only standard solution, b) chromatogram of a matrix-matched standard solution, and c) chromatogram of sample C. 102

3. Coexistence of Microplastics and Plastic-related Chemicals in Soil

3.1. Investigating the Impact of Microplastics on Triphenyl Phosphate Adsorption in Soil: Insights into Environmental Factors and Soil Properties

Figure 1. Overview of the experimental setup, including the preparation of soil-only, MP-only, and soil-MP systems, experimental conditions, and analytical processes for TPhP quantification and MPs photooxidation assessment. 111

Figure 2. Spectra of MPs under varying aging conditions in MPs-only systems. ATR-FTIR spectra (a, c, e) spanning the wavenumber range of 4000–400 cm^{-1} versus

transmittance (%), with two distinct ranges highlighted in green (3600–3000 and 1800–1500 cm^{-1}), for PP-MPs, PS-MPs, and EVA-MPs. Raman spectra (b, d, f) covering a Raman shift range of 3500–100 cm^{-1} versus intensity are presented for PP-MPs, PS-MPs, and EVA-MPs, respectively..... 113

Figure 3. Temporal variation in TPhP concentration (µg/L) over 168 h (a, c, e) and adsorption capacity (µg/$g_{adsorbent}$) of TPhP in soil-MP systems (b, d, f) for soil + PP-MPs, soil + PS-MPs, and soil + EVA-MPs..... 115

Figure 4. Variation of equilibrium adsorption capacity (qe, $\mu g_{TPhP}/g_{adsorbent}$) across different systems of soil-only and soil-MPs subjected to varying aging conditions of pH and radiation..... 115

Figure 5. ATR-FTIR and Raman spectra from soil-MP systems. ATR-FTIR spectra (a, c, e) spanning the wavenumber range of 4000–400 cm^{-1} versus transmittance (%), with two distinct ranges highlighted in green (3600–3000 and 1800–1500 cm^{-1}), for PP-MPs, PS-MPs, and EVA-MPs, respectively. Raman spectra (b, d, f) covering a Raman shift range of 3500–100 cm^{-1} versus intensity are presented for PP-MPs, PS-MPs, and EVA-MPs. respectively. 116

Figure S1. a) Concentration of TPhP in soil-only systems over time, showing the temporal variation in TPhP concentration within the soil matrix; b) Adsorption capacity (qt) expressed as µg of TPhP per g of adsorbent in soil-only systems over time (t, h). 121

Figure S2. pH at point zero charge for a) soil-only, b) soil + PP-MPs, c) soil + PS-MPs; and d) soil + EVA-MPs..... 122

Figure S3. Images of MPs from MP-only systems captured using a Leica DM2700 microscope equipped with a 50x objective lens. Each image corresponds to MPs subjected to different aging conditions in MPs-only systems: pristine (a-c); pH 5.5 with fluorescent light (d-f); pH 5.5 with UV radiation (g-i); pH 4.0 with UV radiation (j-l); and pH 7.0 with UV radiation (m-o). Column 1: PP- MPs; column 2: PS-MPs; column 3: EVA-MPs. 123

Figure S4. Images of contact angles from MPs systems captured using a AFWCAMVM high-resolution. Each image corresponds to MPs subjected to different aging conditions in MPs-only systems: pristine (a-c); pH 5.5 with fluorescent light (d-f); pH 5.5 with UV

radiation (g-i); pH 4.0 with UV radiation (j-l); and pH 7.0 with UV radiation (m-o). Column 1: PP-MPs; column 2: PS-MPs; column 3: EVA-MPs. 124

Figure S5. Images of contact angles from MPs captured using a AFWCAMVM high-resolution. Each image corresponds to MPs subjected to different aging conditions in soil-MPs systems: pristine (a-c); pH 5.5 with fluorescent light (d-f); pH 5.5 with UV radiation (g-i); pH 4.0 with UV radiation (j-l); and pH 7.0 with UV radiation (m-o). Column 1: PP-MPs; column 2: PS-MPs; column 3: EVA-MPs. 125

Figure S6. Images of MPs from soil-MPs systems subjected to various conditions, captured using a Leica DM2700 microscope equipped with a 50x objective lens. Column 1: PP-MPs; column 2: PS-MPs; and column 3: EVA-MPs. a-c: pristine MPs; d-f: exposed MPs to pH 5.5 with fluorescent light; g-i: exposed MPs to pH 5.5 with UV radiation; j-l: exposed MPs to pH 4.0 with UV radiation; and m-o: exposed MPs to pH 7.0 with UV radiation. Note: Some images reveal soil fragments adhering to the surface of MPs, indicating potential interactions between microparticles and soil components during aging processes. 126

4. Extracting Microplastics from Soil

4.1. Screening for Microplastics in Agricultural Soils: Applying Green Chemistry Principles in Extraction and Analysis

Figure 1. Overview of the experimental steps for microplastic extraction from agricultural soil samples. Created with BioRender.com. 139

Figure 2. a) Samples prior to digestion, taken 15 minutes before the process; b) EVA-MPs after centrifugation; c) EVA-MPs after filtration; d) PS-MPs after centrifugation; e) PP-MPs after centrifugation; f) PS-MPs and PP-MPs after filtration. Photographs captured using an OPPO Reno 8 Lite smartphone. 143

Figure 3. Images and Raman spectra of the MP identified as poly(ethylene-co-1-butene) in sample E. a), b), and c) White-transparent fragment from replica 1, repetition 1 (score 95.58%): microscope image, µ-Raman image, and spectrum, respectively. d), e), and f) White-transparent fragment from replica 2, repetition 2 (score 95.58%): microscope image, µ-Raman image, and spectrum, respectively. g), h), and j) White-transparent fragment from replica 2, repetition 3 (score 94.32%): microscope image, µ-Raman image, and spectrum, respectively. 149

Figure 4. Results of AGREE analysis for the method. Scores range from 0.0 (red) to 1.0 (dark green), with higher scores indicating more desirable outcomes. The score for each principle is provided in parentheses. 151

Figure 1S. a-i) Images of the filters obtained in three extractions for control, sandy soil, and Lufa 2.2 soil captured using an OPPO Reno8 Lite smartphone; j-l) µ-Raman images for blank, sandy soil, and Lufa 2.2 soil captured using a Leica DM2700 microscope with a 50x objetctive. 163

Figure 2S. Normalized Raman spectra obtained for digestion degradation tests for spikes containing 1, 2 and 5% of MP. a) PP-MPs, b) PS-MPs, c) EVA-MPs, d) TWP-MPs, e) LDPE-MPs, and f) PA 6-MPs. Spectra collected from 100 to 3500 cm^{-1}, using 633 nm He-Ne laser as the excitation light source. 164

Figure 3S. Images of the filters obtained in three extractions for spikes containing 5% TWP, referring to: a), d) and g) digestion degradation tests; b), e) and h) recovery tests with sandy soil; c), f) and j) recovery tests with Lufa 2.2 soil. The images were captured using an OPPO Reno8 Lite smartphone. 165

Figure 4S. Images of the filters obtained in three extractions for spikes containing 5% LDPE, referring to: a), d) and g) digestion degradation tests; b), e) and h) recovery tests with sandy soil; c), f) and j) recovery tests with Lufa 2.2 soil. The images were captured using an OPPO Reno8 Lite smartphone. 165

Figure 5S. Images of the filters obtained in three extractions for spikes containing 5% PA 6, referring to: a), d) and g) digestion degradation tests; b), e) and h) recovery tests with sandy soil; c), f) and j) recovery tests with Lufa 2.2 soil. The images were captured using an OPPO Reno8 Lite smartphone..... 166

Figure 6S. µ-Raman images of TWP-MPs, LDPE-MPs and PA 6-MPs, captured using a Leica DM2700 microscope with a 50x objective. a) digestion degradation tests for TWP 1%, 1st extraction; b) Sand + TWP 1%, 3rd extraction; c) Lufa 2.2 soil + TWP 1%, 1st extraction; d) digestion degradation tests for LDPE 1%, 1st extraction; e) Sand + LDPE 2%, 3rd extraction; f) Lufa 2.2 soil + LDPE; g) digestion degradation tests for PA 6 2%, 3rd extraction; h) Sand + PA 6 2%, 2nd extraction; and i) Lufa 2.2 soil + PA 6 2%, 2nd extraction. 166

Figure 7S. Images of the filters obtained in three extractions for each fraction of Sample A. The images were captured using an OPPO Reno8 Lite smartphone. 167

Figure 8S. Images of the filters obtained in three extractions for each fraction of Sample B. The images were captured using an OPPO Reno8 Lite smartphone 167

Figure 9S. Output of PublicSpectra for two mesoplastics in samples D and E. a) Yellow-orange film in sample D with inconclusive identification. b) White-transparent film in sample E identified as PP-based, specified as propylene-ethylene block copolymer. 170

Figure 10S. Images of non-identified suspects in samples D and E. a) and b) red-pink fragment in sample D; c) and d) white-transparent fiber in sample D; e) and f) white-transparent fragment in sample E [5.00-1.00 mm]; g) and h) blue-green fragment in sample E [40-1.2 µm]. Images a) and g) were captured with OPPO Reno8 Lite smartphone, while c) and e) were collected with an inverted microscope at 5x ampliation. 171

List of Abbreviations

ABS	2 ACRYLONITRILE BUTADIENE STYRENE
ACN	ACETONITRILE
AGREE	ANALYTICAL GREENNESS METRIC APPROACH
AsA	ASCORBIC ACID
ATBC	ACETYL TRIBUTYL CITRATE
ATR	ATTENUATED TOTAL REFLECTANCE
b	SLOPE OF THE LINEAR REGRESSION
BaP	BENZO(a)PYRENE
BBP	BUTYL BENZYL PHTHALATE
BDCIPP	BIS(1,3-DICHLORO-2-PROPYL) PHOSPHATE
BDE(S)	BROMINATED DIPHENYL ETHER(S)
BDE 28	2,4,4′-TRIBROMODIPHENYL ETHER
BDE 47	4,4′-TETRABROMODIPHENYL ETHER
BDE 99	2,2′,4,4′,5-PENTABROMODIPHENYL ETHER
BDE 100	2,2′,4,4′,6-PENTABROMODIPHENYL ETHER
BDE 153	2,2′,4,4′,5,5′-HEXABROMODIPHENYL ETHER
BDE 154	2,2′,4,′,5,6′-HEXABROMODIPHENYL ETHER
BDE 183	2,2′,3,4,4′,5′,6-HEPTABROMODIPHENYL ETHER
BDE 209	DECABROMODIPHENYL ETHER
BTBPE	1,2-BIS(2,4,6-TRIBROMOPHENOXY) ETHANE
C	CONCENTRATION
C_0	INITIAL CONCENTRATION
C_t	CONCENTRATION OF TPHP AT A GIVEN TIME
CARS	COHERENT ANTI-STOKES RAMAN SCATTERING
CAT	CATALASE
CB	SAMPLIQ CARBON SPE BULK SORBENT
CEFIC	EUROPEAN CHEMICAL INDUSTRY COUNCIL
CDPP	CRESYLDIPHENYLPHOSPHATE
CL_h	HEPATIC CLEARANCE
CL_{HLM}	HUMAN LIVER MICROSOMES CLEARANCE
CL_{renal}	RENAL CLEARANCE
CoRAP	COMMUNITY ROLLING ACTION PLAN
CYP	CYTOCHROME

CYP450	CYTOCHROME P450
DBA	DIBENZ[a,h]ANTHRACENE
DBDPE	DECABROMODIPHENYL ETHANE
DBP	DIBUTYL PHTHALATE
DCHP	DICYCLOHEXYL PHTHALATE
DDD	1,1-DICHLORO-2,2-BIS-4-CHLOROPHENYL-ETHYLENE
DDE	1,1-DICHLORO-2,2-BIS-4-CHLOROPHENYL-ETHENE
DDT	1,1,1-TRICHLORO-2,2-BIS-4-CHLOROPHENYL-ETHANE
DEHA	DI(2-ETHYLHEXYL) ADIPATE
DEHP	BIS (2-ETHYLHEXYL) PHTHALATE
DEP	DIETHYL PHTHALATE
DiBP	DI-ISOBUTYL PHTHALATE
DiDP	DIISODECYL PHTHALATE
DiHP	DIISOHEPTYL PHTHALATE
DINCH	DI-(ISO-NONYL)-CYCLOHEXANE-1,2-DICARBOXYLATE
DiNP	DI-ISONONYL PHTHALATE
DM	DRY MATTER
DMP	DIMETHYL PHTHALATE
DNA	DEOXYRIBONUCLEIC ACID
DnBP	DI-N-BUTYL PHTHALATE
DNHP	DIHEXYL PHTHALATE
DnOP	DI-N-OCTYL PHTHALATE
DPHP	DIPHENYLPHOSPHATE
DPP	DIPROPYL PHTHALATE
DSC	DIFFERENTIAL SCANNING CALORIMETRY
d-SPE	DISPERSIVE SOLID-PHASE EXTRACTION
DW	DRY WEIGHT
ECD	ELECTRON CAPTURE DETECTION
ECHA	EUROPEAN CHEMICALS AGENCY
EDX	ENERGY DISPERSIVE X-RAY SPECTROSCOPY
EGA	EVOLVED GAS ANALYSIS.
EHDPP	2-ETHYLHEXYL DIPHENYL PHOSPHATE
EH-TBB	2-ETHYLHEXYL-2,3,4,5-TETRABROMOBENZOATE
eI	ELECTRON IMPACT
EPA	ENVIRONMENTAL PROTECTION AGENCY

EPDM	ETHYLENE PROPYLENE DIENE MONOMER
ER	ENDOPLASMATIC RETICULUM
EuPC	EUROPEAN PLASTICS CONVERTERS
EU	EUROPEAN UNION
EVA	ETHYLENE VINYL ACETATE
FE	FIELD EMISSION
FLD	FLUORESCENCE DETECTOR
FLU	FLUORANTHENE
FPD	FLAME PHOTOMETRIC DETECTION
FPS	FOAMED POLYSTYRENE
FT-IR/FTIR	FOURIER TRANSFORM INFRARED
GAC	GREEN ANALYTICAL CHEMISTRY
GAPI	GREEN ANALYTICAL PROCEDURE INDEX
GC	GAS CHROMATOGRAPHY
GSH	GLUTATHIONE
GST	GLUTATHIONE-S-TRANSFERASE
HBB	HEXABROMOBENZENE
HBCDD	HEXABROMOCYCLODODECANE
HCH	HEXACHLOROCYCLOHEXANES
HDPE	HIGH-DENSITY POLYETHYLENE
HEHP	HEXYL 2-ETHYLHEXYL PHTHALATE
HepG2	HUMAN LIVER CELLS
HGMS	HIGH-GRADIENT MAGNETIC SEPARATION
HPLC	HIGH-PERFORMANCE LIQUID CHROMATOGRAPHY
HS	HEADSPACE
HSP 70	HEAT SHOCK PROTEIN 70
ICP	INDUCTIVELY COUPLED PLASMA
IS	INTERNAL STANDARD
JAMSS	JAMSTEC MICROPLASTIC-SEDIMENT SEPARATOR
K_{OC}	ORGANIC CARBON-TO-WATER PARTITION COEFFICIENT
K_{OW}	OCTANOL-WATER PARTITION COEFFICIENTS
KWS	KORONA–WALZEN–SCHEIDER
LC	LIQUID CHROMATOGRAPY
LCA	LIFE CYCLE ASSESSMENT
LC-UV	LIQUID CHROMATOGRAPHY WITH UV DETECTION
LDPE	LOW-DENSITY POLYETHYLENE

LOD(S)	LIMIT OF DETECTION(S)
LOQ(S)	LIMIT OF QUANTIFICATION(S)
LRI	LONG-RANGE RESEARCH INITIATIVES
LW	LIPID WEIGHT
m	MASS
MDA	MALONDIALDEHYDE
MDL	METHOD DETECTION LIMIT
ME	MATRIX EFFECT
MEHHP	2-ETHYL-5-HYDROXYHEXYL) PHTHALATE
MEPS	MICROEXTRACTION BY PACKED SORBENTS
µ-FTIR	FOURIER TRANSFORM INFRARED MICROSCOPY
µ-RAMAN	RAMAN MICROSCOPY
MLOD	METHOD LIMIT OF DETECTION
MP(S)	MICROPLASTIC(S)
MPAE(S)	PHTHALATE MONOESTER(S)
mPE	METALLOCENE POLYETHYLENE
MPSS	MUNICH PLASTIC SEDIMENT SEPARATOR
mRNA	MESSENGER RIBONUCLEIC ACID
MS	MASS SPECTROMETRY
MSF	MAGNETIC SEEDED FILTRATION
MS/MS	TANDEM MASS SPECTROMETRY
MSPD	MATRIX SOLID-PHASE DISPERSION
MT	METALLOTHIONEIN
N.a.	NOT AVAILABLE
NBBS	N-BUTYL BENZENESULFONAMIDE
NBFR(S)	NOVEL BROMINATED FLAME RETARDANT(S)
ND/N.D.	NOT DETECTED
NMR	NUCLEAR MAGNETIC RESONANCE SPECTROSCOPY
NP(S)	NANOPLASTIC(S)
NRRT	NEUTRAL RED RETENTION TIME
OC	ORGANIC CARBON
OCP(S)	ORGANOCHLORINE PESTICIDE(S)
OECD	ORGANISATION FOR ECONOMIC CO-OPERATION AND DEVELOPMENT
OM	ORGANIC MATTER
OPE(S)	ORGANOPHOSPHORUS FLAME RETARDANT(S)

OPP(S)	ORGANOPHOSPHORUS PESTICIDE(S)
OTM	OLIVE TAIL MOMENT
PA	POLYAMIDE
PA 6	POLYAMIDE 6
PAE(S)	PHTHALATE ACID ESTER(S)
PAH(S)	POLYCYCLIC AROMATIC HYDROCARBON(S)
3-PBA	PHENOXYBENZOIC ACID
PBAT	POLY(BUTYLENE ADIPATE-CO-TEREPHTHALATE
PBB(S)	POLYBROMINATED BIPHENYL(S)
PBEB	PENTABROMOETHYLBENZENE
PBDE(S)	POLYBROMINATED DIPHENYL ETHER(S)
PBDPP	P,P′-1,3-PHENYLENE P,P,P′,P′-TETRAPHENYL ESTER PHOSPHATE
PBT	PENTABROMOTOLUENE
PC	POLYCARBONATE
PCB(S)	POLYCHLORINATED BIPHENYL(S)
PCB 28	2,4,4′-TRICHLOROBIPHENY
PCB 118	2,3′,4,4′,5′-PENTACHLOROBIPHENYL
PCB 153	2,2′,4,4′,5,5′-HEXACHLOROBIPHENYL
PCB 180	3,4,4′,5,5′-HEPTACHLOROBIPHENYL
PAD	PHOTODIODE ARRAY DETECTOR
PE	POLYETHYLENE
PET	POLYETHYLENE TEREPHTHALATE
PEVA	POLYETHYLENE VINYL ACETATE
pH_{PZC}	pH AT THE POINT OF ZERO CHARGE
pH_W	pH IN WATER
PLA	POLYLACTIC ACID
PMOC(S)	PERSISTENT MOBILE ORGANIC COMPOUND(S)
POD	PEROXIDASE
POP(S)	PERSISTENT ORGANIC POLLUTANT(S)
PP	POLYPROPYLENE
PS	POLYSTYRENE
PSA	PRIMARY SECONDARY AMINE
PTE(S)	POTENTIALLY TOXIC ELEMENT(S)
PTFE	POLYTETRAFLUOROETHYLENE
PU	POLYURETHANE

PUR	POLYURETHANE
PVC	POLYVINYL-CHLORIDE
PVP	POLYVINYLPYRROLIDONE
PY	PYROLYSIS
PYR(S)	PYRETHROID PESTICIDE(S)
QA	QUALITY ASSURENCE
QC	QUALITY CONTROL
q_e	ADSORPTION CAPACITY AT EQUILIBRIUM
q_t	ADSORPTION CAPACITIE
QuEChERS	QUICK, EASY, CHEAP, EFFECTIVE, RUGGED, AND SAFE
RE	RECOVERY RATE
REACH	REGISTRATION, EVALUATION AND AUTHORISATION OF CHEMICALS
RoHS	RESTRICTION OF HAZARDOUS SUBSTANCES
ROS	REACTIVE OXYGEN SPECIES
RSD	RELATIVE STANDARD DEVIATION
R^2	COEFFICIENT OF DETERMINATION
SD	STANDARD DEVIATION
SDG(S)	SUSTAINABLE DEVELOPMENT GOAL(S)
SEM	SCANNING ELECTRON MICROSCOPY
SERS	SURFACE-ENHANCED RAMAN SPECTROSCOPY
SIM	SELECTED ION MONITORING
SIN	SUBSTITUTE IT NOW
SLE	SOLID-LIQUID EXTRACTION
SMI	THE SEDIMENT-MICROPLASTIC ISOLATION
SOD	SUPEROXIDE DISMUTASE
SPE	SOLID PHASE EXTRACTION
sPLE	SELECTIVE PRESSURIZED LIQUID EXTRACTION
SPME	SOLID-PHASE MICROEXTRACTION
$S_{Y/X}$	STANDARD DEVIATION OF THE RESIDUAL
SS	SEWAGE SLUDGE
TBBPA	TETRABROMOBISPHENOL A
TBECH	1,2-DIBROMO-4-(1,2 DIBROMOETHYL) CYCLOHEXANE
TBEP	TRIS(2-CHLOROETHYL) PHOSPHATE
TBOEP	TRIS (2-BUTOXYETHYL) PHOSPHATE
TBP	TRIBUTYL PHOSPHATE

TCEP	TRIS(2-CHLOROETHYL) PHOSPHATE
TCIPP	TRIS(1-CHLORO-2-PROPYL) PHOSPHATE
TCP	TRICRESYL PHOSPHATE
TCPP	TRIS(2-CHLORO-1-METHYLETHYL) PHOSPHATE
TDBPP	TRIS(2,3-DIBROMOPROPYL) PHOSPHATE
TDCPP	TRIS(1,3-DICHLORO-2-PROPYL) PHOSPHATE
TDCIPP	TRIS(1,3-DICHLORO-2-PROPYL) PHOSPHATE
TED	THERMAL DESORPTION
TEHP	TRI(2-ETHYLHEXYL) PHOSPHATE
TEP	TRIETHYL PHOSPHATE
TiBP	TRI-ISO-BUTYLPHOSPHATE
TGA	THERMOGRAVIMETRIC ANALYSIS
TMP	TRIMETHYL PHOSPHATE
TMPP	TRIS(METHYLPHENYL) PHOSPHATE
TnBP	TRI-N-BUTYL PHOSPHATE
TOC	TOTAL ORGANIC CARBON
TOTM	TRIOCTYL TRIMELLITATE
TPhP	TRIPHENYL PHOSPHATE
TPP	TRIPROPYL PHOSPHATE
TPrP	TRIPROPYL PHOSPHATE
TRWMPS	TIRE AND ROAD-WEAR MICROPARTICLES
TWP	TIRE WEAR PARTICLES
US	UNITED STATES
USA	UNITED STATES OF AMERICA
UV	ULTRAVIOLET
V	VOLUME
WCA	WATER CONTACT ANGLE
WTP	WATER TREATMENT PLANT
WWTP(S)	WASTEWATER TREATMENT PLANT(S)
XPS	X-RAY PHOTOELECTRON SPECTROSCOPY
X-RAY CT	X-RAY COMPUTED TOMOGRAPHY
Z-SEP	SUPEL QUE Z-SEP BULK

Introduction

Contextualization and Thesis Outline

The economic (r)evolution of the last century has significantly reduced poverty and improved the quality of life. This economic growth model followed a "take-make-consume-throw away" pattern, which undeniably contributed to societal development but also led to environmental pressures (Esposito, Tse and Soufani, 2018). This linear economic model, characterized by a one-way flow of materials and energy, relies heavily on nonrenewable resources and their contribution to environmental degradation, pollution, and waste accumulation (Pichlak and Szromek, 2022). If current consumption levels persist, by 2030, resources equivalent to two Earths will be required to meet the needs of a growing population (Esposito, Tse and Soufani, 2018; Werle and Sobek, 2019), leading to increased waste generation, particularly plastic waste (Werle and Sobek, 2019; United Nations, 2023). Exceptional situations, such as the COVID-19 pandemic, have exacerbated this issue by increasing plastic waste from single-use medical products (Amato-Lourenço *et al.*, 2020).

Plastics, primarily produced from fossil fuels, dominate the industry, accounting for 90.6% of production. Mechanically recycled plastics make up 8.9%, bio-based plastics 0.5%, and both chemically recycled and carbon-captured plastics each constitute less than 0.1%. In 2022, global plastic production reached 400.3 million tons, with Asia leading at 52%, followed by North America (17%) and Europe (14%). In Europe, the highest demand for plastics comes from the packaging industry (39%), followed by the building and construction industries (23%) (Plastics Europe, 2023). Since the 1950s, the vast majority of pristine plastic produced has become waste, with minimal recycling and significant amounts ending up in landfills or leaking from waste collection systems (Geyer, Jambeck and Law, 2017). Research forecasts that by 2050, 26 billion metric tons of plastic will be produced (Geyer, Jambeck and Law, 2017), potentially resulting in more plastic in the ocean than fish (VishnuRadhan, Eldho and David, 2019).

Plastic pollution has significant environmental impacts, including contributions to climate change through greenhouse gas (GHG) emissions from the plastic life cycle (Jambeck and Walker-Franklin, 2023). Currently, annual GHG emissions from plastic production and consumption are estimated at 1.8 gigatons of carbon dioxide equivalent (Gt CO_2e), potentially increasing to 8 Gt CO_2e by 2050 (Bauer *et al.*, 2022). Addressing this challenge requires raising awareness, reducing and reusing plastics, ending single-use plastic production, enhancing waste management, promoting recycling and upcycling, and exploring renewable materials (Bauer *et al.*, 2022). In response to these concerns, alternative waste management strategies have been implemented, such as the EU

Directive (EU) 2018/852, which establishes recycling targets for plastic packaging of 50% by 2025 and 55% by 2030 (Council of the European Union, 2018). The use of post-consumer recycled plastics, as well as the production of bio-based polymers, is increasing globally (Payne, McKeown and Jones, 2019; Khalid *et al.*, 2021).

Plastic waste is degraded into smaller fragments, such as microplastics (MPs) and nanoplastics through physical, chemical, and biological processes (Bläsing and Adeyemi, 2018). Each plastic type has a distinct formulation, complicating the tracking and impact assessment (Jambeck and Walker-Franklin, 2023). Additives such as plasticizers, stabilizers, flame retardants, and pigments can leach out, posing additional environmental risks (de Souza Machado *et al.*, 2018; Mariano *et al.*, 2021). Plastics also adsorb pollutants, further increasing their environmental impacts (de Souza Machado *et al.*, 2018; He *et al.*, 2018; Mariano *et al.*, 2021).

Almost every ecosystem is now exposed to some level of plastic debris, with soil recognized as the major reservoir. However, our understanding of how MPs and their related chemicals are released, stored, and transported remains limited (de Souza Machado *et al.*, 2018; He *et al.*, 2018; Radford *et al.*, 2021). Agriculture and wastewater treatment plants (WWTPs) are considered primary sources of MPs, with approximately 90% of the captured MPs being retained in sludge within WWTPs, while the remaining 10% flows directly into aquatic systems (Boots et al., 2019; Edo et al., 2020). Although sewage sludge (SS) is considered a fertilizer that can enhance soil properties, its use in a circular economy context may introduce pollutants that are not addressed by current legislation, such as emerging contaminants and MPs. This practice, which is encouraged in the European Union, can lead to the dispersal of these contaminants into the environment (Wang *et al.*, 2019; van den Berg *et al.*, 2020). Further migration of pollutants across different environments poses a significant threat to global contamination and human health (Bergmann *et al.*, 2019; Goodman *et al.*, 2021; Mariano *et al.*, 2021).

Despite the growing body of research, the effects of MPs on organisms, microbiota, and plants are still not fully understood. However, studies have consistently reported negative impacts on various organisms (Lei *et al.*, 2018; Khalid, Aqeel and Noman, 2020; Sánchez-Almeida *et al.*, 2022). Toxicological effects of MPs have been documented in aquatic ecosystems, including reduced growth and increased mortality in fish larvae (Gu *et al.*, 2020), and similar effects in soil invertebrates (Cheng *et al.*, 2020). Studies suggested that humans ingest MPs, with MPs detected in human blood, testicles, and

placentas, indicating exposure from early developmental stages (Ragusa *et al.*, 2021; Leslie *et al.*, 2022; Zhao *et al.*, 2023). However, research is still ongoing to understand the effects of MPs and the associated chemicals on human health. Although studies have proposed different pathways and mechanisms through which these chemicals could impact health, a complete understanding of the issue is still developing (Sousa *et al.*, 2023).

Identifying and extracting MPs remains a critical challenge due to limited analytical methods (Picó and Barceló, 2022) and the difficulty of conducting research in plastic-free environments (Sánchez-Almeida *et al.*, 2022), which hinders the assessment of their distribution and impact. Current methodologies include density separation, sieving, filtration, and various microscopic and spectroscopic techniques. Harmonizing these methods is crucial for accurately comparing results and understanding the ecological implications of MPs (He *et al.*, 2018; Mariano *et al.*, 2021). To thoroughly explore the characteristics of MP pollution, including associated chemicals and ecotoxicological effects, there is a pressing need for enhanced and standardized methods and tools for their extraction, identification, and characterization (He *et al.*, 2018; Mariano *et al.*, 2021). However, the diverse compositions, shapes, sizes, and levels of aging or weathering of MP particles present significant challenges, necessitating the selection of appropriate techniques tailored to specific research objectives, whether for qualitative or quantitative analysis, targeting large (500 µm to 5 mm), small (1–500 µm), or nanoplastics (1 nm to 1 µm). Additionally, the development of these methods has not prioritized environmental sustainability, highlighting the need to design green methods that minimize environmental impact during extraction and analysis processes, in line with the principles of green chemistry and engineering (Picó and Barceló, 2022).

The main objectives of this thesis were to conduct a comprehensive review of MPs and related chemicals, investigate SS as a possible source of soil contamination using Quick Easy Cheap Effective Rugged Safe (QuEChERS) extraction coupled with chromatographic techniques, study the coexistence of MPs and a flame retardant in soil using advanced spectroscopic methods, and to develop a green extraction method for MP in agricultural soils to contribute to a harmonized method and be able to contribute to knowledge about the sources of MP in agriculture. This research project aimed to improve analytical techniques for detecting soil pollutants, deepen our understanding of the sources and interactions between MPs and related chemical contaminants, and provide insights into their prevalence in terrestrial ecosystems. By merging analytical and environmental chemistry, this project contributes to preventing environmental

degradation, protecting soil health, promoting innovative solutions, and supporting the Sustainable Development Goals (SDGs) of the United Nations 2030 Agenda, specifically Goals 15 (Life on Land) and 3 (Good Health and Well-Being). This work is particularly timely given the recent Eurostat report, which highlights progress towards SDGs within the EU. Goals 3 and 15 show moderate movement away from the desired targets, with Goal 15 ranked last (Eurostat, 2024). This underscores the urgent need for enhanced efforts to protect terrestrial ecosystems.

This thesis is organized into several chapters, each dedicated to exploring different aspects of MPs and their environmental impacts, with a particular emphasis on soil interactions. The first chapter, "State of the Art," provides an integrated literature review of the current knowledge gaps (input pathways, transport, and analytical challenges), and ecotoxicological impacts associated with MP contamination and plastic-related chemicals, namely flame retardants. The second chapter, “Sewage Sludge as a Potential Source of Soil Contamination" investigated the presence of emerging micropollutants in SS by using advanced analytical techniques. The third chapter, "Coexistence of Microplastics and Plastic-related Chemicals in Soil," examines the interactions between MPs and the flame-retardant triphenyl phosphate (TPhP) in soil environments. Finally, the fourth chapter, "Extracting Microplastics from Soil," focuses on developing green chemistry-based methods for MP extraction and analysis in agricultural settings. These chapters collectively aim to deepen the understanding of the presence of MPs and plastic-related chemicals in soils.

References

Amato-Lourenço, L.F. *et al.* (2020) ‘An emerging class of air pollutants: Potential effects of microplastics to respiratory human health?’, *Science of the Total Environment*, 749, p. 141676. Available at: https://doi.org/10.1016/j.scitotenv.2020.141676.

Bauer, F. *et al.* (2022) ‘Plastics and climate change breaking carbon lock-ins through three mitigation pathways’, *One Earth*, 5(4), pp. 361–376. Available at: https://doi.org/10.1016/j.oneear.2022.03.007.

van den Berg, P. *et al.* (2020) ‘Sewage sludge application as a vehicle for microplastics in eastern Spanish agricultural soils’, *Environmental Pollution*, 261, p. 114198. Available at: https://doi.org/10.1016/j.envpol.2020.114198.

Bergmann, M. *et al.* (2019) ‘White and wonderful? Microplastics prevail in snow from the

Alps to the Arctic', *Science Advances*, 5(8), pp. 1–11. Available at: https://doi.org/10.1126/sciadv.aax1157.

Bläsing, M. and Adeyemi, K.A. (2018) 'Plastics in soil: Analytical methods and possible sources', *Science of the Total Environment*, 612, pp. 422–435. Available at: https://doi.org/10.1016/j.scitotenv.2017.08.086.

Cheng, Y. *et al.* (2020) 'Combined effects of mulch film-derived microplastics and atrazine on oxidative stress and gene expression in earthworm (Eisenia fetida)', *Science of the Total Environment*, 746, p. 141280. Available at: https://doi.org/10.1016/j.scitotenv.2020.141280.

Council of the European Union (2018) 'Directive (EU) 2018/852 of the European Parliament and of the Council of 30 May 2018', *Official Journal of the European Union*, 2018, pp. 141–154. Available at: https://eur-lex.europa.eu/legal-content/EN/TXT/PDF/?uri=CELEX:32018L0852.

Esposito, M., Tse, T. and Soufani, K. (2018) 'The circular economy: An opportunity for renewal, growth, and stability', *Thunderbird International Business Review*, 60(5), pp. 725–728. Available at: https://doi.org/10.1002/tie.21912.

Eurostat (2024) *Sustainable development in the European Union Monitoring report on progress towards the SDGs in an EU context*. Available at: https://ec.europa.eu/eurostat/about/policies/copyright.

Geyer, R., Jambeck, J. and Law, K. (2017) 'Production, Use, And Fate Of All Plastics Ever Made', *Science Advances*, 3(e1700782), pp. 25–29. Available at: https://doi.org/DOI: 10.1126/sciadv.1700782.

Goodman, K.E. *et al.* (2021) 'Exposure of Human Lung Cells to Polystyrene Microplastics Significantly Retards Cell Proliferation and Triggers Morphological Changes', *Chemical Research in Toxicology*, 34(4), pp. 1069–1081. Available at: https://doi.org/10.1021/acs.chemrestox.0c00486.

Gu, L. *et al.* (2020) 'Inhibitory effects of polystyrene microplastics on caudal fin regeneration in zebrafish larvae', *Environmental Pollution*, 266. Available at: https://doi.org/10.1016/j.envpol.2020.114664.

He, D. *et al.* (2018) 'Microplastics in soils: Analytical methods, pollution characteristics and ecological risks', *Trends in Analytical Chemistry*, 109, pp. 163–172. Available at:

https://doi.org/10.1016/j.trac.2018.10.006.

Jambeck, J.R. and Walker-Franklin, I. (2023) 'The impacts of plastics' life cycle', *One Earth*, 6(6), pp. 600–606. Available at: https://doi.org/10.1016/j.oneear.2023.05.015.

Khalid, A. *et al.* (2021) 'Are bio-based and biodegradable microplastics impacting for blue mussel (Mytilus edulis)?', *Marine Pollution Bulletin*, 167(March), p. 112295. Available at: https://doi.org/10.1016/j.marpolbul.2021.112295.

Khalid, N., Aqeel, M. and Noman, A. (2020) 'Microplastics could be a threat to plants in terrestrial systems directly or indirectly', *Environmental Pollution*, 267, p. 115653. Available at: https://doi.org/10.1016/j.envpol.2020.115653.

Lei, L. *et al.* (2018) 'Microplastic particles cause intestinal damage and other adverse effects in zebrafish Danio rerio and nematode Caenorhabditis elegans', *Science of the Total Environment*, 619–620, pp. 1–8. Available at: https://doi.org/10.1016/j.scitotenv.2017.11.103.

Leslie, H.A. *et al.* (2022) 'Discovery and quantification of plastic particle pollution in human blood', *Environment International*, (March), p. 107199. Available at: https://doi.org/10.1016/j.envint.2022.107199.

Mariano, S. *et al.* (2021) 'Micro and Nanoplastics Identification: Classic Methods and Innovative Detection Techniques', *Frontiers in Toxicology*, 3(February), pp. 1–17. Available at: https://doi.org/10.3389/ftox.2021.636640.

Payne, J., McKeown, P. and Jones, M.D. (2019) 'A circular economy approach to plastic waste', *Polymer Degradation and Stability*, 165, pp. 170–181. Available at: https://doi.org/10.1016/j.polymdegradstab.2019.05.014.

Pichlak, M. and Szromek, A.R. (2022) 'Linking Eco-Innovation and Circular Economy—A Conceptual Approach', *Journal of Open Innovation: Technology, Market, and Complexity*, 8(3), p. 121. Available at: https://doi.org/10.3390/joitmc8030121.

Picó, Y. and Barceló, D. (2022) 'Micro(Nano)plastic analysis: a green and sustainable perspective', *Journal of Hazardous Materials Advances*, 6(100058). Available at: https://doi.org/10.1016/j.hazadv.2022.100058.

Plastics Europe (2023) *Plastics - the fast facts 2023*, *Plastics Europe AISBL*. Brussels. Available at: https://plasticseurope.org/knowledge-hub/plastics-the-fast-facts-2023/.

Radford, F. *et al.* (2021) 'Developing a systematic method for extraction of microplastics in soils', *Analytical Methods*, 13(14), pp. 1695–1705. Available at: https://doi.org/10.1039/d0ay02086a.

Ragusa, A. *et al.* (2021) 'Plasticenta: First evidence of microplastics in human placenta', *Environment International*, 146, p. 106274. Available at: https://doi.org/10.1016/j.envint.2020.106274.

Sánchez-Almeida, R. *et al.* (2022) 'Microplastics Determination in Gastrointestinal Tracts of European Sea Bass (Dicentrarchus labrax) and Gilt-Head Sea Bream (Sparus aurata) from Tenerife (Canary Islands, Spain)', *Polymers*, 14(10), pp. 1–15. Available at: https://doi.org/10.3390/polym14101931.

Sousa, S. *et al.* (2023) 'Accumulation of organophosphorus pollutants in adipose tissue of obese women - metabolic alterations', *Environmental Research*, 239(September). Available at: https://doi.org/10.1016/j.envres.2023.117337.

de Souza Machado, A.A. *et al.* (2018) 'Microplastics as an emerging threat to terrestrial ecosystems', *Global Change Biology*, 24(4), pp. 1405–1416. Available at: https://doi.org/10.1111/gcb.14020.

United Nations (2023) 'The Sustainable Development Goals Report 2023: Special edition', in Jennifer Ross (ed.). New York. Available at: https://unstats.un.org/sdgs.

VishnuRadhan, R., Eldho, T.I. and David, T.D. (2019) 'Can plastics affect near surface layer ocean processes and climate?', *Marine Pollution Bulletin*, 140(October 2018), pp. 274–280. Available at: https://doi.org/10.1016/j.marpolbul.2019.01.052.

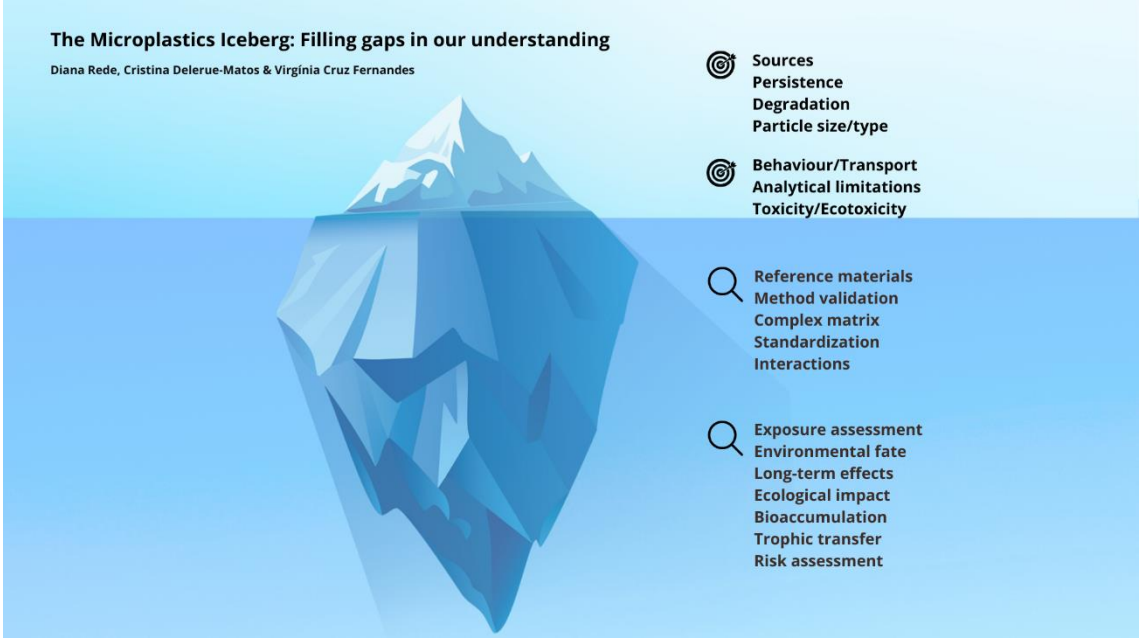
Wang, Y. *et al.* (2019) 'A nationwide survey of 31 organophosphate esters in sewage sludge from the United States', *Science of the Total Environment*, 655, pp. 446–453. Available at: https://doi.org/10.1016/j.scitotenv.2018.11.224.

Werle, S. and Sobek, S. (2019) 'Gasification of sewage sludge within a circular economy perspective: a Polish case study', *Environmental Science and Pollution Research*, 26(35), pp. 35422–35432. Available at: https://doi.org/10.1007/s11356-019-05897-2.

Zhao, Q. *et al.* (2023) 'Detection and characterization of microplastics in the human testis and semen', *Science of the Total Environment*, 877(March), p. 162713. Available at: https://doi.org/10.1016/j.scitotenv.2023.162713.

1. State of the Art

1.1. The Microplastics Iceberg: Filling Gaps in Our Understanding



Published at *Polymers*, 15, 16:3356. (2023). https://doi.org/10.3390/polym15163356

Contribution Statement

The candidate contributed to the paper on environmental contamination by MPs by conducting an integrated literature review covering input pathways, transport mechanisms, analytical challenges, methodological advancements, and the toxicological effects of MPs. Additionally, the candidate authored the original draft of the paper and participated in the review and editing stages. Except for Figure 2, which includes photographs taken by the candidate and assembled using Microsoft® PowerPoint®, all other figures in the paper were created using the Canva platform (http://www.canva.com).

polymers

MDPI

Review

The Microplastics Iceberg: Filling Gaps in Our Understanding

Diana Rede [1,2], Cristina Delerue-Matos [1] and Virgínia Cruz Fernandes [1,*]

[1] REQUIMTE/LAQV, Instituto Superior de Engenharia do Porto, Instituto Politécnico do Porto, Rua Dr. António Bernardino de Almeida, 431, 4249-015 Porto, Portugal; dsgmr@isep.ipp.pt (D.R.); cmm@isep.ipp.pt (C.D.-M.)
[2] Departamento de Química, Faculdade de Ciências, Universidade do Porto, rua do Campo Alegre s/n, 4169-007 Porto, Portugal
* Correspondence: vir@isep.ipp.pt

Abstract: Plastic is an indispensable material in modern society; however, high production rates combined with inadequate waste management and disposal have resulted in enormous stress on ecosystems. In addition, plastics can become smaller particles known as microplastics (MPs) due to physical, chemical, and biological drivers. MP pollution has become a significant environmental problem affecting terrestrial and aquatic ecosystems worldwide. Although the topic is not entirely new, it is of great importance to the field of polymers, drawing attention to specific gaps in the existing literature, identifying future areas of research, and improving the understanding of MP pollution and its environmental impacts. Despite progress in this field, problems remain. The lack of standardized methods for MP sampling, separation, extraction, and detection makes it difficult to collect information and establish links between studies. In addition, the distribution and pathways of MPs in ecosystems remain unknown because of their heterogeneous nature and the complex matrices in which they occur. Second, toxicological tests showed that MPs can be ingested by a wide range of organisms, such as *Danio rerio* and *Eisenia fetida*, resulting in gut obstruction, physical damage, histological changes, and oxidative stress. The uptake of MP and their toxicological effects depend on their shape, size, concentration, and polymer composition. Furthermore, MPs can enter the food chain, raising concerns regarding potential contaminations for human and environmental health. This review paper sheds light on the pressing issue of MP pollution and highlights the need for interdisciplinary collaboration between scientists, policymakers, and industry leaders.

Keywords: plastic pollution; emerging contaminants; analytical methods; ecotoxicity; oxidative stress

check for updates

Citation: Rede, D.; Delerue-Matos, C.; Fernandes, V.C. The Microplastics Iceberg: Filling Gaps in Our Understanding. *Polymers* **2023**, *15*, 3356. https://doi.org/10.3390/polym15163356

Academic Editors: Xinfeng Wei, Emmanuel Richaud and Andrew M. Booth

Received: 20 June 2023
Revised: 3 August 2023
Accepted: 7 August 2023
Published: 10 August 2023

Copyright: © 2023 by the authors. Licensee MDPI, Basel, Switzerland. This article is an open access article distributed under the terms and conditions of the Creative Commons Attribution (CC BY) license (https://creativecommons.org/licenses/by/4.0/).

1. Introduction

Plastic debris and microplastics (MPs) (defined as plastic particles <5 mm) have been widely found in a variety of environmental media, such as air, water, and soil, and their persistence and complexity are considered major global concerns [1,2]. MPs are classified as primary if they are industrially produced, or secondary if they are derived from the fragmentation of larger plastic items [3,4]. Owing to the widespread use and disposal of plastics, as well as the heterogeneity of polymers, the sources of MPs in the environment and the routes of contamination can be difficult to determine. Land-based activities are considered the primary source of MPs, but ocean-related activities such as fishing and shipping can also contribute [5,6]. Typically, MPs tend to be more prevalent in urbanized areas and regions with ineffective waste management, although they can also be dispersed by the airstream and deposited across water and land [7–9]. Information on the presence, fate, and long-term effects of MPs on ecosystems (particularly in freshwater and terrestrial environments) is scarce. Indeed, there is a lack of standardized sampling, pretreatment, extraction, and analysis methods for MPs, making comparisons between studies quite challenging [2,4]. There is growing evidence suggesting that MPs can have negative effects

on individual organisms [10–17]; for instance, MPs ingested by zebrafish (*Danio rerio*) can accumulate in the gut, causing inflammation and oxidative stress in tissues [13].

Research and development of effective methods to detect and monitor MPs in various environmental media is essential because of the significant environmental impact and potential health risks associated with them. The standardization of analytical methods would provide more reliable and robust data, which in turn would facilitate the development of effective regulations to mitigate the impact of MPs, promote the use of alternative materials to plastics, and establish defensible waste management practices. This study provides an integrated literature review on pollution from MPs, focusing on an analytical methodology. The study covers a wide range of studies that examined the sources and transport of MPs into the environment, as well as the concentrations and toxicological effects of MP exposure. It includes both research and reviews that address advances in extraction and detection methods, quantification techniques, and innovations to identify MPs in various environmental matrices while analyzing the pathways of entry involved. To prepare this review, relevant studies were retrieved from the ScienceDirect database covering the period from 2017 to 2023. By summarizing and reviewing the literature on these critical aspects, this review aims to contribute to a deeper understanding of the environmental pollution of MP and to promote progress in the field of analytical methods for their study.

2. Emerging Contamination: From Plastic to Microplastics

Plastics comprise a wide variety of materials that are produced from different sources, namely fossil origins (i.e., crude oil, gas, etc.), renewable (e.g., sugar cane, vegetable oils, etc.), or mineral base (i.e., salt) [18]. Large-scale plastic production began in the early 1950s and products made from these materials are all around playing a fundamental role in a myriad of sectors, such as packaging, construction, electronics, agriculture, textile, cosmetics, among others [19–21]. The use of plastics deeply shapes the development of modern society as they bring safety, hygiene, comfort, and well-being [18,20]. Many types of chemical additives are used in plastic production to improve its properties, including plasticizers, stabilizers, flame retardants, and colorants [22–24]. It is important to note that the characteristics that make plastic materials desirable (hydrophobicity, durability, etc.) are those that make them persistent and prevalent in terrestrial, freshwater, estuarine, coastal, and marine environments [2,25].

In 2021, global plastic production reached 390.7 million tonnes, with Asia being responsible for half of the production followed by North America and Europe. Packaging, building and construction, and the automotive sector were the three biggest end-use markets, with 44%, 18%, and 8% of the consumption, respectively [26]. Fossil-based resins represented 90.2%, and the most produced polymers were polypropylene (PP) (19.3%), low-density polyethylene (PE-LD) (14.4%), polyvinyl-chloride (PVC) (12.9%), high-density polyethylene (PE-HD) (12.5%), polyethylene terephthalate (PET) (6.2%), polyurethane (PUR) (5.5%), and polystyrene (PS) (5.3%). Circular plastics (i.e., recycled and biobased/bioattributed plastics) represent approximately 9.8% of the global production [26]. It was estimated that in 2015, around 8.3 billion tonnes of plastics were produced worldwide, of which 6.3 billion tonnes ended up as waste with 9% being recycled, 12% energetically recovered, and 79% deposited in landfills or leaked out of formal waste collection systems accumulating in terrestrial or marine environments (i.e., single-use packaging) [21,27,28]. According to Plastics Europe, the separate waste collection enables recycling rates 13 times higher than mixed waste collection systems [26].

The different physical properties of each polymer may affect its behavior in the environment. For instance, in the aquatic environment, the tendency of particles to float or settle in sediments is usually related to the density of the polymer [2,9]. However, buoyant particles of PP and PE can sink and be retained within sediments, which means that even when physical properties are well known, predicting the fate of polymers in the environment is very challenging [2,29]. From sediments in deep seas to underwater canyon, encapsulated in Arctic sea ice, or massive accumulations at sea surface waters, such as *the Great Pacific Garbage Patch*, plastic materials have been identified all across the

globe [29–32]. Moreover, the ability of plastics to fuse with volcanic rocks, sediments, and organic materials may lead to the formation of solid rocklike structures, the *plastiglomerates* (Figure 1a) [33,34]. Furthermore, it has been shown that chemical additives can leach out during the life cycle of the product [22,35,36]. At the same time, due to the hydrophobic surface of plastic materials, they can adsorb other chemical contaminants (e.g., metals, polychlorinated biphenyls, polycyclic aromatic hydrocarbons, and/or pesticides) [22,35–37]. Synergistic interactions may occur between them, resulting in an enhancement of the toxicity in living organisms [22,35–38]. It is possible that if plastic particles were taken up by biota, they could act as carriers for other contaminants along the food chain—a *Trojan horse effect* [3,37,39–41].

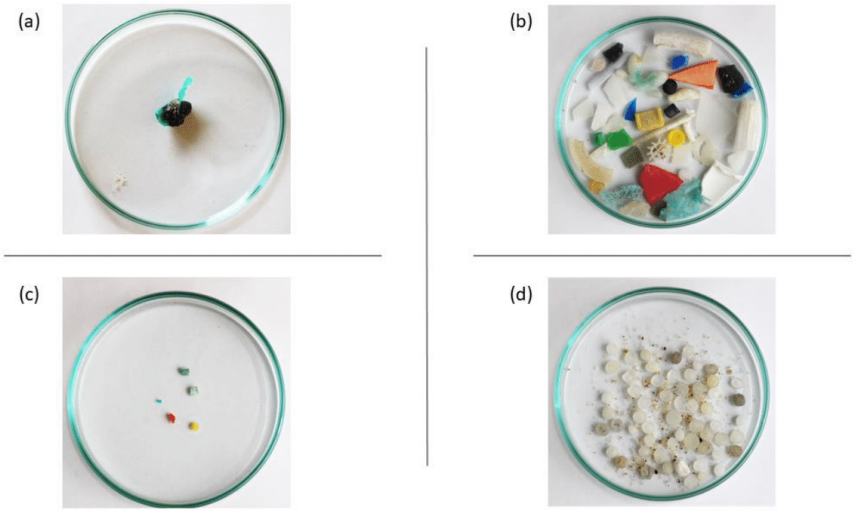


Figure 1. Types of plastic debris found on a beach in Northern Portugal. The plastic materials include: (**a**) a plastiglomerate, (**b**) mesoplastic fragments, (**c**,**d**) microplastics.

Plastic litter can be degraded by physical, chemical, and biological drivers (i.e., ultraviolet radiation, wind or water erosion, etc.) and become smaller pieces, usually classified by size, namely, megaplastics (>100 mm), macroplastics (>20 mm), mesoplastics (20–5 mm, Figure 1b)), MPs (<5 mm, Figure 1c,d), and nanoplastics (NPs) (1 to 1000 nm), although the adopted terminology can vary [7,39,42–44]. Plastic debris was pointed out as a serious environmental issue in the 1970s, though only in 2004 was the term microplastic applied for the first time [9,45]. Currently, environmental contamination caused by MPs is in the public domain, being considered an emerging issue of global interest [16,46,47]. MPs fall into two groups: primary MPs if they are produced for industrial purposes, such as PE microbeads used as exfoliating agents in personal care products; or secondary MPs if they are derived from the fragmentation of larger items [6,39,40]. Secondary MPs correspond to the majority of MPs that can be found in the natural environment [3,48].

Owing to the massive production of plastic materials and the ineffectiveness of waste management and disposal, there is no question about the challenge that plastic pollution represents in our society [36]. The wide variability of plastic types and sizes has hindered the development of standardized extraction and detection methods for MPs in environmental samples [35,49]. There has been an increase in the development of programs and guidelines for assessing marine litter and in the number of studies on the fate and effects of marine compartments [8,45]. However, sources, in situ formation, distribution, transport pathways, interactions, and ecotoxicological effects of MPs and other chemical contaminants on the environment, particularly in terrestrial and freshwater compartments, have not received

sufficient attention, and the data are scattered [39,45]. Both have been seen mainly as sinks and transport routes for MPs to reach the seas and oceans [2,6]. Monitoring programs are generally based on the measurement of chemical concentrations in different compartments. They do not provide useful information on real impacts on organisms and ecosystems, making it difficult to prepare protection and mitigation plans [36,39]. In Europe, approximately 26 million tonnes of plastic waste are produced annually [50]. To tackle plastic pollution and marine litter and to accelerate the transition to a resource-efficient circular plastic economy, the European Commission has established the European Plastics Strategy as part of the Circular Economy Action Plan and the Framework on Biobased, Biodegradable, and Compostable Plastics [50,51]. It brings clarity to consumers and the industry on single-use plastics, plastic packaging, MPs, and circular plastics. It is estimated that between 75,000 and 300,000 tonnes of MPs are released into the environment every year in the EU [50]. While there is still no law in place for MPs, the European Chemical Agency has put forward a proposal for a restriction on MPs intentionally added to mixtures, which is currently under discussion with member state authorities and voting. If adopted, this restriction would reduce the quantity of MPs released to approximately 500,000 tonnes over 20 years [52].

3. The Ubiquity of Microplastics in the Environment: Input Pathways and Transport

The sources of MPs in the environment can be numerous, and the routes of contamination can be difficult to define because of the massive plastic production and consumption (especially single-use packaging), the leakage of plastic from waste streams, and the heterogeneity of polymers [2,6,53]. Land-based activities are pointed out as the main sources of MPs, and as environmental compartments are linked, it is expected that contaminants migrate between them (Figure 2) [5,6]. Moreover, ocean-based activities, such as fishing, aquaculture, and merchant ships, might also release MPs directly into the environment, either by the accidental loss and fragmentation of plastic materials or by illegal dumping of plastic waste at sea [6,41,53]. MPs are likely to be more abundant in urbanized areas as well as in areas where waste management programs are ineffective [2,22,54]. Additionally, lighter plastic items from construction materials, artificial turf, and household dust can be transported by wind action and deposited by atmospheric fallout across water bodies and/or land [8,9,30].

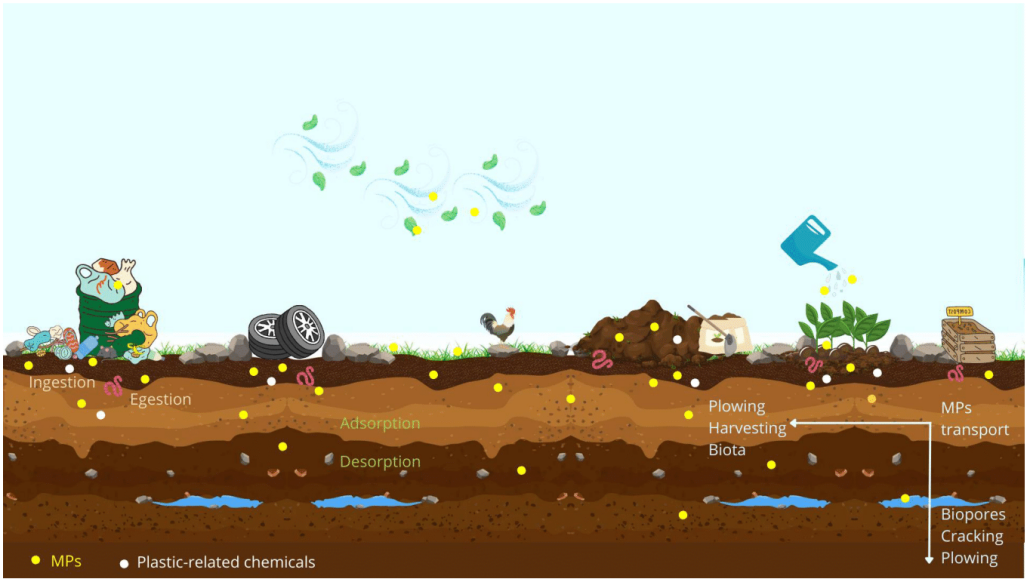


Figure 2. Sources and routes of microplastics and plastic-related chemical pollution in soil environment.

Industrial complexes might contribute to the input of primary MPs into the environment, mostly due to improper handling during production, packaging, and transportation [25,37]. Some examples are plastic resin pellets (commonly known as *nurdles*, Figure 1d), flakes, or plastic powder, used as raw materials in the production of larger items, waste from plastic production, regranulate from plastic recycling, and products containing abrasives [37]. Furthermore, wastewater treatment plants (WWTPs) are thought to be an important land-based source of primary MPs, namely plastic particles from personal care products (i.e., hand cleaners or toothpaste, to name a few) and medical products [3,22,25,55]. In addition, wastewater may contain secondary synthetic microfibers from laundry (i.e., PA), and other plastic debris that, due to inadequate disposition, end up in wastewater streams [2]. The resulting sewage sludge is often disposed of in soil or converted into compost or biosolids (pasteurized sewage sludge) and applied as fertilizer (Figure 2) [25,28,55]. Regarding the effluents of WWTPs, they can be discharged into the aquatic environment or be used as reclaimed water and are frequently seen as a major source of MPs [3,8,25,39,56].

Approximately 95% of MPs captured by WWTPs are retained in the sludge phase [8,55,57]. Every day, large amounts of sewage sludge are produced and widely applied to the soil for agricultural purposes [57,58]. Considering the properties of polymers, it is expected that MPs will remain barely unchanged over time [2,25,59]. For example, the original properties of microfibers, which are considered the most abundant microparticles in natural environments, have been preserved for 15 years after biosolid application [22]. The remaining 5% of MPs that pass through WWTPs are directly and continuously released into aquatic systems [8,25]. As MPs can be retained within sediments and buried close to the outlet of treated wastewater, not all plastic particles discharged into freshwater are transported to marine environments [22,60]. For instance, in industrialized areas, rivers may have higher concentrations of MPs than marine environments [22]. Furthermore, when modern WWTP facilities are not available or in the case of an overflow, wastewater is directly input into aquatic systems without any treatment [2,9]. Nonetheless, it is undeniable that rivers and freshwater bodies are the major carriers of MPs from land to oceans [6,8]. According to Zhang and Liu, only 1% of global plastic waste is directly input into the marine environment, which means that the largest amount is transferred from freshwater and soil [28].

A direct source of secondary MPs is the fragmentation of meso- and macroplastic litter already present in the environment [1,2]. Physical abrasion and ultraviolet radiation are considered to be the driving forces that trigger the fragmentation of plastic items by altering their chemical, physical, and mechanical properties [9,61,62]. Another source of secondary MPs is living organisms that mistake plastic for food [63,64]. For example, caddisfly larvae use external feeding appendages to actively fragment and physically alter plastics [63]. Similarly, earthworms contribute to the biofragmentation of plastic litter, as reported by Kwak and An [64]. In addition, landfills can facilitate the entry of MPs into the environment, either through the loss of plastic materials during waste collection or mismanagement [6,25,54]. MPs can also accumulate in the environment through the fragmentation of tire wear particles, road-marking paints, and particles derived from vehicle components. Tire abrasion particles may be introduced into roadside environments via dust or wash-off, decreasing plant growth even at low concentrations, altering bulk density and soil aeration, and ultimately the biogeochemical cycling [39,54,65,66].

The plastic mulching used in agriculture promotes the incorporation of MPs into the environment [25,39,54]. This widespread agricultural technique contributes to improve production, but plastic-related chemicals such as phthalates (plastic plasticizers) can be released into crops along with MPs [39,54]. Moreover, it is expected that dense polymers remain in the soil and are transported into deeper soil layers by the action of biota, harvesting, ploughing, soil cracking, and wet–dry cycles [64,67,68]. On the other hand, lighter polymers are more likely to be transported across water bodies or land, by the action of wind and water (Figure 2) [8,9]. It is important to note that plastic debris is not only transported by rivers from land to the ocean; plastic litter in the aquatic environment can

return to land due to high tides or floods, reinforcing the idea that pollutants drift between environmental compartments [2,30,39].

4. Unveiling Microplastics in the Environment: Advances and Challenges in Analytics

MPs have been reported worldwide from the water and sediments of Hiroshima Bay (Japan), amended agricultural soil in Mellipilla (Chile), and snow from the Alps (Europe) [30,69–71]. From an analytical point of view, some challenges can be identified, such as the lack of reference material needed for method validation and the inexistence of standardized analysis methods that allow the accurate comparison of results [55,72]. As shown in Table 1, there are differences in MP extraction procedures between the same sample types, such as agricultural soils from the Chai River valley (China) [28] and Middle Franconia (Germany) [58] or freshwater from Lakee Saimaa (Finland) [73] and Lakee Winnipeg (Canada) [3]. Furthermore, analytical methodologies designed for the extraction of MPs from aqueous samples have been adapted to solid samples, such as soil. However, the high complexity of solid matrices, especially if they are rich in organic matter, and the presence of other chemical contaminants (e.g., PAHs) hinder the extraction and identification of MPs [55,74]. Moreover, the degradation of plastics under natural conditions causes changes in the surface and functional groups. This means that depending on the degree of aging, MPs of the same polymer can exhibit different thermochemical properties, which can decrease the accuracy of the analysis [62,75–77]. Concerns regarding cross-contamination have been highlighted and the impossibility of working in a plastic-free environment has been recognized [56,78,79]. It is recommended that the use of plastic materials be avoided and limited as far as possible; however, in some cases, it cannot be eliminated [56]. However, as highlighted by Miller et al. (2021), there is a perceived need for the further development of rigorous study designs in MP research, with relatively few studies currently incorporating comprehensive quality assurance and quality control (QA/QC) measures commonly found in more established fields of trace chemical contaminant monitoring. The pressing need in this area is to establish standardized methods for QA/QC, which should include the systematic collection and reporting of field and laboratory blanks, as well as a careful consideration of background contamination in field samples [80].

In general, the methods reported in the literature are carried out in three main steps: sample pretreatment (e.g., drying, size fractioning, and chemical digestion of organic matter), MP extraction (e.g., sieving or density separation), and the identification of the recovered MPs (Figure 3). The presence of nontarget impurities, such as dust or organic matter, can bias MP identification, and it is more challenging to separate and characterize MPs from samples with a high organic matter content such as soil than from water matrices [54,77]. In fact, the elimination of organic matter is a sore point in sample pretreatment, since it is necessary to avoid or limit the possible damage that oxidizing agents, usually hydrogen peroxide (H_2O_2) [8,78,81,82] or Fenton's reagent [3,28,73,78], may cause in MP particles [3,22,56,81]. For instance, a method developed by Li et al. (2019) for analyzing MPs in soil and sludge samples comprised two digestions to remove organic matter: a first with 30% H_2O_2 at 70 °C and a second with H_2O_2 and sulfuric acid at 70 °C. The authors observed a slight dissolution of PA, possibly owing to the last step of the process [81]. As an alternative to chemical oxidation, Mintenig et al. (2017) developed a greener, multistep, plastic-preserving enzymatic-oxidative method to degrade the organic matter of wastewater from Lower Saxony (Germany), but the process takes 20 days (incubation, 24 h; protease, 48 h; lipase, 96 h; cellulase, 6 d), which is time consuming [56].

Salt-based density separation followed by filtration is the most widely used procedure for extracting MPs [8,28,56,57,69,70,81,83]. However, it is not always easy to float the densest polymers, which can undermine the reliability of the results, because high-density MPs may be underestimated or not reported. To overcome these difficulties, some authors have proposed an oil-based density separation by exploiting the oleophilic properties of plastic materials. Using this technique, it is necessary to rinse the sample with organic solvents (e.g., n-hexane) after extraction to reduce the interference of oil in the identification

analysis [84–87]. Furthermore, aeration and freezing have been used as adjuncts to the density separation process [84,88,89]. However, it is difficult to avoid disturbances in the settled solid phase during filtration when using beakers and clogging when using separation funnels. In addition, laboratory glassware can pose a challenge, as some MPs adhere to glass walls, and in the case of solid samples, more than one filter can be generated per sample [90,91]. To mitigate sample loss caused by repeated filtering or sieving, some authors have developed custom-made labware and devices utilizing density separation/flotation or sieving techniques. These include a small stainless-steel sieve that fits into a 200 mL glass beaker [90], a PTFE cylinder equipped with removable caps and a piston [84], a spiral conveyor operated within a glass separation funnel [92], the Munich Plastic Sediment Separator (MPSS) [93], the Sediment-microplastic Isolation (SMI) [94], and the JAMSTEC Microplastic-sediment Separator (JAMSS) [91]. In 2012, a team of researchers developed the MPSS, a stainless-steel device standing about 1.75 m tall, that uses zinc chloride as a flotation medium. The study reported recovery rates of 100% for larger MPs (1–5 mm) and 95.5% for MPs smaller than 1 mm in spiked and organic matter-free sediments. Zobkov and Esiukova later re-evaluated the extraction efficiencies of MPSS using unprepared sediment samples collected from the Baltic Sea, obtaining results between 13 and 39% [93]. SMI, a portable plastic device, is based on the MPSS's design and is compatible with both coarse and fine beach sediments. It can extract MPs with an average recovery rate of 95.8% in a single step [94]. JAMSS consists of two modified glass plates, with the upper plate attached to an open glass tube and the lower plate attached to a cylindrical glass container [91]. Devices with different sample-processing capabilities can be assembled by modifying the volume of the tube/container. JAMSS is used in combination with a sodium iodine solution and prevents the resuspension of decanted sediments into the supernatant, with recovery rates ranging from 94 to 98% in a single-step extraction [91].

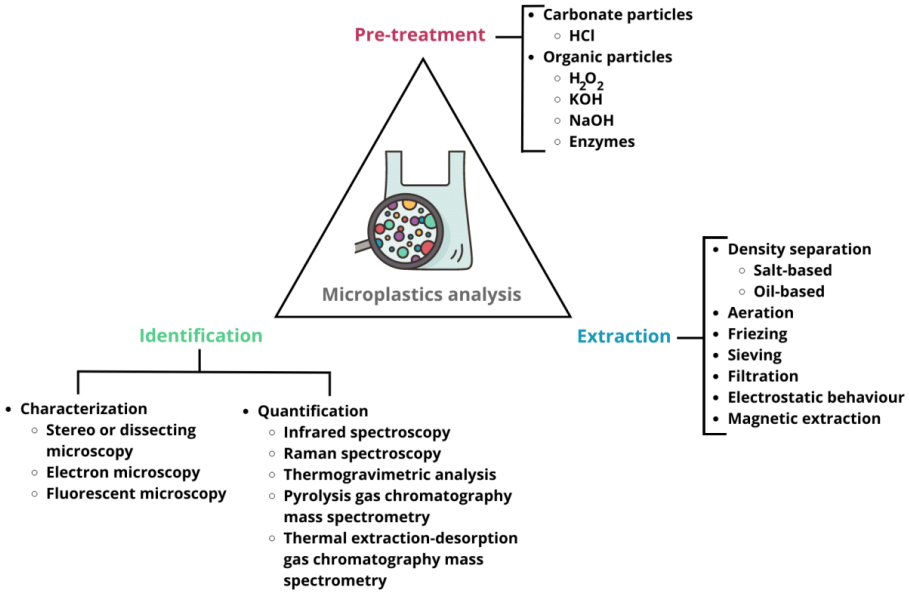


Figure 3. The main steps involved in analysing microplastics in environmental samples: pretreatment, extraction, and identification.

Magnetic and electrostatic techniques have been tested as alternatives to density-based methods for extracting MPs from environmental samples. The aim is to reduce sample loss, avoid toxic salts, improve high-density polymer extraction, and accelerate the experimental

procedure [95–98]. One such technique is magnetic seeded filtration (MSF), which uses seed particles to agglomerate with micro- and nanoscale particles, thereby enabling magnetic separation [95]. Using MSF, Rhein et al. achieved a 95% separation efficiency of MPs from dilute suspensions across a wide range of pH values [95]. Both magnetic and nonmagnetic fractions can be retrieved by the chemical breakup of agglomerates [99]. Moreover, using hydrophobic seed particles, the MSF approach is a promising purification step that may aid in quantifying MP extracted from complex matrices, such as sewage sludge [100]. Hydrophobic iron nanoparticles were tested by Grbic et al. in seawater spiked with PE, PS, PET, PUR, PVC, and PP MPs with recovery rates higher than 90% [96]. The authors applied this technique to extract MPs from freshwater and sediments and recovered 84% and 78% of the MPs, respectively. The adsorption efficiency of modified iron nanoparticles depends on the hydrophobicity and crystallinity of MPs [101]. Furthermore, the presence of organic and inorganic particles in the media hinders the ability of the iron nanoparticles to contact the MPs, which may account for the decreased extraction efficiency observed in sediments [96,98]. Additionally, the extraction process results in the fragmentation of brittle MPs. Moreover, Ramage et al. employed hydrophobized iron nanoparticles along with the high-gradient magnetic separation (HGMS) technique for the extraction of MPs from four soil types, namely, loam, high-carbon loamy sand, sandy loam, and high-clay sandy loam [98]. By utilizing an electromagnetic field and magnetically susceptible wires, HGMS systems can produce steep gradients that result in a net force on the particles, causing their separation via competition between magnetic and gravity settling forces. Magnetic recovery is determined by the ability of the modified iron nanoparticles to bind to the MP surface and particle size, which implies that the polymer type has no impact on it. To implement this method in soils, it is necessary to first extract paramagnetic minerals naturally present in the sample matrix to prevent wire blockage; however, MPs aggregated into clay can also be removed. This technique enables the processing of each sample within 30 min, which marks a significant reduction from the 2–3 days required by the density separation method. The recovery rate obtained (>88%) is dependent on several factors, including MPs' size, soil mineralogy, and carbon content [98]. Regarding electrostatic separation, its application has been limited to beach sand and river sediments [102–104]. This technology is used for metal/plastic waste separation and mineral refinement, and it utilizes a dry separation process to segregate metal particles with a diameter <8 mm from nonconductive materials such as commonly used plastics [102,103]. A scaled-down version of the Korona–Walzen–Scheider electrostatic metal separator system, which is widely used in the recycling industry, has been used to gain insights into the potential application of an electrostatic separation of MPs with diverse characteristics, including density, size, shape, and age [102–104]. Although its application has been limited to sediment testing, it was observed that the recovery of the method was highly dependent on the size of MP particles and sample composition and complexity, namely mineral and organic matter contents [103]. Thus, all the aforementioned procedures can be less efficient and/or more laborious for soil or sludge samples [73].

MPs' identification typically involves two types of analytical techniques: particle-based methods such as microscopy, Fourier transform infrared (FT-IR), or Raman spectroscopy, and mass-based determination methods, such as thermal desorption gas chromatography coupled with mass spectrometry (TED-GC-MS) [104]. Despite the need for further research, there is an increasing concern among politicians and scientists regarding the lack of reliable and comparable data on environmental MP pollution. A survey of existing papers on the study of MPs using FT-IR spectroscopy revealed a lack of information about the experimental setup, which is crucial for scientific reproducibility, indicating poor quality criteria and a lack of control samples and validation in analyses [105]. Moreover, there are currently no established units for reporting MP concentrations. Table 1 displays varying units of MPs concentration reported in studies, such as particles per liter [78], particles per kilogram [69], particles per 50 g dry weight [83], particles per gram [70,73], particles per 50 kg dry weight [58], particles per cubic meter [56], particles per square kilometer [3], and

newtons per liter [30]. If studies do not provide the information needed to compute the unit conversion, it becomes difficult to compare the results and draw conclusions [2,22].

Certain studies solely relied on optical microscopy techniques (dissecting microscopes or stereomicroscopes) to quantify MPs in various environmental samples such as agricultural soil, beach sand, or amended agricultural soil [28,70,83]. No other methods were used to validate the results or identify the types of polymers detected. Naked eye detection can only identify visible particles, but with the use of optical microscopes, particles larger than 0.42 µm can potentially be detected [2,22]. However, visual selection has limitations in terms of accuracy and precision, as it can be difficult to distinguish MPs from other materials, leading to the overestimation of microparticle numbers [22,39,81]. To overcome this, other analytical techniques based on molecular "fingerprint" for identifying polymers, such as FT-IR (including micro-FT-IR or attenuated total reflectance (ATR)-FT-IR) or Raman spectroscopy, have commonly been used, with FT-IR being particularly prevalent. FT-IR enables the detection of MPs as small as <20 µm, whereas Raman spectroscopy can identify MPs as small as <1 µm [2,22]. However, it is worth noting that the irregular surfaces of some polymer particles may interfere with the identification using FT-IR spectroscopy, and the presence of additives such as pigments or plasticizers may interfere with the identification using Raman spectroscopy [106]. Additionally, a sample analysis may require a significant amount of time, ranging from several hours to several days [105]. Mass-based methods facilitate expeditious data acquisition on the types and quantities of polymers in environmental samples. Moreover, these methods entail reduced contamination risks compared with particle-based methods, as they are less susceptible to atmospheric exposure [104]. However, these methods are destructive, which means that information on particle count, size, and shape characteristics cannot be obtained. Examples of mass-determining methods include thermogravimetric analysis (TGA), TED-GC-MS, and pyrolysis in combination with gas chromatography and mass spectrometry (Py-GC-MS) [76,86,107–111]. The application of headspace solid-phase microextraction coupled with gas chromatography and mass spectrometry (HS-SPME-GC-MS) and liquid chromatography with UV detection (LC-UV) had also been explored [87,109,110] Chromatographic techniques enable the determination of monomers as well as plastic additives or chemicals that have been sorbed onto the surface of MPs, such as pesticides or pharmaceuticals. Other relevant techniques, such as Nile red staining combined with fluorescent microscopy, scanning electron microscopy (SEM) (including field emission (FE)-SEM and SEM–energy dispersive X-ray spectroscopy (EDX)), X-ray photoelectron spectroscopy (XPS), differential scanning calorimetry (DSC), and nuclear magnetic resonance (NMR) spectroscopy have been used to obtain information on size, morphology, behavior, and type of MPs [69,78,103,104,111–113].

In summary, the importance of harmonizing standardized analytical methods has been highlighted in numerous studies [104,112]. Additionally, the absence of standardized practices hinders accurate occurrence calculations and makes cross-study comparisons challenging. By understanding the sources of background contamination, researchers can better select appropriate reporting methods and implement additional measures to minimize their impact. Adopting standardized QA/QC procedures is crucial to ensure the accuracy and reliability of MP data, enabling meaningful comparisons between different research studies [80]. Although there may be limited knowledge on the subject, the dedication of the scientific community to the development of reliable analytical methods is evident from the increasing number of recent studies and proposed optimizations. Obviously, all methods have strengths and weaknesses, and their usage should be tailored to align with the research objectives of each study, as they can be complementary or coupled [104,112]. For instance, when using Nile red staining methods, nonplastic hydrophobic particles can be dyed, requiring confirmation via spectroscopic techniques to avoid any overestimation of MPs. Another example is Raman microscopy, which enables the determination of the polymer type, as well as the observation of the morphology, size, and color.

Table 1. Summary of MPs' concentrations in the environment covering a range of compartments. The selected studies had methodological details. (dw: dry weight; WTP: water treatment plant; KWS: Korona–Walzen–Scheider; Py-GC-MS: pyrolysis gas chromatography–mass spectrometry; DSC: differential scanning calorimetry; FT-IR: Fourier transform infrared spectroscopy; μ-FT-IR: micro-FTIR; ATR-FT-IR: attenuated total reflection FTIR; FE-SEM: field-emission scanning electron microscopy; SM-EDX: SEM energy electron microscopy; X-ray CT: X-ray computed tomography; HS-SPME-GC-MS: headspace solid-phase microextraction coupled with gas chromatography and mass spectrometry; LC-UV: liquid chromatography with UV detection; TED-GC-MS: thermal desorption gas chromatography–mass spectrometry; TGA-MS: thermogravimetry–mass spectrometry;. EGA-MS: evolved gas analysis–mass spectrometry).

Sample Type	Location	Study Findings	Pretreatment	Extraction and Identification Techniques	Ref.
Beach sand	The Netherlands	Intertidal zone: 29.10 ± 17.75 MPs per 50 g dw High tidal line: 25.20 ± 12.37 MPS per 50 g dw Supralittoral zone (30 m from the dunes): 21.30 ± 3.62 MPs per 50 g dw Supralittoral zone (10 m from the dunes): 25.90 ± 10.91 MPS per 50 g dw	Samples were dried (48 h, 75 °C), and stored at room temperature for extraction.	Samples were floated in NaCl solution (358.9 g L^{-1}). After mixing for 2 min at 600 rpm, the mixture settled for 6 h, then the supernatant was filtered. MPs were counted on filter papers using a stereomicroscope. NaCl flotation was used.	[83]
Quartz sand Freshwater sediment Beach sand	Germany	99% of the original sample mass was removed without loss of MPs. 150 g quartz sand reduced to 2.34 ± 0.17 g. 150 g freshwater sediment reduced to 2.33 ± 0.13 g. 150 g beach sand reduced to 2.00 ± 0.04 g. 150 g particulate matter reduced to 2.51 ± 0.23 g.	Sample was sieved through 20, 63, 200, 630, and 2000 mm sieves. 20 g of freeze-dried material, 100 mL of bidistilled water, and agate balls were added to each sieve, that was sonicated for 1 min, and sieved manually. The procedure was repeated 10 times and the remaining fractions were centrifuged and dried at 105 °C.	150 g of sample material was spiked with 10 particles of each type of MP. Separation using the KWS electrostatic method, and each fraction was separated 3 times. Samples were digested, subjected to density separation, and characterized by Py-GC-MS.	[102]
Sand River sediment		Mass of sand was reduced by 98% after electrostatic separation. Mass reduction of sediment samples reduced by 70–78% after electrostatic separation, and above 99% after density separation. Recovery of MPs was polymer-specific: PCL: 50 ± 8%–74 ± 9%; LD-PE: 93 ± 9%–114 ± 9%; and PET 82 ± 11%–120 ± 18%.	Samples dried at 60 °C. Particles with diameters >2 mm were removed by sieving. Samples spiked with PCL, LD-PE, and PET (63–200 μm).	Electrostatic separation combined with density separation, identification, and quantification by DSC.	[104]

Table 1. *Cont.*

Sample Type	Location	Study Findings	Pretreatment	Extraction and Identification Techniques	Ref.
Estuarine sediments	Japan	Fenton's reagent affected the size of PE and PET. Recovery rates for density separation using an overflow column with top inflow (OC-T): 90.7% (±7.7% SD) for large MPs (>0.5 mm) and 95.0% (±12.5% SD) for small MPs (<0.5–0.160 mm). 91.7% of stained particles were confirmed as MPs.	2 protocols were tested for organic matter removal: (1) 20 mL of a 30% H_2O_2 added to 60 mL of sample; (2) 20 mL of a 0.05 M Fe(II) solution (2.5 g of $FeSO_4.7H_2O$, 165 mL water and 1 mL of concentrated H_2SO_4) added to 60 mL of sample. Samples were left to react for 24 h at room temperature and then freeze-dried at 80 °C under vacuum.	Density separation was tested using 4 columns, filled with $ZnCl_2$ solution (1.5 g cm^{-3}): an SMI unit; a simple decanting column; an OC-T; and an overflow column with mid-level inflow (OC-M). MPs were concentrated on vacuum glass fiber filters and drops of a Nile red solution (1 mg Nile red dye in 1 mL 99.5% acetone, diluted with 100 mL distilled water) were spread. Stained filters were inspected with a binocular microscope. Automated epifluorescence microscopic image analysis of Nile red-stained filters with FT-IR validation for polymer identification.	[111]
Beach sediments		Foamed polystyrene (FPS) (0.3 to <5 mm): 80–17,500 particles m^{-2}; 5–1206 pieces kg^{-1} dw PE and PP (0.3 to <5 mm): 0–1640 pieces m^{-2}; 0–200 particles kg^{-1} dw	-	Samples floated in saline solution (200 mL:100 mL sediment) for 30 s, settled for 2 min, and then sieved through a 355 µm mesh. The residue was rinsed, vacuum-filtered, and MPs were collected via visual sorting and stereomicroscopy. Identification was done with FT-IR, and structural analysis utilized digital microscopy, FE-SEM, and X-ray CT.	[69]
Bottom sediments		FPS (0.3 to <5 mm): 552–9128 particles m^{-2}; 13–221 particles kg^{-1} dw PE and PP (0.3 to <5 mm): 210–1210 particles m^{-2}; 5–29 particles kg^{-1} dw	Samples sieved through 5.6 mm and 355 µm mesh.		
Bay surface water		FPS (0.3–<5 mm): 0.004–0.06 particles m^{-2} PE and PP (0.3–<5 mm): 0.03–0.17 particles m^{-2}		The residues on the 355 µm mesh were rinsed with distilled water and vacuum-filtered. MPs were collected from samples by visual sorting and stereomicroscopy. Identification was performed using FT-IR and the structure was analyzed by digital microscopy, FE-SEM, and X-ray CT.	
Snow	Arctic and Alps	MPs: 0.02×10^3–154×10^3 N L^{-1} (80% ≤ 25 µm; 98% < 100 µm) Microfibers: 0.043×10^3–10.2×10^3 N L^{-1} (maximum length: 97% < 5 mm; 31% < 500 µm) European fibers were significantly longer than those from Arctic snow.	-	Samples were filtered using aluminum oxide (Al_2O_3) filters and dried in a desiccator for 2 days. Particles retained on filters were analyzed by FT-IR imaging.	[30]
Aqueous solution		Linearity (R^2) > 0.994 Precision: 99.4–99.9%. Limit of detection (LOD): 19–21 µg mL^{-1} Limit of the quantification (LOQ): 74–85 mg mL^{-1}	MPs (PE granules < 300 µm, PET fibers 500 µm, and PS beads 0.5–1 mm) dissolved in a deuterated solvent at 50 °C	Samples were analyzed by NMR spectroscopy.	[113]
Freshwater (inlet WTP)	Czech Republic	1473 ± 34–3605 ± 497 particles L^{-1} Common sizes: 1–10 µm Common types: fibers, spherical, and fragments Common polymers: PET and PP	Oxidize each sample with 20 mL of 0.05 M Fe (II) and 20 mL of 30% H_2O_2, and stir for 30 min at 75 °C in 250 mL of sample. Allow samples to digest for 24 h.	Samples vacuum-filtered in two-step descending-mesh-size, dry PTFE filters (30 °C, 30 min). Particles retained on filters were analyzed by SEM; particles > 10 µm were analyzed by FT-IR; particles 1–10 µm were analyzed by µ-Raman spectroscopy. Elemental analysis was performed on selected particles using SEM-EDX.	[78]
Drinking water (outlet WTP)		338 ± 76–628 ± 28 particles L^{-1} Common sizes: 1–10 µm Common types: fibers, spherical, and fragments Common polymers: PET PP and polyacrylamide			

Table 1. *Cont.*

Sample Type	Location	Study Findings	Pretreatment	Extraction and Identification Techniques	Ref.
Wastewater (effluent)	Germany	MP > 500 µm: 0×10^1–4×10^1 particles m^{-3} MP < 500 µm: 8×10^1–9×10^3 particles m^{-3} Common polymers: PE (59%) and PP (16%)	Samples were incubated at 70 °C for 24 h, then treated with enzymes (protease at 50 °C for 48 h, lipase at 40 °C for 96 h, and cellulase at 50 °C for 6 days). Finally, each sample was filtered through a 500 µm PA net.	<500 µm fractions were filtered with 10 µm stainless-steel screens, and then treated with H_2O_2 (35%) at 37 °C for 48 h, followed by incubation at 50 °C for 24 h. MPs were identified using ATR-FT-IR and µ-FT-IR spectroscopy techniques.	[56]
Sewage sludge		MP > 500 µm: not detected MP < 500 µm: 1×10^3–2.4×10^4 particles kg^{-1} dw	125 g of each sample was diluted in 825 deionized water and then mixed with 400 g solid NaOH (24 h at 60 °C). Samples were neutralized with HCl.	Flotation with NaCl (1.14 g cm^{-3}). After 96 h, supernatants were rinsed over a 500 µm PA net. Residues were visually inspected using an optical microscope and identification was carried out using ATR-FT-IR. Aliquots of fraction <500 µm filtered using 0.2 µm Al_2O_3 filters and analyzed by µ-FT-IR.	
Lake water	Canada	53,000–748,000 particles km^{-2} Common types: fibers (90%), films, and foam	Samples were filtered through a 250 µm mesh sieve and rinsed with deionized water. Each 250 mL sample was oxidized with 20 mL of Fe (II) (0.05 M) and 20 mL of 30% H_2O_2 while stirring for 30 min at 75 °C. Samples digested for 24 h.	Each sample was filtered through a 250 µm sieve. MPs were visually identified using a dissecting microscope and SEM-EDX.	[3]
Lake water	Finland	Total MP: 0.3 ± 0.1 particles L^{-1} Microfibers: 0.2 ± 0.1 particles L^{-1}	Samples were sieved and dried (40 h, 75 °C). Dried samples were oxidized with 20 mL of Fe (II) (0.05 M) and 60 mL of H_2O_2 (30%). Samples settled for 5 min, then were shaken and heated up to 75 °C.	Samples were vacuum-filtrated, and the glass filters were left to dry for 24 h at room temperature. Identification was performed by optical microscopy, FT-IR, and Raman spectroscopy.	[73]
Wastewater (influent)		Total MP: 56.7 ± 12.4 particles L^{-1} Microfibers: 52.6 ± 11.3 particles L^{-1}	Samples were sieved and dried (40 h, 75 °C). Dried samples were oxidized with 20 mL of Fe (II) (0.05 M) and 20 mL of H_2O_2 (30%). Samples settled for 5 min, then were agitated and heated up to 75 °C.		
Sewage sludge		Activated sludge: 23 ± 4.2 particles g^{-1} dw microfibers: 21.7 ± 4.6 particles g^{-1} Digested sludge: 170.9 ± 28.7 particles g^{-1} dw microfibers: 161.0 ± 25.5 particles g^{-1}	Samples were stirred and subsamples (0.1 g dw) were dried at 45 °C for1 8 h.	Identification was performed by optical microscopy, FT-IR and Raman spectroscopy.	
Wastewater (influent)	Spain	Primary effluent (451 ± 106 particles L^{-1}) Fragment length: 53–2100 µm Fiber length: 104–4000 µm Secondary effluent (26 ± 14 particles L^{-1}) Fragment length: 41–2890 µm Fiber length: 144–1824 µm	Filtration through 3 stainless steel meshes (375, 104 and 25 µm). Filters were exposed to H_2O_2 (33%) at 50 °C. After 20–24 h, the filters were rinsed with deionized water.	NaCl flotation was conducted, and samples were stirred for 24 h followed by settling for 24 h. Both supernatant and sediment were then filtered. Identification was performed using stereomicroscopy and µ-FT-IR.	[8]
Sewage sludge		Wet sludge (314 ± 145 particles L^{-1}) fragment length: 36–377 µm fibers length: 213–4716 µm Dry sludge (302 ± 83 particles L^{-1}) fragment length: 29–533 µm fibers length: 71–2224 µm	30 mL of H_2O_2 (33%) was added to 1 g of sludge (at 50 °C).		

Table 1. *Cont.*

Sample Type	Location	Study Findings	Pretreatment	Extraction and Identification Techniques	Ref.
Sewage sludge	China	5553–13,460 particles kg^{-1} Common polymers: PET, PE, and polyacrylonitrile	Samples were dried, sieved, and predigested with 30% H_2O_2 at 70 °C.	Three flotation solutions (NaI, $ZnCl_2$, and NaCl) with respective densities of 1.8, 1.5, and 1.2 g cm^{-3} were compared. Four membrane types (quartz, glass fiber, PTFE, and nylon) were tested for vacuum filtration of the supernatant. MPs on the membranes were digested with 30% H_2O_2 and H_2SO_4 at 70 °C for identification using stereomicroscopy and µ-FT-IR.	[81]
Soil		420–1290 particles kg^{-1} Common polymers: PP, PE			
Alluvial soil	Slovenia	Recovery rate: Oil-based extraction: >97% for all vessels in alluvial soil; 80% for modified syringes in compost. Salt-based extraction: >93% and >98% for alluvial soil and compost, respectively The $ZnCl_2$ solution could be reused up to 20 times without losing the desired density, reducing cost and environmental impact. Protocol was chosen to extract PE, PP, PS, PVC, and PET at various concentrations (10, 25, and 50 MPs) with cumulative recoveries >93% for all spiked MPs.	-	Oil-based extraction: 30 mL of H_2O and 3 mL of olive oil were added to the sample. The vessel was capped and shaken. After 2 h of standing, the samples were frozen overnight at −18 °C. The frozen oil layer was removed, melted, and filtered through a GF/C filter (47 mm). The MPs were rinsed with n-hexane and H_2O. Salt-based extraction: $ZnCl_2$ solution (1.6 g cm^{-3}; pH 3) was filtered with GF/C filter. The sample was transferred to 50 mL centrifuge tube and a $ZnCl_2$ solution was added to the 50 mL mark. After shaking for 30 s, it was centrifuged at 9000 rpm for 15 min. The supernatant was filtered through a GF/C filter. For compost, an oxidation step was performed by submerging the filter in 60 mL of Fenton's reagent for 2 h under constant stirring. The oxidized sample was filtered through a GF/C filter. The optimal extraction method was tested on samples spiked with 10, 25, and 50 MPs. Identification of MPs via HS-SPME-GC-MS.	[87]
Biowaste compost			10 g of compost with MPs (10 and 20 MPs of LDPE or PET) was added to 60 mL of Fenton's reagent and left for 2 h under constant stirring. The sample was filtered through the GF/C filter, and the sample remaining on the filter was oxidized using 50 mL of NaOH (1M) under constant stirring overnight at 50 °C. The sample was filtered through a 100 µm stainless-steel mesh.		
Lagooning sludge	Morocco	Fresh sludge: $40.5 \pm 11.9 \times 10^3$ kg^{-1} (dw) Dewatered sludge: $36 \pm 9.7 \times 10^3$ kg^{-1} (dw). Sludge dewatering resulted in a loss of MPs <500 µm. The quantity of MPs in compost varied with the proportion of sewage sludge.	20 g of dry sample treated with Fenton's reagent (H_2O_2 30% (*v*/*v*) + $FeSO_4$ solution 20 mg mL^{-1}).	For Py-GC/MS analysis, 1 mg of the freeze-dried sample was used. For Nile red staining, 1 g of digested sample was mixed with 50 µL Nile red (1 mg mL^{-1}) and incubated on a shaker at 100 rpm for 60 min. MPs were separated using a $ZnCl_2$ solution (1.38 g cm^{-1}) and centrifuged. The supernatant was filtered through 0.45 µm cellulose nitrate filters with a graduated grid (100 µm). The filter paper was observed using a fluorescence microscope under blue light. Identification of suspected MPs using Raman spectroscopy	[112]
Soil Sediment Compost Sewage sludge Suspended particles of WWTP Indoor dust	Germany	Recoveries rates for PET: 94.5–107.1% Limit of determination 0.031 mg PET Limit of quantification 0.121 mg PET PET mass contents in environmental samples: <LOQ in agriculture soil up to 57,000 mg kg^{-1} in dust samples.		20 g of sample was mixed with 20 mL of 1-butanol and 1 g of potassium hydroxide pellets. The mixture was heated to 115 °C in an oil bath under constant stirring for 1 h. Then, 50 mL of ultrapure water was added, and the system was mixed for 1 h at 300 rpm. The extract was vacuum-filtrated using a glass-fiber filter. Next, 10 mL of the aqueous phase was diluted (1:10) with ultrapure water, and the pH was adjusted to 2.5, using HCl (10%). Determination of the monomers, terephthalic acid, using LC-UV. Mass content verification using TED-GC-MS.	[110]

Table 1. *Cont.*

Sample Type	Location	Study Findings	Pretreatment	Extraction and Identification Techniques	Ref.
Biosolids	Ireland	4196–15,385 particles kg^{-1} dw. Common polymers: HDPE, PE, PET, PP, and PA. Common types: fibers (75.8%), fragments, films, and spheres	Biosolids treated by composting or thermal drying (TD): samples were soaked in water for 1 week, then transferred to a water bath (30 °C) for 24 h and shacked for 12 h. The samples were sieved through a 250 µm mesh. Biosolids treated by lime stabilization (LS) and biosolids treated by anaerobic digestion (AD): samples were soaked in tap water and washed through 250, 212, 63, and 45 µm sieves.	TD and AD Extraction: each sample (40 g) was elutriated. The extracted mixture was filtered through a 250 µm mesh, rinsed with $ZnCl_2$ (1 M), and brought to a volume of 300 mL. The mixture was shaken (1 min) and settled (20 min). The settled material was drained, and the remaining sample was filtered (glass-fiber filter).LS Extraction: 10 g from each sample was filtered. Identification: Stereomicroscopy, ATR-FT-IR, and SEM.	[57]
Compost	Finland	Mean recovery rate: 90.5% for PE, PU, polycarbonate (PC), PET, PVC, and PS; 30% for tire wear particles (TWP). Sewage sludge compost: 2 acrylonitrile (butadiene styrene) (ABS) fragments, and 1 PE fiber. Biowaste compost: 1 PE fragment, 1 PET fiber, 1 ABS fragment and 1 blend ABS/PET fiber.	10 mL H_2O_2 (30%), 1 mL of $FeSO_4.7H_2O$ (2 mmol L^{-1}), 1 mL of protocatechuic acid (2 mmol L^{-1}), and 5 mL of H_2O were added to 1 g of soil. Samples were kept in the hood for 1 h and then in the oven (40 °C) overnight.	Oxidized samples were transferred to custom-made PTFE tubes with 3 mL of olive oil, left to stand for 2 h, and frozen at −40 °C. Samples were filtered using glass microfiber filters. Filters were rinsed with water and n-hexane, air dried, and the MPs were collected with tweezers for identification with ATR-FT-IR. Each sample was extracted three times.	[84]
Agriculture soil		Mean recovery rate: 96.5% for PE, PU, PC, PET, PVC, and PS; 43% for TWP. 1 ABS fiber and PS fragment detected in soil from Mäkelä.			
Amended agricultural soil	Chile	18–41 particles g^{-1} Common types: microfibers	Samples were milled (porcelain mortar), sieved (<1 mm), and dried.	5 g of each sample was mixed with 20 mL of deionized water, centrifuged, and filtered with filter paper. 20 mL of NaCl was added to the sample, which was centrifuged and filtered with filter paper. 20 mL of $ZnCl_2$ was added, centrifuged, and filtered with filter paper. MPs identified by stereomicroscopy.	[70]
Agricultural soil	Chai river valley, China	0–5 cm layer: Fibers: 11,130–24,850 particles kg^{-1} Strings: 10–60 particles kg^{-1} Films: 460–1110 particles kg^{-1} fragments: 230–1360 particles kg^{-1} 5–10 cm layer: Fibers: 9780–26,940 particles kg^{-1} Strings: 40–70 particles kg^{-1} Films: 410–1290 particles kg^{-1} Fragments: 170–15,700 particles kg^{-1}	10 mL of H_2O_2 (35%) was added incrementally to 30.0 g of soil sample. $FeSO_4$ (10%, 1 mL) was added, and sample was heated on sand bath (50 °C). After organic matter destruction, $FeSO_4$ (10%, 1 mL) and NaOH (0.5 M, 30 mL) were added. Volumes were adjusted to 150 mL with distilled water, sonicated, and centrifuged.	Supernatant was collected and 150 mL of a saturated NaI solution (1.8 g cm^{-3}) was added to the soil, followed by centrifugation. The procedure was repeated. The collected supernatant was filtered (1, 0.25, and 0.05 mm mesh). H_2O_2 (2 mL) was added for the digestion of labile organic. Solids were washed with distilled water, transferred to clean glass containers and oven-dried at 80 °C. MPs were optically sorted by a dissecting microscope.	[28]

Table 1. *Cont.*

Sample Type	Location	Study Findings	Pretreatment	Extraction and Identification Techniques	Ref.
Agricultural soil	Middle Franconia, Germany	0–1.25 particles kg^{-1} dw 16 particles per 50 kg dw (5–1 mm): PE (62.50%, 10 particles) PP (25.00%, 4 particles)	Soil aggregates dissolved by adding 20 mL of H_2O_2 to 500 mL of sample. Size fractioning using sieves with mesh size of 5 and 1 mm. The procedure was repeated until all aggregates were dissolved.	MPs optically sorted under a magnifying lamp and by stereomicroscopy. Identification and quantification carried out by ATR-FT-IR.	[58]
Soil	United Kingdom	Average recoveries using high-gradient magnetic separation (HGMS) system: 96% for fibers and 92% for MPs in loam; 91% for fibers and 87% for MPs in high-carbon loamy sand; 96% for fibers and 89% for MPs in sandy loam; 97% for fibers; and 94% for MPs in high-clay sandy loam. Agricultural soil: HGMS extracted an average of 14 ± 4 fibers and 3 ± 1 MPs per 8 g sample extracted using HGMS; 8 ± 3 fibers and 1 ± 1 MPs per 8 g sample extracted by density separation.	20 mL of ethanol was added to 4 g of soil spiked with 30 MPs (<1% (w/w)) which were prepared in the laboratory. Magnetic soil particle removal for each soil sample using HGMS system. MPs magnetized with modified iron nanoparticles.	HGMS: the sample was introduced in the system and the retained fraction containing MPs was filtered onto 1.2 µm Whatman GF/C glass-microfiber membrane filters. Density separation: 50 mL of a saturated zinc bromide solution (density ≈ 2.4 g mL^{-3}) was added to the soil. The sample was shaken at 300 rpm for 5 min and settled overnight. The recovered material was treated with 10 mL 30% H_2O_2 for 1 h at 60 °C and filtered. The MPs were counted directly on the filter using a stereo microscope. ATR-FT-IR was used to confirm the compositions of the MPs.	[98]
Loamy sand (standard)	Germany	LOD: 0.07 wt % PET; LOQ: 1.72 wt % PET. MS signal intensities linearly responding to MPs concentrations.	Samples (with 1.61 ± 0.15 wt % organic matter) spiked with 0.23–4.59 wt % PET recycled MPs.	Calibration series was prepared with a standard loamy sand with 1.61 ± 0.15% organic content. DL-cysteine was used as the internal standard. PET quantified by TGA-MS.	[114]
Soil (standard)		Validation parameters for plastic contents of 250 µg g^{-1}: $R^2 > 0.996$, LOD: 1–86 ng Precision: 3.2–7.2% Recoveries: 70–128% The addition of nontarget polymers (PET, PVC and TWP) did not interfere with the quantification of the analytes.	Each reference soil (4 g) was spiked with 0.2 and 1.0 mg of PE, PP, and PS. Three clean-up protocols were tested: (1) adding 8 mL of methanol to the sample and agitating it for 60 min at 150 rpm, followed by centrifugation and evaporation of the supernatant; (2) performing Fenton digestion by adding 10 mL of $FeSO_4.7H_2O$ solution (20 g L^{-1}, pH 2) and 10 mL of H_2O_2 (30%) to the spiked soil, followed by 60 min in an ice bath and heating to 60 °C; (3) adding 4 mL of $KAl(SO_4)_2.12H_2O$ solution (500 mgL^{-1}) to the soil, shaking for 60 min at 150 rpm and evaporation. Nonspiked soil and soil spiked with 0.2 mg of nontargeted plastics were also included for testing	Polymers extracted using 1,2,4-trichlorobenzene (TCB) and liquid sample aliquots analyzed by Py-GC-MS.	[115]
Road Dust	Korea	Tire and road-wear microparticles (TRWMPs): 6,400–39,738 µg/g. Average concentration of TRWMPs in the industrial area of 22,581 µg/g and in the residential area of 9054 µg/g.	Moisture content was removed at 120 °C.	TGA to compare the thermal profile of road dust and tire tread particles; EGA-MS analysis to compare the organic composition of road dust and tire tread powder; identification and quantification of TRWMPs using Py-GC-MS.	[77]

5. (Eco)Toxicological Effects of Microplastics

Considering the presence of MPs in the environment (Table 1), it is very likely that terrestrial and aquatic organisms can find and interact with MP particles present in their ecosystems [2]. Studies have suggested that MPs can be ingested by fish [10–17], crustaceans [38,116,117], nematodes [16], arthropods [118], and annelids [25,119,120], or can be absorbed by plants such as *Lolium perenne* [25], *Allium fistulosum* [121], and *Lepidium sativum* [122] (Table 2). The great challenge in assessing the toxicological effects of MPs derives from the fact that MPs are not homogeneous but rather a mixture of particles of different shapes, sizes, and compositions, which can act as vehicles for the transfer of additives and other chemical contaminants [116,123]. Most additives are attached to the polymer matrix via weak van der Waals forces, which means that they can leach from the matrix and become available for uptake (ingestion/sorption) [24,38,124]. PS microspheres are often used as model particles in toxicological tests because PS is one of the most produced polymers and is commonly found in the environment [116]. However, other polymers that contain many additives, such as PVC, are also abundant in the environment and need to be considered [1,18].

The ingestion of MPs is closely related to the size and shape of the particle, type of polymer, concentration, and physiological and behavioral characteristics of the organism itself (Figure 4) [15,16,38,119,120]. It is more likely that, in the environment, organisms are more exposed to irregularly shaped secondary MPs, which could potentially cause more injury and stronger gut inflammation than would spherical shapes [10,11,13,38]. Additionally, depending on their size, MPs and/or their chemical additives can pass through the intestinal wall and reach other body tissues, which may result in trophic transfers into and up the food chain [2,12,116]. The accumulation of MPs in the gills, gut, and liver may cause obstruction, physical damage, histological changes in the intestines, changes in lipid metabolism, liver metastasis, behavioral changes, growth and developmental inhibition, endocrine disruption, energy disturbance, oxidative stress, immune and neurotransmission dysfunction, and genotoxicity [10,11,13,15]. Even if plastic is excreted, there is evidence suggesting that retention time in the intestine is longer than that observed for food [2].

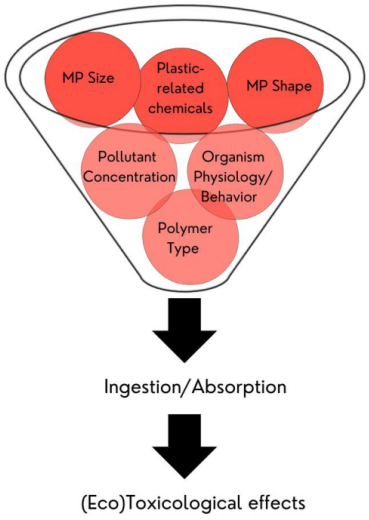


Figure 4. Factors that lead to the ingestion or absorption of microplastics causing potential ecotoxicological and toxicological impacts.

In a study from Choi et al., the effects of irregular and spherical PE microparticles on swimming behavior, gene expression, and *Cyprinodon variegatus* larvae were compared [10]. No mortality or malformations were observed in the larvae; however, there was a decrease in swimming activity that was more pronounced in the presence of irregular MPs. In addition, the MPs ingested by *C. variegatus* passed into the digestive system, causing a distension of the intestinal lumen. Exposure to both shapes of MPs slightly increased cellular reactive oxygen species (ROS), causing a differential regulation of genes related to oxidative stress (*Cat* and *Sod3*). *Sod3* gene expression was induced for both shapes at 50 mg L^{-1}, whereas *Cat* gene expression was induced at 250 mg L^{-1} of spherical MPs and at 50 mg L^{-1} of irregular MPs. Moreover, catalase (CAT) activity, an antioxidant-related enzyme, significantly increased after exposure to 50 mg L^{-1} of irregular MPs [10]. The influence of MPs' shape was also studied in *Carassius auratus* by Jabeen et al. [11]. The fish were exposed to ethylene vinyl acetate (EVA) fibers, PS fragments, and PA pellets via food amended with MPs for six weeks, and no mortality was observed. However, the organism showed a significant weight loss, and fibers were found in the gills, gastrointestinal tract, and feces. The fragments and pellets were chewed, and then expelled, and a histological examination revealed a breakage of the dermal layer with hemorrhages in the lower jaws. Moreover, although MPs did not accumulate in the organs of *C. auratus*, changes in liver tissue (passive hyperemia, dilated sinusoid, and hydrophilic vacuolization) were detected. They may be related to the stress induced by the chemical additives released during chewing and ingestion [11]. Similarly, Qiao et al. reported that the shapes of PS microparticles had a significant influence on their uptake by *Dania rerio* [13]. The study suggested that all shapes accumulated in the gut with the following order of magnitude: fibers (8.0 μg mg^{-1}) > fragments (1.7 μg mg^{-1}) > spheres (0.5 μg mg^{-1}), causing damage to the mucosa and an increased permeability, inflammation, and interruption of metabolism. Furthermore, fibers induced a higher activity of superoxide dismutase (SOD) (antioxidant-related enzyme), which may be due to the long residence time, higher accumulation, and larger physical damage in the gut [13].

It is not clear whether an irregular shape is the main condition that promotes the bioaccumulation of MPs. Since there is evidence that some organisms (such as *C. auratus*) select the food based on its morphology, the size of the MPs also seems to influence their accumulation in the organs [11,16]. A study involving *D. rerio* focused on the effects of small-sized MPs in the digestive system and found that exposure to PS microspheres (5 μm) resulted in a significant increase in CAT and SOD activity in the intestine [14]. A histological analysis revealed inflammation, bowel wall thinning, villi formation, and epithelial damage. Disturbances in the gut biota have also been identified: a decreased number of proteobacteria and an increased number of fusobacteria [14]. This microbiota dysbiosis could be associated with the development of metabolic disorders [13,14]. Moreover, in their study, Lei et al., exposed *Caenorhabditis elegans* nematodes to MPs of PS with different sizes (ranging from 0.1 to 5.0 μm) and to MPs of PA, PE, PP, and PVC, all of which were approximately 70 μm in size [16]. They found that PS particles measuring 1 μm were the most abundant in the digestive system, causing oxidative stress and pronounced alterations in intestinal calcium levels.

A study by Zimmermann et al. compared the effects of different types of MP (PVC, PUR, and polylactic acid (PLA)) and their additives on the mortality, reproduction, and body lengths of *Daphnia magna* [38]. All MP particles had irregular shapes and rough surfaces and were identified in the gastrointestinal tract of *D. magna*; however, only exposure to PLA increased mortality. The mean body length of adults was significantly lower when exposed to PVC, PUR, and PLA, whereas reproduction was affected and significantly reduced by exposure to PLA and PUR microparticles [38]. Regarding the contribution of plastic additives to MPs' toxicity, the study showed that chemical additives leached from PVC were the main driver for the toxicity induced in *D. magna*, reinforcing the idea that toxicological effects can be mediated by both particles and chemicals [38]. In addition, this study highlights that biopolymers (such as PLA) are not necessarily less toxic to organisms

than fossil-based polymers, a perspective that is also shared by Boots et al. in a study with perennial ryegrass (*L. perenne*) [25].

Given the importance of soil biota in maintaining the structure and function of soil ecosystems, it is essential to investigate the impact of MPs on these organisms [25,119,125]. Studies reporting the exposure and ecological effects of MPs in soil are emerging, as it is recognized as a primary source of MP pollution [25,122]. Earthworms, considered ecosystem engineers, are widely used in ecotoxicological tests due to their sensitivity to toxic substances [25,119]. In a study by Jiang et al., *Eisenia fetida* exposed to concentrations of 10–1000 μg kg^{-1} of PS fragments (100–1300 nm) presented damage to intestinal cells and changes in the activity of antioxidant enzymes glutathione (GSH) and SOD [119]. Moreover, the exposure to 1300 nm MPs at 1000 μg kg^{-1} resulted in the highest accumulation rate. The comet assay revealed that DNA damage in coelomocytes (phagocytic leukocytes) depends on the size and concentration of MPs, and *E. fetida* exposed to a concentration of 1000 μg kg^{-1} with a size of 1300 nm experienced the greatest damage to their DNA [119]. Another study found that exposure to PVC microparticles significantly inhibited the growth and reproduction of springtail *Folsomia candida* by 16.8 and 28.8%, respectively, while also altering the microbiota of the collembolan gut. Higher values of nitrogen and carbon isotopes (δ15N and δ13C) were observed in the tissues, and this alteration may be due to the response of growth rate and metabolic turnover [118]. Likewise, Selonen et al. observed that microsized tire particles (<180 μm) spiked in soil or food reduced reproduction and survival rates and a decrease in the acetylcholinesterase activity of soil invertebrate species (enchytraeid worm *Enchytraeus crypticus*, *F. candida*, and woodlouse *Porcellio scaber*) [65]. Moreover, tire-particle-related chemicals such as benzothiazole and zinc act as neuroinhibitory, affecting the neurological processes of *P. scaber* by reducing the acetylcholinesterase activity [65]. These observations indicate that even at low concentrations, MPs can be ingested by soil organisms and potentially affect their survival and metabolic processes, highlighting the potential for accumulation/magnification of MPs along the soil detrital food web [16,27]. These accumulated substances may also be transferred to predators such as insects, birds, and small mammals [126–128]. For instance, Kwon et al. found that oral exposure to PS-MPs can lead to their accumulation in the microglial cells of the mouse brain, causing morphological changes and potentially leading to cell death [125]. These findings are particularly significant because they suggest that PS-MPs can cross the blood–brain barrier in humans affecting the immune response in the central nervous system.

While studies on the impacts of MPs in soil systems have mainly focused on animals, the effects of MPs on plants have also been observed; however, the number of studies on this topic remains relatively limited [32,129]. MPs can have both direct and indirect harmful effects on plants. Indirect effects include alterations to soil structure, which can impact root growth, nutrient immobilization, shifts in soil microbial communities, and root symbionts, potentially leading to reduced fertility and contaminant transportation and leaching [32,66,129]. The direct effects of MPs on plants include the clogging of seed pores, reduction in germination rates, and accumulation in plant tissues [32,129]. It is important to note that different plants can be affected by MPs to differing degrees with different mechanisms and effects [32]. Moreover, terrestrial plants are temporary sinks of atmospheric MPs. In the top 11 green countries, there could be 0.13 trillion pieces of MPs attached to leaves. Though there is no direct evidence of impaired plant function at environmental concentrations, the long-term ecological effects of MPs should be investigated [130].

Pignattelli et al. investigated how acute (6 days) and chronic (21 days) exposure to four different types of MPs (PP, PE, PVC, and PE + PVC) affected the growth and biochemical responses of garden cress (*L. sativum*) [122]. The study found that acute exposure to PE had adverse effects on the germination rate, plant height, leaf number, and fresh biomass production. On the other hand, chronic exposure to PP and PE negatively impacted germination rate, leaf number, and biomass produced. Moreover, PVC was found to be the most toxic MP with the highest production of H_2O_2 and depletion of ascorbic acid

(AsA), suggesting that different MPs act in different ways [122]. In other study the impact of sewage sludge containing MPs on the growth, biomass production, and yield of tomato plants (*Lycopersicon esculentum* Mill.) was examined over a period of 109 days. Plants grown in soils mixed with sludge showed a more pronounced growth while fruit production was delayed and reduced [131]. These findings suggest that plants are vulnerable to the impacts of MPs, although more research is needed to fully understand whether the effects on terrestrial plants are due to the MPs themselves, their chemical-related contaminants, or both. What about the effects of NPs on terrestrial plants? Li et al. studied the effects of PS-NPs (100–700 nm) on *Cucumis sativus* growth using Hoagland nutrient solution [132]. The results showed that different sizes of PS-NPs had varying effects on plant metabolic pathways: 700 nm PS-NPs increased the levels of the oxidative stress markers in leaves, such as malondialdehyde (MDA), proline, and H_2O_2; and 100 nm PS-NPs decreased chlorophyll and soluble sugar contents in the leaves. Additionally, the study found that the degradation of PS-NPs into benzene rings in cucumber leaves may be the main factor affecting chlorophyll and sugar metabolism, suggesting harmful effects on plant growth and development. Nevertheless, further research in this field is necessary [132].

It is possible that MPs could contaminate human food and therefore enter the human diet. In fact, plastic fragments have been found in a range of food sources, including seafood, bottled water, salt, honey, edible fruits and vegetables, and even infant milk powder [127,133–138]. Additionally, airborne particles with sizes ranging from 1 nm and 20 µm can also be inhaled by humans [139,140]. Plastic fragments have been found on both the maternal and fetal sides of human placentas, suggesting that exposure to plastic debris may occur during fetal development [141]. Moreover, studies have shown that certain types of MPs, such as PS-MPs and PE-MPs, can cause alterations to the shape of lung cells, slowing down their metabolism [142], and causing genomic instabilities in human peripheral lymphocytes [143], respectively. These findings suggest that MPs that humans encounter via ingestion or inhalation can potentially enter the bloodstream, become bioavailable, and translocate to organs [140]. Therefore, it is critical to conduct further research to fully understand the fate and transport mechanisms of MPs in the environment, their ability to sorb and transfer organic and inorganic contaminants, and the potential long-term effects of exposure. This is essential for conducting effective risk assessments and developing strategies to mitigate the potential impact of MPs on human health.

Table 2. Illustrative toxicological effects observed in diverse organisms, including fishes, crustaceans, nematodes, arthropods, and annelids, and plants, caused by MPs of varying shapes, types, and sizes.

Species	Exposure Characteristics	Toxicological Effects/Findings	Ref.
Artemia salina	PS (spherical; 5 µm); 1–100 mg L^{-1}; 48 h and 14-day exposure tests	Deformation of epithelial cells in the midgut region after both acute exposures at 100 mg/L and chronic exposure at 1 mg L^{-1}	[117]
Carassius auratus	EVA (fiber; 0.7–5.0 mm), PS (fragments; 2.5–3.0 mm), PA (pellet; 4.9–5.0 mm); 6 weeks of exposure	Fibers detected in gills, gastrointestinal tract and feces; severe alterations in the livers of fish exposed to fibers; severe breakage of the dermal layer with hemorrhages in the lower jaws of fish exposed to fragments; hypertrophy of mucous cells in the lower jaw in fish exposed to pellet.	[11]
Cyprinodon variegatus	PE (spherical, 150–180 µm; irregular, 6–350 µm); 50 and 250 mg L^{-1}; 4-day exposure test	Intestinal distention provoked by the accumulation of MPs in the digestive system; decrease in swimming activities; oxidative stress induced by irregularly shaped MPs.	[10]

Table 2. *Cont.*

Species	Exposure Characteristics	Toxicological Effects/Findings	Ref.
Danio rerio	PS (fibers, fragments, beads); 50–500 μg L^{-1}; 21-day exposure test	Shape-dependent accumulation in the gut: fibers > fragments > beads; mucosal damage and increased permeability; inflammation and metabolism disruption; gut microbiota dysbiosis and bacteria alterations.	[13]
	PS (spherical; 5 μm); 50–500 μg L^{-1}; 21-day exposure test	Accumulation of MPs in the gut; inflammation and oxidative stress in the gut tissues; gut microbiome perturbations: *Proteobacteria* decreased and *Fusobacteria* increased.	[14]
	PS (spherical; 50–500 nm); 0.1–10 mg L^{-1}; 14-day exposure test	Tissue of the amputated plane was penetrable by MPs; inhibition of fin regeneration, both morphologically and functionally, of amputated larvae.	[15]
	PA, PE, PP, PVC (~70 μm); PS (0.1–5.0 μm); 0.001–10.0 mg L^{-1}; 10-day exposure test	PA, PE, PP, and PVC caused intestinal damage including cracking of villi and splitting of enterocytes.	[16]
	MPs: PS (700 nm)	Signs of accumulation of particles around the heart region and within the blood stream; systemic immune responses; lipid metabolism and toxicity pathway significantly enriched.	[17]
	Fertilized eggs exposed to MPs (2 mg/L, red fluorescent spherical polymer particles), copper (Cu), and Cu + MPs, 96 h exposure	MPs did not significantly impact the early life stages of zebrafish; increased mortality, inhibition hatching rate, oxidative stress, AChE inhibition, and behavioral changes in zebrafish in the presence of Cu; antagonistic response of MPs to Cu.	[144]
Dicentrachus labrax	Mixture of environmental MPs (35.29% PEVA; 5.88% HDPE; 17.65% PE; 11.76% LDPE; 23.53% PA; 5.88% PP); fragments and fibers (5–1 mm and 1 mm–300 μm)	Imbalance in the enzymatic defense mechanisms after a short-term exposure to MPs ranging from 1 mm to 300 μm.	[47]
Mytilus edulis	PLA (<250 μm); 10 μg/L and 100 μg L^{-1} 8-day exposure test	No significant signs of oxidative stress or neurotoxicity; slight increase in CAT and glutathione-S-Transferase (GST) biomarker activities was observed.	[145]
Sparus aurata L.	PVC (40–150 μm); 100 and 500 mg kg^{-1}; 30-day exposure test	Ingestion did not produce any significant alteration in humoral and cellular immunity; evidence of cellular and oxidative stress and damage in the liver and kidney.	[12]
Daphnia magna	PVC, PUR and PLA (<59 μm); 10–500 mg L^{-1}	PVC toxic to reproduction; PLA reduced survival.	[38]
	PS (6 μm); 5–300 mg L^{-1}; 120 h and 80-day exposure tests	EC_{50} of 34.3 (19.8–59.3) mg L^{-1} for juveniles and 52 (17.7–152.3) mg L^{-1}; growth rate of mother animals and the body size of newborn declined with increasing dose of MPs.	[116]
Caenorhabditis elegans	PA, PE, PP, PVC (~70 μm); PS (0.1–5.0 μm); 0.5–10.0 mg m^{-2}; 2-day exposure test	5.0 mg m^{-2} significantly inhibited survival rates, body length, and reproduction; oxidative stress and changes in intestinal calcium levels.	[16][l]
Coturnix japonica	Naturally aged PS (fragments); 9-day oral exposure tests; three experimental groups (0, 11, and 22 MPs per day)	Lower body mass; increased ROS levels in muscle and liver, and higher production of MDA in various organs; reduction in SOD activity in the liver and intestine; MPs' size and shape altered as they moved through the gastrointestinal tract.	[146]
Eisenia andrei	Tire particles (<600 μm) and PS (<500 μm, containing 1% hexabromocyclododecane (HBCD)); 28-day exposure test	No mortality, morphological, or avoidance behavior changes observed; AChE activity was not significantly affected after 14 and 28 days.	[147]
Eisenia fetida	PS (fragments, 100–1300 nm); 100–1000 μg kg^{-1}; 14-day exposure test	Intestinal cells were damaged; changes in GSH level and SOD activity; induction of damages in DNA.	[119]
Enchytraeus crypticus	PA and PVC (13–18 μm; 90–150 μm); 20–120 g kg^{-1}; 21-day exposure test	EC_{50} of 108 ± 8.5 g kg^{-1} for PA 13–18 μm size range; 25% reduction in reproduction for PA 90–50 μm.	[120]

Table 2. *Cont.*

Species	Exposure Characteristics	Toxicological Effects/Findings	Ref.
Folsomia Candida	PVC (80–250 µm); 1 g Kg^{-1} dw; 56-day exposure test	Alterations of microbial community of the gut; significant reduction in body weight and reproduction; carbon and nitrogen contents increased in tissues.	[118]
Aporrectodea rosea	PLA, HDPE and fibers	The biomass of *A. rosea* exposed to HDPE was significantly reduced.	[25]
Allium fistulosum	PE (fibers); PA (spherical); PE, PS, Polyester, and PET (fragments)	Changes in biomass, tissue elemental composition, root traits, and soil microbial activities.	[121]
Cucumis sativus L.	PS-NPs (100, 300, 500, and 700 nm); 10 mg mL^{-1}, 65-day exposure test	Decreased biomass induced by 300 nm PS-NPs; decreased chlorophyll content and soluble sugar induced by 300 nm PS-NPs; increase in the contents of MDA and proline in leaves induced by 700 nm PS-NPs.	[132]
Lepidium sativum	PP, PE, PVC, PE + PVC (0.125 mm); 184 ± 4 mg kg^{-1}	Effect on growth; induction of oxidative stress.	[122]
Lycopersicon esculentum Mill	One-month-old plants transplanted outdoors into 3.3 L terracotta pots with five different soil compositions: control, manure control, and soil + sewage sludge 109-days exposure test	Lower crop in plants grown under soil mixed with sewage sludge.	[131]
Lolium perenne	PLA, HDPE and fibers	Germination decreased with PE and fibers; reduction in shoot height with PLA; increase in chlorophyll a/chlorophyll b ratio suggesting a stronger inhibition of chlorophyll b synthesis in response to MPs.	[25]
Oryza sativa	PS and PTFE (~10 mm) combined with arsenic (As) III in Hoagland nutrient solution; 0.04 g L^{-1} MPs + 1.6 mg L^{-1} As(III); 0.1 g L^{-1} MPs + 3.2 mg L^{-1} As (III); and 0.2 g L^{-1} MPs + 4.0 mg L^{-1} As (III)	PS and PTFE hinder root growth and transpiration; As (III) damages chloroplast structure, reducing photosynthetic capacity and biomass, and impairing antioxidant enzyme structure, leading to membrane lipid peroxidation and membrane structure destruction; the presence of MPs restricts the uptake of As(III) in rice seedlings, reducing its content in tissues.	[148]
Triticum aestivum	LDPE, PET, PBT and starch-based biodegradable MP	Biodegradable MPs inhibited wheat growth and decreased the fruits and the shoot biomass.	[149]
Vicia faba	PS (5 µm and 100 nm); 10–100 mg L^{-1}; 48 h exposure test	Inhibition of growth; induction of oxidative damage; accumulation of 100 nm sized MPs in root.	[150]

6. What Does the Future Hold?

Plastic pollution has gained attention due to the accumulation of waste in natural ecosystems and the breakdown of plastics into MPs via physical, chemical, and biological drivers. Identifying the sources of MPs in the environment is challenging due to factors such as a high plastic production and consumption, leakage from waste streams, and polymer heterogeneity. The distribution and pathways of MPs in ecosystems remain unsuccessfully understood. Toxicological tests have revealed that MPs can be ingested by a variety of organisms, including, but not limited to, fish, crustaceans, nematodes, arthropods, and annelids. There is evidence that MPs accumulate in the gills, gut, and liver of these organisms, causing gut obstruction, behavioral changes, and physical and histological damage. Moreover, MPs can enter the food chain, with potential consequences for human and environmental health. The shape, size, and concentration, composition of MPs as well as the characteristics of the organism and the environment in which they are found may contribute to the observed morphological and toxicological effects.

Assessing the toxicity of MPs is challenging due to their heterogeneous nature and the fact that they can act as carriers for other chemicals that they absorb from the surrounding media. Future studies should focus on the effects of a realistic mixture of polymers, using environmentally relevant concentrations, to understand the extent effects of MPs. The field is claiming standardization may enable a direct comparison between studies and the use of environmentally relevant exposure concentrations in (eco)toxicological assays. However,

several key challenges must be overcome to achieve this goal. These challenges include the absence of reference materials for method validation, the use of nonstandardized analytical methods, and difficulties associated with complex matrices rich in organic matter.

The future of MP research involves further investigation into the long-term effects of MPs on the environment and human health. Additionally, there is a need for increased interdisciplinary collaboration between scientists, policymakers, and industry leaders to address the issue of MP pollution comprehensively. The world population is expected to increase in the coming decades, which will translate into increased environmental pressures, consumption of raw materials, and waste generated. It is naive to think that plastic pollution will be solved with the transition to bioplastics and biobased plastics, whose environmental impacts of production (e.g., use of land and water resources) are still under discussion. Additionally, biobased plastics can still generate waste and MPs, which are not proven to be less dangerous than oil-based MPs. Tackling plastic pollution requires a comprehensive and holistic approach that includes not only the production and disposal aspects but also focuses on consumption patterns concerning single-use plastics and explores potential methods to minimize waste generation.

Funding: Diana Rede thanks FCT/MCTES (Fundação para a Ciência e Tecnologia and Ministério da Ciência, Tecnologia e Ensino Superior) and ESF (European Social Fund) through NORTE 2020 (Programa Operacional Região Norte) for her PhD grant ref. SFRH/BD/147404/2019. Additionally, this work also received financial support through the BiodivRestore Joint Call 2020–2021, which is part of the European Union's Horizon 2020 research and innovation program, under grant agreement No. 101003777-BiodivRestore-406/DivRestore/0002/2020-BioReset, focusing on "Biodiversity restoration and conservation of inland water ecosystems for environmental and human well-being".

Institutional Review Board Statement: Not applicable.

Data Availability Statement: Not applicable.

Acknowledgments: This work has received support from national funds of Portugal, specifically from the FCT/ MCTES, through the following projects: UIDB/50006/2020, UIDP/50006/2020, and LA/P/0008/2020. The authors would also like to express their gratitude to the FCT for the support through project number 2022.15094.CBM (a bilateral cooperation between Portugal and France under the 2023–2024 person program), and project number 49190WH (PHC PESSOA 2023).

Conflicts of Interest: The authors declare no conflict of interest.

References

1. Danso, D.; Chow, J.; Streit, W.R. Plastics: Environmental and Biotechnological Perspectives on Microbial Degradation. *Appl. Environ. Microbiol.* **2019**, *85*, e01095-19. [CrossRef]
2. Horton, A.A.; Walton, A.; Spurgeon, D.J.; Lahive, E.; Svendsen, C. Microplastics in freshwater and terrestrial environments: Evaluating the current understanding to identify the knowledge gaps and future research priorities. *Sci. Total Environ.* **2017**, *586*, 127–141. [CrossRef] [PubMed]
3. Anderson, P.J.; Warrack, S.; Langen, V.; Challis, J.K.; Hanson, M.L.; Rennie, M.D. Microplastic contamination in Lake Winnipeg, Canada. *Environ. Pollut.* **2017**, *225*, 223–231. [CrossRef] [PubMed]
4. Qi, R.; Jones, D.L.; Li, Z.; Liu, Q.; Yan, C. Behavior of microplastics and plastic film residues in the soil environment: A critical review. *Sci. Total Environ.* **2019**, *703*, 134722. [CrossRef]
5. Li, Y.; Chang, Q.; Duan, H.; Liu, Y.; Zhang, J.; Li, J. Occurrence, levels and profiles of brominated flame retardants in daily-use consumer products on the Chinese market. *Environ. Sci. Process. Impacts* **2019**, *21*, 446–455. [CrossRef] [PubMed]
6. Kawecki, D.; Nowack, B. Polymer-Specific Modeling of the Environmental Emissions of Seven Commodity Plastics As Macro- and Microplastics. *Environ. Sci. Technol.* **2019**, *53*, 9664–9676. [CrossRef]
7. Gago, J.; Windsor, F.M.; Durance, I.; Horton, A.A.; Thompson, R.C.; Tyler, C.R.; Ormerod, S.J.; Vazquez, A.; Carlos, J.; Zeferino, A.; et al. *Standardised Protocol for Monitoring Microplastics in Seawater*; JPI-Oceans BASE-MAN project; JPI Oceans AISBL: Brussels, Belgium, 2018.
8. Edo, C.; González-Pleiter, M.; Leganés, F.; Fernández-Piñas, F.; Rosal, R. Fate of microplastics in wastewater treatment plants and their environmental dispersion with effluent and sludge. *Environ. Pollut.* **2020**, *259*, 113837. [CrossRef]
9. Bellasi, A.; Binda, G.; Pozzi, A.; Galafassi, S.; Volta, P.; Bettinetti, R. Microplastic Contamination in Freshwater Environments: A Review, Focusing on Interactions with Sediments and Benthic Organisms. *Environments* **2020**, *7*, 30. [CrossRef]

10. Choi, J.S.; Jung, Y.-J.; Hong, N.-H.; Hong, S.H.; Park, J.-W. Toxicological effects of irregularly shaped and spherical microplastics in a marine teleost, the sheepshead minnow (*Cyprinodon variegatus*). *Mar. Pollut. Bull.* **2018**, *129*, 231–240. [CrossRef]
11. Jabeen, K.; Li, B.; Chen, Q.; Su, L.; Wu, C.; Hollert, H.; Shi, H. Effects of virgin microplastics on goldfish (*Carassius auratus*). *Chemosphere* **2018**, *213*, 323–332. [CrossRef]
12. Espinosa, C.; Cuesta, A.; Esteban, M.Á. Effects of dietary polyvinylchloride microparticles on general health, immune status and expression of several genes related to stress in gilthead seabream (*Sparus aurata* L.). *Fish Shellfish Immunol.* **2017**, *68*, 251–259. [CrossRef] [PubMed]
13. Qiao, R.; Sheng, C.; Lu, Y.; Zhang, Y.; Ren, H.; Lemos, B. Microplastics induce intestinal inflammation, oxidative stress, and disorders of metabolome and microbiome in zebrafish. *Sci. Total Environ.* **2019**, *662*, 246–253. [CrossRef]
14. Qiao, R.; Deng, Y.; Zhang, S.; Wolosker, M.B.; Zhu, Q.; Ren, H.; Zhang, Y. Accumulation of different shapes of microplastics initiates intestinal injury and gut microbiota dysbiosis in the gut of zebrafish. *Chemosphere* **2019**, *236*, 124334. [CrossRef] [PubMed]
15. Gu, L.; Tian, L.; Gao, G.; Peng, S.; Zhang, J.; Wu, D.; Huang, J.; Hua, Q.; Lu, T.; Zhong, L.; et al. Inhibitory effects of polystyrene microplastics on caudal fin regeneration in zebrafish larvae. *Environ. Pollut.* **2020**, *266*, 114664. [CrossRef] [PubMed]
16. Lei, L.; Wu, S.; Lu, S.; Liu, M.; Song, Y.; Fu, Z.; Shi, H.; Raley-Susman, K.M.; He, D. Microplastic particles cause intestinal damage and other adverse effects in zebrafish *Danio rerio* and nematode *Caenorhabditis elegans*. *Sci. Total Environ.* **2018**, *619–620*, 1–8. [CrossRef]
17. Veneman, W.J.; Spaink, H.P.; Brun, N.R.; Bosker, T.; Vijver, M.G. Pathway analysis of systemic transcriptome responses to injected polystyrene particles in zebrafish larvae. *Aquat. Toxicol.* **2017**, *190*, 112–120. [CrossRef]
18. Plastics–The Facts 2019. *An Analysis of European Plastics Production, Demand and Waste Data*; Plastics Europe: Brussels, Belgium, 2019.
19. Namazi, H. Polymers in our daily life. *Bioimpacts* **2017**, *7*, 73–74. [CrossRef]
20. Payne, J.; McKeown, P.; Jones, M.D. A circular economy approach to plastic waste. *Polym. Degrad. Stab.* **2019**, *165*, 170–181. [CrossRef]
21. Independent Group of Scientists Appointed by the Secretary-General. *Global Sustainable Development Report 2019: The Future is Now–Science for Achieving Sustainable Development*; United Nations: New York, NY, USA, 2019.
22. De Souza Machado, A.A.; Kloas, W.; Zarfl, C.; Hempel, S.; Rillig, M.C. Microplastics as an emerging threat to terrestrial ecosystems. *Glob. Chang. Biol.* **2018**, *24*, 1405–1416. [CrossRef]
23. UNEP. *Frontiers 2018/2019 Emerging Issues of Environmental Concern*; United Nations Environment Programme: Nairobi, Kenya, 2019; ISBN 978-92-807-3553-6.
24. Fred-Ahmadu, O.H.; Bhagwat, G.; Oluyoye, I.; Benson, N.U.; Ayejuyo, O.O.; Palanisami, T. Interaction of chemical contaminants with microplastics: Principles and perspectives. *Sci. Total Environ.* **2020**, *706*, 135978. [CrossRef]
25. Boots, B.; Russell, C.W.; Green, D.S. Effects of Microplastics in Soil Ecosystems: Above and Below Ground. *Environ. Sci. Technol.* **2019**, *53*, 11496–11506. [CrossRef]
26. Plastics–The Facts 2022. Plastics Europe, Brussels, Belgium. 2022. Available online: https://plasticseurope.org/knowledge-hub/plastics-the-facts-2022/ (accessed on 15 May 2023).
27. Chae, Y.; An, Y.-J. Current research trends on plastic pollution and ecological impacts on the soil ecosystem: A review. *Environ. Pollut.* **2018**, *240*, 387–395. [CrossRef]
28. Zhang, G.S.; Liu, Y.F. The distribution of microplastics in soil aggregate fractions in southwestern China. *Sci. Total Environ.* **2018**, *642*, 12–20. [CrossRef]
29. Lebreton, L.; Slat, B.; Ferrari, F.; Sainte-Rose, B.; Aitken, J.; Marthouse, R.; Hajbane, S.; Cunsolo, S.; Schwarz, A.; Levivier, A.; et al. Evidence that the Great Pacific Garbage Patch is rapidly accumulating plastic. *Sci. Rep.* **2018**, *8*, 4666. [CrossRef]
30. Bergmann, M.; Mützel, S.; Primpke, S.; Tekman, M.B.; Trachsel, J.; Gerdts, G. White and wonderful? Microplastics prevail in snow from the Alps to the Arctic. *Sci. Adv.* **2019**, *5*, eaax1157. [CrossRef]
31. Ross, P.S.; Chastain, S.; Vassilenko, E.; Etemadifar, A.; Zimmermann, S.; Quesnel, S.-A.; Eert, J.; Solomon, E.; Patankar, S.; Posacka, A.M.; et al. Pervasive distribution of polyester fibres in the Arctic Ocean is driven by Atlantic inputs. *Nat. Commun.* **2021**, *12*, 106. [CrossRef]
32. Rillig, M.C.; Lehmann, A.; Machado, A.A.d.S.; Yang, G. Microplastic effects on plants. *New Phytol.* **2019**, *223*, 1066–1070. [CrossRef]
33. Corcoran, P.L.; Jazvac, K. The consequence that is plastiglomerate. *Nat. Rev. Earth Environ.* **2020**, *1*, 6–7. [CrossRef]
34. De-la-Torre, G.E.; Pizarro-Ortega, C.I.; Dioses-Salinas, D.C.; Rakib, R.M.J.; Ramos, W.; Pretell, V.; Ribeiro, V.V.; Castro, Í.B.; Dobaradaran, S. First record of plastiglomerates, pyroplastics, and plasticrusts in South America. *Sci. Total Environ.* **2022**, *833*, 155179. [CrossRef]
35. He, D.; Luo, Y.; Lu, S.; Liu, M.; Song, Y.; Lei, L. Microplastics in soils: Analytical methods, pollution characteristics and ecological risks. *TrAC Trends Anal. Chem.* **2018**, *109*, 163–172. [CrossRef]
36. Wright, S.L.; Kelly, F.J. Plastic and Human Health: A Micro Issue? *Environ. Sci. Technol.* **2017**, *51*, 6634–6647. [CrossRef]
37. Pozo, K.; Urbina, W.; Gómez, V.; Torres, M.; Nuñez, D.; Přibylová, P.; Audy, O.; Clarke, B.; Arias, A.; Tombesi, N.; et al. Persistent organic pollutants sorbed in plastic resin pellet—"Nurdles" from coastal areas of Central Chile. *Mar. Pollut. Bull.* **2020**, *151*, 110786. [CrossRef]
38. Zimmermann, L.; Göttlich, S.; Oehlmann, J.; Wagner, M.; Völker, C. What are the drivers of microplastic toxicity? Comparing the toxicity of plastic chemicals and particles to *Daphnia magna*. *Environ. Pollut.* **2020**, *267*, 115392. [CrossRef]

39. Bläsing, M.; Amelung, W. Plastics in soil: Analytical methods and possible sources. *Sci. Total Environ.* **2018**, *612*, 422–435. [CrossRef]
40. Anbumani, S.; Kakkar, P. Ecotoxicological effects of microplastics on biota: A review. *Environ. Sci. Pollut. Res.* **2018**, *25*, 14373–14396. [CrossRef]
41. Smith, M.; Love, D.C.; Rochman, C.M.; Neff, R.A. Microplastics in Seafood and the Implications for Human Health. *Curr. Environ. Health Rep.* **2018**, *5*, 375–386. [CrossRef]
42. Gasperi, J.; Wright, S.L.; Dris, R.; Collard, F.; Mandin, C.; Guerrouache, M.; Langlois, V.; Kelly, F.J.; Tassin, B. Microplastics in air: Are we breathing it in? *Curr. Opin. Environ. Sci. Health* **2018**, *1*, 1–5. [CrossRef]
43. ter Halle, A.; Ghiglione, J.F. Nanoplastics: A Complex, Polluting Terra Incognita. *Environ. Sci. Technol.* **2021**, *55*, 14466–14469. [CrossRef]
44. Gigault, J.; ter Halle, A.; Baudrimont, M.; Pascal, P.-Y.; Gauffre, F.; Phi, T.-L.; El Hadri, H.; Grassl, B.; Reynaud, S. Current opinion: What is a nanoplastic? *Environ. Pollut.* **2018**, *235*, 1030–1034. [CrossRef]
45. Barboza, L.G.A.; Vethaak, A.D.; Lavorante, B.R.B.O.; Lundebye, A.-K.; Guilhermino, L. Marine microplastic debris: An emerging issue for food security, food safety and human health. *Mar. Pollut. Bull.* **2018**, *133*, 336–348. [CrossRef]
46. Henderson, L.; Green, C. Making sense of microplastics? Public understandings of plastic pollution. *Mar. Pollut. Bull.* **2020**, *152*, 110908. [CrossRef]
47. Zitouni, N.; Bousserrhine, N.; Missawi, O.; Boughattas, I.; Chèvre, N.; Santos, R.; Belbekhouche, S.; Alphonse, V.; Tisserand, F.; Balmassiere, L.; et al. Uptake, tissue distribution and toxicological effects of environmental microplastics in early juvenile fish *Dicentrarchus labrax*. *J. Hazard. Mater.* **2020**, *403*, 124055. [CrossRef]
48. Hüffer, T.; Metzelder, F.; Sigmund, G.; Slawek, S.; Schmidt, T.C.; Hofmann, T. Polyethylene microplastics influence the transport of organic contaminants in soil. *Sci. Total Environ.* **2019**, *657*, 242–247. [CrossRef]
49. Besseling, E.; Quik, J.T.K.; Sun, M.; Koelmans, A.A. Fate of nano- and microplastic in freshwater systems: A modeling study. *Environ. Pollut.* **2017**, *220*, 540–548. [CrossRef]
50. European Commission. *Communication from the Commission to the European Parliament, the Council, the European Economic and Social Committee and the Committee of the Regions: A European Strategy for Plastics in a Circular Economy*; European Commission: Brussels, Belgium, 2018.
51. European Commission. *Communication from the Commission to the European Parliament, the Council, the European Economic and Social Committee and the Committee of the Regions: EU Policy Framework on Biobased, Biodegradable and Compostable Plastics*; European Commission: Brussels, Belgium, 2022.
52. European Commission. *Amending Annex XVII to Regulation (EC) No 1907/2006 of the European Parliament and of the Council Concerning the Registration, Evaluation, Authorisation and Restriction of Chemicals (REACH) as Regards Synthetic Polymer Microparticles-Draft*; European Commission: Brussels, Belgium, 2022.
53. Kawecki, D.; Wu, Q.; Gonçalves, J.S.; Nowack, B. Polymer-specific dynamic probabilistic material flow analysis of seven polymers in Europe from 1950 to 2016. *Resour. Conserv. Recycl.* **2021**, *173*, 105733. [CrossRef]
54. da Costa, J.P.; Paço, A.; Santos, P.S.M.; Duarte, A.C.; Rocha-Santos, T. Microplastics in soils: Assessment, analytics and risks. *Environ. Chem.* **2019**, *16*, 18–30. [CrossRef]
55. Hurley, R.R.; Lusher, A.L.; Olsen, M.; Nizzetto, L. Validation of a Method for Extracting Microplastics from Complex, Organic-Rich, Environmental Matrices. *Environ. Sci. Technol.* **2018**, *52*, 7409–7417. [CrossRef]
56. Mintenig, S.M.; Int-Veen, I.; Löder, M.G.J.; Primpke, S.; Gerdts, G. Identification of microplastic in effluents of waste water treatment plants using focal plane array-based micro-Fourier-transform infrared imaging. *Water Res.* **2017**, *108*, 365–372. [CrossRef]
57. Mahon, A.M.; O'connell, B.; Healy, M.G.; O'connor, I.; Officer, R.; Nash, R.; Morrison, L. Microplastics in Sewage Sludge: Effects of Treatment. *Environ. Sci. Technol.* **2017**, *51*, 810–818. [CrossRef]
58. Piehl, S.; Leibner, A.; Löder, M.G.J.; Dris, R.; Bogner, C.; Laforsch, C. Identification and quantification of macro- and microplastics on an agricultural farmland. *Sci. Rep.* **2018**, *8*, 17950. [CrossRef]
59. Rillig, M.C.; Ingraffia, R.; de Souza Machado, A.A. Microplastic Incorporation into Soil in Agroecosystems. *Front. Plant Sci.* **2017**, *8*, 1805. [CrossRef]
60. van Weert, S.; Redondo-Hasselerharm, P.E.; Diepens, N.J.; Koelmans, A.A. Effects of Nanoplastics and Micro-plastics on the Growth of Sediment-Rooted Macrophytes. *Sci. Total Environ.* **2019**, *654*, 1040–1047. [CrossRef]
61. Luo, H.; Zhao, Y.; Li, Y.; Xiang, Y.; He, D.; Pan, X. Aging of microplastics affects their surface properties, thermal decomposition, additives leaching and interactions in simulated fluids. *Sci. Total Environ.* **2020**, *714*, 136862. [CrossRef]
62. Fernández-González, V.; Andrade-Garda, J.M.; López-Mahía, P.; Muniategui-Lorenzo, S. Impact of weathering on the chemical identification of microplastics from usual packaging polymers in the marine environment. *Anal. Chim. Acta* **2021**, *1142*, 179–188. [CrossRef]
63. Valentine, K.; Cross, R.; Cox, R.; Woodmancy, G.; Boxall, A.B.A. Caddisfly Larvae are a Driver of Plastic Litter Breakdown and Microplastic Formation in Freshwater Environments. *Environ. Toxicol. Chem.* **2022**, *41*, 3058–3069. [CrossRef]
64. Kwak, J.I.; An, Y.-J. Length- and polymer-dependent ecotoxicities of microfibers to the earthworm *Eisenia andrei*. *Comp. Biochem. Physiol. Part C Toxicol. Pharmacol.* **2022**, *257*, 109354. [CrossRef]

65. Selonen, S.; Dolar, A.; Kokalj, A.J.; Sackey, L.N.A.; Skalar, T.; Fernandes, V.C.; Rede, D.; Delerue-Matos, C.; Hurley, R.; Nizzetto, L.; et al. Exploring the impacts of microplastics and associated chemicals in the terrestrial environment–Exposure of soil invertebrates to tire particles. *Environ. Res.* **2021**, *201*, 111495. [CrossRef]
66. Leifheit, E.F.; Kissener, H.L.; Faltin, E.; Ryo, M.; Rillig, M.C. Tire abrasion particles negatively affect plant growth even at low concentrations and alter soil biogeochemical cycling. *Soil Ecol. Lett.* **2022**, *4*, 409–415. [CrossRef]
67. Rillig, M.C.; Ziersch, L.; Hempel, S. Microplastic transport in soil by earthworms. *Sci. Rep.* **2017**, *7*, 1362. [CrossRef]
68. Lwanga, E.H.; Gertsen, H.; Gooren, H.; Peters, P.; Salánki, T.; van der Ploeg, M.; Besseling, E.; Koelmans, A.A.; Geissen, V. Incorporation of microplastics from litter into burrows of *Lumbricus terrestris*. *Environ. Pollut.* **2017**, *220*, 523–531. [CrossRef]
69. Sagawa, N.; Kawaai, K.; Hinata, H. Abundance and size of microplastics in a coastal sea: Comparison among bottom sediment, beach sediment, and surface water. *Mar. Pollut. Bull.* **2018**, *133*, 532–542. [CrossRef] [PubMed]
70. Corradini, F.; Meza, P.; Eguiluz, R.; Casado, F.; Huerta-Lwanga, E.; Geissen, V. Evidence of microplastic accumulation in agricultural soils from sewage sludge disposal. *Sci. Total Environ.* **2019**, *671*, 411–420. [CrossRef] [PubMed]
71. Caruso, G.; Bergami, E.; Singh, N.; Corsi, I. Plastic occurrence, sources, and impacts in Antarctic environment and biota. *Water Biol. Secur.* **2022**, *1*, 100034. [CrossRef]
72. Seghers, J.; Stefaniak, E.A.; La Spina, R.; Cella, C.; Mehn, D.; Gilliland, D.; Held, A.; Jacobsson, U.; Emteborg, H. Preparation of a reference material for microplastics in water—Evaluation of homogeneity. *Anal. Bioanal. Chem.* **2021**, *414*, 385–397. [CrossRef] [PubMed]
73. Lares, M.; Ncibi, M.C.; Sillanpää, M.; Sillanpää, M. Occurrence, identification and removal of microplastic particles and fibers in conventional activated sludge process and advanced MBR technology. *Water Res.* **2018**, *133*, 236–246. [CrossRef] [PubMed]
74. Thomas, D.; Schütze, B.; Heinze, W.M.; Steinmetz, Z. Sample Preparation Techniques for the Analysis of Microplastics in Soil—A Review. *Sustainability* **2020**, *12*, 9074. [CrossRef]
75. Andrade, J.; Fernández-González, V.; López-Mahía, P.; Muniategui, S. A low-cost system to simulate environmental microplastic weathering. *Mar. Pollut. Bull.* **2019**, *149*, 110663. [CrossRef]
76. Zhu, K.; Jia, H.; Sun, Y.; Dai, Y.; Zhang, C.; Guo, X.; Wang, T.; Zhu, L. Long-term phototransformation of microplastics under simulated sunlight irradiation in aquatic environments: Roles of reactive oxygen species. *Water Res.* **2020**, *173*, 115564. [CrossRef]
77. Youn, J.-S.; Kim, Y.-M.; Siddiqui, M.Z.; Watanabe, A.; Han, S.; Jeong, S.; Jung, Y.-W.; Jeon, K.-J. Quantification of tire wear particles in road dust from industrial and residential areas in Seoul, Korea. *Sci. Total Environ.* **2021**, *784*, 147177. [CrossRef]
78. Pivokonsky, M.; Cermakova, L.; Novotna, K.; Peer, P.; Cajthaml, T.; Janda, V. Occurrence of microplastics in raw and treated drinking water. *Sci. Total Environ.* **2018**, *643*, 1644–1651. [CrossRef]
79. da Costa, J.P.; Reis, V.; Paço, A.; Costa, M.; Duarte, A.C.; Rocha-Santos, T. Micro(nano)plastics–Analytical challenges towards risk evaluation. *TrAC Trends Anal. Chem.* **2019**, *111*, 173–184. [CrossRef]
80. Miller, E.; Sedlak, M.; Lin, D.; Box, C.; Holleman, C.; Rochman, C.M.; Sutton, R. Recommended best practices for collecting, analyzing, and reporting microplastics in environmental media: Lessons learned from comprehensive monitoring of San Francisco Bay. *J. Hazard. Mater.* **2021**, *409*, 124770. [CrossRef] [PubMed]
81. Li, Q.; Wu, J.; Zhao, X.; Gu, X.; Ji, R. Separation and identification of microplastics from soil and sewage sludge. *Environ. Pollut.* **2019**, *254*, 113076. [CrossRef]
82. Li, Q.; Zeng, A.; Jiang, X.; Gu, X. Are microplastics correlated to phthalates in facility agriculture soil? *J. Hazard. Mater.* **2021**, *412*, 125164. [CrossRef] [PubMed]
83. Besley, A.; Vijver, M.G.; Behrens, P.; Bosker, T. A standardized method for sampling and extraction methods for quantifying microplastics in beach sand. *Mar. Pollut. Bull.* **2017**, *114*, 77–83. [CrossRef] [PubMed]
84. Scopetani, C.; Chelazzi, D.; Mikola, J.; Leiniö, V.; Heikkinen, R.; Cincinelli, A.; Pellinen, J. Olive oil-based method for the extraction, quantification and identification of microplastics in soil and compost samples. *Sci. Total Environ.* **2020**, *733*, 139338. [CrossRef]
85. Song, X.; Wu, X.; Song, X.; Zhang, Z. Oil extraction following digestion to separate microplastics from mussels. *Chemosphere* **2021**, *289*, 133187. [CrossRef]
86. Kononov, A.; Hishida, M.; Suzuki, K.; Harada, N. Microplastic Extraction from Agricultural Soils Using Canola Oil and Unsaturated Sodium Chloride Solution and Evaluation by Incineration Method. *Soil Syst.* **2022**, *6*, 54. [CrossRef]
87. Prosenc, F.; Leban, P.; Šunta, U.; Kralj, M.B. Extraction and Identification of a Wide Range of Microplastic Polymers in Soil and Compost. *Polymers* **2021**, *13*, 4069. [CrossRef] [PubMed]
88. Han, X.; Lu, X.; Vogt, R.D. An optimized density-based approach for extracting microplastics from soil and sediment samples. *Environ. Pollut.* **2019**, *254*, 113009. [CrossRef] [PubMed]
89. Constant, M.; Billon, G.; Breton, N.; Alary, C. Extraction of microplastics from sediment matrices: Experimental comparative analysis. *J. Hazard. Mater.* **2021**, *420*, 126571. [CrossRef] [PubMed]
90. Nakajima, R.; Lindsay, D.J.; Tsuchiya, M.; Matsui, R.; Kitahashi, T.; Fujikura, K.; Fukushima, T. A small, stainless-steel sieve optimized for laboratory beaker-based extraction of microplastics from environmental samples. *Methodsx* **2019**, *6*, 1677–1682. [CrossRef] [PubMed]
91. Nakajima, R.; Tsuchiya, M.; Lindsay, D.J.; Kitahashi, T.; Fujikura, K.; Fukushima, T. A new small device made of glass for separating microplastics from marine and freshwater sediments. *PeerJ* **2019**, *7*, e7915. [CrossRef] [PubMed]
92. Enders, K.; Lenz, R.; Sul, J.A.I.D.; Tagg, A.S.; Labrenz, M. When every particle matters: A QuEChERS approach to extract microplastics from environmental samples. *Methodsx* **2020**, *7*, 100784. [CrossRef]

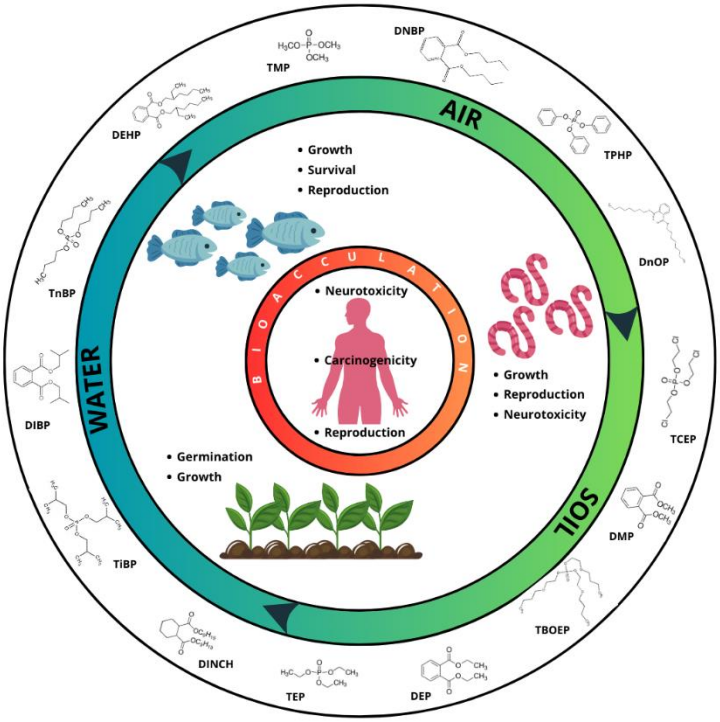
93. Zobkov, M.B.; Esiukova, E.E. Evaluation of the Munich Plastic Sediment Separator efficiency in extraction of microplastics from natural marine bottom sediments. *Limnol. Oceanogr. Methods* **2017**, *15*, 967–978. [CrossRef]
94. Coppock, R.L.; Cole, M.; Lindeque, P.K.; Queirós, A.M.; Galloway, T.S. A small-scale, portable method for extracting microplastics from marine sediments. *Environ. Pollut.* **2017**, *230*, 829–837. [CrossRef]
95. Rhein, F.; Scholl, F.; Nirschl, H. Magnetic seeded filtration for the separation of fine polymer particles from dilute suspensions: Microplastics. *Chem. Eng. Sci.* **2019**, *207*, 1278–1287. [CrossRef]
96. Grbic, J.; Nguyen, B.; Guo, E.; You, J.B.; Sinton, D.; Rochman, C.M. Magnetic Extraction of Microplastics from Environmental Samples. *Environ. Sci. Technol. Lett.* **2019**, *6*, 68–72. [CrossRef]
97. Budhiraja, V.; Mušič, B.; Krzan, A. Magnetic Extraction of Weathered Tire Wear Particles and Polyethylene Microplastics. *Polymers* **2022**, *14*, 5189. [CrossRef]
98. Ramage, S.J.F.F.; Pagaling, E.; Haghi, R.K.; Dawson, L.A.; Yates, K.; Prabhu, R.; Hillier, S.; Devalla, S. Rapid extraction of high- and low-density microplastics from soil using high-gradient magnetic separation. *Sci. Total Environ.* **2022**, *831*, 154912. [CrossRef]
99. Rhein, F.; Kaiser, S.; Rhein, M.; Nirschl, H. Agglomerate processing and recycling options in magnetic seeded filtration. *Chem. Eng. Sci.* **2021**, *238*, 116577. [CrossRef]
100. Rhein, F.; Nirschl, H.; Kaegi, R. Separation of Microplastic Particles from Sewage Sludge Extracts Using Magnetic Seeded Filtration. *Water Res. X* **2022**, *17*, 100155. [CrossRef] [PubMed]
101. Shi, X.; Zhang, X.; Gao, W.; Zhang, Y.; He, D. Removal of microplastics from water by magnetic nano-Fe_3O_4. *Sci. Total Environ.* **2022**, *802*, 149838. [CrossRef] [PubMed]
102. Felsing, S.; Kochleus, C.; Buchinger, S.; Brennholt, N.; Stock, F.; Reifferscheid, G. A new approach in separating microplastics from environmental samples based on their electrostatic behavior. *Environ. Pollut.* **2018**, *234*, 20–28. [CrossRef] [PubMed]
103. Enders, K.; Tagg, A.S.; Labrenz, M. Evaluation of Electrostatic Separation of Microplastics from Mineral-Rich Environmental Samples. *Front. Environ. Sci.* **2020**, *8*, 112. [CrossRef]
104. Kurzweg, L.; Schirrmeister, S.; Hauffe, M.; Adomat, Y.; Socher, M.; Harre, K. Application of electrostatic separation and differential scanning calorimetry for microplastic analysis in river sediments. *Front. Environ. Sci.* **2022**, *10*, 1–12. [CrossRef]
105. Andrade, J.M.; Ferreiro, B.; López-Mahía, P.; Muniategui-Lorenzo, S. Standardization of the minimum information for publication of infrared-related data when microplastics are characterized. *Mar. Pollut. Bull.* **2020**, *154*, 111035. [CrossRef] [PubMed]
106. Oßmann, B.E.; Sarau, G.; Holtmannspötter, H.; Pischetsrieder, M.; Christiansen, S.H.; Dicke, W. Small-sized microplastics and pigmented particles in bottled mineral water. *Water Res.* **2018**, *141*, 307–316. [CrossRef]
107. Dümichen, E.; Eisentraut, P.; Bannick, C.G.; Barthel, A.-K.K.; Senz, R.; Braun, U. Fast identification of microplastics in complex environmental samples by a thermal degradation method. *Chemosphere* **2017**, *174*, 572–584. [CrossRef]
108. Castelvetro, V.; Corti, A.; Biale, G.; Ceccarini, A.; Degano, I.; La Nasa, J.; Lomonaco, T.; Manariti, A.; Manco, E.; Modugno, F.; et al. New methodologies for the detection, identification, and quantification of microplastics and their environmental degradation by-products. *Environ. Sci. Pollut. Res.* **2021**, *28*, 46764–46780. [CrossRef]
109. Šunta, U.; Prosenc, F.; Trebše, P.; Bulc, T.G.; Kralj, M.B. Adsorption of acetamiprid, chlorantraniliprole and flubendiamide on different type of microplastics present in alluvial soil. *Chemosphere* **2020**, *261*, 127762. [CrossRef] [PubMed]
110. Müller, A.; Goedecke, C.; Eisentraut, P.; Piechotta, C.; Braun, U. Microplastic analysis using chemical extraction followed by LC-UV analysis: A straightforward approach to determine PET content in environmental samples. *Environ. Sci. Eur.* **2020**, *32*, 85. [CrossRef]
111. Vermeiren, P.; Muñoz, C.; Ikejima, K. Microplastic identification and quantification from organic rich sediments: A validated laboratory protocol. *Environ. Pollut.* **2020**, *262*, 114298. [CrossRef] [PubMed]
112. El Hayany, B.; El Fels, L.; Quénéa, K.; Dignac, M.-F.; Rumpel, C.; Gupta, V.K.; Hafidi, M. Microplastics from lagooning sludge to composts as revealed by fluorescent staining- image analysis, Raman spectroscopy and pyrolysis-GC/MS. *J. Environ. Manag.* **2020**, *275*, 111249. [CrossRef] [PubMed]
113. Peez, N.; Janiska, M.-C.; Imhof, W. The first application of quantitative 1H NMR spectroscopy as a simple and fast method of identification and quantification of microplastic particles (PE, PET, and PS). *Anal. Bioanal. Chem.* **2019**, *411*, 823–833. [CrossRef] [PubMed]
114. David, J.; Steinmetz, Z.; Kučerík, J.; Schaumann, G.E. Quantitative Analysis of Poly(ethylene terephthalate) Microplastics in Soil via Thermogravimetry–Mass Spectrometry. *Anal. Chem.* **2018**, *90*, 8793–8799. [CrossRef]
115. Steinmetz, Z.; Kintzi, A.; Muñoz, K.; Schaumann, G.E. A simple method for the selective quantification of polyethylene, polypropylene, and polystyrene plastic debris in soil by pyrolysis-gas chromatography/mass spectrometry. *J. Anal. Appl. Pyrolysis* **2020**, *147*, 104803. [CrossRef]
116. Eltemsah, Y.S.; Bøhn, T. Acute and chronic effects of polystyrene microplastics on juvenile and adult *Daphnia magna*. *Environ. Pollut.* **2019**, *254*, 112919. [CrossRef]
117. Suman, T.Y.; Jia, P.-P.; Li, W.-G.; Junaid, M.; Xin, G.-Y.; Wang, Y.; Pei, D.-S. Acute and chronic effects of polystyrene microplastics on brine shrimp: First evidence highlighting the molecular mechanism through transcriptome analysis. *J. Hazard. Mater.* **2020**, *400*, 123220. [CrossRef]
118. Zhu, D.; Chen, Q.L.; An, X.L.; Yang, X.R.; Christie, P.; Ke, X.; Wu, L.H.; Zhu, Y.G. Exposure of Soil Collembolans to Micro-plastics Perturbs Their Gut Microbiota and Alters Their Isotopic Composition. *Soil Biol. Biochem.* **2018**, *116*, 302–310. [CrossRef]

119. Jiang, X.; Chang, Y.; Zhang, T.; Qiao, Y.; Klobučar, G.; Li, M. Toxicological effects of polystyrene microplastics on earthworm (*Eisenia fetida*). *Environ. Pollut.* **2020**, *259*, 113896. [CrossRef] [PubMed]
120. Lahive, E.; Walton, A.; Horton, A.A.; Spurgeon, D.J.; Svendsen, C. Microplastic particles reduce reproduction in the terrestrial worm *Enchytraeus crypticus* in a soil exposure. *Environ. Pollut.* **2019**, *255*, 113174. [CrossRef] [PubMed]
121. de Souza Machado, A.A.; Lau, C.W.; Kloas, W.; Bergmann, J.; Bachelier, J.B.; Faltin, E.; Becker, R.; Görlich, A.S.; Rillig, M.C. Microplastics Can Change Soil Properties and Affect Plant Performance. *Environ. Sci. Technol.* **2019**, *53*, 6044–6052. [CrossRef] [PubMed]
122. Pignattelli, S.; Broccoli, A.; Renzi, M. Physiological responses of garden cress (*L. sativum*) to different types of microplastics. *Sci. Total Environ.* **2020**, *727*, 138609. [CrossRef]
123. Batel, A.; Linti, F.; Scherer, M.; Erdinger, L.; Braunbeck, T. Transfer of benzo[*a*]pyrene from microplastics to *Artemia* nauplii and further to zebrafish via a trophic food web experiment: CYP1A induction and visual tracking of persistent organic pollutants. *Environ. Toxicol. Chem.* **2016**, *35*, 1656–1666. [CrossRef]
124. Rodrigues, J.P.; Duarte, A.C.; Santos-Echeandía, J.; Rocha-Santos, T. Significance of interactions between microplastics and POPs in the marine environment: A critical overview. *TrAC Trends Anal. Chem.* **2019**, *111*, 252–260. [CrossRef]
125. Kwon, W.; Kim, D.; Kim, H.-Y.; Jeong, S.W.; Lee, S.-G.; Kim, H.-C.; Lee, Y.-J.; Kwon, M.K.; Hwang, J.-S.; Han, J.E.; et al. Microglial phagocytosis of polystyrene microplastics results in immune alteration and apoptosis *in vitro* and *in vivo*. *Sci. Total Environ.* **2022**, *807*, 150817. [CrossRef]
126. Beriot, N.; Peek, J.; Zornoza, R.; Geissen, V.; Lwanga, E.H. Low density-microplastics detected in sheep faeces and soil: A case study from the intensive vegetable farming in Southeast Spain. *Sci. Total Environ.* **2021**, *755*, 142653. [CrossRef]
127. Alma, A.M.; de Groot, G.S.; Buteler, M. Microplastics incorporated by honeybees from food are transferred to honey, wax and larvae. *Environ. Pollut.* **2023**, *320*, 121078. [CrossRef]
128. Luo, Y.; Wang, L.; Cao, T.; Chen, J.; Lv, M.; Wei, S.; Lu, S.; Tian, X. Microplastics are transferred by soil fauna and regulate soil function as material carriers. *Sci. Total Environ.* **2023**, *857*, 159690. [CrossRef]
129. Khalid, N.; Aqeel, M.; Noman, A. Microplastics could be a threat to plants in terrestrial systems directly or indirectly. *Environ. Pollut.* **2020**, *267*, 115653. [CrossRef] [PubMed]
130. Liu, K.; Wang, X.; Song, Z.; Wei, N.; Li, D. Terrestrial plants as a potential temporary sink of atmospheric microplastics during transport. *Sci. Total Environ.* **2020**, *742*, 140523. [CrossRef] [PubMed]
131. Hernández-Arenas, R.; Beltrán-Sanahuja, A.; Navarro-Quirant, P.; Sanz-Lazaro, C. The effect of sewage sludge containing microplastics on growth and fruit development of tomato plants. *Environ. Pollut.* **2021**, *268*, 115779. [CrossRef] [PubMed]
132. Li, Z.; Li, R.; Li, Q.; Zhou, J.; Wang, G. Physiological response of cucumber (*Cucumis sativus* L.) leaves to polystyrene nanoplastics pollution. *Chemosphere* **2020**, *255*, 127041. [CrossRef]
133. Rahman, A.; Sarkar, A.; Yadav, O.P.; Achari, G.; Slobodnik, J. Potential human health risks due to environmental exposure to nano- and microplastics and knowledge gaps: A scoping review. *Sci. Total Environ.* **2021**, *757*, 143872. [CrossRef]
134. Praveena, S.M.; Ariffin, N.I.S.; Nafisyah, A.L. Microplastics in Malaysian bottled water brands: Occurrence and potential human exposure. *Environ. Pollut.* **2022**, *315*, 120494. [CrossRef]
135. Conti, G.O.; Ferrante, M.; Banni, M.; Favara, C.; Nicolosi, I.; Cristaldi, A.; Fiore, M.; Zuccarello, P. Micro- and nano-plastics in edible fruit and vegetables. The first diet risks assessment for the general population. *Environ. Res.* **2020**, *187*, 109677. [CrossRef]
136. Sivagami, M.; Selvambigai, M.; Devan, U.; Velangani, A.A.J.; Karmegam, N.; Biruntha, M.; Arun, A.; Kim, W.; Govarthanan, M.; Kumar, P. Extraction of microplastics from commonly used sea salts in India and their toxicological evaluation. *Chemosphere* **2020**, *263*, 128181. [CrossRef]
137. Zhang, Q.; Liu, L.; Jiang, Y.; Zhang, Y.; Fan, Y.; Rao, W.; Qian, X. Microplastics in infant milk powder. *Environ. Pollut.* **2023**, *323*, 121225. [CrossRef]
138. Compa, M.; Ventero, A.; Iglesias, M.; Deudero, S. Ingestion of microplastics and natural fibres in *Sardina pilchardus* (Walbaum, 1792) and *Engraulis encrasicolus* (Linnaeus, 1758) along the Spanish Mediterranean coast. *Mar. Pollut. Bull.* **2018**, *128*, 89–96. [CrossRef]
139. Amato-Lourenço, L.F.; dos Santos Galvão, L.; de Weger, L.A.; Hiemstra, P.S.; Vijver, M.G.; Mauad, T. An emerging class of air pollutants: Potential effects of microplastics to respiratory human health? *Sci. Total Environ.* **2020**, *749*, 141676. [CrossRef] [PubMed]
140. Leslie, H.A.; van Velzen, M.J.M.; Brandsma, S.H.; Vethaak, A.D.; Garcia-Vallejo, J.J.; Lamoree, M.H. Discovery and quantification of plastic particle pollution in human blood. *Environ. Int.* **2022**, *163*, 107199. [CrossRef] [PubMed]
141. Ragusa, A.; Svelato, A.; Santacroce, C.; Catalano, P.; Notarstefano, V.; Carnevali, O.; Papa, F.; Rongioletti, M.C.A.; Baiocco, F.; Draghi, S.; et al. Plasticenta: First evidence of microplastics in human placenta. *Environ. Int.* **2021**, *146*, 106274. [CrossRef] [PubMed]
142. Goodman, K.E.; Hare, J.T.; Khamis, Z.I.; Hua, T.; Sang, Q.-X.A. Exposure of Human Lung Cells to Polystyrene Microplastics Significantly Retards Cell Proliferation and Triggers Morphological Changes. *Chem. Res. Toxicol.* **2021**, *34*, 1069–1081. [CrossRef] [PubMed]
143. Çobanoğlu, H.; Belivermiş, M.; Sıkdokur, E.; Kılıç, Ö.; Çayır, A. Genotoxic and cytotoxic effects of polyethylene microplastics on human peripheral blood lymphocytes. *Chemosphere* **2021**, *272*, 129805. [CrossRef]

144. Santos, D.; Félix, L.; Luzio, A.; Parra, S.; Cabecinha, E.; Bellas, J.; Monteiro, S.M. Toxicological effects induced on early life stages of zebrafish (*Danio rerio*) after an acute exposure to microplastics alone or co-exposed with copper. *Chemosphere* **2020**, *261*, 127748. [CrossRef]
145. Khalid, A.; Zalouk-Vergnoux, A.; Benali, S.; Mincheva, R.; Raquez, J.-M.; Bertrand, S.; Poirier, L. Are bio-based and biodegradable microplastics impacting for blue mussel (*Mytilus edulis*)? *Mar. Pollut. Bull.* **2021**, *167*, 112295. [CrossRef]
146. de Souza, S.S.; Freitas, Í.N.; Gonçalves, S.d.O.; da Luz, T.M.; Araújo, A.P.d.C.; Rajagopal, R.; Balasubramani, G.; Rahman, M.; Malafaia, G. Toxicity induced via ingestion of naturally-aged polystyrene microplastics by a small-sized terrestrial bird and its potential role as vectors for the dispersion of these pollutants. *J. Hazard. Mater.* **2022**, *434*, 128814. [CrossRef]
147. Lackmann, C.; Velki, M.; Šimić, A.; Müller, A.; Braun, U.; Ečimović, S.; Hollert, H. Two types of microplastics (polystyrene-HBCD and car tire abrasion) affect oxidative stress-related biomarkers in earthworm *Eisenia andrei* in a time-dependent manner. *Environ. Int.* **2022**, *163*, 107190. [CrossRef]
148. Dong, Y.; Gao, M.; Song, Z.; Qiu, W. Microplastic particles increase arsenic toxicity to rice seedlings. *Environ. Pollut.* **2020**, *259*, 113892. [CrossRef]
149. Qi, Y.; Yang, X.; Pelaez, A.M.; Lwanga, E.H.; Beriot, N.; Gertsen, H.; Garbeva, P.; Geissen, V. Macro- and micro- plastics in soil-plant system: Effects of plastic mulch film residues on wheat (*Triticum aestivum*) growth. *Sci. Total Environ.* **2018**, *645*, 1048–1056. [CrossRef] [PubMed]
150. Jiang, X.; Chen, H.; Liao, Y.; Ye, Z.; Li, M.; Klobučar, G. Ecotoxicity and genotoxicity of polystyrene microplastics on higher plant *Vicia faba*. *Environ. Pollut.* **2019**, *250*, 831–838. [CrossRef] [PubMed]

Disclaimer/Publisher's Note: The statements, opinions and data contained in all publications are solely those of the individual author(s) and contributor(s) and not of MDPI and/or the editor(s). MDPI and/or the editor(s) disclaim responsibility for any injury to people or property resulting from any ideas, methods, instructions or products referred to in the content.

1.2. Plastic-Related Chemicals: Occurrence in Environment and Ecotoxicological Impact



Chapter 16 included in the book "Toxic Effects of Micro- and Nanoplastics: Environment, Food and Human Health," published by Scrivener Publishing LLC (2024). https://doi.org/10.1002/9781394238163.ch16

Contribution Statement

The candidate contributed to this book chapter by conducted a literature review on plastic additives, focusing particularly on plasticizers and flame retardants. Additionally, the candidate drafted the original content of the chapter and participated in the review and editing stages. The graphical abstract and Figure 1 were created using the Canva platform, accessible at (http://www.canva.com).

16

Plastic-Related Chemicals: Occurrence in Environment and Ecotoxicological Impacts

Diana Rede[1,2], Cristina Delerue-Matos[1] and Virgínia Cruz Fernandes[1]*

[1]REQUIMTE/LAQV, Instituto Superior de Engenharia do Porto, Instituto Politécnico do Porto, Porto, Portugal
[2]Departamento de Química e Bioquímica, Faculdade de Ciências, Universidade do Porto, Porto, Portugal

Abstract
The presence of plastic additives such as plasticizers and flame retardants, in different environments raises concerns about their impact on organisms and health. Plastic additives are found indoors, in water, in the soil, and in biota entering the body through dietary and non-dietary sources, potentially causing health issues. Studies have revealed significant findings, including increased oxidative stress, altered antioxidant enzyme activities, DNA damage, gene expression changes, and a modified gut microbiome in plasticizer-exposed earthworms. These effects occur even at low concentrations, indicating potential soil toxicity and the need for further investigation. Additionally, wheat plants can absorb and metabolize plasticizers, posing concerns about their bioaccumulation in the food chain and associated health risks. Flame retardants used for fire safety raise concerns owing to their persistence in the environment, ability to bioaccumulate, and associated health risks. These additives harm organisms such as marine mussels, fish, and soil inhabitants, affecting their immune, reproductive, endocrine, and neurological systems. Research has linked exposure to developmental, reproductive, endocrine, and neurotoxic effects, especially in infants and children. Although progress has been made in understanding the toxicological aspects of plastic additives, knowledge gaps remain regarding their basic toxicological data, metabolic pathways, and potentially harmful effects, particularly for non-prioritized additives.

Keywords: Additives, plasticizers, PAEs, flame retardants, OPEs, bioaccumulation, oxidative stress, endocrine-disrupting chemicals

16.1 Introduction

The pervasive presence of plastic debris in natural ecosystems has made plastic pollution a prominent concern as plastic materials have become an indispensable part of modern society, serving a wide range of applications [1, 2]. Plastic production incorporates a diverse range of additives, classified into the following categories: functional additives, fillers, reinforcements, and colorants (Figure 16.1). Functional additives include plasticizers,

**Corresponding author*: vir@isep.ipp.pt

Inamuddin, Tariq Altalhi and Virgínia Cruz Fernandes (eds.) Toxic Effects of Micro- and Nanoplastics: Environment, Food and Human Health, (347–374) © 2024 Scrivener Publishing LLC

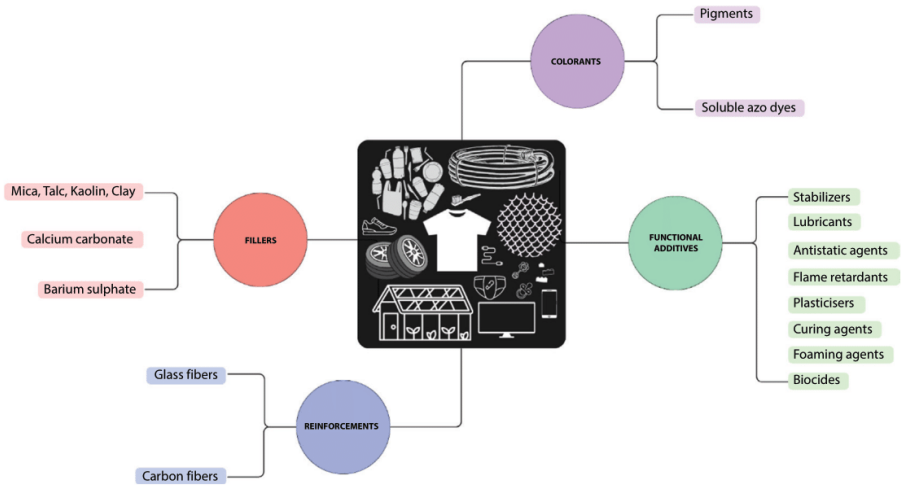


Figure 16.1 Four main categories of additives are used to maximize the performance and versatility of everyday plastics.

flame retardants, stabilizers, antistatic agents, curing agents, lubricants, foaming agents, and biocides. The colorants include soluble azo dyes and pigments. Fillers are composed of materials such as kaolin, mica, talc, clay, calcium carbonate, and barium sulfate. Finally, reinforcements involve substances such as carbon and glass fibers [2].

The incorporation of additives is essential in the production of plastics to meet various requirements for specific purposes, such as increasing the bulk, improving mechanical strength and flexibility, enhancing electrical conductivity, adding color, delaying oxidation, and preventing ignition [1, 3]. However, as additives are incorporated into plastics to modify the polymer structure, they might also affect the sorption capacity of the polymer [1]. Moreover, additives have a weak bond with polymers and therefore have the potential to leach out over time, influenced by the physicochemical properties of the additive and its surroundings, and the size of both the polymer pores and additive molecules [1, 3, 4]. This leaching process can be accelerated when plastic waste is exposed to UV degradation and/or high temperature [3, 5].

Within the environment, several plastic additives have been identified as endocrine disruptors or toxic, raising concerns about their potential impact. Examples are phthalates, bisphenol A, nonylphenols, polybrominated diphenyl ethers, and metals [1, 3, 5, 6]. These additives have been found in various environments, highlighting the need for a comprehensive understanding of their ecotoxicological effects. In 2019, the European Chemicals Agency (ECHA) collaborated with PlasticEurope, Cefic, European Plastics Converters (EuPC), academics, and representatives from European Union (EU) member states to publish a comprehensive inventory of plastic additives used in the EU under REACH regulation. The initiative registered additives with an annual production exceeding 100 tons. The resulting inventory (available at https://echa.europa.eu/pt/mapping-exercise-plastic-additives-initiative) comprises 418 functional additives and provides information on

commonly associated polymers and typical concentration ranges. The additives include stabilizers, antioxidants, nucleating agents, pigments, antistatic agents, plasticizers, and flame retardants [7].

The ecotoxicological consequences of plastic-related chemicals can be deepened by acknowledging the diverse range of additives used in plastic production and their potential environmental impacts. In the following sections, we explore the specific categories of plastic-related chemicals, namely plasticizers and flame retardants, and examine their effects on both the environment and living organisms.

16.2 Plasticizers

Plasticizers improve the processability of polymers, enhance the flexibility and toughness of the final products, and are among the most commonly used additives in the industry [2, 8]. They comprise different chemical families such as phthalate acid esters (PAEs) (also known as ortho-phthalates esters or phthalates), benzoate esters, aliphatic dibasic acid esters (adipates, azelates, sebacates, and citrates), terephthalate esters (including bisphenol A), and trimellitate esters, among others [2, 7, 9].

Annually, 7.5 million tons of plasticizers are consumed worldwide. Within Europe, the yearly utilization of additives amounts to approximately 1.35 million tons, with over 85% employed in flexible PVC applications such as electric cables, flooring, wall coverings, and coatings [2, 7, 9, 10]. Among plasticizers, PAEs such as dibutyl phthalate (DBP) and bis (2-ethylhexyl) phthalate (DEHP) are the most widely consumed because of their exceptional compatibility with PVC [1, 11, 12].

PAEs have emerged as significant environmental pollutants and are classified as endocrine-disrupting chemicals with antiandrogenic properties, posing a significant risk to the human endocrine, reproductive, and respiratory systems [10, 13–17]. The United States Environmental Protection Agency (US EPA) includes DEHP, diethyl phthalate (DEP), di-n-butyl phthalate (DnBP), butyl benzyl phthalate (BBP), dimethyl phthalate (DMP), and di-n-octyl phthalate (DnOP) as priority pollutants [18]. The EU restricts the marketing of toys and childcare articles containing DEHP, BBP, DBP, and di-isobutyl phthalate (DiBP) at a concentration by weight, individually or in combination, greater than or equal to 0.1% [19]. Moreover, non-phthalate plasticizers (e.g., di(2-ethylhexyl) adipate (DEHA), trioctyl trimellitate (TOTM), acetyl tributyl citrate (ATBC)), and di-(iso-nonyl)-cyclohexane-1,2-dicarboxylate (DINCH)) have been used to replace phthalate plasticizers in various industrial applications, such as fabric coatings, food-packing materials, children's toys, and electrical cables [10, 11, 20]. However, due to the scarcity of information on the toxicity of these replacement plasticizers, there is a lack of understanding of the potential human health implications associated with chronic exposure [21].

16.2.1 Presence and Accumulation of PAEs in the Environment

PAEs have been extensively reported in air [18], wastewater [13], soil [10, 18], sludge [22], food [23], drinking water [14], and sediment [11] (Table 16.1). The presence of PAEs in soil has received significant attention because of the intensive application of plastics in

Table 16.1 Occurrence of plasticizers in the environment, concentration ranges, and matrix sources (time span: 2017–2023).

PAE	Concentration	Matrix, Location	Ref.
Dimethyl phthalate (DMP)	64.6–126 pg m^{-3}	Outdoor air, China	[23]
	135–176 pg g^{-3}	Indoor air, China	
	<0.01 μg m^{-3}	(Greenhouse) air, China	[18]
	<0.01 μg kg^{-1}	(Greenhouse) soil, China	
	2.9–16.7 ng g^{-1} dw	Soil, China	[10]
	0.05–197 ng g^{-1} dw	Sediment, Korea	[11]
	14.31 ± 26.28 ng L^{-1}	Drinking water, China	[14]
	6.8–400 ng L^{-1}	Freshwater, Uganda	[8]
	16.7–37.4 ng L^{-1}	River water, China	[23]
	0.0006–1.12 μg g^{-1} dw	Sewage sludge, China	[22]
	<LOD–4.93 μg L^{-1}	Influent WWTP, Poland	[13]
	<LOD–6.50 μg L^{-1}	Effluent WWTP, Poland	
	2.46–24.6 μg L^{-1}	(Active) landfill leachates, Poland	
	7.77–26.3 μg L^{-1}	(Close) landfill leachates, Poland	
	2.66–3.67 ng g^{-1} dw	Fish, China	[23]
	4.18–5.96 ng g^{--} dw	Pig, China	
	3.36–3.68 ng g^{-1} dw	Chicken, China	
	3.53–3.82 ng g^{-1} dw	Cattle, China	
	21.0–38.4 ng g^{-1} dw	Vegetables, China	
Diethyl phthalate (DEP)	400–966 pg m^{-3}	Outdoor air, China	
	297–549 pg g^{-3}	Indoor air, China	
	<0.01 μg m^{-3}	(Greenhouse) air, China	[18]
	0.01–0.02 μg kg^{-1}	(Greenhouse) soil, China	
	1.9–7.2 ng g^{-1} dw	Soil, China	[10]
	0.07–10.3 ng g^{-1} dw	Sediment, Korea	[11]
	5.905 ± 11.57 ng L^{-1}	Drinking water, China	[14]
	38–1,100 ng L^{-1}	Freshwater, Uganda	[8]

(*Continued*)

Table 16.1 Occurrence of plasticizers in the environment, concentration ranges, and matrix sources (time span: 2017–2023). (*Continued*)

PAE	Concentration	Matrix, Location	Ref.
	8.63–57.4 ng L^{-1}	River water, China	[23]
	0.0003–1.41 μg g^{-1} dw	Sewage sludge, China	[22]
	<LOD–4.05 μg L^{-1}	Influent WWTP, Poland	[13]
	<LOD–3.26 μg L^{-1}	Effluent WWTP, Poland	
	<LOD–14.5 μg L^{-}	(Active) landfill leachates, Poland	
	0.19–9.48 μg L^{-1}	(Close) landfill leachates, Poland	
	0.57–1.64 ng g^{-1} dw	Fish, China	[23]
	1.80–16.7 ng g^{-1} dw	Pig, China	
	0.33–1.44 ng g^{-1} dw	Chicken, China	
	0.35–0.81 ng g^{-1} dw	Cattle, China	
	2.42–69.1 ng g^{-1} dw	Vegetables, China	
Di-isobutyl phthalate (DiBP)	172–708 pg m^{-3}	Outdoor air, China	
	90.1–152 pg g^{-3}	Indoor air, China	
	0.01–0.05 μg m^{-3}	(Greenhouse) air, China	[18]
	0.16–0.58 μg kg^{-1}	(Greenhouse) soil, China	
	9.4–123.2 ng g^{-1} dw	Soil, China	[10]
	<0.02–11.2 ng g^{-1} dw	Sediment, Korea	[11]
	103.8 ± 310.5 ng L^{-1}	Drinking water, China	[14]
	77.4–205 ng L^{-1}	River water, China	[23]
	0.0003–5.92 μg g^{-1} dw	Sewage sludge, China	[22]
	<LOD–93.1 μg L^{-1}	Influent WWTP, Poland	[13]
	<LOD–76.2 μg L^{-1}	Effluent WWTP, Poland	
	<LOD–7.39 μg L^{-1}	(Active) landfill leachates, Poland	
	<LOD–4.33 μg L^{-1}	(Close) landfill leachates, Poland	
	2.00–2.40 ng g^{-1} dw	Fish, China	[23]
	4.20–12.9 ng g^{-1} dw	Pig, China	
	1.30–3.73 ng g^{-1} dw	Chicken, China	

(*Continued*)

Table 16.1 Occurrence of plasticizers in the environment, concentration ranges, and matrix sources (time span: 2017–2023). (*Continued*)

PAE	Concentration	Matrix, Location	Ref.
	1.57–2.36 ng g^{-1} dw	Cattle, China	
	0.63–77.8 ng g^{-1} dw	Vegetables, China	
Di-n-butyl phthalate (DnBP)	319–666 pg m^{-3}	Outdoor air, China	
	146–334 pg g^{-3}	Indoor air, China	
	0.01–0.03 μg m^{-3}	(Greenhouse) air, China	[18]
	0.14–0.55 μg kg^{-1}	(Greenhouse) soil, China	
	9.2–100.7 ng g^{-1} dw	Soil, China	[10]
	0.48–56.2 ng g^{-1} dw	Sediment, Korea	[11]
	595.9 ± 1794 ng L^{-1}	Drinking water, China	[14]
	135–801 ng L^{-1}	River water, China	[23]
	0.0004–5.31 μg g^{-1} dw	Sewage sludge, China	[22]
	21.0–44.5 ng g^{-1} dw	Fish, China	[23]
	26.4–34.0 ng g^{-1} dw	Pig, China	
	17.9–24.7 ng g^{-1} dw	Chicken, China	
	19.6–22.3 ng g^{-1} dw	Cattle, China	
	155–338 ng g^{-1} dw	Vegetables, China	
Benzyl butyl phthalate (BBP)	N.D.—209 pg m^{-3}	Outdoor air, China	
	32.4–64.7 pg g^{-3}	Indoor air, China	
	<0.01 μg m^{-3}	(Greenhouse) air, China	[18]
	<0.01–0.02 μg kg^{-1}	(Greenhouse) soil, China	
	<0.15–1,322 ng g^{-1} dw	Sediment, Korea	[11]
	0.0011–0.0149 μg g^{-1} dw	Sewage sludge, China	[22]
	0.53–1.35 ng L^{-1}	River water, China	[23]
	0.12–1.19 ng g^{-1} dw	Fish, China	
	0.41–1.16 ng g^{-1} dw	Pig, China	
	0.17–0.42 ng g^{-1} dw	Chicken, China	
	0.17–0.92 ng g^{-1} dw	Cattle, China	
	1.03–1.68 ng g^{-1} dw	Vegetables, China	

(*Continued*)

Table 16.1 Occurrence of plasticizers in the environment, concentration ranges, and matrix sources (time span: 2017–2023). (*Continued*)

PAE	Concentration	Matrix, Location	Ref.
Dibutyl phthalate (DBP)	3.5–16,000 ng L^{-1}	Freshwater, Uganda	[8]
	<LOD–65.6 μg L^{-1}	Influent WWTP, Poland	[13]
	<LOD–365.8 μg L^{-1}	Effluent WWTP, Poland	
	<LOD–6.34 μg L^{-1}	(Active) landfill leachates, Poland	
	0.27–2.41 μg L^{-1}	(Close) landfill leachates, Poland	
Di(2-ethylhexyl) phthalate (DEHP)	713–2,600 pg m^{-3}	Outdoor air, China	[23]
	1,550–2,300 pg g^{-3}	Indoor air, China	
	0.03–1.32 μg m^{-3}	(Greenhouse) air, China	[18]
	0.04–1.04 μg kg^{-1}	(Greenhouse) soil, China	
	36.9–1142.2 ng g^{-1} dw	Soil, China	[10]
	1.00–2740 ng g^{-1} dw	Sediment, Korea	[11]
	178.2 ± 422.0 ng L^{-1}	Drinking water, China	[14]
	210–23,000 ng L^{-1}	Freshwater, Uganda	[8]
	73.3–261 ng L^{-1}	River water, China	[23]
	0.326–67.8 μg g^{-1} dw	Sewage sludge, China	[22]
	<LOD–143.3 μg L^{-1}	Influent WWTP, Poland	[13]
	<LOD–27.1 μg L^{-1}	Effluent WWTP, Poland	
	<LOD–249 μg L^{-1}	(Active) landfill leachates, Poland	
	<LOD–143 μg L^{-1}	(Close) landfill leachates, Poland	
	2.05–52.4 ng g^{-1} dw	Fish, China	[23]
	1.00–9.09 ng g^{-1} dw	Pig, China	
	1.83–30.5 ng g^{-1} dw	Chicken, China	
	N.D.–6.78 ng g^{-1} dw	Cattle, China	
	12.6–75.9 ng g^{-1} dw	Vegetables, China	
Di-isononyl phthalate (DINP)	21.3–553 ng g^{-1} dw	Sediment, Korea	[11]
	<LOD–142.8 μg L^{-1}	Influent WWTP, Poland	[13]
	<LOD–25.2 μg L^{-1}	Effluent WWTP, Poland	

(*Continued*)

Table 16.1 Occurrence of plasticizers in the environment, concentration ranges, and matrix sources (time span: 2017–2023). (*Continued*)

PAE	Concentration	Matrix, Location	Ref.
Diisodecyl phthalate (DiDP)	<3.92–169 ng g^{-1} dw	Sediment, Korea	[11]
Dicyclohexyl phthalate (DCHP)	6.9 ng g^{-1} dw	Soil, China	[10]
	0.0014–0.0836 μg g^{-1} dw	Sewage sludge, China	[22]
Dihexyl phthalate (DNHP)	1.5 ng g^{-1} dw	Soil, China	[10]
Hexyl 2-ethylhexyl phthalate (HEHP)	8.7 ng g^{-1} dw		
Dipropyl phthalate (DPP)	<LOD–80.3 μg L^{-1}	Influent WWTP, Poland	[13]
	<LOD–31.2 μg L^{-1}	Effluent WWTP, Poland	
	<LOD–0.96 μg L^{-1}	(Active) landfill leachates, Poland	
	<LOD–11.4 μg L^{-1}	(Close) landfill leachates, Poland	
Diisoheptyl phthalate (DiHP)	<LOD–61.7 μg L^{-1}	Influent WWTP, Poland	
	<LOD–17.7 μg L^{-1}	Effluent WWTP, Poland	
Di-n-octyl Phthalate (DNOP)	0.50–1.06 ng L^{-1}	River water, China	[23]
	0.0036–0.0687 μg g^{-1} dw	Effluent WWTP, Poland	[22]
	N.D.–0.22 ng g^{-1} dw	Fish, China	[23]
	N.D.–0.13 ng g^{-1} dw	Pig, China	
	0.13–0.15 ng g^{-1} dw	Chicken, China	
	N.D.–0.14 ng g^{-1} dw	Cattle, China	
	N.D.–1.37 ng g^{-1} dw	Vegetables, China	
Di(2-ethylhexyl) adipate (DEHA)	12–6,100 ng L^{-1}	Sewage sludge, China	[8]
N-butyl benzenesulfonamide (NBBS)	7.5–200 ng L^{-1}	Freshwater, Uganda	

N.D., not detected; LOD, limit of detection; dw, dry weight.

agriculture, such as mulching and greenhouse cultivation, as well as improper plastic disposal methods, atmospheric deposition, sludge disposal, irrigation with reclaimed water, and landfilling [10, 13, 16, 22]. However, the extent to which PAEs are released from the use and aging of agricultural plastic film remains uncertain, as it is influenced by their concentration, film material, and thickness [15]. Furthermore, it is worth mentioning that

a quick search yields numerous Chinese studies in this field. China's dominance as the primary global producer of vegetables is closely linked to its position as the leading producer and consumer of agricultural films such as mulch and shed. In fact, China boasts an extensive agricultural film coverage area of over 253,333 km^2, which accounts for about 90% of the world's total greenhouse vegetable production [24]. Consequently, it comes as no surprise that soils from China exhibit some of the highest levels of PAEs globally, posing a significant human health risk through soil ingestion and the consumption of contaminated food [17].

Li *et al.* (2021) carried out a study investigating the distribution of 17 PAEs congeners at the soil-air interface in plastic-covered greenhouses from autumn to spring. The highest concentrations of PAEs, whether in the air or soil, were recorded during spring [18]. DEHP was identified as the dominant congener detected in the soil during spring and in the air during both seasons, whereas DiBP was the major congener detected in the soil during autumn. The researchers concluded that the concentrations of both Σ17 PAEs and individual congeners in the greenhouse system are influenced by the partition coefficient of each congener and seasonal variation, which in turn are affected by temperature and farming practices [18]. Furthermore, the study demonstrated that the soil acts as a sink, adsorbing leached PAEs from plastic debris, as even restricted compounds such as DEHP or DnBP, were still detected [18].

Zhu *et al.* (2019) conducted another study to assess the presence of nine PAE congeners in sludge from 46 WWTPs. The study identified DEHP as the predominant congener, followed by DBP and DiBP. Researchers estimated the daily intake of DBP and DEHP from soil amended with sludge, suggesting minor exposure to humans [22]. Kotowska *et al.* (2020) concluded that the efficiency of PAE removal from wastewater through activated sludge depends on the chemical properties of each congener and the amount of coagulant used during the purification process in WWTPs [13]. Moreover, phthalate monoesters (MPAEs), the primary degradation products of PAEs, are typically excreted in urine and frequently detected in wastewater and drinking water [10, 14]. The presence of MPAEs in these environmental matrices highlights the possibility of human exposure to PAEs, leading to concerns regarding their potential impact on human health. For example, the overall intake of DEHP can be estimated from the concentration of mono (2-ethyl-5-hydroxyhexyl) phthalate (MEHHP) in urine [14].

He *et al.* (2020) collected samples from various sources, including indoor and outdoor air, river water, fish, vegetables, and domestic livestock (pigs, chickens, and cattle), in an agricultural region. In all sampled matrices, DEHP, DMP, DEP, BBP, DiBP, and DnBP were detected. Among these PAEs, DnBP is the major congener detected in animal and plant tissues. Vegetable samples exhibited, highest levels of PAEs (330 ng g^{-1} dw), pig samples (51.3 ng g^{-1} dw), fish samples (49.2 ng g^{-1} dw), chicken samples (44.8 ng g^{-1} dw), and cattle samples (30.7 ng g^{-1} dw) [23]. Edwards *et al.* (2021) searched for PAEs and replacement plasticizers in 64 food samples, including hamburgers and chicken burritos, obtained from fast food restaurants in the USA. The results indicated that all tested plasticizers were present in all food samples analyzed. DnBP exhibited the highest incidence, detected in 81% of the samples, followed by DEHP at 70%. In addition, the replacement plasticizers DINCH and DEHA were detected in 14% and 41% of the analyzed samples, respectively [21]. The prevalence of DnBP detected in both studies may be related to its extensive use and may indicate a risk of bioaccumulation within organisms.

16.2.2 Ecotoxicological Effects of PAEs

Given the widespread occurrence of plasticizers in distinct environmental settings, as stated in Table 16.1, it is expected that organisms in terrestrial and aquatic ecosystems encounter and interact with these compounds, which can also be associated with humans. Despite advancements in understanding the toxicological aspects of PAEs, there are still gaps in knowledge regarding their basic toxicological data, metabolic pathways, and potentially harmful effects. This is particularly true for PAEs that are currently not included in the US EPA list [25].

In the ecotoxicology assessment of soil, invertebrates are commonly employed due to their high reproductive capacity, widespread presence, easy collection, and strong interaction with soil [26]. Earthworms, such as *Eisenia fetida*, play a crucial role as indicators of soil pollution due to their importance in soil processes, their sensitivity to environmental contaminants, and their contribution of up to 60% of the total biomass of soil-dwelling animals. These organisms effectively assess the impact of contaminants on soil inhabitants, serving as a dependable benchmark for measuring toxicity and ensuring the safety of the soil environment [27–29].

Studies on the effects of specific plasticizers, such as DEHP and DBP, on earthworms have revealed significant findings. In the case of DEHP, increasing concentrations led to increased malondialdehyde (MDA) and metallothionein (MT) content, elevated superoxide dismutase (SOD) activity, heat shock protein 70 (HSP 70) expression, and genotoxicity parameters of *E. fetida*. Nonetheless, at a low DEHP concentration of 1 mg kg^{-1}, noticeable decreases in peroxidase (POD) activity and neutral red retention time (NRRT) were observed, along with alterations in mitochondrial membrane potential difference values [28]. Similarly, earthworms exposed to various concentrations of DBP exhibited increased antioxidant enzyme activities, apart from the lowest concentration tested, which was 0.1 mg kg^{-1}. Elevated concentrations of DBP led to the excessive production of reactive oxygen species (ROS), causing DNA damage in earthworm coelomocytes and significant increments in MDA content [27]. Furthermore, the exposure of *E. fetida* to di-isononyl phthalate (DiNP) affected the gut microbiome, leading to a decrease in the Chao index and alterations in the abundance of *Chloroflexi*, *Proteobacteria*, and *Ottowia* in the surrounding soil [30]. Additionally, a dose–response correlation was observed between DNA damage and the plasticizers DMP, DnOP, and BBP. Among them, DMP exhibited the highest Olive Tail Moment (OTM) value, indicating the most significant DNA damage, followed by DnOP and BBP [26]. These findings emphasize the potential of PAEs to induce oxidative stress, cytotoxicity, and DNA damage in soil organisms. Moreover, Wu *et al.* (2022) investigated the impact of three PAEs (DEHP, DBP, and DMP) on soil metabolic functions and revealed their disruptive effects on the complexity of the symbiotic network among soil bacterial communities, resulting in a reduction of bacterial interactions. Notably, exposure to DBP caused substantial alterations in the soil metabolite profile, with 100 metabolites showing upregulation and 72 showing downregulation among 172 differential metabolites. Furthermore, the analysis of pathway enrichment provided insight into the effects of DBP, as it was found to interfere with 43 metabolic pathways, including fundamental processes such as residual steroid metabolism and plasticizer metabolism [31].

In a study reported by Gao *et al.* (2019), it was found that wheat plants can absorb and metabolize PAEs, with translocation of the compounds from roots to aboveground tissues

influenced by soil type and PAES concentrations. Higher stress concentrations resulted in increased DBP content in wheat tissues, although the content decreased as the plants continued to grow. The presence of DBP metabolites in both soil and plant tissues indicates that wheat plants can efficiently metabolize DBP into monoesters. This metabolic process was facilitated by the increased content of glutathione S-transferase (GST) and cytochrome P450 (CYP450), suggesting the existence of similar pathways for DBP metabolism and detoxification between plants and mammals [32]. Moreover, DBP adversely affects the germination and growth of *Brassica rapa var. chinensis*, disrupting antioxidant defense and phytohormone balance. It also leads to shifts in microbial populations, particularly in rhizosphere soil and roots, which can impact nutrient availability and ecosystem functions [33]. The ecotoxicological impacts of DBP on vegetables, coupled with the accumulation of DBP or its metabolites in tissues, can potentially increase health risks through the process of bioaccumulation in the food web [26]. These findings underscore the potential hazards linked to PAE exposure through the intake of vegetables cultivated in contaminated soils.

Although soil is commonly identified as a significant reservoir of PAEs, it is important to acknowledge that these compounds have also been found in the aquatic environment. Therefore, it is to be expected that aquatic organisms are affected by the presence of PAEs. Indeed, DBP has been found to induce lipid peroxidation, oxidative stress, and DNA damage in zebra fish (*Dania rerio*) [34]. Similarly, DEHP has been shown to disrupt thyroid hormone activity, reducing the eye size and total body length of Japanese medaka (*Oryzias latipes*) [35]. These findings suggest that exposure to PAEs can lead to cellular damage, developmental abnormalities, and potential health risks to aquatic organisms.

16.2.3 Human Exposure to PAEs

There is a recognized association between phthalate exposure and adverse effects on the endocrine, reproductive, and cardiovascular systems in humans. The concern surrounding human exposure to PAEs is significant because these compounds can be absorbed by a variety of routes, including inhalation, ingestion, and dermal absorption by a variety of sources, including food (e.g., fish, livestock, and vegetables), water, air, dust, and soil [14, 17, 23]. This concern is supported by the high detection frequencies of PAE metabolites in human matrices [36]. It is important to note that human exposure pathways may vary in regions with different PAE sources [23].

Concerning PAE-contaminated soil, both the food chain and dermal adsorption are pointed out as the primary routes of human exposure to these pollutants. The utilization of shed films, specifically PVC or metallocene polyethylene (mPE), which have DEHP concentrations above 140,000 mg kg^{-1} and total PAE concentrations ranging from 2.59 to 359 mg kg^{-1}, illustrates the potential ecological impact of PAEs in agricultural environments [15]. DEHP is readily released into the environment from films at high concentrations and can be absorbed by plant leaves, thus presenting a potential risk of PAE exposure through ingestion. Wang *et al.* (2021) concluded that the DEHP content in the air of plastic greenhouses, particularly those with mPE and PVC films, exceeds the acceptable levels set by the US EPA [15]. Furthermore, Zhou *et al.* (2021) evaluated the non-carcinogenic and carcinogenic risks associated with exposure to PAEs in Huang-Huai-Hai (China). The researchers focused on both non-dietary and dietary exposures to determine the major pathways impacting human health. The study found that the non-carcinogenic risk from dietary DBP

was higher in soils used for vegetable production than in soils used for other crops due to the higher concentration of this substance. For DEHP, the relationship was reversed, except for children in Tianjin Province. The differences in DEHP risk among provinces were influenced by various factors, including the DEHP concentration in each cropping system and the dietary habits of the population. In provinces where DEHP concentrations in vegetable and cropland soils were comparable, population dietary habits emerged as the most important factor influencing the non-carcinogenic risk associated with DEHP. However, in regions with significant differences in DEHP concentrations, soil concentrations were found to be the most important determinant of non-carcinogenic risk from DEHP. Children are more susceptible to non-carcinogenic risks from exposure to PAEs that are not ingested in the diet. Therefore, to accurately assess the health risks associated with PAEs, it is essential to fully consider the type and concentration of PAEs and the dietary habits of the population [25]. This comprehensive approach ensures a more accurate estimation of the potential health effects of PAE exposure.

16.3 Flame Retardants

Flame retardants are used to prevent the ignition of a particular material or to slow the development of a fire. Rather than being chemically bonded, flame retardants are typically blended with polymeric materials. This property facilitates the release of these compounds into the environment through processes such as leaching, volatilization, and abrasion, which can affect various environmental compartments [37–39]. For several decades, halogenated flame retardants, including polybrominated biphenyls (PBBs), polybrominated diphenyl ethers (PBDEs), hexabromocyclododecane (HBCDD), and tetrabromobisphenol A (TBBPA), have been extensively used in various materials such as plastics in electronics, printed circuit boards, and insulation [40, 41]. These compounds exhibit resistance to degradation by chemical, biological, and photolytic processes, making them persistent organic pollutants (POPs) [40, 42].

Owing to their lipophilic nature, halogenated flame retardants have the potential to bioaccumulate in human, animal, and plant tissues, which may lead to adverse environmental and human health effects [42–45]. In fact, exposure to PBDEs has been associated with several human health effects, including diabetes, thyroid disorders, and impairments in executive functions and attention control [41, 44, 46, 47]. Consequently, these chemical compounds have become a matter of international concern, leading to restrictions and legislative bans. For instance, in the EU, the use of BDEs and PBDEs in electrical and electronic devices, systems, and toys is regulated by the European Restriction of Hazardous Substances (RoHS) Directive (2002/95/EC). Moreover, commercial formulations of PBDEs, specifically octabromodiphenyl ether and pentabromodiphenyl ether, were classified as persistent organic pollutants (POPs) and listed for elimination in Annex A of the Stockholm Convention in 2009. In 2013, HBCDD was also added to the list, and in 2017, decabromodiphenyl ether (BDE 209) was added, leading to restrictions on its production, use, or marketing in 2019 [40, 42].

The restrictions have resulted in an increase in the manufacture and use of substitute products such as novel brominated flame retardants (NBFRs) and organophosphorus flame retardants (OPEs) [41, 48]. The recognition of NBFRs as environmental pollutants has

emerged relatively recently, as they have replaced PBDEs in many products [41, 49]. For instance, decabromodiphenyl ethane (DBDPE) is being employed as a replacement for BDE 209 [47]. Recent studies have demonstrated that NBFRs follow the same release mechanisms as PBDEs and exhibit comparable hazardous characteristics when released into the environment, raising concerns about potential environmental and human health impacts [47, 49].

OPEs, which are used not only as flame retardants but also as plasticizers and defoamers, are extensively used in several industries such as plastics, furniture, textiles, construction, electronics, vehicles, and petroleum [37, 48]. OPEs have been hypothesized to be less harmful to human and environmental health due to their shorter half-lives and less persistence than older flame retardants; however, it is worth noting that OPEs have already been detected in water, air, soil, sediments, biota, plants, and biological samples (e.g., urine and breast milk) [38, 45, 50–53]. Despite this, there are limited regulations in place for OPEs [53–55]. Nevertheless, recent toxicological and epidemiological studies suggest that certain OPEs, including tris(2-chloroethyl)phosphate (TCEP), are suspected to be linked to reproductive toxicity, neurotoxicity, endocrine disruption, and carcinogenicity [51, 55]. Therefore, the presence of OPEs in the environment may pose risks to human health via multiple pathways, including dermal contact, inhalation, and both dietary and non-dietary ingestion.

16.3.1 Presence and Accumulation of Flame Retardants in the Environment

In response to the recognition of adverse health effects, the production of PBDE formulations has been phased out in many countries due to guidelines restricting these substances. However, PBDEs can still be detected in several environmental compartments, either due to poor waste management or because products containing them are still in use. Thus, despite the cessation of production, the legacy of PBDEs remains a concern because they can persist in the environment for long periods of time, bioaccumulate, and affect health. For example, a study by Falandysz *et al.* (2019) examined PBDE concentrations in oils and canned livers from the Baltic Sea and North Atlantic from 1972 to 2017. Total concentrations of BDEs varied between 9.9 and 415 ng g^{-1} in oils, while they ranged between 10.5 and 13 ng g^{-1} in canned livers. In all samples, 4,4′-tetrabromodiphenyl ether (BDE-47) was the predominant PBDE, with the highest concentration of 308 ng g^{-1} measured in a Baltic cod liver oil sample from the year 1993 [56].

NBFRs have been reported in atmospheric samples from various regions, including Europe, America, Asia, and Africa. The concentrations of NBFRs in these samples were higher than or comparable to those of PBDEs [49]. A study conducted in Australia analyzed 30 soil samples from different industrial and non-industrial areas. Six NBFRs were detected in 24 of the samples, namely 2-ethylhexyl-2,3,4,5-tetrabromobenzoate (EH-TBB), pentabromoethylbenzene (PBEB), 1,2-bis(2,4,6-tribromophenoxy) ethane (BTBPE), pentabromotoluene (PBT), hexabromobenzene (HBB), and decabromodiphenylethane (DBDPE), with concentrations ranging from non-detectable levels to 384 ng g^{-1} dw. HBB was the predominant compound, while DBDPE had the highest concentrations. The study highlights that electronic polymer manufacturing and waste recycling activities are significant sources of soil pollution in NBFRs. In contrast, non-industrial areas showed minimal impacts. These findings suggest that, similar to PBDEs, NBFRs have the potential to contaminate soil [49].

In a study by Xiong *et al.* (2021), nine NBFRs were detected in soil moss (*Sanionia uncinata*) and lichen (*Usnea aurantiaco-atra*) from Antarctica. The dominant NBFR found was decabromodiphenylethane (DBDPE). Although NBFR concentrations were low, their presence suggests long-range atmospheric transport and deposition into soil, as with the banned BFRs. Moreover, NBFR concentrations were found to be higher in plant samples than in soil samples, indicating a potential for bioaccumulation in wildlife [39]. Furthermore, it should be noted that as the different environmental compartments are interconnected, translocation of contaminants is also expected to occur in aquatic environments.

Regarding OPEs, their concentrations in the environment have shown a gradual increase over time, which is believed to be directly linked to their growing use following the phase-out of halogenated flame retardants. OPEs have higher vapor pressures than PBDEs and can be more readily released into the atmosphere by processes such as volatilization or combustion of products and materials containing them. They can then become airborne and be deposited in water bodies or on land. Environmental measurements have provided clear evidence that OPEs exhibit long-range environmental transport and accumulation comparable to PBDEs, despite initial expectations, classifying them as persistent mobile organic compounds (PMOCs) [55]. Studies indicate that OPEs can indeed bioaccumulate in aquatic environments, including fish, where these compounds gradually accumulate in the tissues over time. Fish are exposed to OPEs primarily through the ingestion of contaminated food and water [38, 57]. In a study conducted by He *et al.* [38] in an agricultural area in Chongqing, China, the concentrations of OPEs in various biotic samples were investigated. The results showed that fish samples with a concentration of 960 ng g^{-1} lw had the highest OPE levels. This was followed by chicken samples with a concentration of 676 ng g^{-1} lw, while samples from cattle had a concentration of 545 ng g^{-1} lw, and samples from pigs exhibited the lowest concentration of 535 ng g^{-1} lw. This bioaccumulation process raises concerns that OPEs may enter the food chain.

High concentrations of triphenyl phosphate (TPhP), tricresyl phosphate (TCP), tri(2-ethylhexyl) phosphate (TEHP), and tris(2-chloroethyl) phosphate (TCEP) have been detected in Lake Victoria, Uganda. The concentrations found were N.D.–8,100 ng L^{-1} for TCP, 24–6,500 ng L^{-1} for TCEP, 54–4,300 ng L^{-1} for TPhP, and N.D.–4,300 ng L^{-1} for TEHP. The high concentrations may be attributed to the lack of strict regulations for the disposal of OPE-containing industrial waste, but also to atmospheric deposition [8]. In a study by Wang *et al.* [48], 75 sewage sludge samples from 67 WWTPs were analyzed and a mean concentration of 1,290 ng g^{-1} dw (∑20 OPEs) was found, with tributoxyethyl phosphate (TBEP) and TEHP being the most abundant compounds. These findings highlight that OPEs can accumulate in sewage sludge and can transfer from soil to crops when applied as fertilizers in agriculture.

In plants, the accumulation of OPEs varies among different cultivars, as observed by Hu *et al.* [45], with carrots (*Daucus carota L.*) exhibiting a higher preference for OPE enrichment compared to maize (*Zea mays L.*). The behavior of OPEs in the soil-plant system is affected by the characteristics of both plant (lipid content) and OPES (hydrophobicity and molecular geometry). OPEs exhibit a broad range of K_{OW}, indicating diverse environmental behavior within congeners. Plants with a high lipid content tend to accumulate hydrophobic chemicals, and this accumulation is influenced by root lipid substances, primarily affecting the distribution of organic compounds near the root epidermis. Although the specific role of plant lipid content in the uptake and movement of OPEs remains unclear, it may contribute to the overall fate of OPEs in the soil-plant system. Additionally, OPEs with

electron-ring substituents such as tris(methylphenyl) phosphate (TMPP), TPhP, tris(1,3-dichloro-2-propyl) phosphate (TDCPP), and TCPP have higher potential for uptake by plant roots compared to OPEs with open-chain substituents such as tri-n-butyl phosphate (TnBP), 2-ethylhexyl diphenyl phosphate (EHDPP), TEP, TEHP, TCEP, and TBOEP. The variance in uptake ability can be attributed to the electron-rich structure of OPEs, which enables stronger non-covalent interactions and promotes their enhanced sorption onto charged surfaces of roots [45]. Furthermore, hydrolysis of organophosphate triesters into their metabolites was observed in the cell wall of wheat plants (*Triticum aestivum L.*), suggesting that organophosphate diesters have higher stability in plants compared to organophosphate triesters [58].

A study conducted in China investigated the occurrence and distribution of 14 OPEs in 65 road dust samples. Among the OPEs analyzed, tris(2-chloro-1-methylethyl) phosphate (TCPP) was the most abundant, with a concentration of 384 mg kg^{-1} [59]. Another study conducted at a recycling facility concluded that primitive outdoor recycling operations and open storage of waste were the primary factors for the release and dispersion of OPEs into the soil and surrounding dust. The levels of TCEP, TPhP, and TMPP in the soil indicated a significant ecotoxicological risk at the outdoor waste recycling facilities. In addition to the risk of environmental contamination, the study also highlighted the occupational risk associated with working at these recycling sites. Workers may be exposed through dermal contact, ingestion, or inhalation, which may pose health risks [60]. Table 16.2 provides some examples of the presence of NBFR and OPE in the environment. The table includes information on concentration ranges and the sources of these flame retardants in several matrices.

16.3.2 Ecotoxicological Effects of Flame Retardants

Owing to their lipophilic nature, high octanol-water partition coefficients (K_{OW}) values, and poor water solubility, numerous flame retardants tend to persist in water bodies and sediments. The persistence of flame retardants in aquatic environments raises substantial concerns due to their potential to bioaccumulate and trigger harmful effects in exposed organisms [57]. Pollutants can have a dual effect on organisms, directly impacting their immune, reproductive, or endocrine systems while also leading to diverse changes in bioenergetics and the development of tissues and specimens [61].

Marine mussels such as *Mytilus galloprovincialis* are commonly employed as bioindicators owing to their ability to accumulate and withstand high concentrations of environmental pollutants. The exposure of *M. galloprovincialis* to environmentally relevant concentrations of BDE-47 was found to significantly affect cell activity within the digestive gland. The limited elimination of BDE-47 through biotransformation, observed after a 30-day period, may have long-term effects on the growth, survival, and reproduction of *M. galloprovincialis* [61]. In juvenile crucian carp (*Carassius auratus*), exposure to environmentally relevant doses of HBCDD resulted in the accumulation of the substance primarily in liver and muscle tissue. The decrease in thyroxine and total triiodothyronine levels indicated a disruption in the thyroid hormone function of *C. auratus* [62]. Thyroid function plays an essential role in regulating various physiological processes, including cell development, thermoregulation, metabolism, growth, and reproduction. TPhP also affects thyroid function in fish, mammals, and birds. In Japanese quail (*Coturnix japonica*), TPhP exposure did not affect

Table 16.2 Occurrence of NBFRs and OPES in the environment, concentration ranges, and matrix sources (time span: 2017–2023). N.D., not detected; MDL, method detection limit; LOD, limit of detection; dw, dry weight; lw, lipid weight.

Substances	Concentration	Matrix, Location	Ref.
Decabromodiphenyl ethane (DBDPE)	N.D.–384 ng g^{-1} dw	Soil manufacturing industries, Australia	[49]
	N.D.–295 ng g^{-1} dw	Soil waste disposal facilities, Australia	
1,2-Bis(2,4,6-tribromophenoxy) ethane (BTBPE)	N.D.–63.8 ng g^{-1} dw	Soil, manufacturing industries, Australia	
	N.D.–11.4 ng g^{-1} dw	Soil, waste disposal facilities, Australia	
2-Ethylhexyl-2,3,4,5-tetrabromobenzoate (EH-TBB)	N.D.–1.79 ng g^{-1} dw	Soil, waste disposal facilities, Australia	
Pentabromotoluene (PBT)	N.D.–0.10 ng g^{-1} dw	Soil, waste disposal facilities, Australia	
Hexabromobenzene (HBB)	N.D.–1.37 ng g^{-1} dw	Soil, manufacturing industries, Australia	
	N.D.–90.9 ng g^{-1} dw	Soil, waste disposal facilities, Australia	
Trimethyl phosphate (TMP)	3.03 μg kg^{-1} dw	Road dust, China	[59]
	3.81–242 ng g^{-1} lw	Fish, China	[38]
	0.69–50.0 ng g^{-1} lw	Pig, China	
	1.59–15.6 ng g^{-1} lw	Chicken, China	
	N.D.–18.2 ng g^{-1} lw	Cattle, China	
	N.D.–1.39 ng g^{-1} lw	Vegetables, China	
Tris(methylphenyl) phosphate (TMPP)	61.6 μg kg^{-1} dw	Road dust, China	[59]
	35.2–100 ng g^{-1} dw	Sludge cake, USA	[71]
	20.1–405 ng L^{-1}	WW influent, USA	
	11.5–181 ng g^{-1} lw	Fish, China	35]
	4.59–315 ng g^{-1} lw	Pig, China	
	8.00–1,090 ng g^{-1} lw	Chicken, China	
	10.8–97.0 ng g^{-1} lw	Cattle, China	
	0.81–20.8 ng g^{-1} lw	Vegetables, China	

(*Continued*)

Table 16.2 Occurrence of NBFRs and OPES in the environment, concentration ranges, and matrix sources (time span: 2017–2023). N.D., not detected; MDL, method detection limit; LOD, limit of detection; dw, dry weight; lw, lipid weight. (*Continued*)

Substances	Concentration	Matrix, Location	Ref.
Triethyl phosphate (TEP)	<LOD–29 ng L^{-1}	Freshwater, Uganda	[8]
	53.7 μg kg^{-1} dw	Road dust, China	[59]
	2.99–189 ng g^{-1} dw	Sludge cake, USA	[71]
	184–775 ng L^{-1}	WW influent, USA	
	N.D.–0.42 ng g^{-1} dw	Farmland soil, China	[60]
	1.90–18.1 ng g^{-1} lw	Fish, China	[38]
	N.D.–8.02 ng g^{-1} lw	Pig, China	
	0.94–9.52 ng g^{-1} lw	Chicken, China	
	2.39–14.8 ng g^{-1} lw	Cattle, China	
	N.D.–0.95 ng g^{-1} lw	Vegetables, China	
Tripropyl phosphate (TPrP)	<LOD	Road dust, China	[59]
	4.57–14.0 ng g^{-1} lw	Fish, China	35]
	N.D.–15.4 ng g^{-1} lw	Pig, China	
	2.61–55.6 ng g^{-1} lw	Chicken, China	
	4.44–24.2 ng g^{-1} lw	Cattle, China	
	N.D.–2.04 ng g^{-1} lw	Vegetables, China	
Tri-n-butylphosphate (TnBP)	41.1 μg kg^{-1} dw	Road dust, China	[59]
	13.8–106 ng g^{-1} dw	Sludge cake, USA	[71]
	50.8–649 ng L^{-1}	WW influent, USA	
	<MDL–4.59 ng g^{-1} dw	Farmland soil, China	[60]
	37.0–2,380 ng g^{-1} lw	Fish, China	[38]
	24.7–217 ng g^{-1} lw	Pig, China	
	30.2–1,260 ng g^{-1} lw	Chicken, China	
	49.7–461 ng g^{-1} lw	Cattle, China	
	N.D.–2.04 ng g^{-} lw	Vegetables, China	
Tributyl phosphate (TBP)	9.6–500 ng L^{-1}	Freshwater, Uganda	[8]

(*Continued*)

Table 16.2 Occurrence of NBFRs and OPES in the environment, concentration ranges, and matrix sources (time span: 2017–2023). N.D., not detected; MDL, method detection limit; LOD, limit of detection; dw, dry weight; lw, lipid weight. (*Continued*)

Substances	Concentration	Matrix, Location	Ref.
Tri-iso-butylphosphate (TiBP)	20.3 μg kg^{-1} dw	Road dust, China	[59]
	0.608–131 ng g^{-1} dw	Sludge cake, USA	[71]
	57.9–102 ng L^{-1}	WW influent, USA	
	<MDL–4.68 ng g^{-1} dw	Farmland soil, China	[60]
	N.D.–312 ng g^{-1} lw	Fish, China	[38]
	20.1–141 ng g^{-1} lw	Pig, China	
	28.6–262 ng g^{-1} lw	Chicken, China	
	23.9–370 ng g^{-1} lw	Cattle, China	
	1.18–9.55 ng g^{-1} lw	Vegetables, China	
Tris(2-chloro-1-methylethyl) phosphate (TCPP)	25–600 ng L^{-1}	Freshwater, Uganda	[8]
	1,010 μg kg^{-1} dw	Road dust, China	[59]
Tris(1-chloro-2-propyl)phosphate (TCIPP)	132–661 ng g^{-1} dw	Sludge cake, USA	[71]
	820–145,000 ng L^{-1}	WW influent, USA	
	<MDL–16.8 ng g^{-1} dw	Farmland soil, China	[60]
Tributoxyethylphosphate (TBEP)	73.8 μg kg^{-1} dw	Road dust, China	[59]
Tripropyl phosphate (TPP)	3.07–10.3 ng g^{-1} dw	Sludge cake, USA	[71]
	5.65–45.8 ng L^{-1}	WW influent, USA	
Tri(2-ethylhexyl) phosphate (TEHP)	<LOD–4,300 ng L^{-1}	Freshwater, Uganda	[8]
	5.97 μg kg^{-1} dw	Road dust, China	[59]
	607–2,750 ng g^{-1} dw	Sludge cake, USA	[71]
	13.1–1,850 ng L^{-1}	WW influent, USA	
	1.26–45.7 ng g^{-1} dw	Farmland soil, China	[60]
Tris(2-chloroethyl) phosphate (TCEP)	24–6,500 ng L^{-1}	Freshwater, Uganda	[8]
	397 μg kg^{-1} dw	Road dust, China	[59]
	48.6–109 ng g^{-} dw	Sludge cake, USA	[71]
	195–8,450 ng L^{-1}	WW influent, USA	

(*Continued*)

Table 16.2 Occurrence of NBFRs and OPES in the environment, concentration ranges, and matrix sources (time span: 2017–2023). N.D., not detected; MDL, method detection limit; LOD, limit of detection; dw, dry weight; lw, lipid weight. (*Continued*)

Substances	Concentration	Matrix, Location	Ref.
	1.72–3.79 ng g^{-1} dw	Farmland soil, China	[60]
	17.1–159 ng g^{-1} lw	Fish, China	[38]
	11.1–116 ng g^{-1} lw	Pig, China	
	9.31–135 ng g^{-1} lw	Chicken, China	
	15.3–123 ng g^{-1} lw	Cattle, China	
	1.54–5.26 ng g^{-1} lw	Vegetables, China	
Tricresyl phosphate (TCP)	<LOD–8,100 ng L^{-1}	Freshwater, Uganda	[8]
Triphenyl phosphate (TPhP)	54–4,300 ng $^{-1}$	Freshwater, Uganda	[8]
	103 μg kg^{-1} dw	Road dust, China	[59]
	223–688 ng g^{-1} dw	Sludge cake, USA	[71]
	187–845 ng L^{-1}	WW influent, USA	
	0.53–8.33 ng g^{-1} dw	Farmland soil, China	[60]
	211–18,912 ng g^{-1}	Indoor air (homes and offices), Spain	[72]
	172–12,853 ng g^{-1}	Indoor air (homes and offices), Netherlands	
	3.49–59.6 ng g^{-1} lw	Fish, China	[38]
	2.64–36.4 ng g^{-1} lw	Pig, China	
	3.76–92.1 ng g^{-1} lw	Chicken, China	
	3.82–4.44 ng g^{-1} lw	Cattle, China	
	N.D.–2.21 ng g^{-1} lw	Vegetables, China	
Cresyldiphenylphosphate (CDPP)	33.0 μg kg^{-1} dw	Road dust, China	[59]
2-Ethylhexyl diphenyl phosphate (EHDPP)	22 μg kg^{-1} dw		
	22.2 μg kg^{-1} dw		
	7.7–730 ng L^{-1}	Freshwater, Uganda	[8]
	121–427 ng g^{-1} dw	Sludge cake, USA	[71]

(*Continued*)

Table 16.2 Occurrence of NBFRs and OPES in the environment, concentration ranges, and matrix sources (time span: 2017–2023). N.D., not detected; MDL, method detection limit; LOD, limit of detection; dw, dry weight; lw, lipid weight. (*Continued*)

Substances	Concentration	Matrix, Location	Ref.
	1.12–4.58 ng g^{-} dw	Farmland soil, China	[60]
Tris (2-butoxyethyl)phosphate (TBOEP)	21.1–59.9 ng g^{-1} dw		
	N.D.–112 ng g^{-1} lw	Fish, China	[38]
	3.49–38.9 ng g^{-1} lw	Pig, China	
	N.D.–119 ng g^{-1} lw	Chicken, China	
	9.56–62.6 ng g^{-1} lw	Cattle, China	
	0.62–4.45 ng g^{-1} lw	Vegetables, China	
	2,490–13,500 ng g^{-1} dw	Sludge cake, USA	[71]
	129–69,500 ng L^{-1}	WW influent, USA	
Tris(2,3-dibromopropyl) phosphate (TDBPP)	288–397 ng g^{-1} dw	Sludge cake, USA	
	370–530 ng L^{-1}	WW influent, USA	
Tris(1,3-dichloro-2-propyl) phosphate (TDCPP)	431–1,700 ng g^{-1} dw	Sludge cake, USA	
	259–3,450 ng L^{-1}	WW influent, USA	
	37.2 μg kg^{-1} dw	Road dust, China	[59]
	<MDL–28.3 ng g^{-1} dw	Farmland soil, China	[60]
	N.D.–381 ng g^{-1} lw	Fish, China	[38]
	16.0–163 ng g^{-1} lw	Pig, China	
	8.82–110 ng g^{-1} lw	Chicken, China	
	N.D.–117 ng g^{-1} lw	Cattle, China	
	N.D.–5.86 ng g^{-1} lw	Vegetables, China	
p,p′-1,3-Phenylenep,p,p′,p′-tetraphenylesterphosphate (PBDPP)	54.1–555 ng g^{-1} dw	Sludge cake, USA	[71]
	99.0–2,660 ng L^{-1}	WW influent, USA	
Diphenylphosphate (DPHP)	10.9–210 ng g^{-1} dw	Sludge cake, USA	
	30.0–1,290 ng L^{-1}	WW influent, USA	
	106–1,251 ng g^{-1}	Indoor air (homes and offices), Spain	[72]
	151–4,189 ng g^{-1}	Indoor air (homes and offices), Netherlands	

mRNA expression of thyroid-related genes, but it had differential effects on thyroid structure and activity in males and females. Males showed increased thyroid structure at high TPhP exposure, whereas females had suppressed thyroid structure and activity across all TPhP exposure levels. In addition, highly-TPhP-exposed females showed a decrease in circulating free triiodothyronine levels [63].

The presence of flame retardants can also lead to ecotoxicological effects on soil inhabitants, including earthworms. Exposure to BDE-209 and BDE-47 can induce toxic effects in *E. fetida*, affecting various biological processes including nerve activities, osmoregulation, the tricarboxylic acid cycle, energy metabolism, and amino acid metabolism [64]. Moreover, when exposed to soil contaminated with tris(2-butoxyethyl) phosphate (TBOEP), *E. fetida* experienced various detrimental effects. These included the inhibition of acetylcholinesterase activity, leading to neurotoxicity. Moreover, there was a decrease in the rate of weight gain, indicating developmental toxicity, and a reduction in the number of juveniles, indicating reproductive toxicity [65]. Additionally, it has been observed that TnBP can accumulate in earthworm cerebral ganglions, reducing glutamate levels and increasing Ca^{2+} concentration, resulting in an osmotic imbalance in the nervous tissue and leading to apoptotic cell death. Moreover, exposure to 1,2-dibromo-4-(1,2 dibromoethyl) cyclohexane (TBECH), a NBFR, was found to induce toxic effects on *Z. mays L.*, specifically inducing or inhibiting GST and CYP activities and gene expressions, suggesting its bioaccumulation and biotransformation within the plant [66]. These toxic effects on important physiological pathways of terrestrial organisms highlight the potential harm that flame retardants can cause to the environment and human health.

16.4 Human Exposure to Flame Retardants

As a result of the widespread use of flame retardants in the environment, flame retardants can be encountered by humans through multiple pathways, including inhalation of airborne compounds, ingestion of contaminated water and food, or dermal contact with products containing flame retardants [8, 38, 45, 67].

The frequent hand-to-mouth and object-to-mouth behaviors of children increase their susceptibility to bioaccumulating lipophilic compounds, including flame retardants, from indoor dust in comparison to adults [67]. Although accumulation through dietary exposure and breastfeeding is possible, non-dietary pathways, particularly exposure through house dust, play a more substantial role in the accumulation process among children [53, 67, 68]. In a multi-country European study, the presence of PBDEs in the blood of children from four countries and OPEs in the urine of children from eight countries was examined. This study revealed that the levels of BDE-47 in blood samples recently collected from children were similar to or lower than those found in adult samples from previous years, indicating that regulations on PBDEs have effectively reduced human exposure to these compounds. This means that the concentrations of OPEs require careful evaluation due to their extensive occurrence and potential endocrine-disrupting effects, which in turn impact cognitive ability, reproduction, and metabolism. Bis(1,3-dichloro-2-propyl) phosphate (BDCIPP) and diphenyl phosphate (DPHP), which are metabolites of TDCIPP and TPhP, respectively, were found to be widely distributed across Europe with minimal variations between countries, possibly influenced by open market conditions. The authors of

this study faced difficulties in identifying specific lifestyle factors that could be attributed to flame retardant concentrations. However, they observed correlations between flame retardant concentrations and factors such as socioeconomic status, cleaning practices, and the physical characteristics of residences [53].

The liver is widely acknowledged as the primary site of toxicity for xenobiotic compounds in mammals [68, 69]. In a recent study by Saquib *et al.* (2022), transcriptomic changes caused by TBEP were demonstrated in human liver cells (HepG2). This study revealed the activation of cancer pathway genes following exposure to TBEP. Furthermore, TBEP induced DNA damage and disrupted the cell cycle, resulting in apoptosis of HepG2 cells. Additionally, TBEP was found to increase oxidative stress levels (triggered by reactive oxygen species (ROS) and nitric oxide), induce the influx of Ca^{2+}, and disrupt mitochondrial function in liver cells. These findings provide valuable information regarding the potential cytotoxic effects of TBEP on liver cells and are supported by the study conducted by Zhou *et al.* [69]. Nevertheless, depending on whether the OPEs are aryl, halogenated, or alkyl, their effects on ROS production, DNA damage, and endoplasmic reticulum (ER) stress can vary. For instance, elevated ER stress was observed after exposure to aryl-OPEs, while alkyl-OPEs contributed to the overproduction of ROS and DNA damage, and induced cytotoxicity and apoptosis [68].

Metabolic processes mediated by CYP450 and phase II enzymes such as GST in human hepatic fractions significantly contribute to the metabolism of OPEs, resulting in the formation of hydroxylated and dealkylated metabolites. Consequently, renal excretion is the primary pathway for the elimination of OPEs such as TCEP [52, 70]. A Chinese study estimated the renal (CL_{renal}) and hepatic (CL_h) clearance rates of OPEs and their corresponding diester metabolites in the human body using 30 paired samples of human plasma urine. CL_{renal} values were estimated based on the concentration of organophosphate diester metabolites in urine, whereas CL_h was estimated by extrapolating the *in vitro* intrinsic clearance data of organophosphate diester metabolites in human liver microsomes (CL_{HLM}). The study reported that the median total concentration of OPEs in plasma varied from 0.53 to 6.52 ng mL^{-1}. Additionally, the total concentration of metabolites in urine ranged from 0.35 to 5.95 ng mL^{-1}. The CL_{renal} of TPhP, TCEP, and TDCIPP were estimated to be 68.9, 50.9, and 33.3 mL/kg/day, respectively. Similarly, the CL_h presented the same order, with TPhP having the highest clearance rate (166 mL/kg/day), followed by TCEP (35.3 mL/kg/day), and TDCIPP (20.6 mL/kg/day). The CL_{HLM} of these three OPEs decreased in the following order: TPhP (0.0308 mL/mg protein/min), TDCIPP (0.0034 mL/mg protein/min), and TCEP (0.0006 mL/mg protein/min). The discrepancies between the CL_{renal} and CL_{HLM} trends, as observed for TDCIPP, suggest that the clearance of OPEs in humans is influenced by both their intrinsic metabolic characteristics and their affinity for plasma proteins. The binding of OPEs to plasma proteins can reduce CL_{renal}, thereby explaining the observed differences. This study suggests that the half-lives of chlorinated OPEs (TCEP and TDCIPP) in humans, estimated based on CL_h, are longer than those of aryl-OPEs (TPhP and EHDPP) and alkyl-OPEs (TnBP and TBOEP) [70]. Furthermore, BDCIPP has been detected in the urine of more than 90% of Americans, indicating widespread exposure to TDCIPP in the population. Epidemiological studies have revealed sex-specific associations between metabolic syndrome and urinary BDCPP levels, a known risk factor for conditions such as heart disease, stroke type, and type 2 diabetes. The potential effect of TDCIPP exposure on glucose regulation was studied using a mouse model [52].

16.5 Conclusion

Plastic additives play a key role in improving the properties and performance of polymers. However, caution is needed in their use, as their occurrence and persistence in the environment have raised concerns regarding their potential ecotoxicological effects. Studies focusing on earthworms have provided significant insights into the effects of specific plasticizers, such as DEHP and DBP, suggesting the potential toxicity of PAEs in soils. Furthermore, wheat plants have been found to absorb and metabolize PAEs, indicating the possibility of bioaccumulation through the food web. Despite advancements in the understanding of the toxicology of PAEs, there are still gaps in knowledge regarding their toxicological data, metabolic pathways, and harmful effects, especially for non-prioritized PAEs. Flame retardants are known to persist in the environment and accumulate in organisms, posing a risk to ecosystems. They have been detected in indoor environments, water bodies, and food items, with potential adverse health effects as ongoing research suggests associations with developmental, reproductive, endocrine, and neurotoxic effects, particularly in infants and children. While certain additives have been linked to adverse effects, more studies are needed to understand their long-term consequences and establish comprehensive regulatory frameworks. It is vital to continue exploring alternatives to unsafe additives and promote plastic waste management practices to mitigate potential risks to the environment and human health.

Acknowledgments

This work received financial support from national funds of Portugal, specifically from the Fundação para a Ciência e a Tecnologia (FCT)/Ministério da Ciência, Tecnologia e Ensino Superior (MCTES), through the following projects: UIDB/50006/2020, UIDP/50006/2020, and LA/P/0008/2020. The authors express their gratitude to the FCT/MCTES for their support through project MTS/SAS/0077/2020 (Honey+—New reasons to care honey from the Natural Park of Montesinho: A bioindicator of environmental quality and its therapeutic potential), project number 2022.15094.CBM (a Bilateral Cooperation between Portugal and France under the 2023-2024 Person Program), project number 49190WH (PHC PESSOA 2023) and BiodivRestore Joint Call 2020–2021-European Union's Horizon 2020 research and innovation programme under grant agreement No 101003777-BiodivRestore-406/DivRestore/0002/2020, "BioReset—Biodiversity restoration and conservation of inland water ecosystems for environmental and human well-being." Diana thanks FCT/MCTES and the European Social Fund (ESF) through NORTE 2020 (Programa Operacional Região Norte) for her PhD grant SFRH/BD/147404/2019.

References

1. Fred-Ahmadu, O.H., Bhagwat, G., Oluyoye, I., Benson, N.U., Ayejuyo, O.O., Palanisami, T., Interaction of chemical contaminants with microplastics: Principles and perspectives. *Sci. Total Environ.*, 706, 135978, 2020.

2. Hahladakis, J.N., Velis, C.A., Weber, R., Iacovidou, E., Purnell, P., An overview of chemical additives present in plastics: Migration, release, fate and environmental impact during their use, disposal and recycling. *J. Hazard. Mater.*, 344, 179–199, 2018.
3. Horton, A.A., Walton, A., Spurgeon, D.J., Lahive, E., Svendsen, C., Microplastics in freshwater and terrestrial environments: Evaluating the current understanding to identify the knowledge gaps and future research priorities. *Sci. Total Environ.*, 586, 127–141, 2017.
4. Li, Q., Zeng, A., Jiang, X., Gu, X., Are microplastics correlated to phthalates in facility agriculture soil? *J. Hazard. Mater.*, 412, 125164, 2021.
5. Luo, H., Zhao, Y., Li, Y., Xiang, Y., He, D., Pan, X., Aging of microplastics affects their surface properties, thermal decomposition, additives leaching and interactions in simulated fluids. *Sci. Total Environ.*, 714, 136862, 2020.
6. Hermabessiere, L., Dehaut, A., Paul-Pont, I., Lacroix, C., Jezequel, R., Soudant, P., Duflos, G., Occurrence and effects of plastic additives on marine environments and organisms: A review. *Chemosphere*, 182, 781–793, 2017.
7. European Chemicals Agency, ECHA (The European Chemicals Agency), in: *Encyclopedia of Toxicology*, Third Edition, P. Wexler, (Ed.), pp. 263–264, Academic Press, Oxford, 2014.
8. Nantaba, F., Palm, W.U., Wasswa, J., Bouwman, H., Kylin, H., Kümmerer, K., Temporal dynamics and ecotoxicological risk assessment of personal care products, phthalate ester plasticizers, and organophosphorus flame retardants in water from Lake Victoria, Uganda. *Chemosphere*, 262, 127716, 2021.
9. Saghir, S.A., Absorption, in: *Encyclopedia of Toxicology*, Third Edition, P. Wexler, (Ed.), pp. 1–6, Academic Press, Oxford, 2014.
10. Hu, A., Qiu, M., Liu, H., Xu, Y., Tao, Y., Yang, G., He, Y., Xu, J., Lu, Z., Simultaneous determination of phthalate diesters and monoesters in soil using accelerated solvent extraction and ultra-performance liquid chromatography coupled with tandem mass spectrometry. *J. Chromatogr. A*, 1626, 461347, 2020.
11. Lee, Y.S., Lim, J.E., Lee, S., Moon, H.B., Phthalates and non-phthalate plasticizers in sediment from Korean coastal waters: Occurrence, spatial distribution, and ecological risks. *Mar. Pollut. Bull.*, 154, 111119, 2020.
12. Li, Q., Wu, J., Zhao, X., Gu, X., Ji, R., Separation and identification of microplastics from soil and sewage sludge. *Environ. Pollut.*, 254, 113076, 2019.
13. Kotowska, U., Kapelewska, J., Sawczuk, R., Occurrence, removal, and environmental risk of phthalates in wastewaters, landfill leachates, and groundwater in Poland. *Environ. Pollut.*, 267, 115643, 2020.
14. Ding, M., Kang, Q., Zhang, S., Zhao, F., Mu, D., Zhang, H., Yang, M., Hu, J., Contribution of phthalates and phthalate monoesters from drinking water to daily intakes for the general population. *Chemosphere*, 229, 125–131, 2019.
15. Wang, Y., Wang, F., Xiang, L., Gu, C., Redmile-Gordon, M., Sheng, H., Wang, Z., Fu, Y., Bian, Y., Jiang, X., Risk assessment of agricultural plastic films based on release kinetics of phthalate acid esters. *Environ. Sci. Technol.*, 55, 3676, 2021.
16. He, W., Yang, H., Pu, Q., Li, Y., Novel control strategies for the endocrine-disrupting effect of PAEs to pregnant women in traffic system. *Sci. Total Environ.*, 851, 158269, 2022.
17. Lü, H., Mo, C.H., Zhao, H.M., Xiang, L., Katsoyiannis, A., Li, Y.W., Cai, Q.Y., Wong, M.H., Soil contamination and sources of phthalates and its health risk in China: A review. *Environ. Res.*, 164, 417–429, 2018.
18. Li, Y., Wang, J., Yang, S., Zhang, S., Occurrence, health risks and soil-air exchange of phthalate acid esters: A case study in plastic film greenhouses of Chongqing, China. *Chemosphere*, 268, 128821, 2021.

19. Commission Regulation (EU) 2016/26 of 13 Jan 2016 amending Annex XVII to Regulation (EC) No 1907/2006 of the European Parliament and of the Council concerning the Registration, Evaluation, Authorisation and Restriction of Chemicals (REACH) as regards nonylphenol ethoxylates. *Focus Surfactants*, 2016, 5–6, 2016.
20. Correia-Sá, L., Schütze, A., Norberto, S., Calhau, C., Domingues, V.F., Koch, H.M., Exposure of Portuguese children to the novel non-phthalate plasticizer di-(iso-nonyl)-cyclohexane-1,2-dicarboxylate (DINCH). *Environ. Int.*, 102, 79–86, 2017.
21. Edwards, L., McCray, N.L., VanNoy, B.N., Yau, A., Geller, R.J., Adamkiewicz, G., Zota, A.R., Phthalate and novel plasticizer concentrations in food items from U.S. fast food chains: A preliminary analysis. *J. Expo. Sci. Environ. Epidemiol.*, 32, 366–373, 2022.
22. Zhu, Q., Jia, J., Zhang, K., Zhang, H., Liao, C., Spatial distribution and mass loading of phthalate esters in wastewater treatment plants in China: An assessment of human exposure. *Sci. Total Environ.*, 656, 862–869, 2019.
23. He, M.J., Lu, J.F., Wang, J., Wei, S.Q., Hageman, K.J., Phthalate esters in biota, air and water in an agricultural area of western China, with emphasis on bioaccumulation and human exposure. *Sci. Total Environ.*, 698, 134264, 2020.
24. Ma, T., Zhou, W., Chen, L., Li, Y., Luo, Y., Wu, P., Phthalate esters contamination in vegetable–soil system of facility greenhouses in Jingmen, central China and the assessment of health risk. *Environ. Geochem. Health*, 42, 2703–2721, 2020.
25. Zhou, B., Zhao, L., Sun, Y., Li, X., Weng, L., Li, Y., Contamination and human health risks of phthalate esters in vegetable and crop soils from the Huang-Huai-Hai region of China. *Sci. Total Environ.*, 778, 146281, 2021.
26. Song, P., Gao, J., Li, X., Zhang, C., Zhu, L., Wang, J., Wang, J., Phthalate induced oxidative stress and DNA damage in earthworms (Eisenia fetida). *Environ. Int.*, 129, 10–17, 2019.
27. Wang, G., Wang, J., Zhu, L., Wang, J., Li, H., Zhang, Y., Liu, W., Gao, J., Oxidative Damage and Genetic Toxicity Induced by DBP in Earthworms (Eisenia fetida). *Arch. Environ. Contam. Toxicol.*, 74, 527–538, 2018.
28. Ma, T., Zhou, W., Chen, L., Wu, L., Christie, P., Zhang, H., Luo, Y., Toxicity effects of di-(2-ethylhexyl) phthalate to Eisenia fetida at enzyme, cellular and genetic levels. *PloS One*, 12, e0173957, 2017.
29. Li, X., Li, N., Wang, C., Wang, A., Kong, W., Song, P., Wang, J., Occurrence of Phthalate Acid Esters (PAEs) in Protected Agriculture Soils and Implications for Human Health Exposure. *Bull. Environ. Contam. Toxicol.*, 109, 548, 2022.
30. Zhang, Y., Yang, Z., Li, X., Song, P., Wang, J., Effects of diisononyl phthalate exposure on the oxidative stress and gut microorganisms in earthworms (Eisenia fetida). *Sci. Total Environ.*, 822, 153563, 2022.
31. Wu, C., Ma, Y., Wang, D., Shan, Y., Song, X., Hu, H., Ren, X., Ma, X., Luo, J., Cui, J., Ma, Y., Microbiology combined with metabonomics revealing the response of soil microorganisms and their metabolic functions exposed to phthalic acid esters. *Ecotoxicol. Environ. Saf.*, 233, 113338, 2022.
32. Gao, M., Dong, Y., Zhang, Z., Song, Z., Metabolism and distribution of dibutyl phthalate in wheat grown on different soil types. *Chemosphere*, 236, 124293, 2019.
33. Ge, J., Cheng, J., Li, Y., Li, Q.X., Yu, X., Effects of dibutyl phthalate contamination on physiology, phytohormone homeostasis, rhizospheric and endophytic bacterial communities of Brassica rapa var. chinensis. *Environ. Res.*, 189, 109953, 2020.
34. Song, P., Jiang, N., Zhang, K., Li, X., Li, N., Zhang, Y., Wang, Q., Wang, J., Ecotoxicological evaluation of zebrafish liver (Danio rerio) induced by dibutyl phthalate. *J. Hazard. Mater.*, 425, 128027, 2022.

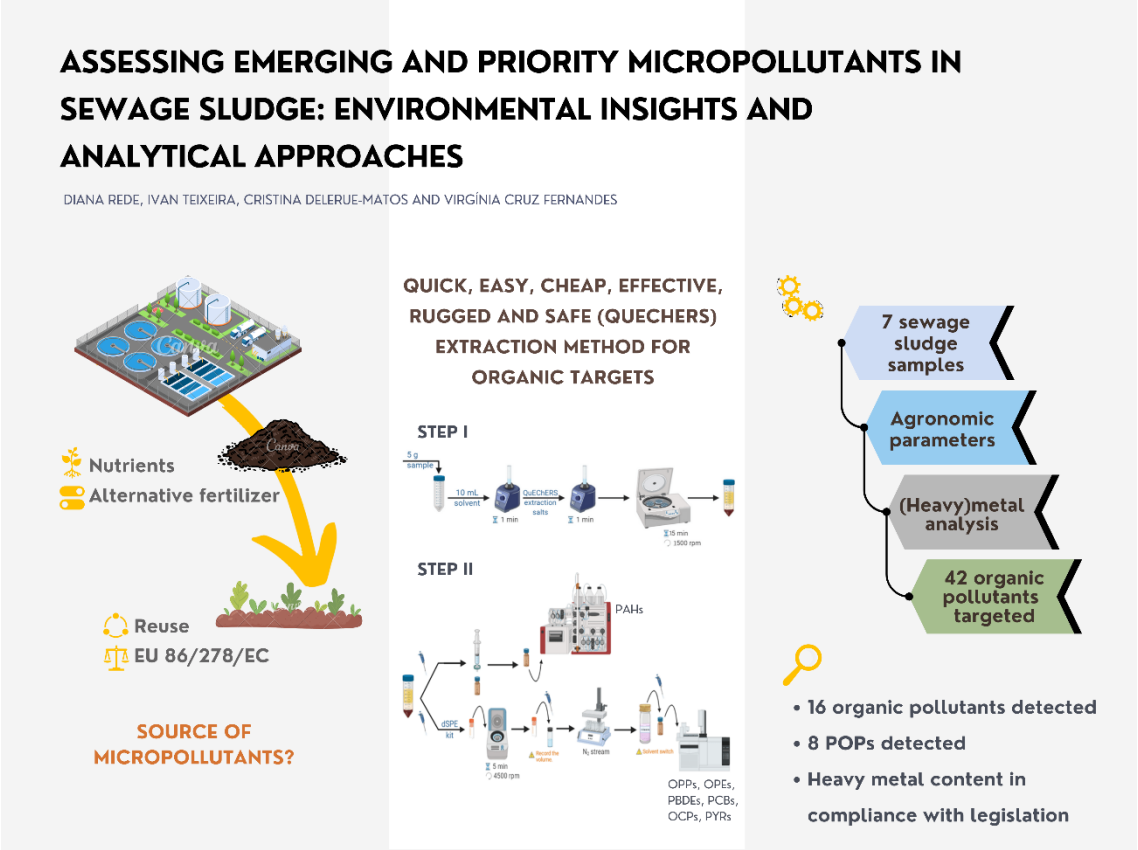
35. Horie, Y., Nomura, M., Ramaswamy, B.R., Harino, H., Yap, C.K., Okamura, H., Thyroid hormone disruption by bis-(2-ethylhexyl) phthalate (DEHP) and bis-(2-ethylhexyl) adipate (DEHA) in Japanese medaka Oryzias latipes. *Aquat. Toxicol.*, 252, 106312, 2022.
36. Rocha, B.A., Asimakopoulos, A.G., Barbosa, F., Kannan, K., Urinary concentrations of 25 phthalate metabolites in Brazilian children and their association with oxidative DNA damage. *Sci. Total Environ.*, 586, 152–162, 2017.
37. Chen, S., Tan, Z., Qi, Y., Ouyang, C., Sorption of tri-n-butyl phosphate and tris(2-chloroethyl) phosphate on polyethylene and polyvinyl chloride microplastics in seawater. *Mar. Pollut. Bull.*, 149, 110490, 2019.
38. He, M.J., Lu, J.F., Wei, S.Q., Organophosphate esters in biota, water, and air from an agricultural area of Chongqing, western China: Concentrations, composition profiles, partition and human exposure. *Environ. Pollut.*, 244, 388–397, 2019.
39. Xiong, S., Hao, Y., Li, Y., Yang, R., Pei, Z., Zhang, Q., Jiang, G., Accumulation and influencing factors of novel brominated flame retardants in soil and vegetation from Fildes Peninsula, Antarctica. *Sci. Total Environ.*, 756, 144088, 2021.
40. Martín-Pozo, L., de Alarcón-Gómez, B., Rodríguez-Gómez, R., García-Córcoles, M.T., Çipa, M., Zafra-Gómez, A., Analytical methods for the determination of emerging contaminants in sewage sludge samples. A review. *Talanta*, 192, 508–533, 2019.
41. Bu, Q., Wu, D., Xia, J., Wu, M., Liu, X., Cao, Z., Yu, G., Polybrominated diphenyl ethers and novel brominated flame retardants in indoor dust of different microenvironments in Beijing, China. *Environ. Int.*, 122, 159–167, 2019.
42. Li, Y., Chang, Q., Duan, H., Liu, Y., Zhang, J., Li, J., Occurrence, levels and profiles of brominated flame retardants in daily-use consumer products on the Chinese market. *Environ. Sci. Process. Impacts*, 21, 446–455, 2019.
43. Dunnick, J.K., Pandiri, A.R., Merrick, B.A., Kissling, G.E., Cunny, H., Mutlu, E., Waidyanatha, S., Sills, R., Hong, H.L., Ton, T.V., Maynor, T., Recio, L., Phillips, S.L., Devito, M.J., Brix, A., Carcinogenic activity of pentabrominated diphenyl ether mixture (DE-71) in rats and mice. *Toxicol. Reports.*, 5, 615, 2018.
44. Vuong, A.M., Yolton, K., Dietrich, K.N., Braun, J.M., Lanphear, B.P., Chen, A., Exposure to polybrominated diphenyl ethers (PBDEs) and child behavior: Current findings and future directions. *Horm. Behav.*, 101, 94–104, 2018.
45. Hu, B., Jiang, L., Zheng, Q., Luo, C., Zhang, D., Wang, S., Xie, Y., Zhang, G., Uptake and translocation of organophosphate esters by plants: Impacts of chemical structure, plant cultivar and copper. *Environ. Int.*, 155, 106591, 2021.
46. Vuong, A.M., Braun, J.M., Webster, G.M., Thomas Zoeller, R., Hoofnagle, A.N., Sjödin, A., Yolton, K., Lanphear, B.P., Chen, A., Polybrominated diphenyl ether (PBDE) exposures and thyroid hormones in children at age 3 years. *Environ. Int.*, 117, 339–347, 2018.
47. Fernandes, V.C., Luts, W., Delerue-Matos, C., Domingues, V.F., Improved QuEChERS for analysis of polybrominated diphenyl ethers and novel brominated flame retardants in capsicum cultivars using gas chromatography. *J. Agric. Food Chem.*, 68, 3260–3266, 2020.
48. Wang, Y., Kannan, P., Halden, R.U., Kannan, K., A nationwide survey of 31 organophosphate esters in sewage sludge from the United States. *Sci. Total Environ.*, 655, 446–453, 2019.
49. McGrath, T.J., Morrison, P.D., Ball, A.S., Clarke, B.O., Detection of novel brominated flame retardants (NBFRs) in the urban soils of Melbourne, Australia. *Emerg. Contam.*, 3, 23–31, 2017.
50. Chokwe, T.B. and Okonkwo, J.O., Occurrence, distribution and ecological risk assessment of organophosphorus flame retardants and plasticizers in sediment samples along the Vaal River catchment, South Africa. *Emerg. Contam.*, 5, 173–178, 2019.
51. Lippold, A., Harju, M., Aars, J., Blévin, P., Bytingsvik, J., Gabrielsen, G.W., Kovacs, K.M., Lyche, J.L., Lydersen, C., Rikardsen, A.H., Routti, H., Occurrence of emerging brominated flame

retardants and organophosphate esters in marine wildlife from the Norwegian Arctic. *Environ. Pollut.*, 315, 120395, 2022.
52. Tenlep, S.Y.N., Weaver, M., Chen, J., Vsevolozhskaya, O., Morris, A.J., Rashid, C.S., Tris(1,3-dichloro-2-propyl) phosphate is a metabolism-disrupting chemical in male mice. *Toxicol. Lett.*, 374, 31–39, 2023.
53. van der Schyff, V., Kalina, J., Govarts, E., Gilles, L., Schoeters, G., Castaño, A., Esteban-López, M., Kohoutek, J., Kukučka, P., Covaci, A., Koppen, G., Andrýsková, L., Piler, P., Klánová, J., Jensen, T.K., Rambaud, L., Riou, M., Lamoree, M., Kolossa-Gehring, M., Vogel, N., Weber, T., Göen, T., Gabriel, C., Sarigiannis, D.A., Sakhi, A.K., Haug, L.S., Murinova, L.P., Fabelova, L., Tratnik, J.S., Mazej, D., Melymuk, L., Exposure to flame retardants in European children—Results from the HBM4EU aligned studies. *Int. J. Hyg. Environ. Health*, 247, 114070, 2023.
54. Bai, C.L., Liu, L.Y., Hu, Y.B., Zeng, E.Y., Guo, Y., Microplastics: A review of analytical methods, occurrence and characteristics in food, and potential toxicities to biota. *Sci. Total Environ.*, 806, 150263, 2022.
55. Blum, A., Behl, M., Birnbaum, L.S., Diamond, M.L., Phillips, A., Singla, V., Sipes, N.S., Stapleton, H.M., Venier, M., Organophosphate ester flame retardants: Are they a regrettable substitution for polybrominated diphenyl ethers? *Environ. Sci. Technol. Lett.*, 6, 638–649, 2019.
56. Falandysz, J., Smith, F., Steel, Z., Fernandes, A.R., PBDEs in cod (Gadus morhua) liver products (1972–2017): Occurrence and human exposure. *Chemosphere*, 232, 63–69, 2019.
57. Robinson, S.A., Young, S.D., Brinovcar, C., McFee, A., De Silva, A.O., Ecotoxicity assessment and bioconcentration of a highly brominated organophosphate ester flame retardant in two amphibian species. *Chemosphere*, 260, 127631, 2020.
58. Gong, X., Wang, Y., Pu, J., Zhang, J., Sun, H., Wang, L., The environment behavior of organophosphate esters (OPEs) and di-esters in wheat (Triticum aestivum L.): Uptake mechanism, *in vivo* hydrolysis and subcellular distribution. *Environ. Int.*, 135, 105405, 2020.
59. Li, W., Shi, Y., Gao, L., Wu, C., Liu, J., Cai, Y., Occurrence, distribution and risk of organophosphate esters in urban road dust in Beijing, China. *Environ. Pollut.*, 241, 566–575, 2018.
60. Wang, Y., Sun, H., Zhu, H., Yao, Y., Chen, H., Ren, C., Wu, F., Kannan, K., Occurrence and distribution of organophosphate flame retardants (OPFRs) in soil and outdoor settled dust from a multi-waste recycling area in China. *Sci. Total Environ.*, 625, 1056–1064, 2018.
61. Messina, C.M., Espinosa Ruiz, C., Regoli, F., Manuguerra, S., D'Agostino, F., Avellone, G., Sprovieri, M., Santulli, A., BDE-47 exposure modulates cellular responses, oxidative stress and biotransformation related-genes in Mytilus galloprovincialis. *Fish Shellfish Immunol.*, 107, 537–546, 2020.
62. Dong, H., Lu, G., Yan, Z., Liu, J., Yang, H., Nkoom, M., Bioconcentration and effects of hexabromocyclododecane exposure in crucian carp (Carassius auratus). *Ecotoxicology*, 27, 313–324, 2018.
63. Guigueno, M.F., Head, J.A., Letcher, R.J., Karouna-Renier, N., Peters, L., Hanas, A.M., Fernie, K.J., Early life exposure to triphenyl phosphate: Effects on thyroid function, growth, and resting metabolic rate of Japanese quail (Coturnix japonica) chicks. *Environ. Pollut.*, 253, 899–908, 2019.
64. Liang, R., Chen, J., Shi, Y., Lu, Y., Sarvajayakesavalu, S., Xu, X., Zheng, X., Khan, K., Su, C., Toxicological effects on earthworms (Eisenia fetida) exposed to sub-lethal concentrations of BDE-47 and BDE-209 from a metabolic point. *Environ. Pollut.*, 240, 653–660, 2018.
65. Wu, X., Zhu, Y., Yang, M., Zhang, J., Lin, D., Biological responses of Eisenia fetida towards the exposure and metabolism of tris (2-butoxyethyl) phosphate. *Sci. Total Environ.*, 811, 152285, 2022.

66. Huang, H., Guo, B., Wang, D., Kang, Y., Cao, D., Geng, F., Rao, Z., Lv, J., Wen, B., Bioaccumulation and biotransformation of tetrabromoethylcyclohexane (TBECH) in maize (Zea mays L.): Stereoselective driving roles of plant biomacromolecules. *J. Hazard. Mater.*, 424, 127610, 2022.
67. Zeng, Y., Pan, W., Ding, N., Kang, Y., Man, Y.B., Zeng, L., Zhang, Q., Luo, J., Brominated flame retardants in home dust and its contribution to brominated flame retardants bioaccumulation in children hair. *J. Environ. Sci. Heal. - Part A Toxic/Hazardous Subst. Environ. Eng.*, 55, 1528–1533, 2020.
68. Zhou, Y., Liao, H., Yin, S., Wang, P., Ye, X., Zhang, J., Aryl-, halogenated- and alkyl- organophosphate esters induced oxidative stress, endoplasmic reticulum stress and NLRP3 inflammasome activation in HepG2 cells. *Environ. Pollut.*, 316, 120559, 2023.
69. Saquib, Q., Al-Salem, A.M., Siddiqui, M.A., Ansari, S.M., Zhang, X., Al-Khedhairy, A.A., Tris(2-butoxyethyl) phosphate (TBEP): A flame retardant in solid waste display hepatotoxic and carcinogenic risks for humans. *Chemosphere*, 296, 133977, 2022.
70. Wang, X., Liu, Q., Zhong, W., Yang, L., Yang, J., Covaci, A., Zhu, L., Estimating renal and hepatic clearance rates of organophosphate esters in humans: Impacts of intrinsic metabolism and binding affinity with plasma proteins. *Environ. Int.*, 134, 105321, 2020.
71. Kim, U.J., Oh, J.K., Kannan, K., Occurrence, removal, and environmental emission of organophosphate flame retardants/plasticizers in a wastewater treatment plant in New York State. *Environ. Sci. Technol.*, 51, 7872–7880, 2017.
72. Björnsdotter, M.K., Romera-García, E., Borrull, J., de Boer, J., Rubio, S., Ballesteros-Gómez, A., Presence of diphenyl phosphate and aryl-phosphate flame retardants in indoor dust from different microenvironments in Spain and the Netherlands and estimation of human exposure. *Environ. Int.*, 112, 59–67, 2018.

2. Sewage Sludge as a Potential Source of Soil Contamination

2.1. Assessing Emerging and Priority Micropollutants in Sewage Sludge: Environmental Insights and Analytical Approaches



Published at *Environmental Science Pollution Research* 31, 3152–3168 (2024). https://doi.org/10.1007/s11356-023-30963-1

Contribution Statement

The candidate contributed to this study by developing an analytical method for quantifying 42 organic compounds, including both legislated and non-legislated pollutants, in SS samples collected from seven WWTPs in Northern Portugal. In addition to developing the methodology, the candidate conducted the physicochemical characterization of the SS samples, determined the metal content, and was involved in sample analysis, data processing, drafting the original manuscript, and participating in the reviewing and editing stages of the paper. The graphical abstract was created using BioRender.com and Canva (accessible at https://www.canva.com).

Environmental Science and Pollution Research (2024) 31:3152–3168
https://doi.org/10.1007/s11356-023-30963-1

RESEARCH ARTICLE

Assessing emerging and priority micropollutants in sewage sludge: environmental insights and analytical approaches

Diana Rede[1,2] · Ivan Teixeira[1] · Cristina Delerue-Matos[1] · Virgínia Cruz Fernandes[1]

Received: 23 August 2023 / Accepted: 5 November 2023 / Published online: 12 December 2023
© The Author(s) 2023

Abstract

The application of sewage sludge (SS) in agriculture, as an alternative to manufactured fertilizers, is current practice worldwide. However, as wastewater is collected from households, industries, and hospitals, the resulting sludge could contaminate land with creeping levels of pharmaceuticals, pesticides, heavy metals, polycyclic aromatic hydrocarbons, and microplastics, among others. Thus, the sustainable management of SS requires the development of selective methods for the identification and quantification of pollutants, preventing ecological and/or health risks. This study presents a thorough evaluation of emerging and priority micropollutants in SS, through the lens of environmental insights, by developing and implementing an integrated analytical approach. A quick, easy, cheap, effective, rugged, and safe (QuEChERS) extraction method, coupled with gas chromatography and liquid chromatography, was optimized for the determination of 42 organic compounds. These include organophosphorus pesticides, organochlorine pesticides, pyrethroid pesticides, organophosphate ester flame retardants, polybrominated diphenyl ethers, polychlorinated biphenyls, and polycyclic aromatic hydrocarbons. The optimization of the dispersive-solid phase for clean-up, combined with the optimization of chromatographic parameters, ensured improved sensitivity. Method validation included assessments for recovery, reproducibility, limit of detection (LOD), and limit of quantification (LOQ). Recoveries ranged from 59.5 to 117%, while LODs ranged from 0.00700 to 0.271 μg g^{-1}. Application of the method to seven SS samples from Portuguese wastewater treatment plants revealed the presence of sixteen compounds, including persistent organic pollutants. The quantification of α-endosulfan, an organochlorine pesticide, was consistently observed in all samples, with concentrations ranging from 0.110 to 0.571 μg g^{-1}. Furthermore, the study encompasses the analysis of agronomic parameters, as well as the mineral and metal content in SS samples. The study demonstrates that the levels of heavy metals comply with legal limits. By conducting a comprehensive investigation into the presence of micropollutants in SS, this study contributes to a deeper understanding of the environmental and sustainable implications associated with SS management.

Keywords PCBs · PAHs · Flame retardants · Pesticides · POPs · QuEChERS · Micropollutants · Sewage sludge

Introduction

Sewage sludge (SS) is a solid, semi-solid, or slurry by-product that emerges from treatment processes conducted in wastewater treatment plants (WWTPs) (Martín-Pozo et al. 2019; Campo et al. 2021). In a conventional WWTP, the influent undergoes the following steps: (i) pretreatment (removal of large debris and grit), (ii) primary treatment (separation of suspended solid matter in sedimentation tanks), (iii) secondary treatment (biological cleaning through an activated sludge system), and (iv) (bio)solids handling (thickening, stabilization, dewatering, and disposal) (Venkatesan and Halden 2020; Campo et al. 2021). SS is produced during primary and secondary treatments, and its exact composition varies and is not

Responsible Editor: Ester Heath

✉ Virgínia Cruz Fernandes
vir@isep.ipp.pt

[1] REQUIMTE/LAQV, Instituto Superior de Engenharia do Porto, Instituto Politécnico do Porto, Rua Dr. António Bernardino de Almeida, 431, 4249-015 Porto, Portugal

[2] Departamento de Química e Bioquímica, Faculdade de Ciências, Universidade do Porto, Rua do Campo Alegre S/N, 4169-007 Porto, Portugal

known. The wastewater collected can come from households, industries, healthcare facilities, rainwater runoff, or landfill leachate (Venkatesan and Halden 2020; Hatinoğlu and Sanin 2021). In addition, any chemical compounds used in everyday products such as pharmaceuticals, pesticides, heavy metals, polycyclic aromatic hydrocarbons (PAHs), and microplastics that are not eliminated during wastewater treatment processes can sorb SS (Rossini et al. 2016; Horton et al. 2017; van den Berg et al. 2020; Venkatesan and Halden 2020). Commonly, the disposal routes for SS are land application (such as agricultural, forestry, and reclamation), energy recovery (including incineration and co-combustion), and landfilling. However, improper dumping is still practiced in developing regions (Martín-Pozo et al. 2019; Zhu et al. 2019; Schnell et al. 2020).

Millions of tons of SS are produced annually. For example, the European Union (EU) produces approximately 9 million tons of dry matter of SS. These quantities are expected to increase in the short term (Mohapatra et al. 2016; Chen et al. 2021). According to the United Nations, three out of ten people do not have access to safe drinking water services, and six out of ten people lack access to sanitation facilities. It is estimated that more than 80% of the wastewater resulting from human activities is discharged into the aquatic environment without undergoing any prior treatment (UN DESA 2023). Moreover, existing WWTPs are unable to effectively remove emerging contaminants at trace levels (Paíga et al. 2019). By 2030, with a growing global population, there is an anticipated shortage of approximately 40% of freshwater resources (UN DESA 2023). To meet the strict regulations imposed by the governments and to ensure universal access to water and sanitation (fulfilling the sixth goal of the 2030 Agenda for Sustainable Development), it will be crucial to construct new WWTPs and enhance the existing ones. This will increase SS production (Wyrwicka et al. 2014; Gago et al. 2019). However, the challenge in managing and disposing of SS lies in effectively handling the large quantities generated while adhering to the principles of the circular economy, which prioritize strategies such as reuse and recycling (Campo et al. 2021).

SS has high organic matter and nutrient content; hence, it is considered a valuable resource rather than a waste and is widely used as a fertilizer to enhance crop, pasture, and rangeland production (Martín-Pozo et al. 2019; Hatinoğlu and Sanin 2021). In the EU, the reuse of SS on agricultural land is highly encouraged, in line with the principles of the circular economy. However, to safeguard humans, animals, plants, and the environment, the spread of SS must comply with Council regulations, specifically the Sewage Sludge Directive 86/278/EEC and the EU Working Document on Sewage Sludge. These regulations establish limit values for agronomic parameters, heavy metals, and organic compounds, including polychlorinated dibenzodioxins and dibenzofurans (European Commission 1986; European Comission 2000). Even so, studies have highlighted that potentially toxic elements (PTEs) sorbed onto SS can be transferred to soil, causing its deterioration and the subsequent loss of function (Mahon et al. 2017; Martín-Pozo et al. 2019; Corradini et al. 2019). This can ultimately result in ecological and/or health risks, such as the spread of antibiotic resistance genes (Buta et al. 2021; Yuan et al. 2023), the prevalence of SARS-CoV-2 or its genetic material (Adelodun et al. 2022), the bioaccumulation of metals and PAHs on crops and biota (Zhang et al. 2017; Iglesias et al. 2018; Courtois et al. 2021), or the absorption of microplastics by fungi (Wan et al. 2022). Moreover, it must not be forgotten that hundreds of new synthetic compounds are launched in the global market every year. For example, the USA alone is responsible for the production of 1500 new products annually (Naidu et al. 2021).

To minimize the environmental impact of incorporating SS into soils, it is essential to develop efficient analytical methodologies that enable the extraction and analysis of various contaminants. Typically, the techniques used to extract organic compounds from SS are solid-phase extraction (Liang and Liu 2016), matrix solid-phase dispersion (Sánchez-Brunete et al. 2009), solid–liquid extraction (Chen et al. 2019), the Soxhlet method, and ultrasonic-assisted extraction. The Quick, Easy, Cheap, Effective, Rugged, and Safe (QuEChERS) method, which was initially designed for extracting and purifying contaminants from food samples, has also been successfully used for environmental samples (Guillemet et al. 2009; Guo et al. 2009; Suciu et al. 2015; Barakat et al. 2017; Tomczyk et al. 2020). This method, known for its speed, reliability, and cost-effectiveness, as it does not rely on expensive instrumentation, has previously been applied to sludge samples for the determination of pharmaceuticals, ultraviolet filters, and synthetic musks (Rossini et al. 2016; Ramos et al. 2019). The detection of emerging pollutants in SS is generally achieved using gas chromatography (GC) (Chen et al. 2019) and high-performance liquid chromatography (HPLC) (Castro et al. 2021), typically in conjunction with mass spectrometry (MS). The QuEChERS extraction technique demonstrates excellent performance in terms of efficiency, versatility, and reduction of interferents (such as fats or pigments) that may be present in the sample matrix. This technique produces an extract that is suitable for chromatographic analysis.

Since the environment, especially SS is facing an increasing number of toxic micropollutants that pose proven or potential risks, this study has two main objectives. Firstly, we have developed a simple and rapid method that combines the QuEChERS extraction technique with chromatographic analysis to identify 42 organic compounds from seven chemical families in SS. These include six organophosphorus pesticides (OPPs), five organochlorine pesticides (OCPs), five

pyrethroid pesticides (PYRs), seven organophosphate esters (OPEs), seven polybrominated diphenyl ethers (PBDEs), four polychlorinated biphenyls (PCBs), and eight polycyclic aromatic hydrocarbons (PAHs) in SS. Additionally, we assess the content of agronomic parameters (pH in water (pH_w), dry matter (DM), organic matter (OM) and total organic carbon (TOC)), and mineral and metal content (Co, Mo, Hg, Cd, Ni, Pb, Cr, Cu, Zn, Li, Be, V, As, Se, Rb, Sr, Rh, Sb, Cs, Ba, Ir, Tl, Mg, Ca, Mn, and Fe) using standardized methods. Secondly, our study contributes with data to future considerations on legislation on SS and its application on agricultural land, in the framework of the Action Plan for a New Circular Economy adopted on March 11, 2020, to protect the environment and human health. The developed method was applied to analyze samples from seven different Portuguese WWTPs, collectively serving over 380,000 inhabitants. To the best of our knowledge, our study represents a pioneering effort in two key areas. Firstly, we employed the QuEChERS method for the simultaneous extraction of these emerging and priority organic compounds from SS samples. Secondly, we conducted a comprehensive analysis of Portuguese SS for the presence of multiple organic micropollutants not currently addressed in the existing legislation. Using geographically representative samples from a specific region in Portugal, our findings contribute to a better understanding of contamination and have the potential to drive future legislative measures aimed at reducing these emerging pollutants in SS, providing crucial data for the development of targeted mitigation measures in the region.

Materials and methods

Reagents and materials

Deionized water with a resistivity of 15.8 MΩ cm was obtained using an Elix® 3ADV system (Millipore SAS, Molsheim, France) equipped with a Q-Gard® T1 purification cartridge and a Vent Filter MPK01 for the storage tank (Merck Millipore, Darmstadt, Germany). Nitric acid (HNO_3) (65% w/v) was supplied by Merck (Darmstadt, Germany). Acetonitrile (ACN) from VWR Chemicals, Leicestershire, England, and n-hexane from Merck, Darmstadt, Germany, were of chromatography grade. Reference materials BCR®–667 (sediment) and ISE 918 (soil) were obtained from the Institute for Reference Materials and Measurements (Belgium) and WEPAL-QUASIMEME (Netherlands), respectively. The QuEChERS EN Method salts, primary secondary amine (PSA), C18, SampliQ anhydrous magnesium sulphate ($MgSO_4$), and SampliQ Carbon SPE Bulk Sorbent (CB) were purchased from Agilent Technologies (Santa Clara, California, USA). Additionally, Supel™ QuE Z-Sep (Z-Sep) was acquired from Supelco (Bellefonte, Pennsylvania, USA). OPPs (dimethoate, chlorpyrifos-methyl, parathion-methyl, malathion, chlorpyrifos, and chlorfenvinphos), OPEs (tri-iso-butyl phosphate (TiBP), tri-n-butyl phosphate (TnBP), tris(2-chloroethyl) phosphate (TCEP), triphenyl phosphate (TPhP), tris(2-butoxyethyl) phosphate (TBEP), tris(2-ethylhexyl) phosphate (TEHP), and tri-cresyl phosphate (TCP)), PBDEs ((2,4,4′-tribromodiphenyl ether (BDE 28), 2,2′,4,4′-tetrabromodiphenyl ether (BDE 47), 2,2′,4,4′,5-pentabromodiphenyl ether (BDE 99), 2,2′,4,4′,6-pentabromodiphenyl ether (BDE100), 2,2′,4,4′,5,5′-hexabromodiphenyl ether (BDE 153), 2,2′,4,′,5,6′-hexabromodiphenyl ether (BDE 154), 2,2′,3,4,4′,5′,6-heptabromodiphenyl ether (BDE 183)), PCBs (2,4,4′-trichlorobiphenyl (PCB 28), 2,3′,4,4′,5′-pentachlorobiphenyl (PCB 118), 2,2′,4,4′,5,5′-hexachlorobiphenyl (PCB 153), and 3,4,4′,5,5′-heptachlorobiphenyl (PCB 180)), OCPs (hexachlorocyclohexanes (HCH), α-endosulfan, 2,2-bis(p-chlorophenyl)-1,1-dichloroethylene (p,p″-DDE), dieldrin, and dichlorodiphenyldichloro-ethane (p,p′-DDD)), PYRs (bifenthrin, λ-cyhalothrin, cypermethrin, fenvalerate, and deltamethrin) standards, and dichlorobenzophone (internal standard (IS)) were acquired from Sigma Aldrich and Chemservice (West Chester, Pennsylvania, USA). PAHs (fluoranthene (FLU), benzo[b]fluoranthene, benzo[j]fluoranthene, benzo(a)pyrene (BaP), dibenzo[a,l]pyrene, dibenz[a,h]anthracene (DBA), benzo[ghi]perylene, indeno[1,2,3-cd]pyrene) were obtained from Supelco (Bellefonte, Pennsylvania, USA). All standards were of analytical grade.

Sampling and characteristics of sewage sludges

Sewage sludge samples, which were properly stabilized and dewatered, were collected from seven WWTPs located in three different regions of Northern Portugal. Five of these WWTPs can be found in the Porto region, while the other two are situated in the Viseu and Aveiro regions, as illustrated in Fig. 1S in the Supporting Information. However, all of them receive urban wastewater as well as some industrial and agricultural discharges. The samples were identified from A to G and stored in pre-cleaned glass containers at - 20 °C until analysis. Sample A was collected from a WWTP that serves a population of approximately 285,000 inhabitants. The plant receives an average flow of 39,470 m^3 per day and operates with secondary treatment using the activated sludge process. Samples B, C, D, E, and G were collected from WWTPs with secondary treatment based on an extended aeration system. These plants receive average flows between 380 and 8270 m^3 per day and serve populations of approximately 54,660, 3430, 2260, 2890, and 3430 inhabitants, respectively. Sample F was collected from a WWTP that serves a population of approximately 35,430

inhabitants (3750 m^3 day^{-1}). The WWTP operates with a secondary treatment system, which consists of a trickling filter process followed by an activated sludge process. A mixture of samples, referred to as the *sludge mixture*, was prepared to develop a method for quantifying organic pollutants. The moisture percentages of the individual SS samples were used to calculate adjusted quantities for the sludge mixture, ensuring consistent contributions based on dry-weight (dw). The Supporting Information contains details in section S.1.2 about the methods used to determine pH_w values, DM, OM, TOC contents, and concentrations of trace elements in SS samples.

Standard solutions for the extraction and detection of organic pollutants

Individual stock solutions (2500 µg L^{-1}) of each OPPs, OPEs, PBDEs, PCBs, and OCPs were prepared in n-hexane, while PYRs were prepared in ACN. Reagent-only and matrix-matched calibration standards were prepared for OPPs and OPEs, with concentrations ranging from 20 to 100 µg L^{-1} (0.207–1.034 µg g^{-1}). For PBDEs, PCBs, OCPs, and PYRs, the calibration standards ranged from 10 to 100 µg L^{-1} (0.103–1.034 µg g^{-1}). Calibration standards for PAHs were prepared with concentrations ranging from 0.13 to 20.06 µg L^{-1} (0.00026–0.040 µg g^{-1}, values for BaP). To prepare matrix-matched calibration standards, aliquots of the stock solutions were dried using a nitrogen stream and then re-dissolved in the *sludge mixture* extract.

Sample preparation for the extraction and detection of organic pollutants

The extraction methodology was based on the QuEChERS method described by Fernandes et al. (2012). Briefly, 5 g of the SS sample (wet weight) were placed in a glass tube. Next, 10 mL of ACN was added to the sample and vortexed for 1 min. QuEChERS EN salts (4 g of $MgSO_4$, 1 g of NaCl, 1 g of trisodium citrate dihydrate, and 0.5 g of disodium hydrogen citrate sesquihydrate) were added. The tube was then vortexed for 1 min. The mixture was centrifuged at 2000 rpm for 15 min.

For the assessment of PAHs, 1 mL of supernatant was filtered using a 0.22-µm BGB Analytik PTFE syringe filter with a 13-mm diameter and collected in a 1.5-mL glass vial. The final extract was injected into a liquid chromatograph equipped with photodiode array (PAD) and fluorescence (FLD) detectors, referred to as LC-PDA-FLD (Oliveira et al. 2015). For the analysis of OPPs, OPEs, PBDEs, PCBs, OCPs, and PYRs analysis, the extracts underwent a cleaning process to minimize matrix interference. This was achieved through dispersive solid-phase extraction (d-SPE) using a mixture of sorbents in bulk form. The composition of this mixture was optimized, as shown in Table 1. Initially, a series of five different mixtures (I-V) were tested in SS, A and B. The performance of the procedure was evaluated based on its color removal capability, which determined the selection of sorbents to be included in the d-SPE. Then, in the second set of four bulk mixtures (VI-IX), the recovery rates (RE) and matrix effects (ME) of each target analyte were evaluated within the sludge mixture by adjusting the amounts of sorbents in the d-SPE. The supernatant (1 mL) was added to a 4-mL glass vial containing a mixture of bulk sorbents. It was then vortexed for 1 min and centrifuged at 4500 rpm for 5 min. The clear supernatant was transferred to a 1.5-mL amber glass vial, evaporated to dryness under a gentle nitrogen stream, redissolved with n-hexane, and vortexed. Approximately 150 µL of extract was transferred to a second amber glass vial containing a 250-µL insert and injected into the following instruments for analysis: (i) a gas chromatograph (GC-2010) with a flame photometric detector (FPD) from Shimadzu to quantify OPPs and OPEs; (ii) a gas chromatograph (GC-2010) with an electron capture detector (ECD) from Shimadzu for the quantification of PBDEs, PCBs, OCPs, and PYRs (the internal standard was added prior to analysis); (iii) a gas chromatograph with a mass spectrometry detector (GC-MS) from Thermo Fisher to confirm chlorpyrifos-methyl, malathion, TiBP, TPhP, TEHP, BDE 28, BDE 99, BDE 183, α-endosulfan, PCB 118, cypermethrin, and deltamethrin in the samples. The Supporting Information provides details about the chromatographic methods used in section S.1.3.

Validation of analytical methods for the extraction and detection of organic pollutants

The method was validated according to European Union guidelines (Magnusson and Örnemark 2014; European Commission 2021) for linearity and range, matrix effects (ME), trueness, precision, limit of detection (LOD), and quantification (LOQ) (Bhardwaj et al. 2016; European Commission 2019). Eight concentration levels of matrix-matched standards and reagent-only standards were used to obtain calibration curves, which plotted the peak area against the concentration of the target analyte. The calibration curves enabled the establishment of linearity, expressed as the coefficient of determination (R^2), within the selected range of concentrations. ME was investigated by comparing the slopes between calibration in the matrix and calibration in the reagent for each target analyte (Ponce-Robles et al. 2017).

The trueness of the analytical procedure, expressed as RE, was evaluated by conducting recovery studies. To conduct these studies, the *sludge mixture* was fortified both before (*pre-spike*) and after (*post-spike*) the analytical procedure. Fortifications were made at two levels: OPPs and OPEs at 50 and 75 µg L^{-1} (0.517 and 0.776 µg g^{-1}); OCPs, PBDEs, PCBs,

and PYRs at 20 and 50 µg L^{-1} (0.207 and 0.517 µg g^{-1}); and PAHs at 0.50 and 2.51 µg L^{-1} (0.0010 and 0.0050 µg g^{-1}, values for BaP). Two replicates were conducted for each level on two different days. The RE was determined by comparing the peak areas before and after the spike. In addition, the sorbent mixture used in the d-SPE clean-up was selected based on the ME obtained by comparing the peak areas of the post-spike and the standard in the solvent at a specific concentration level. Precision was studied in terms of intraday and day-to-day repeatability, which are expressed as the relative standard deviation (% RSD) of a series of measurements.

For the analyses performed in GC-FPD, GC-ECD, and LC-PDA-FLD, the LOD and LOQ were determined by considering the residual standard deviation of the linear regression and the slope of the calibration curve (Miller and Miller 2010; Magnusson and Örnemark 2014). Both LOD and LOQ were expressed as the concentration of the target analyte in the sample. Additionally, TCP, deltamethrin, fenvalerate, and λ-cyhalothrin were quantified by summing the peak areas of their respective isomers. Positive results were confirmed by GC-MS, and the identification was carried out using selected ion monitoring (SIM), which involved the use of three ions that were sufficiently selective for each analyte (European Commission 2021).

Results and discussion

Optimization of analytical methodologies for the extraction and detection of organic pollutants

The chromatographic methods for GC-FPD (OPPs and OPEs) and GC-ECD (PBDEs, PCBs, OCPs, and PYRs) were based on previous studies conducted by the research group (Fernandes et al. 2012, 2018, 2020; Correia-Sá et al. 2012; Bragança et al. 2019; Cruz Fernandes et al. 2020 et al. 2020; Dorosh et al. 2021; Sousa et al. 2023). However, due to the high complexity of the SS matrix, modifications were made to achieve maximum sensitivity for identifying and quantifying multiple target analytes. The organic fraction of SS depends on the source of the effluent. However, it typically consists of proteins, humic substances, carbohydrates, and significant amounts of cellular lipids, free fatty acids, and wax/gums. This results in a highly intricate and diverse matrix (Zhu et al. 2017; Chen et al. 2021; Gonzalez et al. 2021).

The sample preparation method was performed using the QuEChERS approach, which is a salting-out extraction technique with an organic solvent (first stage) combined with d-SPE clean-up using sorbents (second stage). In this study, QuEChERS EN salts (4 g $MgSO_4$, 1 g NaCl, 1 g trisodium citrate dihydrate, 0.5 g of disodium hydrogen citrate sesquihydrate) were selected based on previous works described in the literature (Herrero et al. 2014; Maragou et al. 2021). The clean-up step, which is crucial for reducing the matrix effect when analyzing complex samples (Herrero et al. 2014; Ponce-Robles et al. 2017), was optimized in terms of the sorbents and their quantities. The experiments were performed using a standard mixture of 150 mg of $MgSO_4$, 50 mg of PSA, and 50 mg of C18, combined with varying amounts of CB (used for pigment removal) and Z-Sep (used for lipid content removal) (Ponce-Robles et al. 2017; Fernandes et al. 2020). In the first set of d-SPE mixtures tested, it was observed that increasing the amount of CB in the mixture led to a reduction in the intensity of the sample color (Fig. 1). In fact, 50 mg of CB in the d-SPE bulk mixture (A-V and B-V) achieved almost complete color removal. However, it should be noted that using high amounts of CB can lead to the adsorption of the target analytes (Masiá et al. 2015). Thus, since the combinations of CB/Z-Sep also decrease the color intensity in both sample extracts (A-IV: 20 mg/10 mg; B-IV: 10 mg/10 mg), we tested different amounts of these sorbents in the second set of d-SPE. Recovery rates and ME were assessed for each cleanup procedure using a fortified *sludge mixture* before and after the QuEChERS method. The concentration used for the fortified mixture was 50 µg L^{-1} (0.517 µg g^{-1}) for OPPs and OPEs, and 20 µg L^{-1} (0.207 µg g^{-1}) for PBDEs, PCBs, OCPs, and PYRs. Matching reagent-only standards were prepared.

Figure 2a shows the recovery results for different mixtures of bulk sorbents, with mean recoveries ranging from 18.1 to 102.1% (VI), 55.6 to 372.3% (VII), 71.3 to 106.3% (VIII), and 63.9 to 139.7% (IX). Overall, mixtures with lower CB content and higher Z-Sep showed improved RE (%), particularly for PYRs (18.1% (VI) < 55.6% (VII) < 71.3% (VIII) < 73.1% (IX)). Mixture VIII exhibited the lowest RSDs with values of 11.6% for OPPs, 14.7% for OPEs, 13.8% for PBDEs, 26.9% for PCBs, 14.4% for OCPs and 8.0% for PYRs. Figure 2b shows the results of the ME determinations, where chromatographic interferences were observed in all d-SPE mixtures. However, these interferences were reduced in mixture VIII, as no effect was observed for OPPs, OPEs, and PYRs (117.3%, 92.6%, and 107% respectively). On the other hand, signal suppression was noticed for PBDEs, PCBs, and OCPs (60.3%, 39.3%, and 43.8% respectively). Mixture VIII was selected for the clean-up step because it provided acceptable recovery values and had less pronounced matrix interference. This is the first study using a sorbent mixture consisting of 150 mg of $MgSO_4$, 50 mg of PSA, 50 mg of C18, 5 mg of CB, and 20 mg of Z-Sep for extracting OPPs, OPEs, PBDEs, PCBs, OCPs, and PYRs from SS samples.

Validation of the analytical methodologies for the extraction and detection of organic pollutants

The development of a quantification method requires a validation process that ensures precision, robustness, and

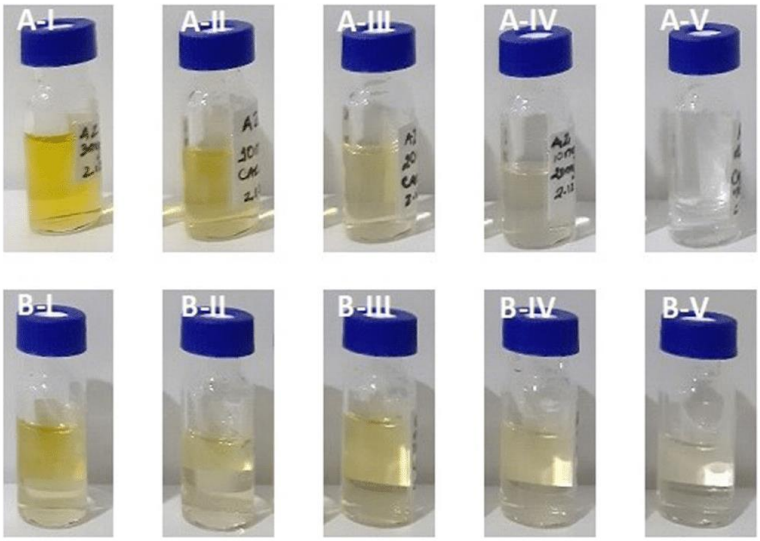


Fig. 1 Color removal with different d-SPE mixtures applied to samples A and B in the first set of clean-ups. The d-SPE tube contained a typical mixture of 150 mg of $MgSO_4$, 50 mg of PSA, and 50 mg of C18 with A-I — 3 mg of CB; A-II — 10 mg of CB; A-III — 20 mg of CB; A-IV — 20 mg of CB and 10 mg of Z-Sep; A-V — 50 mg of CB; B-I — 3 mg of CB; B-II — 6 mg of CB; B-III — 10 mg of CB; B-IV — 10 mg of CB and 10 mg of Z-Sep; B-V — 50 mg of CB

Table 1 Composition of the d-SPE mixtures tested in the two sets

First set					
d-SPE mixture	$MgSO_4$ PSA C18 (mg)	SS A		SS B	
		CB (mg)	Z-Sep (mg)	CB (mg)	Z-Sep (mg)
I	150	3	0	3	0
II	50	10	0	6	0
III	50	20	0	10	0
IV		20	10	10	10
V		50	0	50	0
Second set (*sludge mixture*)					
d-SPE mixture	$MgSO_4$ (mg)	PSA (mg)	C18 (mg)	CB (mg)	Z-Sep (mg)
VI	150	50	50	10	10
VII	150	50	50	5	15
VIII	150	50	50	5	20
IX	150	50	50	5	25

minimization of differences in the matrix effect and/or extraction efficiency among samples (Herrero et al. 2014). The developed method was validated for each compound in terms of the linear range, ME, LODs, LOQs, RE, repeatability (intraday), and reproducibility (day-to-day) (Magnusson and Örnemark 2014; Bhardwaj et al. 2016; European Commission 2019; European Commission 2021). All validation parameters are listed in Table 2.

Linearity was assessed using matrix-matched calibration solutions at eight concentration levels ranging from 0.207 to 1.034 µg g^{-1} for OPPs and OPEs; 0.103 to 1.034 µg g^{-1} for PBDEs, PCBs, OCPs, and PYRs; and 0.00026 to 0.040 µg g^{-1} (values for BaP) for PAHs. The use of matrix-matched calibration reduces the problems related to signal suppression or enhancement (Rajski et al. 2013; European Commission 2019). It has been described as a suitable strategy for analyzing complex matrices, such as SS (Herrero et al. 2013, 2014; Masiá et al. 2015). The coefficients of determination (R^2) were higher than 0.9905 for all compounds, except for parathion methyl, TiBP, and FLU, which had R^2 values of 0.9634, 0.9667, and 0.9816, respectively. The effects of the SS matrix on the extraction efficiency were evaluated by comparing the ratio of the slopes of the matrix-matched and reagent-only calibration curves. An ME closer to 100% suggests no influence from the matrix; an ME within the range of 80–120% indicates

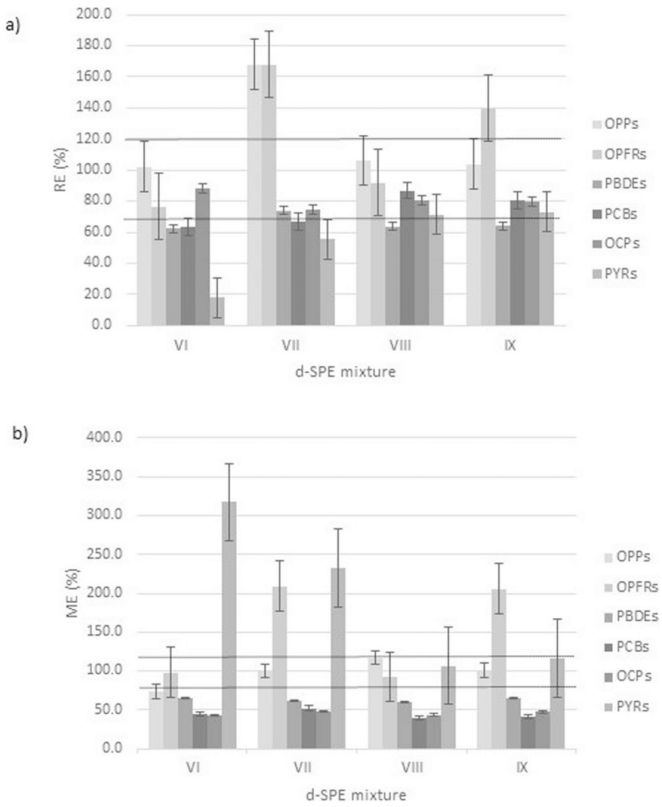


Fig. 2 RE (%) (**a**) and ME (**b**) obtained with the different formulations of d-SPE sorbents (VI–IX) used in the clean-up of the *sludge mixture*. The d-SPE tube contained a typical mixture of 150 mg of $MgSO_4$, 50 mg of PSA, and 50 mg of C18 combined with VI – 10 mg of CB and 10 mg of Z-Sep; VII – 5 mg of CB and 15 mg of Z-Sep; VIII– 5 mg of CB and 20 mg of Z-Sep; IX – 5 mg of CB and 25 mg of Z-Sep

a soft matrix influence, while an ME outside this range reveals medium or strong influence, such as suppression or reinforcement (Rajski et al. 2013; Masiá et al. 2015). Thus, based on the obtained results, the following conclusions can be drawn: five compounds (TCP, deltamethrin, BaP, benzo[ghi]perylene, and indeno[1,2,3-cd]pyrene) did not exhibit ME; ten compounds (TiBP, TPhP, chlorpyrifos, chlorfenvinphos, bifenthrin, fenvalerate, dibenzo[a,l]pyrene, and DBA) showed soft ME; seventeen compounds showed suppressed responses ranging from - 25% (FLU) to - 55% (p,p'-DDE), with an average value of - 38.8%; and ten compounds displayed enhanced responses ranging from + 26% (cypermethrin) to + 93.2% (parathion methyl), with an average value of + 54.1%.

The accuracy was assessed by conducting recovery tests at two levels of contamination. The recoveries were determined by comparing the concentration obtained from the spiked *sludge mixture* (before the extraction process) with the concentration obtained from the spiked extract. The samples were quantified using a combined matrix-matched calibration. According to these guidelines, the mean recoveries of target analytes within the scope of a method should be in the range of 70–120% (RSD ≤ 20%) (European Commission 2019). The recoveries obtained for approximately 40% of the target analytes were outside this range, varying from 49.6% (FLU) to 126% (PCB 28). This variation may be due to the diversity of chemical families included in the study and is consistent with the results reported for the analysis of multiple pharmaceutical families in SS (Peysson and Vulliet 2013). For each chemical family, the average recovery obtained was as follows: PAHs (90.6 ± 21.6%), OPPs (94.3 ± 13.6%), PCBs (84.0 ± 30.0%), OPEs (78.3 ± 8.6%), OCPs (76.8 ± 8.7%), PYRs (69.0 ± 4.6%), and PBDEs (59.5 ± 7.6%).

The precision of the chromatographic methods, expressed as % RSD, was determined by repeatedly injecting a spiked extract of *sludge mixture* at a single concentration level. The concentration levels were 0.207 μg g^{-1} for OPPs and OPEs; 0.103 μg g^{-1} for PBDEs, PCBs, OCPs, and PYRs; and 0.005 μg g^{-1} for PAHs (value for BaP). The obtained intraday RSD values were lower than 20% for all compounds, as were the inter-day RSD values, except for TiBP, which was 21.1%. The obtained results are

Table 2 Coefficient of determination (R^2), limit of detection (LOD) and quantification (LOQ), recovery (RE), matrix effect (ME), repeatability, and reproducibility (%RSD, $n = 2$) of the developed method for the studied compounds

	Target analyte	R^2	LOD (μg g^{-1})	LOQ (μg g^{-1})	RE (%)	ME (%)	Repeatability (%RSD)	Reproducibility (%RSD)
OPPs	Dimethoate	0.9919	0.101	0.307	80.1	164.3**	7.80	18.2
	Chlorpyrifos methyl	0.9915	0.136	0.413	90.6	142**	3.40	6.70
	Parathion methyl	0.9634	0.271	0.821	86.0	193**	0.100	10.4
	Malathion	0.9946	0.109	0.331	87.1	155**	0.500	17.0
	Chlorpyrifos	0.9905	0.145	0.439	107	120	2.40	9.10
	Chlorfenvinphos	0.9947	0.123	0.373	115	115	11.0	14.4
OPEs	TiBP	0.9667	0.102	0.730	91.3	104	7.60	21.1
	TnBP	0.9950	0.106	0.322	86.3	133**	8.80	12.5
	TCEP	0.9925	0.130	0.394	74.0	152**	9.40	10.5
	TPhP	0.9958	0.096	0.292	79.8	107	2.50	5.80
	TBEP	0.9935	0.130	0.393	71.3	192**	6.40	11.6
	TEHP	0.9970	0.0770	0.257	61.9	145**	9.40	6.50
	TCP	0.9942	0.112	0.339	79.9	99.3	8.80	7.30
PCBs	PCB 28[1]	0.9940	0.102	0.341	126	91.91	4.61	11.0
	PCB 118[1]	0.9997	0.0220	0.0750	84.7	49.8*	2.53	12.7
	PCB 153[1]	0.9988	0.0440	0.145	68.0	67.2*	6.36	4.54
	PCB 180[1]	0.9999	0.0150	0.0500	57.5	55.3*	2.31	4.02
PBDEs	BDE 28	0.9998	0.0200	0.0670	72.9	65.6*	5.92	6.78
	BDE 47	0.9999	0.0100	0.0330	62.8	73.1*	6.69	6.56
	BDE 100	0.9973	0.0650	0.216	60.4	48.6*	1.49	3.87
	BDE 99	0.9999	0.0150	0.0500	62.0	63.4*	5.71	7.83
	BDE 154	0.9996	0.0260	0.0850	54.1	66.0*	2.26	8.23
	BDE 153	0.9993	0.0340	0.112	54.6	72.3*	0.120	7.54
	BDE 183	1.0000	0.00800	0.0260	49.7	61.1	3.02	20.0
OCPs	o-HCH	0.9958	0.0800	0.266	86.3	51.5*	3.65	5.59
	α-Endosulfan	0.9997	0.0220	0.074	81.6	56.3*	3.56	14.0
	p,p´-DDE	0.9991	0.0460	0.153	72.1	44.7*	4.13	5.19
	p,p´-DDD	0.9992	0.0350	0.118	67.1	52.4*	2.50	9.0
	Dieldrin	0.9973	0.0640	0.213	73.7	64.9*	5.65	6.0
PYRs	Bifenthrin	0.9949	0.0770	0.255	74.5	97.9	9.02	16.4
	λ-Cyhalothrin	0.9992	0.0420	0.140	63.4	72.1*	8.92	8.16
	Cypermethrin	0.9997	0.0210	0.0710	69.6	126.1**	3.81	10.9
	Fenvalerate	0.9988	0.0420	0.139	64.7	93.7	1.00	6.86
	Deltamethrin	0.9999	0.0150	0.0510	68.0	102.1	4.44	14.8
PAHs	Fluoranthene[1]	0.9816	0.0870	0.290	49.5	75.5*	2.00	7.30
	Benzo[b + j]fluoranthene[1]	0.9982	0.0590	0.196	94.8	139**	2.60	10.6
	Benzo[a]pyrene[1]	0.9985	0.00700	0.0240	103.1	101	1.00	1.20
	Dibenzo[a,l]pyrene	0.9997	0.0110	0.0380	80.0	96.2	4.60	2.40
	Dibenz[a,h]anthracene	0.9988	0.0230	0.0760	118.5	95.1	7.40	18.6
	Benzo[ghi]perylene[1]	0.9994	0.0170	0.0570	96.5	101	4.10	9.90
	Indeno[1,2,3-cd]pyrene[1]	0.9972	0.0140	0.0470	91.6	101	6.40	11.9

[1]Included in working document on sludge

*Signal suppression

**Signal enhancement

acceptable, considering the complexity of the matrix. Therefore, the method can be considered precise. The LODs and LOQs of the GC-FPD, GC-ECD, and LCPDA–FLD methods were determined as 3.3 and 10 times the standard deviation of the residual ($S_{y/x}$) divided by the slope of the linear regression (b), respectively. The LODs ranged from 0.007 to 0.271 μg g^{-1}, while the LOQs ranged from 0.024 to 0.821 μg g^{-1}, depending on the specific compound.

To the best of our knowledge, this is the first instance in which the QuEChERS approach, using citrate buffer and a d-SPE mixture of PSA, C18, $MgSO_4$, CB, and Z-Sep, has been utilized for the simultaneous extraction of six OPPs, four OCPs, six PYRs, seven OPEs, seven PBDEs, four PCBs, and eight PAHs in SS. Nevertheless, there are studies in the literature that support the applicability of the QuEChERS approach for extracting organic pollutants from SS samples. Masiá et al. (2015) used QuEChERS to identify 50 pesticides, five of which were targeted in our study (dimethoate, parathion-methyl, malathion, chlorpyrifos, and chlorfenvinphos). They used 150 mg of $MgSO_4$, 50 mg of C18, and 50 mg of PSA for cleanup and obtained RE ranging from 36 to 120% with 26% inter-day precision. For the five pesticides we both studied, their RE ranged from 40 to 101%. This addition of CB to the d-SPE mixture improves the % RE of OPPs. Ramos et al. (2019) used the QuEChERS method to extract synthetic musk compounds from SS. The d-SPE contained 500 mg of $MgSO_4$, 410 mg of C18, and 315 mg of PSA, and the recoveries ranged from 75 to 122%, with interday and intraday precision of 1–8%. Peysson and Vulliet (2013) applied the QuEChERS approach to determine 17 hormonal steroids and 119 pharmaceutical compounds in SS, obtaining recoveries ranging from 15 to 131%. Herrero et al. (2014) evaluated the QuEChERS method, which involved using citrate buffer for extraction and Z-sep + as a cleaning material, to detect benzotriazoles, benzothiazoles, and benzenesulfonamide derivatives in SS. They achieved over 80% RE for all compounds, with less than 15% intra- and inter-day RSD values. The results of our study indicate that the proposed methodology is a suitable and flexible approach for quantifying OPPs, OPEs, PBDEs, PCBs, OCPs, PYRs, and PAHs in SS, with RE comparable or better than those reported in the literature. The applicability of the method was demonstrated by analyzing seven samples and comparing the results with published data.

Assessment of physical, chemical, and micropollutant levels in sewage sludge samples

Analysis of physical, chemical, and elemental characteristics of sewage sludge samples

The physicochemical analysis of SS samples collected from different WWTPs included pH_w, DM, OM, TOC, nutrients, heavy metals, and other trace elements, such as (Table S2 in the Supporting Information). The variation in sample composition may be related to the origin of the wastewater and the type of treatment process used. For instance, the heavy metal content mainly depends on the proximity of WWTPs to industrial sites (Halecki et al. 2016). The mean pH_w values varied between 6.08 (B and E) and 8.42 (A), indicating a slightly acidic to slightly alkaline pH_w. The DM content of the SS samples ranged from 13.4 to 24.1%, and the OM content varied in the range of 68.7 to 85.8%. Sample A, collected from a WWTP that utilizes an activated sludge process for secondary treatment, exhibited the highest DM content and the lowest OM content. In Portugal, the agricultural use of SS from WWTPs is regulated by Decree-Law No. 276/2009. This law transposes Council Directive 86/278/EEC into national legislation (Ministério do Ambiente do Ordenamento do Território e do Desenvolvimento Regional 2009). According to the current legislation, the concentration of heavy metals must not exceed the following limits: 16 mg kg^{-1} dw for Hg, 20 mg kg^{-1} dw for Cd, 300 mg kg^{-1} dw for Ni, 750 mg kg^{-1} dw for Pb, 1000 mg kg^{-1} dw for Cr and Cu, and 2500 mg kg^{-1} dw for Zn. In the current study, the heavy metal content was found to be within the legal limits, significantly lower than the maximum allowed by the regulations, and consistent with the values reported in the literature (Halecki et al. 2016). Overall, the sample with the highest concentration of PTEs is C followed by A, G, D, F, E, and B.

Generally, studies on the effect of SS application on soil have focused on the variation in topsoil properties (~ 0–20 cm), once it corresponds to the incorporation depth of organic materials, but what about subsoil properties? Hechmi et al. (2021) studied unvegetated semi-arid soils treated with excessive doses of SS for four years. OM, N, P, and K accumulation was monitored in two soil profiles (0–20 and 20–40 cm), while Cu, Zn, Pb, and Ni contents and enzyme activities were assessed. Results showed that the SS application improved OM content in light-textured soils, enriching surface, and subsoil profiles with macronutrients. Moreover, the accumulation of heavy metals from SS did not inhibit essential microbial activities. This suggests that reusing SS can improve soil quality in semi-arid regions without causing significant environmental impacts. Additionally, Zhao et al. (2021) investigated the effect of SS on bacterial communities in forest plantation soils. Results showed an increased abundance of Bacteroidetes, Actinobacteria, and Chloroflexi, but not Acidobacteria, Proteobacteria, and Verrucomicrobia. Changes in keystone bacterial groups and an increase in the interactions among community members were observed, indicating community instability and adaptation to new conditions. These findings are of

particular importance as microorganisms play a crucial role in soil fertility and stability. They are involved in biogeochemical cycles and the degradation of contaminants (Courtois et al. 2021). What about the effects on plants? Iglesias et al. (2018) analyzed 13 PTEs in barley and maize crops and soils amended with SS for 15 years. The results showed an increase in the amount of Pb, Hg, Zn, and Ag in cropland soils. However, the total PTEs contents remained below the thresholds established by US and European regulations. Yet, these regulations do not consider the mobility, extractability, and transfer of PTEs to plants, as pointed out by the authors.

Levels of organic pollutants in sewage sludge samples

Table 3 displays the levels of organic pollutants that were detected and quantified in SS samples after being adjusted for recoveries. Within this monitoring, 16 target compounds were detected: two OPPs (chlorpyrifos-methyl and malathion), four OPEs (TiBP, TPhP, TBEP, and TEHP), one PCB (28), three PBDEs (28, 99, and 183), one OCP (α-endosulfan), two PYRs (cypermethrin and deltamethrin), and three PAHs (FLU, BaP, and DBA). Among the compounds that were detected, eight were identified as persistent organic pollutants (POPs). In each sample, at least two target compounds were detected. Sample C presented the highest number of target compounds and the highest concentration of POPs, whereas F showed the highest concentration of pollutants, followed by E, C, B, A, G, and D. The differences between the samples may be attributed to the composition of the wastewater and/or the characteristics of each treatment system. The presence of pollutants from OPPs, OPEs, PCBs, PBDEs, and PYRs was confirmed through GC-MS analysis. Only TBEP has not been confirmed. To the best of our knowledge, no previous studies have been published on the concentrations of the target compounds in SS from WWTPs located in other regions of Portugal. The EU Sludge Directive establishes maximum concentration values for various substances in sludge intended for agricultural reuse. These substances include halogenated organic compounds, linear alkylbenzene sulfonate, di(2-ethylhexyl)phthalate, nonylphenols and nonyl ethoxylates with one or two ethoxy groups,

Table 3 Concentrations (μg g^{-1} dw) of OPPs, OPEs, PBDEs, PCBs, OCPs, PYRs, and PAHS in sewage sludge collected from municipal wastewater treatment plants located in the north of Portugal ($n = 6$; ND– not detected; <LOQ– below method quantification limit)

Target analyte		SS samples						
		A	B	C	D	E	F	G
OPPs	Chlorpyrifos methyl	ND	ND	<LOQ	ND	ND	ND	ND
	Malathion	ND	ND	ND	<LOQ	ND	ND	ND
OPEs	TiBP	ND	ND	ND	ND	ND	26.8 ± 0.013	ND
	TPhP	ND	ND	ND	<LOQ	2.05 ± 0.012	ND	ND
	TBEP	ND	1.06 ± 0.19	ND	ND	ND	ND	ND
	TEHP	ND	ND	ND	ND	ND	1.53 ± 0.023	ND
PCBs	PCB 118	0.302 ± 0.056	ND	ND	ND	ND	ND	ND
PBDEs	BDE 28	0.128 ± 0.027	<LOQ	ND	ND	ND	ND	ND
	BDE 99	ND	ND	0.0540 ± 0.012	ND	ND	<LOQ	ND
	BDE 183	<LOQ	ND	ND	ND	ND	ND	ND
OCPs	α-Endosulfan	0.110 ± 0.007	0.170 ± 0.005	0.490 ± 0.084	0.571 ± 0.037	0.366 ± 0.010	0.282 ± 0.019	0.286 ± 0.022
PYRs	Cypermethrin	0.0870 ± 0.012	ND	0.0573 ± 0.011	ND	ND	<LOQ	ND
	Deltamethrin	0.254 ± 0.0560	ND	ND	<LOQ	ND	ND	ND
PAHs	Fluoranthene	ND	ND	0.435 ± 0.0042	ND	ND	ND	0.401 ± 0.0143
	Benzo[a] pyrene	ND	ND	0.0442 ± 0.0002	ND	0.0418 ± 0.00003	ND	ND
	Dibenz[a,h] anthracene	ND	ND	<LOQ	ND	ND	ND	<LOQ
Total pollutant load per SS sample (μg g^{-1} dw)		0.881	1.26	2.25	0.571	2.46	28.6	0.687
Total POP load per SS sample (μg g^{-1} dw)		0.540	0.170	1.02	0.571	0.408	0.282	0.687
Number of pollutants detected per SS sample		6	3	7	4	3	5	2

PAHs (acenaphthene, phenanthrene, fluorene, FLU, pyrene, benzo(b + j + k)fluoranthene, BaP, benzo(ghi)perylene, and indeno(1, 2, 3-c, d)pyrene); PCBs (congeners 28, 52, 101, 118, 138, 153, and 180), and polychlorinated dibenzodioxins and dibenzofurans. Compounds belonging to the OPPs, OPEs, PYRs, OCPs, and PBDEs chemical families are not covered by the Sludge Directive. Table S3 in the Supporting Information displays the results for the 42 compounds, and Table S4 shows concentrations from the literature.

Organophosphorus pesticides Dimethoate, parathion-methyl, chlorpyrifos, and chlorfenvinphos were not detected in any sample. However, chlorpyrifos-methyl and malathion were detected in samples C and D, respectively, but their quantities were not determined. OPPs are used to control insect pests, such as weevils or flies, in stored cereals or crops. Products containing chlorpyrifos-methyl as an active ingredient were withdrawn from the EU in 2020 due to their potential toxic effects on human health such as genotoxic potential and developmental neurotoxicity in children (European Commission 2020; European Food Safety Authority 2019). Malathion has been used as a substitute for DDT, and there is a positive association between oral exposure levels and non-Hodgkin's lymphoma and aggressive prostate cancer; however, the evidence is limited (Mohamed et al. 2010; World Health Organization 2016). As far as we are aware, the presence of these pesticides in SS has not been reported, with the exception of chlorpyrifos, which was detected at concentrations ranging from 0.45 to 703 ng g^{-1} and from non-detected to 0.181 ng g^{-1} (Masiá et al. 2015; Maragou et al. 2021). This may be explained by the fact that OPPs, such as malathion, can serve as a carbon and phosphorus source in activated sludge biological processes (Mohamed et al. 2010). Published data show that malathion has an affinity for adsorbing onto the surface of microplastics (Wang et al. 2020).

Pyrethroid pesticides PYRs in SS samples were evaluated because they are commonly used in agriculture, veterinary, and domestic fields to control insects (Bragança et al. 2018). PYRs were not detected in samples B, E, and G. Only one previous study has reported the presence of PYRs in SS, with bifenthrin, λ-cyhalothrin, and deltamethrin detected at concentrations ranging from < 0.005 to 0.0800 mg/kg dw, < 0.01 to 0.471, and < 0.0005 to 0.171 mg/kg dw, respectively (Maragou et al. 2021). However, PYR residues have been reported in effluents and influents of WWTPs (Weston et al. 2013; Firouzsalari et al. 2019), as well as in soil (Ariyani et al. 2020; Deng et al. 2020). These pesticides are known for their affinity for OM and low water solubility (Cycon and Piotrowska-Seget 2016; Horton et al. 2018). For instance, Ziajahromi et al. (2018) described the sorption of bifenthrin to organic carbon in river water and polyethylene microparticles present in the soil as a process that reduces the bioavailability and toxicity of this compound. However, it has been suggested that microplastics can act as vectors for the uptake of pollutants by organisms (Horton et al. 2018). In addition, soil bacteria, such as *Bacillus* sp., can degrade several PYRs into phenoxybenzoic acid (3-PBA), the general metabolic product of these pesticides. 3-PBA is known for its endocrine-disrupting activity and can be toxic to non-target organisms (Chen et al. 2012; Cycon and Piotrowska-Seget 2016). Moreover, seeds of *Cucumis sativus* (*C. sativus*) exposed to cypermethrin, deltamethrin, and λ-cyhalothrin and 3-PBA for seven days showed that certain PYRs can impact the germination and early growth of plants. Exposure to 3-PBA negatively impacted the seed germination of *C. sativus*. Cypermethrin affected the roots, shoots, and leaves, while deltamethrin only affected root length. Chlorophyll and total carotenoid contents increased with exposure to cypermethrin and deltamethrin exposure, while λ-cyhalothrin had no statistically significant effects on germination, seedling development, or pigment content (Bragança et al. 2018).

Organophosphate esters OPEs are a class of organophosphorus flame retardants that have been extensively used as alternatives to halogenated flame retardants (PBDEs) in plastics, electronic equipment, and textiles (Gao et al. 2016; Liang and Liu 2016; Wang et al. 2019). Their presence has been described in various environmental matrices, such as water, soil, sediments, air, biota, and human samples (Wang et al. 2018; Chokwe and Okonkwo 2019). In 2005, Marklund et al. estimated that 49% of the total annual amount of OPEs received by Swedish WWTPs were degraded, 50% were emitted in the effluents, and 1% ended up in the sludge (Marklund et al. 2005). Furthermore, in a typical WWTP, hydrophobic interactions play an important role in the sorption of OPEs to activated sludge and their subsequent biodegradation (Liang and Liu 2016). The removal of OPEs is favored under aerobic conditions, as the enzyme activity is higher and oxidation reactions are more likely to occur. Under anaerobic conditions, triphenyl OPEs (e.g., TPhP) are more likely to biodegrade (> 70%) than chlorinated OPEs (e.g., TCEP) and alkyl OPEs (e.g., TiBP) (Yang et al. 2021). Within the group of OPEs targeted in the present study, four compounds (TiBP, TPhP, TEHP, and TBEP) were detected in four SS samples and were quantified in three samples (B, E, and F). Sample F exhibited high levels of total OPEs (28.3 ± 0.013 µg g^{-1} dw; Fig. 2S in the Supporting Information). This was followed by sample E (2.05 ± 0.012 µg g^{-1} dw; Fig. 3S in the Supporting Information) and sample B (1.06 ± 0.19 µg g^{-1} dw). TiBP (26.8 ± 0.013 µg g^{-1} dw) was the most abundant compound, possibly due to its structure, which includes branched hydrocarbon chains. This structural feature increases its resistance to biodegradation (Liang and

Liu 2016). A survey conducted from 2008 to 2014 investigated 14 OPEs in the sludge of eight Chinese WWTPs. TEHP and TCP were the predominant congeners found, with mean concentrations of 233 and 137 µg/kg, respectively (Gao et al. 2016). Concentrations of OPEs gradually increased over time, which is believed to be directly linked to the increased consumption of these compounds. Recently, Wang et al. (2019) analyzed 75 SS samples from 67 WWTPs in the USA. They found a median concentration of 1290 ng g^{-1} dw (∑20 OPEs). The most abundant congeners detected were TBEP and TEHP, with mean concentrations ranging from undetectable to 28,300 ng g^{-1} dw and 26.5 to 857 ng g^{-1} dw, respectively. Thus, the potential for the accumulation of OPEs in SS and their migration from soil to crops should be considered. Organic pollutants can be taken up by plants through active and passive mechanisms, which depend on the physicochemical properties and concentrations of the compounds in the surrounding environment (Gong et al. 2020). The study conducted by Gong et al. investigated the accumulation, translocation, and transformation of TCEP, TnBP, and TPhP, as well as their diester hydrolysis metabolites (namely bis(2-chloroethyl) phosphate (BCEP), di-n-butyl phosphate (DnBP), and diphenyl phosphate (DPhP)), in wheat (*Triticum aestivum* L.) plants through hydroponic experiments. TnBP, DnBP, TPhP, and DPhP primarily accumulated in the roots, while TCEP and BCEP were mainly transported to the shoots due to their hydrophilic nature. Moreover, the hydrolysis of OPEs occurs in the cell wall, so organophosphate diesters are more stable in plants than organophosphate triesters. Therefore, the possible biological effects of these compounds on the environment deserve more attention (Gong et al. 2020).

Persistent organic pollutants The POPs of interest in this study belong to the chemical families of PCBs, PBDEs, OCPs, and PAHs. Even at low concentrations, these chemicals can accumulate in the food chain and cause harmful effects on both human health (e.g., carcinogenic, immunological, reproductive, and developmental effects) and the environment (Pozo et al. 2020). Among the four PCB congeners analyzed, only PCB 118 was detected and quantified in sample A, at a concentration of 0.302 ± 0.056 µg g^{-1} dw, which is below the EU limit proposed for these compounds (0.8 mg kg^{-1} dw, as shown in Fig. 4S of the Supporting Information). Additionally, the concentration in sample A was below the range of concentrations documented in Egyptian, which ranges from 897 to 2350 µg/kg, dw, as reported by Barak et al. in 2017.

Concerning PBDEs, three congeners were detected in four samples: BDE 28 (0.128 ± 0.027 µg g^{-1} dw; B: < LOQ), BDE 99 (C:0.0540 ± 0.012 µg g^{-1} dw; F: < LOQ), and BDE 183 (A < LOQ). BDE 99 is the primary component of the penta-BDE formulation, whereas BDE 183 is the primary component of octa-BDE. Both commercial PBDE formulations are listed in *Annex A (Elimination)* of the Stockholm Convention (UNEP 2009). The presence of certain PBDEs congeners in the SS samples has been documented in the scientific literature (Sánchez-Brunete et al. 2009; Wang et al. 2013; Zhao et al. 2022, 2023). For instance, six congeners were found in 19 SS samples collected from WWTPs in the province of Madrid, with concentrations ranging from 20.9 to 736.9 ng g^{-1} dw (Sánchez-Brunete et al. 2009). In another study of Spanish SS samples, the concentration of ∑PPBDEs ranged from 16.2 to 45.6 ng g^{-1} dw (Martínez-Moral and Tena 2014). Owing to their flame retardant properties, PBDEs have been widely used in plastic production (Gaylor et al. 2013). PBDEs and plastic polymers do not bind chemically, allowing these compounds to migrate into the surrounding environment and (bio)accumulate. In addition, these compounds are lipophilic and are prone to causing adverse effects on the endocrine system, especially in the regulation of thyroid hormones (Martínez-Moral and Tena 2014). Moreover, Gaylor et al. (2013) conducted a study on the absorption of PBDEs by earthworms (*Eisenia fetida*) in artificial soil. The soil was supplemented with anaerobically digested biosolids, composted biosolids, penta-BDE-spiked polyurethane foam microparticles, and penta-BDE-spiked artificial soil. The study found that *E. fetida* accumulated penta-PBDE from both biosolids and plastic waste, indicating the potential for PBDEs to bioaccumulate and transfer through food chains.

The accumulation of OCPs compounds in SS stems from their persistent nature, adsorption capacity for solid particles, and hydrophobic character (Barakat et al. 2017; Ademoyegun et al. 2020). In this study, α-endosulfan was the only analyte detected in all samples, with concentrations ranging from 0.110 ± 0.007 to 0.571 ± 0.037 µg g^{-1} dw. This OCP is one of two technical endosulfan isomers that were banned worldwide during the 1970s and 1980s (Somtrakoon and Pratumma 2012). However, in 2017, α-endosulfan was detected in SS samples from Egypt (ranging from 3.24 to 76.8 µg kg^{-1}) (Barakat et al. 2017), and in 2020, it was found in South Africa with concentrations ranging from 8 to 99 ng g^{-1} dw (Ademoyegun et al. 2020).

Regarding PAHs, the EU sludge directive recommends that ∑PAHs should not exceed 6 mg kg^{-1} dw in sludge used for agricultural reclamation. The presence of PAHs in SS samples has been extensively reported worldwide. For example, in Taiwan, the concentration of ∑16 PAHs was found to be 0.5332–1.0666 µg kg^{-1} dw (Chen et al. 2019). In Poland, the concentration ranged from 8625 to 13,833 µg kg^{-1} dw (Tomczyk et al. 2020). In Italy, the concentration ranged from 0.01 to 1.48 mg kg^{-1} dw and 0.04 to 3.91 mg kg^{-1} dw (Suciu et al. 2015). In this study, sample C exhibited the highest levels of total PAHs (0.479 ± 0.0044 µg g^{-1} dw; Fig. 5S from the Supporting Information). It was followed

by sample G (0.401 ± 0.014 µg g^{-1} dw) and sample E (0.0418 ± 0.00003 µg g^{-1} dw). FLU (a 3-ring PAH) was the most abundant compound (C: 0.435 ± 0.0042 µg g^{-1} dw; G: 0.401 ± 0.014 µg g^{-1} dw), followed by BaP (a 5-ring PAH) and DBA (a 5-ring PAH), both prioritized for their teratogenic, mutagenic, and carcinogenic characteristics (Wołejko et al. 2018). Samples A, B, D, and F had no detectable congeners.

Overall, the results showed that the developed QuEChERS methodology can be coupled with chromatographic techniques such as GC-FPD, GC-ECD, GC-MS, and LC-PDA-FLD to monitor a wide range of chemical classes in SS. The QuEChERS extraction method enables the use of small amounts of sample and solvent, reducing sample preparation time, and facilitating the use of eco-friendly solvents, especially when compared to classical methods such as Soxhlet, all while demonstrating high efficiency (Perestrelpo et al. 2019). The complexity of the matrix presents challenges in sample preparation for the development of reliable analytical methods, with the cleanup step being crucial. The levels of pollutants in the SS varied among different samples, which could be attributed to both the composition of each wastewater and the distinct characteristics of each treatment system. Sorption–desorption phenomena determine the fate of organic micropollutants in WWTPs. Moreover, the interaction of organic pollutants with activated sludge influences their bioavailability to microorganisms and the subsequent biodegradation during biological treatment (Madrid et al. 2020). The lack of data on SS contamination by organic pollutants, possibly due to the complexity of the matrix, and the potential negative effects on the environment, such as the possibility of migration from soils to crops, are reflected in the challenges of implementing legislation (Calderón-Preciado et al. 2013; Suciu et al. 2015). On the one hand, the reuse of SS allows for the substitution of synthetic fertilizers and the utilization of waste that is abundant in organic nutrients. On the other hand, this practice can pose risks to both the environment and human health, as micropollutants have the potential to accumulate in SS (Martín-Pozo et al. 2019; Madrid et al. 2020). Hence, more studies are needed in the future to evaluate the exposure of SS to soil, particularly those that encompass different chemical families, as they provide a more realistic representation.

Conclusion

The developed method, based on the QuEChERS approach, allows for the simultaneous extraction and analysis of 42 target analytes from complex SS matrices. Purification of the extracts was a critical step because commercial d-SPEs did not prove to be the most efficient. Therefore, CB and Z-Sep had to be added. Thus, it was possible to obtain clean extracts for analysis by gas chromatography. The procedure provided good recoveries and reproducibility, enabling the quantification of all target analytes while minimizing the time needed for sample preparation. Accurate quantification was achieved by using calibration standards that were matched to the matrix. The method yielded satisfactory performance, with a mean recovery ranging from 50 to 126%, and a reproducibility ≤ 21% (RSD). The protocol was successfully applied to seven SS samples, and at least two target compounds were detected in each sample. Of the 42 targeted analytes, 16 were detected at concentrations ranging from 0.0420 to 26.8 µg g^{-1} dw. Of these, eight are listed as POPs and were detected with concentrations ranging from < LOQ to 0.571 µg g^{-1} dw. The pesticide α-endosulfan was quantified in all samples, with concentrations ranging from 0.110 to 0.571 µg g^{-1} dw. Even if the detected compounds meet the legal limits (when applicable) or occur in relatively low concentrations, it should not be forgotten that little is known about the toxic effects that such a mixture may have on human health. For the past 36 years, the Sewage Sludge Directive has aimed at the correct use of SS in agriculture, while safeguarding soil, vegetation, animals, and humans. Furthermore, under the European Green Deal, there is a need to move from a linear economic model to a circular one that is capable of increasing resource efficiency. Consequently, sludge application to agricultural soils may increase in the coming years, particularly in semi-arid areas. In addition, all products used daily, such as pharmaceuticals, can end up in WWTPs and potentially accumulate in SS. Therefore, the inherent nature of the SS matrix and the dynamic behavior of pollutants in the environment make it necessary to broaden the scope of chemical compounds covered by the legislation.

Supplementary Information The online version contains supplementary material available at https://doi.org/10.1007/s11356-023-30963-1.

Acknowledgements The authors thank the Fundação para a Ciência e a Tecnologia (FCT)/Ministério da Ciência, Tecnologia e Ensino Superior (MCTES) for the project Honey+–New reasons to care honey from the Natural Park of Montesinho: A bioindicator of environmental quality and its therapeutic potential (MTS/SAS/0077/2020) and the PhD grant number SFRH/BD/147404/2019 (Diana Rede). The authors also would like to thank Marta Oliveira (PhD) and Paula Paíga (MEng) for technical assistance with HPLC; Professor Agostinho Almeida, Edgar Pinto (PhD), and Rui Azevedo (MSc) for technical assistance with ICP-MS; and Engineer João Sabino Vilaça from SimDOURO for kindly providing the samples used in the study.

Author contribution Diana Rede contributed to conceptualization, methodology development, and sample analysis, and was involved in the writing of the original draft as well as the review and editing stages. Ivan Teixeira played a role in methodology development and conducted sample analysis. Cristina Delerue-Matos provided supervision, managed resources, acquired funding, and contributed to the review of the manuscript. Virgínia Cruz Fernandes provided supervision, contributed to conceptualization and methodology development, and participated in the review and editing stages of the writing process.

Funding Open access funding provided by FCT|FCCN (b-on). This work was supported by a Portuguese national fund (FCT/MCTES) through the projects UIDB/50006/2020, UIDP/50006/2020, and LA/P/0008/2020.

Data availability Not applicable.

Declarations

Ethics approval and consent to participate Not applicable.

Consent for publication Not applicable.

Competing interests The authors declare no competing interests.

Open Access This article is licensed under a Creative Commons Attribution 4.0 International License, which permits use, sharing, adaptation, distribution and reproduction in any medium or format, as long as you give appropriate credit to the original author(s) and the source, provide a link to the Creative Commons licence, and indicate if changes were made. The images or other third party material in this article are included in the article's Creative Commons licence, unless indicated otherwise in a credit line to the material. If material is not included in the article's Creative Commons licence and your intended use is not permitted by statutory regulation or exceeds the permitted use, you will need to obtain permission directly from the copyright holder. To view a copy of this licence, visit http://creativecommons.org/licenses/by/4.0/.

References

Adelodun B, Kumar P, Odey G et al (2022) A safe haven of SARS-CoV-2 in the environment: prevalence and potential transmission risks in the effluent, sludge, and biosolids. Geosci Front 19. https://doi.org/10.1016/j.gsf.2022.101

Ademoyegun OT, Okoh OO, Okoh AI (2020) Organochlorine pesticides in selected sewage sludge in South Africa: assessment and method validation. Polish J Environ Stud 29:1021–1028. https://doi.org/10.15244/pjoes/97391

Ariyani M, Pitoi MM, Koesmawati TA et al (2020) Pyrethroid residues on tropical soil of an Indonesian tea plantation: analytical method development, monitoring, and risk assessment. Sustain Environ Res 30:15. https://doi.org/10.1186/s42834-020-00055-7

Barakat AO, Khairy MA, Mahmoud MR (2017) Organochlorine pesticides and polychlorinated biphenyls in sewage sludge from Egypt. J Environ Sci Heal - Part A Toxic/hazardous Subst Environ Eng 52:750–756. https://doi.org/10.1080/10934529.2017.1303313

Bhardwaj SK, Dwivedia K, Agarwala DD (2016) A review: GC method development and validation. Int J Anal Bioanal Chem 6(1):1–7

Bragança I, Lemos PC, Barros P et al (2018) Phytotoxicity of pyrethroid pesticides and its metabolite towards Cucumis sativus. Sci Total Environ 619–620:685–691. https://doi.org/10.1016/j.scitotenv.2017.11.164

Bragança I, Lemos PC, Delerue-Matos C, Domingues VF (2019) Assessment of pyrethroid pesticides in topsoils in NorthernPortugal. Water Air Soil Pollut 230:166. https://doi.org/10.1007/s11270-019-4209-7

Buta M, Hubeny J, Zieliński W et al (2021) Sewage sludge in agriculture — the effects of selected chemical pollutants and emerging genetic resistance determinants on the quality of soil and crops — a review. Ecotoxicol Environ Saf 214:112070. https://doi.org/10.1016/j.ecoenv.2021.112070

Calderón-Preciado D, Matamoros V, Savé R et al (2013) Uptake of microcontaminants by crops irrigated with reclaimed water and groundwater under real field greenhouse conditions. Environ Sci Pollut Res 20:3629–3638. https://doi.org/10.1007/s11356-013-1509-0

Campo G, Cerutti A, Lastella C et al (2021) Production and destination of sewage sludge in the piemonte region (Italy): the results of a survey for a future sustainable management. Int J Environ Res Public Health 18:3556. https://doi.org/10.3390/ijerph18073556

Castro G, Ramil M, Cela R, Rodríguez I (2021) Identification and determination of emerging pollutants in sewage sludge driven by UPLC-QTOF-MS data mining. Sci Total Environ 778. https://doi.org/10.1016/j.scitotenv.2021.146256

Chen S, Hu W, Xiao Y et al (2012) Degradation of 3-phenoxybenzoic acid by a Bacillus sp. PLoS ONE 7:1–12. https://doi.org/10.1371/journal.pone.0050456

Chen M, Oshita K, Mahzoun Y et al (2021) Survey of elemental composition in dewatered sludge in Japan. Sci Total Environ 752:141857. https://doi.org/10.1016/j.scitotenv.2020.141857

Chen CF, Ju YR, Lim YC et al (2019) Determination of polycyclic aromatic hydrocarbons in sludge from water and wastewater treatment plants by GC-MS. Int J Environ Res Public Health 16:2604. https://doi.org/10.3390/ijerph16142604

Chokwe TB, Okonkwo JO (2019) Occurrence, distribution and ecological risk assessment of organophosphorus flame retardants and plasticizers in sediment samples along the Vaal River catchment, South Africa. Emerg Contam 5:173–178. https://doi.org/10.1016/j.emcon.2019.05.003

Corradini F, Meza P, Eguiluz R et al (2019) Evidence of microplastic accumulation in agricultural soils from sewage sludge disposal. Sci Total Environ 671:411–420. https://doi.org/10.1016/j.scitotenv.2019.03.368

Correia-Sá L, Fernandes VC, Carvalho M et al (2012) Optimization of QuEChERS method for the analysis of organochlorine pesticides in soils with diverse organic matter. J Sep Sci 35:1521–1530. https://doi.org/10.1002/jssc.201200087

Courtois P, Rorat A, Lemiere S et al (2021) Medium-term effects of Ag supplied directly or via sewage sludge to an agricultural soil on Eisenia fetida earthworm and soil microbial communities. Chemosphere 269. https://doi.org/10.1016/j.chemosphere.2020.128761

Cruz Fernandes V, Freitas M, Pacheco JG et al (2020) Evaluation of the QuEChERS and magnetic micro dispersive solid-phase extraction of brominated flame retardants in red fruits with determination by GC/MS. Food Chem 309:125572. https://doi.org/10.1016/j.foodchem.2019.125572

Cycon M, Piotrowska-Seget Z (2016) Pyrethroid-degrading microorganisms and their potential for the bioremediation of contaminated soils: a review. Front Microbiol 7:1–26. https://doi.org/10.3389/fmicb.2016.01463

Deng F, Sun J, Dou R et al (2020) Contamination of pyrethroids in agricultural soils from the Yangtze River Delta. China Sci Total Environ 731:139181. https://doi.org/10.1016/j.scitotenv.2020.139181

Dorosh O, Fernandes VC, Moreira MM, Delerue-Matos C (2021) Occurrence of pesticides and environmental contaminants in vineyards: case study of Portuguese grapevine canes. Sci Total Environ 791:148395. https://doi.org/10.1016/j.scitotenv.2021.148395

European Commission (1986) Council directive 86/278/EEC of 12 June 1986 on the protection of the environment, and in particular of the soil, when sewage sludge is used in agriculture. Of J L181(L181):6–12

European Commission (2000) Working document on sludge 27 April 2000 - ENV.E.3/LM (3rd draft). Accessed 22 Aug 2023

European Commission (2019) Method validation procedures for pesticide residues analysis in food and feed. SANTE/12682/2019:1–49. Accessed 22 Aug 2023

European Commission (2020) Commission implementing regulation (EU) 2020/17 of 10 January 2020. Official Journal of the European Union L 7/11-L 7/13. Accessed 22 Aug 2023

European Commission (2021) Guidance document on pesticide analytical methods for risk assessment and post-approval control and monitoring purposes. SANTE/2020/12830, Rev. 1:1–50 Accessed 22 Aug 2023

European Food Safety Authority (2019) Statement on the available outcomes of the human health assessment in the context of the pesticides peer review of the active substance chlorpyrifos-methyl. EFSA J 17(8):581017. https://doi.org/10.2903/j.efsa.2019.5810

Fernandes VC, Domingues VF, Mateus N, Delerue-Matos C (2012) Analysing organochlorine pesticides in strawberry jams using GC-ECD, GC-MS/MS and QuEChERS sample preparation. Food Addit Contam - Part A 29:1074–1084. https://doi.org/10.1080/19440049.2012.682319

Fernandes VC, Freitas M, Pacheco JPG et al (2018) Magnetic dispersive micro solid-phase extraction and gas chromatography determination of organophosphorus pesticides in strawberries. J Chromatogr A 1566:1–12. https://doi.org/10.1016/j.chroma.2018.06.045

Fernandes VC, Luts W, Delerue-Matos C, Domingues VF (2020) Improved QuEChERS for analysis of polybrominated diphenyl ethers and novel brominated flame retardants in Capsicum cultivars using gas chromatography. J Agric Food Chem 68:3260–3266. https://doi.org/10.1021/acs.jafc.9b07041

Firouzsalari NZ, Shakerkhatibi M, Pourakbar M et al (2019) Pyrethroid pesticide residues in a municipal wastewater treatment plant: occurrence, removal efficiency, and risk assessment using a modified index. J Water Process Eng 29. https://doi.org/10.1016/j.jwpe.2019.100793

Gago J, Windsor FM, Durance I et al (2019) Standardised protocol for monitoring microplastics in seawater. Mar Pollut Bull 90:96

Gao L, Shi Y, Li W et al (2016) Occurrence and distribution of organophosphate triesters and diesters in sludge from sewage treatment plants of Beijing, China. Sci Total Environ 544:143–149. https://doi.org/10.1016/j.scitotenv.2015.11.094

Gaylor MO, Harvey E, Hale RC (2013) Polybrominated diphenyl ether (PBDE) accumulation by earthworms (Eisenia fetida) exposed to biosolids-, polyurethane foam microparticle-, and penta-BDE-amended soils. Environ Sci Technol 47:13831–13839. https://doi.org/10.1021/es403750a

Gong X, Wang Y, Pu J et al (2020) The environment behavior of organophosphate esters (OPEs) and di-esters in wheat (Triticum aestivum L.): Uptake mechanism, in vivo hydrolysis and subcellular distribution. Environ Int 135:105405. https://doi.org/10.1016/j.envint.2019.105405

Gonzalez A, van Lier JB, de Kreuk MK (2021) The role of growth media on composition, bioconversion and susceptibility for mild thermal pre-treatment of waste activated sludge. J Environ Manage 298:113491. https://doi.org/10.1016/j.jenvman.2021.113491

Guillemet TA, Maesen P, Delcarte É et al (2009) Factors influencing microbiological and chemical composition of South-Belgian raw sludge. Biotechnol Agron Société Environ 13:249–255

Guo L, Zhang B, Xiao K et al (2009) Levels and distributions of polychlorinated biphenyls in sewage sludge of urban wastewater treatment plants. J Environ Sci 21:468–473. https://doi.org/10.1016/S1001-0742(08)62293-7

Halecki W, Michał G, Gambus F, Abram R (2016) The potential of hydrated and dehydrated sewage sludge discharges from soil reclamation appliances. Fresenius Environ Bull 25:1935–1941

Hatinoğlu MD, Sanin FD (2021) Sewage sludge as a source of microplastics in the environment: a review of occurrence and fate during sludge treatment. J Environ Manage 295:113028. https://doi.org/10.1016/j.jenvman.2021.113028

Hechmi S, Hamdi H, Mokni-Tlili S et al (2021) Variation of soil properties with sampling depth in two different light-textured soils after repeated applications of urban sewage sludge. J Environ Manage 297. https://doi.org/10.1016/j.jenvman.2021.113355

Herrero P, Borrull F, Marcé RM, Pocurull E (2013) Determination of polyether ionophores in urban sewage sludge by pressurised liquid extraction and liquid chromatography-tandem mass spectrometry: study of different clean-up strategies. J Chromatogr A 1285:31–39. https://doi.org/10.1016/j.chroma.2013.02.034

Herrero P, Borrull F, Pocurull E, Marcé RM (2014) A quick, easy, cheap, effective, rugged and safe extraction method followed by liquid chromatography-(Orbitrap) high resolution mass spectrometry to determine benzotriazole, benzothiazole and benzenesulfonamide derivates in sewage sludge. J Chromatogr A 1339:34–41. https://doi.org/10.1016/j.chroma.2014.02.081

Horton AA, Walton A, Spurgeon DJ et al (2017) Microplastics in freshwater and terrestrial environments: evaluating the current understanding to identify the knowledge gaps and future research priorities. Sci Total Environ 586:127–141. https://doi.org/10.1016/j.scitotenv.2017.01.190

Horton AA, Vijver MG, Lahive E et al (2018) Acute toxicity of organic pesticides to Daphnia magna is unchanged by co-exposure to polystyrene microplastics. Ecotoxicol Environ Saf 166:26–34. https://doi.org/10.1016/j.ecoenv.2018.09.052

Iglesias M, Marguí E, Camps F, Hidalgo M (2018) Extractability and crop transfer of potentially toxic elements from mediterranean agricultural soils following long-term sewage sludge applications as a fertilizer replacement to barley and maize crops. Waste Manag 75:312–318. https://doi.org/10.1016/j.wasman.2018.01.024

Liang K, Liu J (2016) Understanding the distribution, degradation and fate of organophosphate esters in an advanced municipal sewage treatment plant based on mass flow and mass balance analysis. Sci Total Environ 544:262–270. https://doi.org/10.1016/j.scitotenv.2015.11.112

Madrid F, Rubio-Bellido M, Morillo E (2020) Extraction of nonylphenol, pyrene and phenanthrene from sewage sludge and composted biosolids by cyclodextrins and rhamnolipids. Sci Total Environ 715:136986. https://doi.org/10.1016/j.scitotenv.2020.136986

Magnusson B, Örnemark U (2014) Eurachem guide: The fitness for purpose of analytical methods – a laboratory guide to method validation and related topics, 2nd ed. Available from https://www.eurachem.org

Mahon AM, O'Connell B, Healy MG et al (2017) Microplastics in sewage sludge: effects of treatment. Environ Sci Technol 51:810–818. https://doi.org/10.1021/acs.est.6b04048

Maragou NC, Balayiannis G, Karanasios E et al (2021) Targeted multiresidue method for the analysis of different classes of pesticides in agro-food industrial sludge by liquid chromatography tandem mass spectrometry. Molecules 26:6888. https://doi.org/10.3390/molecules26226888

Marklund A, Andersson B, Haglund P (2005) Organophosphorus flame retardants and plasticizers in Swedish sewage treatment plants. Environ Sci Technol 39:7423–7429. https://doi.org/10.1021/es0510131

Martínez-Moral MP, Tena MT (2014) Use of microextraction by packed sorbents following selective pressurised liquid extraction for the determination of brominated diphenyl ethers in sewage sludge by gas chromatography-mass spectrometry. J Chromatogr A 1364:28–35. https://doi.org/10.1016/j.chroma.2014.08.075

Martín-Pozo L, de Alarcón-Gómez B, Rodríguez-Gómez R et al (2019) Analytical methods for the determination of emerging contaminants in sewage sludge samples. A Review Talanta 192:508–533. https://doi.org/10.1016/j.talanta.2018.09.056

Masiá A, Vásquez K, Campo J, Picó Y (2015) Assessment of two extraction methods to determine pesticides in soils, sediments and

sludges. Application to the Túria River Basin. J Chromatogr A 1378:19–31. https://doi.org/10.1016/j.chroma.2014.11.079
Miller JN, Miller JC (2010) Statistics and chemometrics for analytical chemistry, 6th edn. Pearson Education Limited
Ministério do Ambiente do Ordenamento do Território e do Desenvolvimento Regional (2009) Decreto-Lei N.276/2009. Diário da República n 192, Série I 2 Outubro 2009 7154–7165. Accessed 22 Aug 2023
Mohamed ZK, Ahmed MA, Fetyan NA, Elnagdy SM (2010) Isolation and molecular characterisation of malathion-degrading bacterial strains from waste water in Egypt. J Adv Res 1:145–149. https://doi.org/10.1016/j.jare.2010.03.007
Mohapatra DP, Cledón M, Brar SK, Surampalli RY (2016) Application of wastewater and biosolids in soil: occurrence and fate of emerging contaminants. Water Air Soil Pollut 227:77. https://doi.org/10.1007/s11270-016-2768-4
Naidu R, Biswas B, Willett IR et al (2021) Chemical pollution: a growing peril and potential catastrophic risk to humanity. Environ Int 156:106616. https://doi.org/10.1016/j.envint.2021.106616
Oliveira M, Slezakova K, Delerue-Matos C et al (2015) Polycyclic aromatic hydrocarbons: levels and phase distributions in preschool microenvironment. Indoor Air 25:557–568. https://doi.org/10.1111/ina.12164
Paíga P, Correia M, Fernandes MJ et al (2019) Assessment of 83 pharmaceuticals in WWTP influent and effluent samples by UHPLC-MS/MS: Hourly variation. Sci Total Environ 648:582–600. https://doi.org/10.1016/j.scitotenv.2018.08.129
Perestrelpo R, Silva P, Porto-Figueira P et al (2019) QuEChERS — fundamentals, relevant improvements, applications and future trends _ Elsevier Enhanced Reader.pdf. Anal Chim Acta 1070:1–28
Peysson W, Vulliet E (2013) Determination of 136 pharmaceuticals and hormones in sewage sludge using quick, easy, cheap, effective, rugged and safe extraction followed by analysis with liquid chromatography-time-of-flight-mass spectrometry. J Chromatogr A 1290:46–61. https://doi.org/10.1016/j.chroma.2013.03.057
Ponce-Robles L, Rivas G, Esteban B et al (2017) Determination of pesticides in sewage sludge from an agro-food industry using QuEChERS extraction followed by analysis with liquid chromatography-tandem mass spectrometry. Anal Bioanal Chem 409:6181–6193. https://doi.org/10.1007/s00216-017-0558-5
Pozo K, Urbina W, Gómez V et al (2020) Persistent organic pollutants sorbed in plastic resin pellet - "nurdles" from coastal areas of Central Chile. Mar Pollut Bull 151. https://doi.org/10.1016/j.marpolbul.2019.110786
Rajski Ł, Lozano A, Uclés A et al (2013) Determination of pesticide residues in high oil vegetal commodities by using various multi-residue methods and clean-ups followed by liquid chromatography tandem mass spectrometry. J Chromatogr A 1304:109–120. https://doi.org/10.1016/j.chroma.2013.06.070
Ramos S, Homem V, Santos L (2019) Development and optimization of a QuEChERS-GC–MS/MS methodology to analyse ultraviolet-filters and synthetic musks in sewage sludge. Sci Total Environ 651:2606–2614. https://doi.org/10.1016/j.scitotenv.2018.10.143
Rossini D, Ciofi L, Ancillotti C et al (2016) Innovative combination of QuEChERS extraction with on-line solid-phase extract purification and pre-concentration, followed by liquid chromatography-tandem mass spectrometry for the determination of non-steroidal anti-inflammatory drugs and their metaboli. Anal Chim Acta 935:269–281. https://doi.org/10.1016/j.aca.2016.06.023
Sánchez-Brunete C, Miguel E, Tadeo JL (2009) Analysis of polybrominated diphenyl ethers in sewage sludge by matrix solid-phase dispersion and isotope dilution GC-MS. J Sep Sci 32:109–117. https://doi.org/10.1002/jssc.200800479
Schnell M, Horst T, Quicker P (2020) Thermal treatment of sewage sludge in Germany: a review. J Environ Manage 263:110367. https://doi.org/10.1016/j.jenvman.2020.110367
Somtrakoon K, Pratumma S (2012) Phytotoxicity of heptachlor and endosulfan sulfate contaminants in soils to economic crops. J Environ Biol 33:1097–1101
Sousa S, Rede D, Cruz Fernandes V et al (2023) Accumulation of organophosphorus pollutants in adipose tissue of obese women-metabolic alterations. Environ Res 239. https://doi.org/10.1016/j.envres.2023.117337
Suciu NA, Lamastra L, Trevisan M (2015) PAHs content of sewage sludge in Europe and its use as soil fertilizer. Waste Manag 41:119–127. https://doi.org/10.1016/j.wasman.2015.03.018
Tomczyk B, Siatecka A, Jędruchniewicz K et al (2020) Polycyclic aromatic hydrocarbons (PAHs) persistence, bioavailability and toxicity in sewage sludge- or sewage sludge-derived biochar-amended soil. Sci Total Environ 747. https://doi.org/10.1016/j.scitotenv.2020.141123
UNEP (2009) Stockholm convention on persistent organic pollutants (POPs) as amended in 2009: Text and annexes. Available from https://wedocs.unep.org/20.500.11822/27568
UN DESA (2023) The sustainable development goals report 2023: special edition - July 2023. Available from https://unstats.un.org/sdgs/report/2023/. Accessed 22 Aug 2023
van den Berg P, Huerta-Lwanga E, Corradini F, Geissen V (2020) Sewage sludge application as a vehicle for microplastics in eastern Spanish agricultural soils. Environ Pollut 261:114198. https://doi.org/10.1016/j.envpol.2020.114198
Venkatesan AK, Halden RU (2020) Using national sewage sludge data for chemical ranking and prioritization. Curr Opin Environ Sci Heal 14:10–15. https://doi.org/10.1016/j.coesh.2019.10.006
Wan X, Huang H, Liao Z et al (2022) The distribution and risk of microplastics discharged from sewage treatment plants in terrestrial and aquatic compartment. J Environ Manage 314:115067. https://doi.org/10.1016/j.jenvman.2022.115067
Wang X, Xi B, Huo S et al (2013) Characterization, treatment and releases of PBDEs and PAHs in a typical municipal sewage treatment plant situated beside an urban river, East China. J Environ Sci (china) 25:1281–1290. https://doi.org/10.1016/S1001-0742(12)60201-0
Wang Y, Sun H, Zhu H et al (2018) Occurrence and distribution of organophosphate flame retardants (OPFRs) in soil and outdoor settled dust from a multi-waste recycling area in China. Sci Total Environ 625:1056–1064. https://doi.org/10.1016/j.scitotenv.2018.01.013
Wang Y, Kannan P, Halden RU, Kannan K (2019) A nationwide survey of 31 organophosphate esters in sewage sludge from the United States. Sci Total Environ 655:446–453. https://doi.org/10.1016/j.scitotenv.2018.11.224
Wang T, Yu C, Chu Q et al (2020) Adsorption behavior and mechanism of five pesticides on microplastics from agricultural polyethylene films. Chemosphere 244. https://doi.org/10.1016/j.chemosphere.2019.125491
Weston DP, Ramil HL, Lydy MJ (2013) Pyrethroid insecticides in municipal wastewater. Environ Toxicol Chem 32:2460–2468. https://doi.org/10.1002/etc.2338
Wołejko E, Wydro U, Jabłońska-Trypuć A et al (2018) The effect of sewage sludge fertilization on the concentration of PAHs in urban soils. Environ Pollut 232:347–357. https://doi.org/10.1016/j.envpol.2017.08.120
World Health Organization (2016) Use of malathion for vector control: Report of a WHO meeting Geneva, 16-17 May 2016. Available from https://www.who.int/publications/i/item/9789241510578. Accessed 22 Aug 2023
Wyrwicka A, Steffani S, Urbaniak M (2014) The effect of PCB-contaminated sewage sludge and sediment on metabolism of

cucumber plants (cucumis sativus L.). Ecohydrol Hydrobiol 14:75–82. https://doi.org/10.1016/j.ecohyd.2014.01.003

Yang X, Fan D, Gu W et al (2021) Aerobic and anaerobic biodegradability of organophosphates in activated sludge derived from kitchen garbage biomass and agricultural residues. Front Bioeng Biotechnol 9:1–14. https://doi.org/10.3389/fbioe.2021.649049

Yuan Q, Zhang H, Qin C et al (2023) Impact of emerging pollutant florfenicol on enhanced biological phosphorus removal process: focus on reactor performance and related mechanisms. Sci Total Environ 859:160316. https://doi.org/10.1016/j.scitotenv.2022.160316

Zhang S, Yao H, Lu Y et al (2017) Uptake and translocation of polycyclic aromatic hydrocarbons (PAHs) and heavy metals by maize from soil irrigated with wastewater. Sci Rep 7:1–11. https://doi.org/10.1038/s41598-017-12437-w

Zhao Q, Chu S, He D et al (2021) Sewage sludge application alters the composition and co-occurrence pattern of the soil bacterial community in southern China forestlands. Appl Soil Ecol 157:103744. https://doi.org/10.1016/j.apsoil.2020.103744

Zhao J, Qin C, Sui M et al (2022) Understanding the mechanism of polybrominated diphenyl ethers reducing the anaerobic co-digestion efficiency of excess sludge and kitchen waste. Environ Sci Pollut Res 29:41357–41367. https://doi.org/10.1007/s11356-022-18795-x

Zhao J, Zhang H, Guan D et al (2023) New insights into mechanism of emerging pollutant polybrominated diphenyl ether inhibiting sludge dark fermentation. Bioresour Technol 368:128358. https://doi.org/10.1016/j.biortech.2022.128358

Zhu F, Wu X, Zhao L et al (2017) Lipid profiling in sewage sludge. Water Res 116:149–158. https://doi.org/10.1016/j.watres.2017.03.032

Zhu Q, Jia J, Zhang K et al (2019) Spatial distribution and mass loading of phthalate esters in wastewater treatment plants in China: an assessment of human exposure. Sci Total Environ 656:862–869. https://doi.org/10.1016/j.scitotenv.2018.11.458

Ziajahromi S, Kumar A, Neale PA, Leusch FDL (2018) Environmentally relevant concentrations of polyethylene microplastics negatively impact the survival, growth and emergence of sediment-dwelling invertebrates. Environ Pollut 236:425–431. https://doi.org/10.1016/j.envpol.2018.01.094

Publisher's Note Springer Nature remains neutral with regard to jurisdictional claims in published maps and institutional affiliations.

Supportingy Information

Assessing Emerging and Priority Micropollutants in Sewage Sludge: Environmental Insights and Analytical Approaches

Diana Rede[1,2], Ivan Teixeira[1], Cristina Delerue-Matos[1], and Virgínia Cruz Fernandes[1,*]

[1]REQUIMTE/LAQV, Instituto Superior de Engenharia do Porto, Instituto Politécnico do Porto, Rua Dr. António Bernardino de Almeida, 431, 4249-015 Porto, Portugal
[2]Departamento de Química e Bioquímica, Faculdade de Ciências, Universidade do Porto, Rua do Campo Alegre s/n, 4169– 007 Porto, Portugal.

*Corresponding author: vir@isep.ipp.pt

S.1 Materials and Methods

S.1.1 Sampling Sites

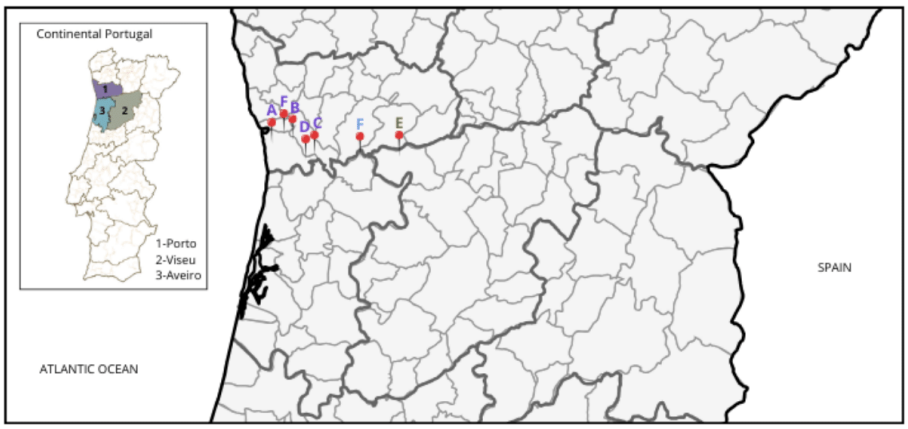


Fig. 1S Map of the sampling sites located in Continental Portugal - Sampling sites (A to F) across the Porto, Viseu and Aveiro regions (1 to 3)

S.1.2 Physical, Chemical, and Elemental Characterization of Sewage Sludge

The physicochemical characterization of the samples was carried out according to standardized methods. All parameters were analyzed in duplicate, and blanks were also prepared. For instance, the pH in water (pH_w) was determined using SW-846 Test Method 9045D: Soil and Waste pH from EPA

(USEPA, 1986). The measurements were performed at room temperature in a 1:2 (m/V) SS/water suspension using an electronic pH meter (micropH 2002 Crison, Spain) after 20-minute of contact time. Dry matter (DM) and organic matter (OM) content were assessed according to EN 12457-4 (CEN, 2002) and the Laboratory Guide for Conducting Soil Tests and Plant Analysis (J.B.Jones, 2001), respectively. DM was determined by weighing the difference, using a forced-draft oven (J.P. Selecta S.A 2000200), where the samples were placed overnight at 105 °C. OM was estimated using the loss-on-ignition methodology. The previous dried samples were placed into a muffle furnace (Nabertherm-B 180, Germany) at 450 °C for 4 hours. Total carbon (TOC) was determined using a Shimadzu TOC-Vscn E200V analyzer with SSM-5000A Solid Sample Module (Shimadzu Corporation, Kyoto, Japan).

For the determination of mineral and metal content, samples were digested using HNO_3, in open vessels covered with a watch glass and heated conventional (APHA, 1992). After cooling, the volume of the digested samples was adjusted to 10 mL using deionized water. The concentrations of Co, Mo, Hg, Cd, Ni, Pb, Cr, Cu, Zn, Li, Be, V, As, Se, Rb, Sr, Rh, Sb, Cs, Ba, Ir, Tl, Mg, Ca, Mn, and Fe were determined using Ion Coupled Plasma Mass Spectrometry (ICP-MS) performed with a Thermo Fisher Scientific (Bremen, Germany) iCAP™ Q instrument, which was equipped with a MicroMist™ nebulizer (Glass Expansion, Port Melbourne Vic, Australia). The instrument also included a Peltier-cooled baffled cyclonic spray chamber, a standard quartz torch, and a two-cone interface design with Ni sample and skimmer cones., High-purity argon (99.9997%; Praxair, Portugal) was used as the carrier gas. Prior to use, all the labware was properly soaked in 10% HNO_3 and rinsed with deionized water.

S.1.3 Chromatographic Analysis

PAHs were quantified using an LC system (Shimadzu Corporation, Kyoto, Japan), equipped with an LC-20AD pump, DGU-20AS degasser, and photodiode array SPD-M20A, as well as fluorescence RF-10AXL detectors. The LC system was operated using LC Solution Shimadzu software. Chromatographic separation was performed at 20 ± 1 °C by injecting 15.0 µL of sample extracts onto a NUCLEOSIL® 100-5 C18 PAH column (150 x 4.0 mm and 5 µm particle size) from Macherey–Nagel (Duren, Germany), with a flow rate of 0.8 mL min^{-1}. The chromatographic conditions consisted of a

mixture of 50% ACN and 50% ultrapure water. Then, the elution gradient was increased to 100% over 15 minutes, and these conditions were maintained for an additional 13 minutes (Oliveira et al., 2015).

OPPs and **OPEs** were determined using a Shimadzu GC-FPD operated by the Shimadzu GC Solution software. The injector and detector temperatures were maintained at 250 and 290 °C, respectively. 1.0 µL of the sample solution was injected in splitless mode on a capillary column TRB-5 (30 m in length, 0.32 mm in inner diameter (i.d.), with a 0.25 µm film thickness, manufactured by Teknokroma, Barcelona, Spain). The GC oven temperature was programmed as follows: 100 °C for 1 min, ramped at 20 °C min^{-1} to 150 °C, held for 1 min, ramped at 2 °C min^{-1} to 180 °C, held for 2 min, and finally ramped at 20 °C min^{-1} to 290 °C, and held at the final temperature for 5 min. Helium (purity 99.99% from Linde Sogás) was used at a pressure of 83.6 KPa, linear velocity of 25.4 cm s^{-1}, and flow rate of 1 mL min^{-1}.

The analysis of **PBDEs**, **PCBs**, **OCPs**, and **PYRs** was performed in splitless mode with a 2 µL injection volume using a GC-ECD operated by GC Solution Shimadzu software. A capillary column, Zebron-5MS (30 m × 0.25 mm × 0.25 µm), from Phenomenex Spain, was used. The oven temperature was initially set at 40 °C (held for 1 min), then increased to 120 °C at a rate of 15 °C min^{-1} per minute and held for 1 min. After the temperature was increased to 200 °C at a rate of 10 °C min^{-1} (held for 1 min), it was further increased to 290 °C at a rate of 7 °C min^{-1} and maintained for 10 min. The injector and detector temperatures were set at 250 °C and 300 °C, respectively. The flow rate of the helium carrier gas (Nippon Gases, Portugal) was set at 1.3 mL min^{-1} with a linear velocity of 32.7 cm s^{-1}, and the nitrogen make-up gas (Nippon Gases, Portugal) at a rate of 30 mL min^{-1}.

GC-MS analyses were performed using a Thermo Fisher Scientific instrument (Waltham, USA) coupled with an ion trap mass detector (Thermo Polaris). The analytes were separated on a Zebron-5ms capillary column (30 m × 250 µm i.d., 0.25 µm thickness, Phenomenex, Spain). The oven temperature was initially maintained at 40 °C for 1 minute, and then the temperature was increased to 290 °C as follows: 120 °C at a rate of 15 °C per minute, held for 1 minute; 150 °C (10 °C per minute), held for 1 minute; 180 °C (10 °C per minute), held for 1 minute; 200 °C (10 °C per minute), held for 1 minute; and 290 °C (10 °C per minute), held for 10 minutes. The helium carrier gas (purity ≥ 99.999%) was maintained at a constant flow rate of 1.0 mL/min. The temperatures of the inlet, ion source, and transfer

line were maintained at 250 °C. The injection volume of 1 µL entered the GC-MS system in splitless mode. The mass spectrometer was operated with electron impact (eI) ionization (-70 eV) with a filament current of 200 µA in the SIM and tandem MS modes. The retention time, precursor, and fragment ions are listed in Table S1. At least three fragment ions were monitored for each compound. To maximize the detector signal, the most abundant and characteristic ion in the spectrum was selected for confirmation.

Table S1: SIM program used to confirm the OPPs, OPEs, PCBs, PBDEs, OCPs, and PYRs detected in the SS samples.

Compound	m/z	Retention time (min)	Dwell time (ms)
TiBP	99,155, 211, 265	13.16	99
Chlorpyrifos-methyl	109, 125, 197, 286	19.07	286
Malathion	93, 99, 125, 158, 173	20.01	173
α-endosulfan	195, 241, 265, 277	21.82	195
PCB118	145, 184, 219, 254, 256, 326	23.28	326
BDE 28	168, 223, 247, 406	23.42	406
TPhP	77, 169, 215, 233, 326	24.66	215
TEHP	57, 99, 113, 211, 323	24.91	99
BDE 99	404, 564, 566	27.78	404
Cypermethrin	91, 127, 152, 163	28.11	163
Deltamethrin	77, 93, 172, 209, 253	30.13	253
BDE 183	561, 564, 723	34.17	561

S.2 Results

S.2.1 Physical, Chemical, and Elemental Characterization of Sewage Sludge Samples

Table S2: Physicochemical properties, heavy metals, and other trace elements content of SS samples (n=2) (mean ± SD) (ND = Not detected).

Parameter	Sewage Sludge Samples						
	A	B	C	D	E	F	G
pH	8.42	6.08	7.98	6.61	6.08	6.93	7.38
DM (%)	24.1	15.5	17.0	14.4	13.4	20.7	19.8
OM (% dw)	68.7	85.1	74.1	85.8	81.5	85.2	73.5
Primary nutrients							
TOC (%)	36.8	40.5	32.8	27.3	16.8	44.3	35.2
Secondary nutrients							
Ca (mg kg^{-1}dw)	12,473	2,857	10,541	10,162	7,579	12,265	13,016
Mg (mg kg^{-1}dw)	1,619	1,129	2,743-	2,927	1,799	2,242	2,779
Micro nutrients							

Co (mg kg^{-1}dw)	2.35	1.26	60.2	2.31	1.57	1.56	2.84
Mo (mg kg^{-1}dw)	3.23	2.14	4.93	3.75	2.88	3.06	4.00
Mn (mg kg^{-1}dw)	105	43.6	643	75.2	108	71.6	127
Fe (mg kg^{-1}dw)	3,957	1,412	8,856	2,867	3,041	2,247	6,994
Heavy metals							
Hg (mg kg^{-1}dw)	0.060	0.050	0.110	0.170	0.190	0.050	0.210
Cd (mg kg^{-1}dw)	0.730	0.290	7.89	0.790	0.660	0.810	1.10
Ni (mg kg^{-1}dw)	59.5	16.5	110	29.7	14.2	11.0	20.1
Pb (mg kg^{-1}dw)	27.8	8.51	38.3	22.8	14.9	20.6	32.9
Cr (mg kg^{-1}dw)	125	12.3	32.2	27.7	13.9	12.7	25.2
Cu (mg kg^{-1}dw)	172	115	246	181	140	179	269
Zn (mg kg^{-1}dw)	906	238	2187	634	453	689	935
Other trace elements							
Li (mg kg^{-1}dw)	7.80	1.44	7.01	3.55	8.37	3.67	16.9
Be (mg kg^{-1}dw)	0.450	0.190	2.62	0.180	0.550	0.330	1.34
V (mg kg^{-1}dw)	6.71	1.52	9.62	5.56	4.42	5.32	8.69
As (mg kg^{-1}dw)	5.07	2.22	13.3	6.50	8.24	5.59	8.62
Se (mg kg^{-1}dw)	3.17	2.89	6.80	2.62	2.54	2.53	3.80
Rb (mg kg^{-1}dw)	8.67	3.72	8.95	6.63	1.38	5.42	19.8
Sr (mg kg^{-1}dw)	66.7	14.4	67.8	106.4	26.2	42.7	37.7
Rh (mg kg^{-1}dw)	ND	ND	ND	ND	ND	ND	0.860
Sb (mg kg^{-1}dw)	0.120	0.050	0.250	0.150	0.060	0.560	0.060
Cs (mg kg^{-1}dw)	2.06	0.850	2.61	1.99	5.22	3.33	4.45
Ba (mg kg^{-1}dw)	232	40.8	303	99.3	71.1	110	154
Ir (mg kg^{-1}dw)	ND	ND	0.190	ND	ND	1.33	1.34
Tl (mg kg^{-1}dw)	0.110	0.0500	0.310	0.0800	0.140	0.150	0.210

S.2.2 Levels of Organic Pollutants in Sewage Sludge Samples

Table S3: Concentrations (µg g^{-1} dw) of OPPs, OPEs, PBDEs, PCBs, OCPs, PYRs, and PAHS in sewage sludge collected from municipal wastewater treatment plants located in the north of Portugal (mean values, n=6; ND: not detected; <LOQ: below method quantification limit).

Target analyte		SS samples						
		A	B	C	D	E	F	G
OPPs	Dimethoate	ND	ND	ND	ND	ND	ND	ND
	Chlorpyrifos methyl	ND	ND	<LOQ	ND	ND	ND	ND
	Parathion methyl	ND	ND	ND	ND	ND	ND	ND
	Malathion	ND	ND	ND	<LOQ	ND	ND	ND
	Chlorpyrifos	ND	ND	ND	ND	ND	ND	ND
	Chlorfenvinphos	ND	ND	ND	ND	ND	ND	ND
	∑6 OPP							
OPEs	TiBP	ND	ND	ND	ND	ND	26.8±0.013	ND
	TnBP	ND	ND	ND	ND	ND	ND	ND
	TCEP	ND	ND	ND	ND	ND	ND	ND

	TPhP	ND	ND	ND	<LOQ	2.05±0.012	ND	ND
	TBEP	ND	1.06±0.19	ND	ND	ND	ND	ND
	TEHP	ND	ND	ND	ND	ND	1.53±0.023	ND
.	TCP	ND	ND	ND	ND	ND	ND	ND
	∑7 OPE		1.06±0.19			2.05±0.012	28.3±0.068	
PCBs	PCB 28	ND	ND	ND	ND	ND	ND	ND
	PCB 118	0.302±0.056	ND	ND	ND	ND	ND	ND
	PCB 153	ND	ND	ND	ND	ND	ND	ND
	PCB 180	ND	ND	ND	ND	ND	ND	ND
	∑4 PCB	0.302±0.056						
PBDEs	BDE 28	0.128±0.027	<LOQ	ND	ND	ND	ND	ND
	BDE 47	ND	ND	ND	ND	ND	ND	ND
	BDE 100	ND	ND	ND	ND	ND	ND	ND
	BDE 99	ND	ND	0.054±0.012	ND	ND	<LOQ	ND
	BDE 154	ND	ND	ND	ND	ND	ND	ND
	BDE 153	ND	ND	ND	ND	ND	ND	ND
	BDE 183	<LOQ	ND	ND	ND	ND	ND	ND
	∑7 BDE	0.128±0.027		0.054±0.012				
OCPs	o-HCH	ND	ND	ND	ND	ND	ND	ND
	α-Endosulfan	0.110±0.007	0.170±0.005	0.490±0.084	0.571±0.037	0.366±0.010	0.282±0.019	0.286±0.022
	p,p´-DDE	ND	ND	ND	ND	ND	ND	ND
	p,p´-DDD	ND	ND	ND	ND	ND	ND	ND
	Dieldrin	ND	ND	ND	ND	ND	ND	ND
	∑5 OCP	0.110±0.007	0.170±0.005	0.490±0.084	0.571±0.037	0.366±0.010	0.282±0.019	0.286±0.022
PYRs	Bifenthrin	ND	ND	ND	ND	ND	ND	ND
	λ-Cyhalothrin	ND	ND	ND	ND	ND	ND	ND
	Cypermethrin	0.0870±0.012	ND	0.0573±0.011	ND	ND	<LOQ	ND
	Fenvalerate	ND	ND	ND	ND	ND	ND	ND
	Deltamethrin	0.254±0.0560	ND	ND	<LOQ	ND	ND	ND
	∑5 PYR	0.341±0.068		0.0573±0.011				
PAHs	Fluoranthene	ND	ND	0.435±0.0042	ND	ND	ND	0.401±0.0143
	Benzo[b+j]fluoranthen	ND	ND	ND	ND	ND	ND	ND
	Benzo[a]pyrene	ND	ND	0.0442±0.0002	ND	0.0418±0.00003	ND	ND
	Dibenzo[a,l]pyrene	ND	ND	ND	ND	ND	ND	ND
	Dibenz[a,h]anthracene	ND	ND	<LOQ	ND	ND	ND	<LOQ
	Benzo[ghi]perylene	ND	ND	ND	ND	ND	ND	ND
	Indeno[1,2,3-cd]pyrene	ND	ND	ND	ND	ND	ND	ND
	∑9 PAH			0.479±0.0044		0.0418±0.00003		0.401±0.0143
Total pollutant load per SS sample (µg g^{-1} dw)		0.881	1.26	2.25	0.571	2.46	28.6	0.687
Total POP load per SS sample (µg g^{-1} dw)		0.540	0.170	1.02	0.571	0.408	0.282	0.687
Number of pollutants detected per SS sample		6	3	7	4	3	5	2

Table S4: Literature-reported concentrations for OPPs, OPEs, PBDEs, PCBs, OCPs, PYRs, and PAHS in sewage sludge.

	Target analyte	Concentration	Analytical procedure	Recovery (%)	Method sensitivity	Reference
OPPs	Chlorfenvinfos	ND	QuEChERS-LC-MS/MS	91	LOQ=5 ng g^{-1}	(Masiá et al., 2015)
	Chlorpyrifos	0.45-703 ng g^{-1}		51	LOQ=0.1 ng g^{-1}	
		ND-0.181		-	LOD=25 ng g^{-1} LOQ=50 ng g^{-1}	(Maragou et al., 2021)
	Chlorpyrifos Methyl	ND		-	LOD=25 ng g^{-1} LOQ=50 ng g^{-1}	(Maragou et al., 2021)
	Dimethoate	ND		90	LOQ=5 ng g^{-1}	(Masiá et al., 2015)
	Malathion	ND		101	LOQ=5 ng g^{-1}	(Masiá et al., 2015)
	Parathion-methyl	ND		40	LOQ=10 ng g^{-1}	(Masiá et al., 2015)
PYRs	Bifenthrin	ND-0.0800 mg/kg dw		-	LOD=5 ng g^{-1} LOQ=10 ng g^{-1}	(Maragou et al., 2021)
	λ-cyhalothrin	ND-0.471 mg/kg dw		-	LOD=10 ng g^{-1} LOQ=50 ng g^{-1}	(Maragou et al., 2021)
	deltamethrin	ND-0.171 mg/kg dw		-	LOD=5 ng g^{-1} LOQ=10 ng g^{-1}	(Maragou et al., 2021)
	ß-cyfluthrin	ND		-	LOD=50 ng g^{-1} LOQ=100 ng g^{-1}	(Maragou et al., 2021)
OPEs	TPrP	<LOD	SLE-SPE-LC-MS/MS	102.8	LOD=0.41 µg/kg dw	(Gao et al., 2016)
	TCEP	<LOD-200 µg/kg dw		64.6	LOD=8.72 µg/kg dw	
		ND-317 ng/g dw	SLE-SPE-HPLC-MS/MS	67.0	MDL=0.64 ng/g dw	(Wang et al., 2019)
	TPhP	4.40-66.8 µg/kg dw	SLE-SPE-LC-MS/MS	100.1	LOD=2.02 µg/kg dw	(Gao et al., 2016)
		ND-1170 ng/g dw	SLE-SPE-HPLC-MS/MS	65.4	MDL=0.73 ng/g dw	(Wang et al., 2019)
	TBEP	6.30-281 µg/kg dw	SLE-SPE-LC-MS/MS	144.0	LOD=0.50 µg/kg dw	(Gao et al., 2016)
	TEHP	46.0-1200 µg/kg dw	SLE-SPE-LC-MS/MS	69.6	LOD=1.21 µg/kg dw	
		26.5-857 ng/g dw	SLE-SPE-HPLC-MS/MS	75.0	MDL=1.62 ng/g dw	(Wang et al., 2019)
	TnBP	1.20-286 µg/kg dw	SLE-SPE-LC-MS/MS	99.9	LOD=0.72 µg/kg dw	(Gao et al., 2016)
		ND-6080 ng/g dw	SLE-SPE-HPLC-MS/MS	65.0	MDL=1.70 ng/g dw	(Wang et al., 2019)
	TiBP	LOD-474 µg/kg dw	SLE-SPE-LC-MS/MS	113.4	LOD=0.63 µg/kg dw	(Gao et al., 2016)
		ND-30.7 ng/g dw	SLE-SPE-HPLC-MS/MS	-	MDL=0.15 ng/g dw	(Wang et al., 2019)
PCBs	PCB 28	452-2380 µg/kg dw	Soxhlet-GC-MS	94-105	MDL=0.012 µg/kg	(Barakat et al., 2017)
	PCB 118	897-2350 µg/kg dw			MDL=0.012 µg/kg	
	PCB 153	842-2150 µg/kg dw			MDL=0.012 µg/kg	
	PCB 180	362-722 µg/kg dw			MDL=0.012 µg/kg	
PBDEs.	BDE 28	ND	MSPD-GC-MS	90.7-94.4	LOD=0.06 ng/g LOQ=0.18 ng/g	(Sánchez-Brunete et al., 2009)
		0.30-46.9 ng g^{-1} dw	sPLE-MEPS-GC-MSMS	97	MLOD=0.02 ng g^{-1}	(Martínez-Moral and Tena, 2014)

	BDE47	ND	MSPD-GC-MS	100.5-101.6	LOD=0.08 ng/g LOQ=0.24 ng/g	(Sánchez-Brunete et al., 2009)
		3.6-497 ng g^{-1} dw	sPLE-MEPS-GC-MSMS	94	MLOD=0.02 ng g^{-1}	(Martínez-Moral and Tena, 2014)
	BDE99	ND	MSPD-GC-MS	94.4-103.6	LOD=0.09 ng/g LOQ=0.28 ng/g	(Sánchez-Brunete et al., 2009)
		1.1-892 ng g^{-1} dw	sPLE-MEPS-GC-MSMS	102	MLOD=0.04 ng g^{-1}	(Martínez-Moral and Tena, 2014)
	BDE100	ND-7.6 ng/g	MSPD-GC-MS	98.7-107.5	LOD=0.1 ng/g LOQ=0.35 ng/g	(Sánchez-Brunete et al., 2009)
		5.2-148 ng g^{-1} dw	sPLE-MEPS-GC-MSMS	92	MLOD=0.02 ng g^{-1}	(Martínez-Moral and Tena, 2014)
	BDE153	ND-6.3 ng/g	MSPD-GC-MS	77.9-107.0	LOD=0.25 ng/g LOQ=0.8 ng/g	(Sánchez-Brunete et al., 2009)
	BDE154	ND-17.6 ng/g		79.4-109.3	LOD=0.2 ng/g LOQ=0.68 ng/g	
		2.7-83.5 ng g^{-1} dw	sPLE-MEPS-GC-MSMS	92	MLOD=0.02 ng g^{-1}	(Martínez-Moral and Tena, 2014)
	BDE183	ND-4.3 ng/g	MSPD-GC-MS	77.9-98.0	LOD=0.4 ng/g LOQ=1.4 ng/g	(Sánchez-Brunete et al., 2009)
OCPs	o-HCH	12.8-87.7 µg/kg dw	Soxhlet-GC-MS	90-105	MDL=0.004 µg/kg	(Barakat et al., 2017)
		ND	SLE-GC/µECD	93.6-104.5	LOD=0.31 ng/g LOQ=0.32 ng/g	(Ademoyegun et al., 2020)
	α-Endosulfan	9.62-16.4 µg/kg dw	Soxhlet-GC-MS	90-105	MDL=0.004 µg/kg	(Barakat et al., 2017)
		ND-99 ng/g	SLE-GC/µECD	91.5-99.1	LOD=0.33 ng/g LOQ=1.31 ng/g	(Ademoyegun et al., 2020)
	p,p´-DDE	2.13-22.2 µg/kg dw	Soxhlet-GC-MS	90-105	MDL=0.004 µg/kg	(Barakat et al., 2017)
		12-45 ng/g	SLE-GC/µECD	98.5-107.4	LOD=0.48 ng/g LOQ=0.38 ng/g	(Ademoyegun et al., 2020)
	p,p´-DDD	ND-7.51 µg/kg dw	Soxhlet-GC-MS	90-105	MDL=0.004 µg/kg	(Barakat et al., 2017)
		56-169 ng/g	SLE-GC/µECD	95.6-105	LOD=0.21 ng/g LOQ=0.28 ng/g	(Ademoyegun et al., 2020)
	Dieldrin	ND		83.6-93.6	LOD=0.43 ng/g LOQ=0.54 ng/g	
PAHs	Fluoranthene	0.0067-0.1516 mg/kg dw	SLE-GC-MS	93	DL=0.0022 mg/kg dw	(Chen et al., 2019)
	Benzo[a]pyrene	ND-0.0568 mg/kg dw		92	DL=0.0045 mg/kg dw	
		1-1341 mg kg^{-1} dw	Soxhlet-GC-MS	99	-	(Suciu et al., 2015)
	Dibenz[a,h]anthracene	ND-0.0434 mg/kg dw	SLE-GC-MS	97	DL=0.0045 mg/kg dw	(Chen et al., 2019)
	Benzo[ghi]perylene	0.0008-0.0997 mg/kg dw		97	DL=0.0033 mg/kg dw	
		2-1030 mg kg^{-1} dw	Soxhlet-GC-MS	105	-	(Suciu et al., 2015)
	Indeno[1,2,3-cd]pyrene	ND-0.0754 mg/kg dw	SLE-GC-MS	98	DL=0.0046 mg/kg dw	(Chen et al., 2019)
		1-1310 mg kg^{-1} dw	Soxhlet-GC-MS	68	-	(Suciu et al., 2015)

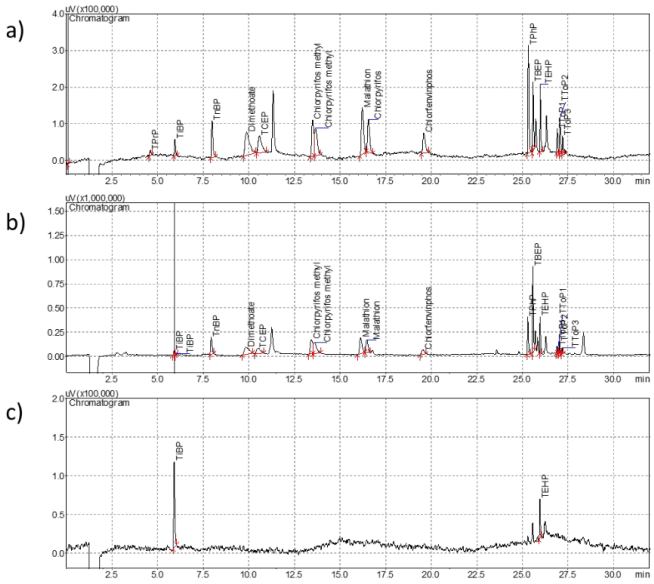


Fig. 2S Chromatographic data for OPPs and OPEs obtained by GC-FPD. a) Chromatogram of a matrix-matched standard solution; b) chromatogram of a reagent-only standard solution; and c) chromatogram of sample F

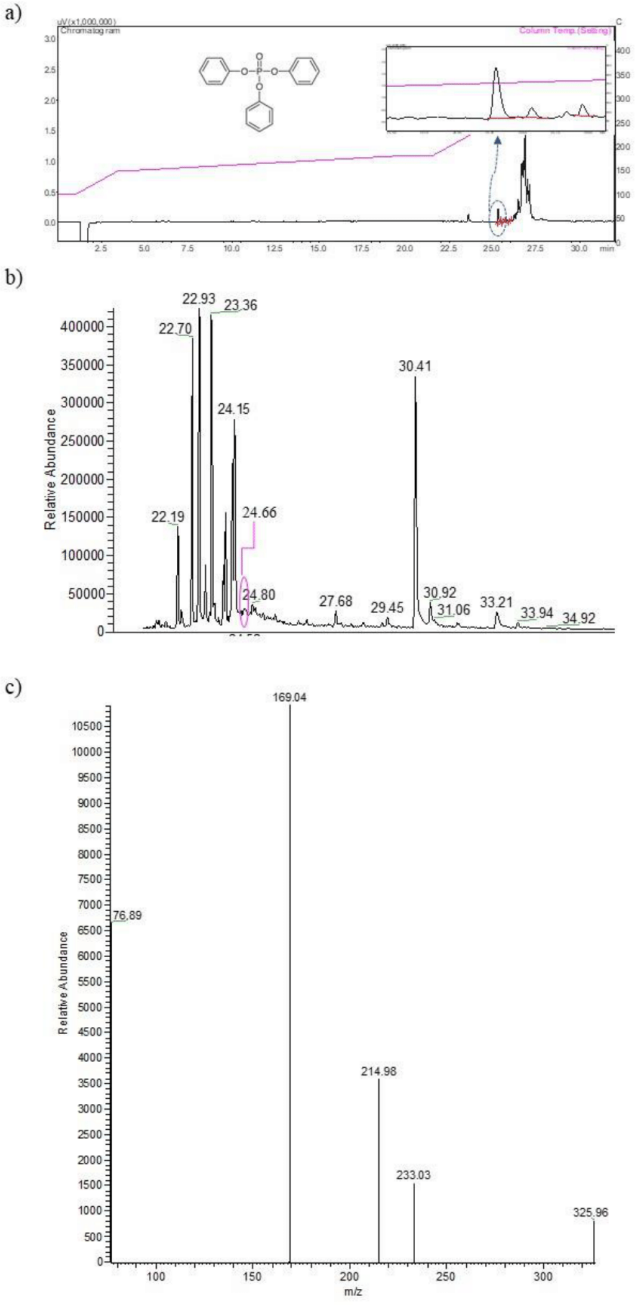


Fig. 3S Chromatographic information of TPhP in sample E: a) chromatogram of sample E obtained by GC-FPD, b) chromatogram of sample E obtained by GC-MS, and c) mass spectrum of TPhP in sample E

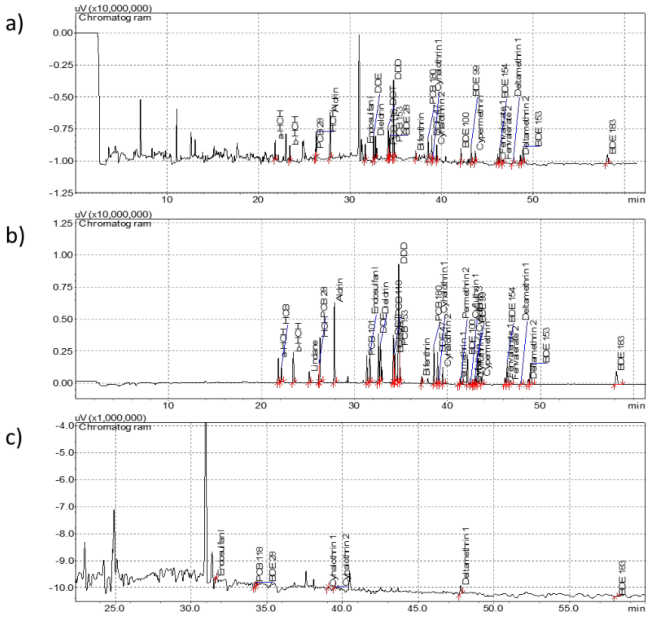


Fig. 4S Chromatographic data for PCBs PBDEs, OCPs, and PYRs obtained using GC-ECD. a) Chromatogram of a matrix-matched standard solution, b) chromatogram of a reagent-only standard solution, and c) chromatogram of sample A

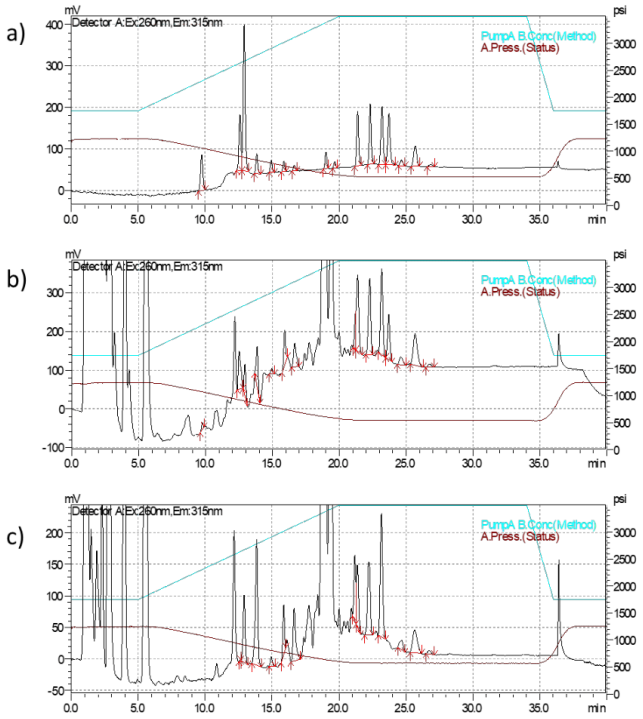


Fig. 5S Chromatographic data for PAHs obtained using LC-PDA-FLD. a) Chromatogram of a reagent-only standard solution, b) chromatogram of a matrix-matched standard solution, and c) chromatogram of sample C

References

Ademoyegun, O.T., Okoh, O.O., Okoh, A.I., 2020. Organochlorine pesticides in selected sewage sludge in South Africa: Assessment and method validation. Polish J. Environ. Stud. 29, 1021–1028. https://doi.org/10.15244/pjoes/97391

APHA, 1992. SM 3050B, in: Andrew D. Eaton, Rodger B. Baird, E.W.R. (Ed.), Standard Methods for the Examination of Water and Wastewater.

Barakat, A.O., Khairy, M.A., Mahmoud, M.R., 2017. Organochlorine pesticides and polychlorinated biphenyls in sewage sludge from Egypt. J. Environ. Sci. Heal. - Part A Toxic/Hazardous Subst. Environ. Eng. 52, 750–756. https://doi.org/10.1080/10934529.2017.1303313

CEN, 2002. EN 12457-4, in: Characterization of Waste -Leaching - Compliance Test for Leaching of Granular Waste Materias and Sludges.

Chen, C.F., Ju, Y.R., Lim, Y.C., Hsieh, S.L., Tsai, M.L., Sun, P.P., Katiyar, R., Chen, C.W., Dong, C. Di, 2019. Determination of polycyclic aromatic hydrocarbons in sludge from water and wastewater treatment plants by GC-MS. Int. J. Environ. Res. Public Health 16, 2604. https://doi.org/10.3390/ijerph16142604

Gao, L., Shi, Y., Li, W., Liu, J., Cai, Y., 2016. Occurrence and distribution of organophosphate triesters and diesters in sludge from sewage treatment plants of Beijing, China. Sci. Total Environ. 544, 143–149. https://doi.org/10.1016/j.scitotenv.2015.11.094

J.B.Jones, 2001. Laboratory Guide for conducting soil tests and plant analysis, Acta Universitatis Agriculturae et Silviculturae Mendelianae Brunensis. CRC Press LLC.

Maragou, N.C., Balayiannis, G., Karanasios, E., Markellou, E., Liapis, K., 2021. Targeted multiresidue method for the analysis of different classes of pesticides in agro-food industrial sludge by liquid chromatography tandem mass spectrometry. Molecules 26, 6888. https://doi.org/10.3390/molecules26226888

Martínez-Moral, M.P., Tena, M.T., 2014. Use of microextraction by packed sorbents following selective pressurised liquid extraction for the determination of brominated diphenyl ethers in sewage sludge by gas chromatography-mass spectrometry. J. Chromatogr. A 1364, 28–35. https://doi.org/10.1016/j.chroma.2014.08.075

Masiá, A., Vásquez, K., Campo, J., Picó, Y., 2015. Assessment of two extraction methods to determine pesticides in soils, sediments and sludges. Application to the Túria River Basin. J. Chromatogr. A 1378, 19–31. https://doi.org/10.1016/j.chroma.2014.11.079

Sánchez-Brunete, C., Miguel, E., Tadeo, J.L., 2009. Analysis of polybrominated diphenyl ethers in sewage sludge by matrix solid-phase dispersion and isotope dilution GC-MS. J. Sep. Sci. 32, 109–117. https://doi.org/10.1002/jssc.200800479

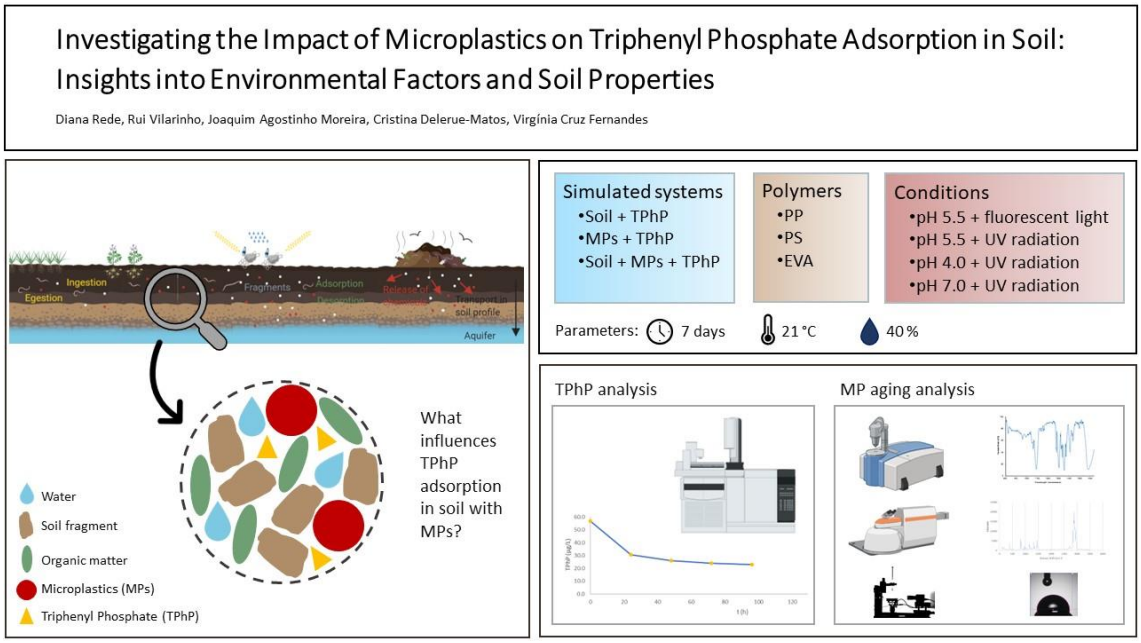
Suciu, N.A., Lamastra, L., Trevisan, M., 2015. PAHs content of sewage sludge in Europe and its use as soil fertilizer. Waste Manag. 41, 119–127. https://doi.org/10.1016/j.wasman.2015.03.018

USEPA, 1986. EPA 9045D, in: Test Methods for Evaluating Solid Waste. Springfield.

Wang, Y., Kannan, P., Halden, R.U., Kannan, K., 2019. A nationwide survey of 31 organophosphate esters in sewage sludge from the United States. Sci. Total Environ. 655, 446–453. https://doi.org/10.1016/j.scitotenv.2018.11.224

3. Coexistence of Microplastics and Plastic-related Chemicals in Soil

3.1. Investigating the Impact of Microplastics on Triphenyl Phosphate Adsorption in Soil: Insights into Environmental Factors and Soil Properties



Published at *Science of The Total Environment* 944, 173745 (2024). https://doi.org/10.1016/j.scitotenv.2024.173745

Contribution Statement

The candidate specifically investigated the adsorption of TPhP in various simulated environments, including soil-only, MP-only, and soil-MP mixtures, using three types of polymers: EVA, PS, and PP. Contributions included planning the experiment, developing the methodology, analyzing samples, and processing data. Additionally, the candidate was responsible for drafting the original manuscript and participated in the reviewing and editing stages of the paper. The graphical abstract and Figure 1 were created in Microsoft® PowerPoint® using stock images from BioRender.com.

Science of the Total Environment 944 (2024) 173745

Contents lists available at ScienceDirect

Science of the Total Environment

journal homepage: www.elsevier.com/locate/scitotenv

Investigating the impact of microplastics on triphenyl phosphate adsorption in soil: Insights into environmental factors and soil properties

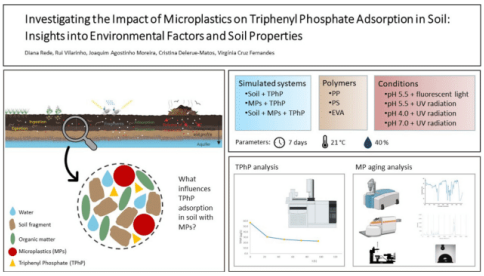
Diana Rede [a,b], Rui Vilarinho [c,d], Joaquim Agostinho Moreira [c,d], Cristina Delerue-Matos [a], Virgínia Cruz Fernandes [a,*]

[a] REQUIMTE/LAQV, Instituto Superior de Engenharia do Porto, Instituto Politécnico do Porto, Rua Dr. António Bernandino de Almeida 431, 4249-015 Porto, Portugal
[b] Departmento de Química e Bioquimica, Faculdade de Ciências, Universidade do Porto, Rua do Campo Alegre s/n, 4169– 007 Porto, Portugal
[c] Departmento de Física e Astronomia, Faculdade de Ciências, Universidade do Porto, Rua do Campo Alegre s/n, 4169–007 Porto, Portugal
[d] IFIMUP—Instituto de Física dos Materiais Avançados, Nanotecnologia e Fotónica, Faculdade de Ciências, Universidade do Porto, Rua do Campo Alegre s/n, 4169–007 Porto, Portugal

HIGHLIGHTS

- TPhP adsorption onto soil particles: crucial insights.
- MPs modify TPhP adsorption in soil environments.
- Environmental factors shape TPhP sorption on soil.
- UV radiation amplifies TPhP adsorption in soil-MP systems.
- MPs exhibiting photooxidation indicators.

GRAPHICAL ABSTRACT



ARTICLE INFO

Editor: Damià Barceló

Keywords:
Polypropylene
Polystyrene
Ethylene-vinyl acetate
Adsorption
Aging
Raman
FTIR

ABSTRACT

Microplastics (MPs) pose significant environmental pollution problems owing to their diverse properties such as various shapes, sizes, compositions, surface features, and levels of degradation. Moreover, their interactions with toxic chemicals and aging processes add complexity to environmental research. This study investigated the adsorption of triphenyl phosphate (TPhP) in soil-only, MP-only, and soil-MP simulated environments under different conditions. The experiment involved three phases: initial exposure to a pH of 5.5 under fluorescent light, subsequent introduction of ultraviolet (UV) radiation, and pH adjustment to 4.0 and 7.0, while maintaining UV exposure, each lasting 7 days. The study found that environmental factors affected TPhP sorption capacity, with higher adsorption observed under UV radiation and acidic conditions. In contrast, the MP-only systems showed no clear trend for TPhP adsorption, suggesting kinetic limitations. When MPs were added to the soil, the adsorption dynamics were altered, with varying adsorption capacities observed for different MP polymers under different aging conditions. ATR-FTIR spectroscopy, micro-Raman spectroscopy, and water contact angle measurements suggested potential photooxidation processes and changes in the surface hydrophobicity of the MPs subjected to simulated environmental conditions. This study provides valuable insights into the interplay

* Corresponding author.
E-mail address: vir@isep.ipp.pt (V.C. Fernandes).

https://doi.org/10.1016/j.scitotenv.2024.173745
Received 3 April 2024; Received in revised form 20 May 2024; Accepted 2 June 2024
Available online 4 June 2024
0048-9697/© 2024 The Authors. Published by Elsevier B.V. This is an open access article under the CC BY license (http://creativecommons.org/licenses/by/4.0/).

between soil properties, MP characteristics, and environmental factors in determining TPhP sorption dynamics in soil-MP environments.

1. Introduction

Plastic debris, particularly microplastics (MPs), have received significant global attention due to their persistence, complexity, and pervasive distribution in ecosystems. MPs can disperse through the airstream and settle in both aquatic and terrestrial environments (Ya et al., 2021; Rede et al., 2023a). In particular, soil tends to accumulate higher levels of MPs compared to aquatic environments due to various land-based sources and disposal practices; however urbanized areas and regions with insufficient waste management tend to exhibit higher levels of MP contamination (Horton et al., 2017; Ya et al., 2023). Terrestrial MPs originate from a variety of sources, including agriculture, waste disposal, urban runoff, industrial processes, transportation, atmospheric deposition, recreational activities, natural degradation, and wildlife interactions (Kole et al., 2017; Ya et al., 2021; Rede et al., 2023a). The impact of MPs in soil is multifaceted, affecting soil physicochemical properties, biota, and potentially, human health. MPs can alter soil structure, pH, and permeability, which in turn can impede plant root growth and impact enzyme activities and soil microorganisms, potentially affecting ecological balance (Prendergast-Miller et al., 2019; Song et al., 2019c; Boots et al., 2019; Kwak and An, 2021; Ya et al., 2023).

A critical aspect in this context is that plastic production involves the incorporation of various additives such as flame retardants, which typically account for 10–20 % of the weight of plastics. Flame retardants decrease the flammability of plastics, slow the spread of fire during combustion, and reduce the risk of catastrophic fires. This is particularly important for preventing small fires from escalating to larger ones, thereby significantly reducing fire hazards (Cheng et al., 2020; Rede et al., 2023a). Despite their slow release rates at ambient temperatures, flame retardants can potentially be released into the environment throughout the lifecycle of materials (via processes such as volatilization, leaching, and abrasion), which poses environmental and ecological risks (Du et al., 2016; Chokwe and Okonkwo, 2019; Cheng et al., 2020). Triphenyl phosphate (TPhP) is an organophosphate ester that is commonly used as a flame retardant and plasticizer for polymers, such as polyvinyl chloride (Du et al., 2016). It is also a metabolite of other flame retardants, such as resorcinol bis diphenylphosphate and bisphenol-a diphenyl phosphate (Dong et al., 2021) and has been found in various environmental matrices worldwide. For instance, it has been detected in freshwater in Uganda (Nantaba et al., 2021), wastewater influent in USA (Kim et al., 2017), sewage sludge in Portugal (Rede et al., 2023b), sediments from the North Pacific to the Arctic Ocean (Ma et al., 2017) and South Africa (Chokwe and Okonkwo, 2019), soil in China (Wang et al., 2018b), indoor air in Spain and Netherlands (Björnsdotter et al., 2018), as well as in living organisms in China (He et al., 2019) and human biological samples (Wang et al., 2020d). Even more alarming is that TPhP has the potential to bioaccumulate, leading to negative consequences (Du et al., 2016; Robinson et al., 2020), such as decreased sperm count and hormone levels in humans (Meeker and Stapleton, 2010). Moreover, in soil, TPhP exhibits high microbiological and chemical stability, and its metabolites and natural attenuation products, such as para-hydroxy triphenyl phosphate, dihydroxylated triphenyl phosphate, diphenyl phosphate, and phenyl phosphate, can pose significant risks to human health (Dong et al., 2021). Consequently, the European Union has included TPhP in the Community Rolling Action Plan (CoRAP) because of its potential for endocrine disruption, high production volumes, and extensive use. It is currently being evaluated for its endocrine-disrupting properties, and the OECD recommends conducting exposure and environmental risk assessments. TPhP has also been added to the Substitute It Now (SIN) list, which is a database maintained by the Swedish NGO ChemSec that identifies substances that are of great concern due to their potential to interfere with endocrine systems (Australian Government, 2023). These classifications underscore the importance of understanding the potential impacts of TPhP on the environment and human health.

Moreover, plastic polymers undergo a series of aging processes, including photoaging, chemical oxidation, and physical abrasion, which induce changes in the material over time and influence their degradation (Fernandez-Gonzalez et al., 2021; Guo et al., 2023; Rede et al., 2023a). These processes are initiated at the surface of the plastic, causing MPs to degrade faster than mesoplastics (20–5 mm) and macroplastics (>20 mm) because of the higher surface-to-volume ratio (Gewert et al., 2015). Observable changes encompass significant alterations in the surface morphology, area, size, oxygen content, molecular structure, surface charge, and crystallinity (Luo et al., 2020; Fernandez-Gonzalez et al., 2021; Guo et al., 2023). Initial signs of degradation include color changes and surface crazing, which lead to cracking, embrittlement, and eventual disintegration as the inner plastic material is exposed to further degradation (Gewert et al., 2018; Luo et al., 2020; Guo et al., 2023). Moreover, aged plastics offer additional sites for the sorption of pollutants, such as pesticides, heavy metals, or pharmaceuticals, from the surrounding environment (Hodson et al., 2017; Puckowski et al., 2021; Guo et al., 2023; Martinho et al., 2023; Zhao et al., 2023). Naturally aged polystyrene (PS) foams, for instance, exhibit a higher specific surface area, micropore area, and degree of oxidation, consequently enhancing oxytetracycline adsorption compared to pristine PS foams (Zhang et al., 2018).

The sorption mechanisms of organic contaminants on MPs include partitioning, surface sorption, and pore filling (Wang et al., 2018a, 2020a). Among these, hydrophobic interactions are the primary mechanism for the adsorption of organic pollutants onto MPs, whereas hydrogen bonding, electrostatic, and π-π interactions are less frequently observed, as indicated by Kinigopoulou et al. (2022). The way in which contaminants adhere to MPs is not only dependent on the properties of the MPs themselves, but also on the properties of the contaminants, such as hydrophobicity, surface charge, and functional groups. Additionally, external factors, such as pH, ionic strength, and dissolved organic matter (OM), can also influence the sorption behavior of contaminants onto MPs. For instance, the pH level determines the charge state of the contaminants, which affects the strength of the electrostatic interactions that drive the sorption process (Wang et al., 2018a, 2020a). An illustrative example is observed when poly(butylene adipate-*co*-terephthalate) (PBAT) undergoes both photoaging and chemical aging, leading to an increase in crystallinity from 29.2 to 52.6 %, which results in the enhancement of its adsorption capacity for tetracycline (Guo et al., 2023).

These alterations affect the properties of MPs, introducing uncertainties in the analytical process and resulting in a diverse range of properties, even within the same polymer type (Luo et al., 2020; Fernandez-Gonzalez et al., 2021). Vibrational spectroscopic techniques, including Fourier-transform infrared spectroscopy (FTIR) and Raman spectroscopy, have proven invaluable in providing insight into the behavior of MPs within their environmental context. These methodologies not only enable the identification of polymer types but also offer an understanding of the molecular and structural alterations that occur during weathering processes (Hiejima et al., 2018; Fernandez-Gonzalez et al., 2021; Guo et al., 2023; Martinho et al., 2023). The degradation of polymers leads to chemical transformations, resulting in the formation of new functional groups such as carbonyl, hydroxyl, vinyl, peroxides, and unsaturated groups (Campanale et al., 2023; Schefer et al., 2023). The formation of these functional groups is frequently correlated with alterations in the wetting behavior of polymers (Binda et al., 2023). For

instance, the introduction of hydrophilic functional groups such as hydroxyl groups can induce a transition from hydrophobic to hydrophilic behavior (Binda et al., 2023; Schefer et al., 2023; Shafea et al., 2023), which can also be assessed through the measurement of water contact angle (WCA) (Wang et al., 2020b; Binda et al., 2023). Moreover, the distinct characteristics of the carbonyl absorption band, characterized by its consistent position, high intensity, and the absence of interfering bands, make it ideal for monitoring the progression of photodegradation by calculating the Carbonyl Index (Almond et al., 2020; Campanale et al., 2023; Schefer et al., 2023).

This study explored the relationship between polymer types and their interactions with chemical pollutants by considering the effects of photoaging and varying pH levels in the soil environment. A simulated soil environment was created by incorporating diverse non-degradable MP granules measuring <5 mm, such as polypropylene (PP), PS, and ethylene-vinyl acetate (EVA), along with TPhP. The oxidation of MPs was analyzed based on wettability using WCA measurements and spectroscopic techniques, including attenuated total reflection (ATR)-FTIR and micro-Raman spectroscopy (μ-Raman). This study provides more information on the interactions between pollutants in soils containing MPs. To the best of our knowledge, this study is the first to investigate the coexistence of TPhP and these polymers in soil, providing new insights into their characteristics and behaviors. This can contribute to extrapolating their behavior beyond laboratory settings and understanding their implications in terrestrial environmental conditions.

2. Materials and methods

2.1. Reagents and materials

Analytical-grade TPhP was acquired from Sigma-Aldrich (Darmstadt, Germany), whereas chromatography-grade n-hexane was obtained from Merck (Darmstadt, Germany). Stock solutions (2000 μg/L) and working standard solutions of TPhP were prepared in n-hexane and stored at 4 °C. Deionized water (15.8 MΩ cm) was obtained using an Elix® Essential Water Purification System equipped with a Progard® TS2 cartridge and a Vent Filter MPK01 for the storage tank (Merck Millipore, Darmstadt, Germany). Sodium hydroxide (NaOH) was obtained from Merck (Darmstadt, Germany) and hydrochloric acid (HCl) was acquired from Sigma-Aldrich (Darmstadt, Germany). Pristine MPs were purchased from Goodfellow Cambridge, Ltd. (Huntington, UK) and included EVA granules (yellow, 3–5 mm), PS granules (colorless, 3–5 mm in diameter), and PP granules (colorless, 5 mm in diameter). Additional details of the MPs are provided in Table S1 (Supporting Information). The Lufa 2.2 standard soil, loamy sand sourced from LUFA Speyer (Speyer, Germany), exhibited the following physicochemical characteristics: a pH of 5.6 ± 0.4 in a 0.01 M $CaCl_2$ solution, an organic carbon content (OC) of 1.61 ± 0.44 %, nitrogen content of 0.18 ± 0.04 %, a cation exchange capacity of 8.5 ± 12.1 meq per 100 g, a maximum water holding capacity of 43.3 ± 5.1 g per 100 g, and a density of 1232 ± 93.8 g per 1000 mL.

2.2. Experimental setup

The study utilized Batch experiments conducted in 20 mL glass vials to investigate the adsorption behavior of TPhP under different environmental conditions. The research design included different systems to explore the dynamic changes in TPhP adsorption behavior over time. These systems were composed of soil, MPs, a combination of both, and a blank experiment with TPhP alone. For each aging condition, eight vials were placed in a climate-controlled chamber (Binder KBW 240, Binder GmbH, Germany) and incubated for seven days at a temperature of 21 °C and a humidity level of 40 %. These vials included soil only (2 g of soil mixed with 10 mL of TPhP at a concentration of 100 mg/L), MPs-only (10 mL of TPhP at a concentration of 100 mg/L + four microparticles of PS-MPs/PP-MPs/EVA-MPs), soil-MPs (2 g of soil mixed with 10 mL of TPhP at a concentration of 100 mg/L + four microparticles of PS-MPs/PP-MPs/EVA-MPs), and a blank control with 10 mL of TPhP at a concentration of 100 mg/L for each exposure test.

The climate chamber was fitted with alternating cycles of 16 h of illumination, provided by Osram T8 Lumilux 18 W lamps emitting 865 lx of daylight at a total output of 12,500 lm, and 8 h of darkness. The experimental setup was adjusted to maintain a consistent temperature, humidity, and pH of 5.5 within the typical range of natural rainfall (usually between 5.5 and 6.0) (Fabian et al., 2023). The system was then subjected to accelerated aging through continuous exposure to UV radiation (UV germicidal lamp E27, 20 W, 250 V, and 254 nm). Subsequently, while maintaining UV light exposure, the pH was adjusted to 4.0, and finally, the pH was adjusted to 7.0.

A daily sampling regimen was established, involving the collection of 1 mL aliquots of the supernatant at 0, 24, 48, 72, 96, 120, 144, and 168 h to determine the TPhP concentration in the solution. Furthermore, MPs were collected at 168 h for structural analysis by using ATR-FTIR and μ-Raman, along with WCA measurements to assess surface alterations. Fig. 1 provides an overview of the experimental procedure of the study, encompassing the preparation of the systems, the tested assay conditions, and the analyses conducted, including TPhP quantification and MPs characterization. The pH was determined at the point of zero charge (pH_{PZC}) for both the soil and soil associated with pristine MPs. Detailed explanations of the experimental procedure are provided in section S.1.2. in the Supporting Information.

The adsorption capacities of the adsorbents (q_t, μg/g), soil, and MPs were determined using the mass balance method and are represented by the ratio of the concentration of TPhP at a given time (C_t, μg/L) to the initial concentration of TPhP (C_0, μg/L) in the presence of an added volume of TPhP solution (V, L) and the specific mass of the added adsorbent (m, g) (Martinho et al., 2022; Sun et al., 2022). The q_t is expressed using the following equation:

$$q_t = \frac{V(C_{0_} C_t)}{m} \quad (1)$$

Equilibrium studies employed the same equation, with the experimental endpoint defined as the time at which equilibrium was reached (Martinho et al., 2022).

2.3. Gas chromatographic analysis of TPhP and analytical performance figure of merit

The TPhP extraction method was adapted from Martinho et al. (2022), involving a liquid-liquid extraction process. This method, performed in a 4 mL vial, consisted of mixing 1 mL of the supernatant of the sample solution with 1 mL of n-hexane, followed by vortex agitation for 1 min. After a 10-min waiting period, 500 μL of the organic phase was filtered using a 0.2 μm PTFE filter and later injected into a gas chromatograph equipped with a flame photometric detector (GC-FPD). To extract TPhP from the MPs, 1 mL of n-hexane was added to each particle, and the same procedure was followed as previously described (Martinho et al., 2022). The calibration standards were prepared at concentrations ranging from 50 to 100 μg/L and underwent a similar liquid-liquid extraction and filtration process.

The TPhP analysis followed the method described by Rede et al. (2023b), with minor modifications. The analysis was conducted using a Shimadzu GC-2010 with FPD (Shimadzu Corporation, Japan) controlled by Shimadzu GC Solution software. The injector and detector temperatures were set to 250 and 290 °C, respectively. Samples (1.0 μL) were injected in splitless mode onto a Phenomenex ZB-5 M Si capillary column (30 m length, 0.25 mm i.d., 0.25 μm film thickness). The temperature program for the GC oven was as follows: initial temperature of 100 °C for 1 min, followed by a gradual increase at a rate of 20 °C per minute up to 170 °C, with a 1-min hold, followed by an increase at a rate of 4 °C per minute up to 210 °C, with a 1-min hold, and a final ramp at 15 °C per minute up to 300 °C, where it remained for 5 min. Helium,

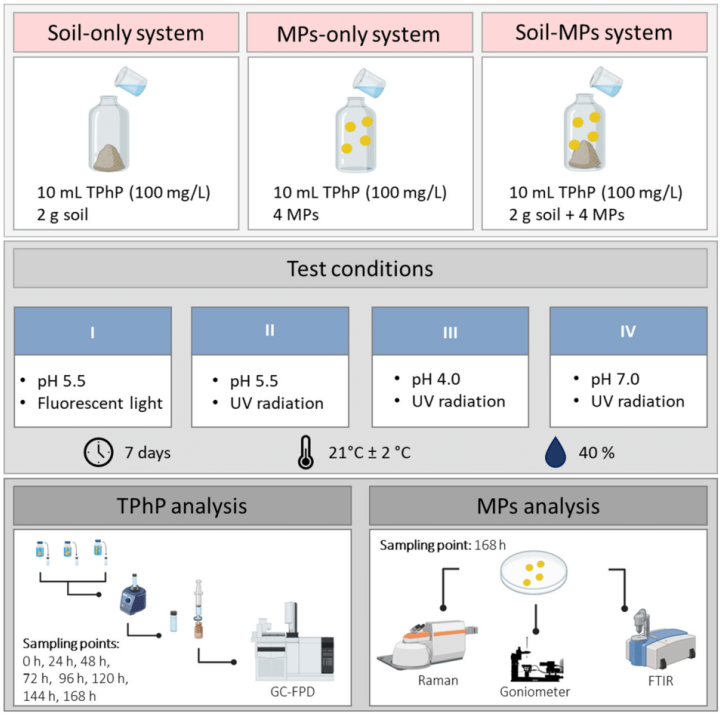


Fig. 1. Overview of the experimental setup, including the preparation of soil-only, MP-only, and soil-MP systems, experimental conditions, and analytical processes for TPhP quantification and MPs photooxidation assessment.

with a purity of 99.99 % from Nippon (Nippon Gases Portugal Unipessoal Lda., Portugal), served as the carrier gas at a pressure of 83.6 KPa, a linear velocity of 25.4 cm per second, and a flow rate of 1 mL per minute.

The validation process involved evaluating linearity range, repeatability, reproducibility, limit of detection (LOD), and limit of quantification (LOQ) (Magnusson and Örnemark, 2014). The calibration curve included five concentration levels. To assess repeatability (intraday) and reproducibility (day-to-day) the relative standard deviation (% RSD) was calculated based on multiple measurements. The values of LOD and LOQ were determined by considering the residual standard deviation of the linear regression and the slope of the calibration curve and were both expressed as the target analyte concentration in the sample (Magnusson and Örnemark, 2014).

2.4. *Experimental procedures for microplastics analysis: ATR-FTIR spectroscopy, μ-Raman spectroscopy, and water contact angle measurements*

The analysis of both pristine MPs and those subjected to various aging procedures involved measurements using ATR-FTIR spectroscopy and μ-Raman spectroscopy as well as determination of wettability through WCA measurements. ATR-FTIR spectroscopy was performed using an FTIR spectrometer (PerkinElmer, Waltham, MA, USA) equipped with a single-reflection attenuated total reflectance diamond. The spectrometer was operated within the 4000–400 cm^{-1} mid-IR region and averaged 32 scans at a resolution of 4 cm^{-1}. All spectra were corrected for light reflectance penetration and baseline displacement.

Micro-Raman spectra were recorded at room temperature using an InVia™ Qontor® confocal Raman spectrometer (Renishaw, United Kingdom), which was equipped with a Leica DM2700 microscope (Ernst Leitz GmbH, Germany), and controlled by WiRE™ 5.2 software (Renishaw Inc., United Kingdom). The spectra were obtained by focusing a 50× objective lens onto each measured MP, with the aid of a 633 nm, 100 mW He—Ne laser source (Hübner Photonics, Kassel, Germany) that was individually regulated for each MP. The scattered light was registered in the 3500–100 cm^{-1} spectral range, and the spectral resolution was >2 cm^{-1}. All spectra underwent pre-processing steps (Araujo et al., 2018) to remove cosmic rays, smooth signals, and correct baselines using OriginPro Version 2024 (OriginLab Corporation, Northampton, MA, USA).

The WCA (θ) of pristine and aged MPs was measured using the sessile drop method with a drop shape analyser, CAM101 (KSV Instruments, Finland). A single drop (10 μL) of deionized water was dispensed onto the surface of the probe using a Hamilton® glass syringe, and a high-resolution camera (model AFWCAMVM, S50 mm, 1:1.8 2/3″, Japan) was used to record the process. The recordings of the droplet geometry were analyzed, and the left and right contact angles were calculated using CAM 200 software, version 3.992, provided by KSV Instruments (Binda et al., 2023; Cramer et al., 2023). This procedure was repeated for each face of the MPs to ensure comprehensive analysis, totalling eight ($n = 8$) measurements per condition. MPs with a WCA above 90° were classified as hydrophobic, while those with a WCA below 90° were considered hydrophilic. This classification is based on established thresholds for defining hydrophobic and hydrophilic surfaces (Binda et al., 2023; Shafea et al., 2023).

3. Results and discussion

3.1. TPhP adsorption dynamics in simulated soil-only systems

In the soil-only system, the concentration of TPhP decreased over time and reached a stable state after 48 h of contact under all four conditions, with approximately 80 % adsorption onto the soil (loamy sand, OC = 1.61 %) (Fig. S1 in the Supporting Information). Previous studies have highlighted the significance of OC in soil, in which higher OC percentages are associated with greater adsorption capacities. For instance, Zheng et al. (2016) observed equilibrium within 420 min in peat soil with 76 % OC, in contrast to the 24-h process observed in clay loam, loamy sand, and loamy sand with sewage sludge amendments (OC content: 4.91 %, 0.47 %, and 2.01 %, respectively) (Zheng et al., 2016) (Cristale et al., 2017). In fact, high-molecular-weight organic compounds with octanol-water partition coefficients (log K_{OW}) exceeding 3.5 tend to adsorb in organic carbon-rich environments. Substances such as TPhP (log K_{OW} 4.63 at 20 °C), with an organic carbon-to-water partition coefficient (K_{OC}) higher than 2000, are expected to be immobile in soil, sediments, sludge, and dust, thereby reducing bioavailability and promoting adsorption (Zheng et al., 2016; Cristale et al., 2017; Wang et al., 2020c; Zhang et al., 2022; Australian Government, 2023). The irreversible bonding of TPhP to OC is primarily attributed to its chemical structure, with aromatic rings facilitating π-π interactions or charge-transfer complexes with soil OM (Cristale et al., 2017; Wang et al., 2018a). Prior studies have also indicated the influence of hydrophobicity on TPhP sorption, as seen in the activated carbon and sediment sorption capacities (Wang et al., 2018a, 2020c).

Variations in the soil adsorption capacity at equilibrium (q_e) of TPhP were observed under diverse pH and UV radiation conditions, with pH 5.5 UV exhibiting the highest capacity, followed by pH 4.0 UV, pH 7.0 UV, and pH 5.5 (0.3586, 0.2940, 0.2762, and 0.1609 $\mu g_{TPhP}/g_{adsorbent}$, respectively). This suggests that the sorption dynamics of sorbate and sorbent are not solely dictated by their intrinsic characteristics but are also influenced by environmental factors. Although research on soil photochemistry is scarce, it has been reported that sunlight induces alterations in the soil matrix. These alterations include dissolved OC, inorganic nitrogen, phosphorus availability, sorption capacity, and the soluble and mineral forms of Fe, Mn, Al, Si, and Ca (Doane et al., 2019). The solubilization of soil OM can be attributed to the degradation of lignin-derived phenols and macromolecular compounds, which absorb UV radiation and undergo direct breakdown (Feng et al., 2011; Doane et al., 2019). Additionally, UV radiation can also influence soil pH, triggering various indirect processes such as the decrease in water-soluble iron levels by breaking down compounds like carboxylic acids (Doane et al., 2019).

Furthermore, the pH can affect both the characteristics of the adsorbent surface and the species of the adsorbate present in the solution (Wang et al., 2018a). When the pH of the solution is below the pH_{PZC} of the soil, its surface becomes positively charged due to the protonation of the functional groups on the soil particles. In contrast, above pH_{PZC}, the surface becomes negatively charged through deprotonation of these functional groups (Wang et al., 2018a). The pH_{PZC} value for the tested soil was determined as 5.9 (Fig. S2 a) in Supporting Information. Moreover, it has been reported that TPhP molecules possess distinct molecular electrostatic potentials, with a negative charge concentrated around oxygen atoms in the P═O group (facilitating electrophilic attack) and a positive charge mainly distributed over hydrogen atoms (susceptible to nucleophilic attack) (Wang et al., 2020c). This implies that the surface charge of soil affects the availability of adsorption sites, thereby influencing the molecular electrostatic potential of TPhP. Our findings suggest a connection between the adsorption capacity of TPhP in soil and both UV radiation exposure and pH fluctuations.

Additionally, TPhP is highly stable in soil and its persistence is influenced by environmental conditions and remediation strategies (Hou et al., 2019; Wang et al., 2020c). Regarding the degradation of TPhP under experimental conditions the available data in the literature appears limited. TPhP exhibits variable degradation rates in different environments, with half-lives ranging from 3 to 12 days in river water/sediment and from 50 to 60 days in pond hydrosoil (Hou et al., 2019). The degradation pathways of TPhP have been elucidated in various studies, revealing multiple mechanisms, including hydrolysis, methoxylation, and hydroxylation (Wang et al., 2016; Hou et al., 2019; Yang et al., 2020; Dong et al., 2022). Advanced oxidation processes demonstrate variable efficiency based on the presence of co-substrates, media properties, and natural OM (Song et al., 2019a, 2019b; Li et al., 2023). Overall, further research is needed to comprehensively understand both the degradation pathways of TPhP, which are influenced by environmental conditions and degradation methods, and the mechanisms governing its adsorption onto soil particles under various environmental conditions.

3.2. TPhP adsorption dynamics in simulated MP-only systems

In our study, despite employing significantly less adsorbent than in the soil-only system (20 times fewer), we anticipated a decrease in the concentration of TPhP. However, the absence of a trend in the MP-only systems suggests that equilibrium was not established under the tested conditions (refer to Table S2 in Supporting Information for example). This lack of equilibrium may be attributed to various factors, such as the kinetics of the adsorption/desorption processes or limitations in experimental conditions, warranting further investigation. In addition, no decrease in the TPhP concentration was observed in the blank controls, indicating that factors such as glass wall sorption, degradation, or solvent evaporation had negligible impacts. The stability of TPhP under different pH conditions, as demonstrated in previous research (OECD SIDS, 2002), underscores the robustness of our findings. However, to the best of our knowledge, the half-life of TPhP at pH 4.0 remains unknown, and the stability observed in blank controls suggests a half-life exceeding 7 days, aligning with its stability in neutral and acidic environments.

Although aged MPs visually resembled pristine polymers (Supporting Information, Fig. S3), and the characteristic peaks of each polymer were detected in the vibrational spectra (Fig. 2) for all MPs, discernible chemical changes on the polymer surface were evident in the FTIR spectra, Raman spectra, and WCA measurements. Shifts in the background intensities observed in the μ-Raman analysis suggest potential aging; nevertheless, these alterations did not seem to pose any detriment under the tested conditions, with the polymer spectra remaining distinctly identifiable. Regarding the FTIR data, the formation of oxygen-containing functional groups resulted in the occurrence of peaks at specific wavenumbers of carbonyls (1850–1650 cm^{-1}) and/or hydroxyls (3300–3600 cm^{-1}), as highlighted in green in Fig. 2, suggesting potential photooxidation aging. This phenomenon was observed for PP and EVA MPs subjected to UV radiation as well as for PS at pH 5.5, which is consistent with findings from other studies documenting the aging of MPs (Andrade and Muniategui, 2019; Binda et al., 2023; Guo et al., 2023; Martinho et al., 2023; Schefer et al., 2023). Additionally, the results of the WCA tests demonstrated slight variations in the hydrophobicity of some MPs across different exposure conditions compared to pristine particles (Table 1 and Fig. S4 in Supporting Information). At pH 5.5, the PP and PS surfaces changed from hydrophobic (WCA > 90°), to hydrophilic (WCA < 90°) suggesting increased hydrophilicity owing to acidic conditions. Exposure to UV radiation at pH 5.5 and 4.0, resulted in a slight decrease in the WCA, further suggesting a trend towards increased hydrophilicity. Similarly, for EVA-MPs, exposure to pH 5.5 and UV radiation also indicated a tendency towards hydrophilicity. Overall, the WCA measurements suggest that both acidic conditions and UV radiation can alter the surface properties of MPs, leading to changes in wettability.

Prior research, including comprehensive literature reviews by Li et al. (2022) and Huang and Wang (2023), has underscored the impact

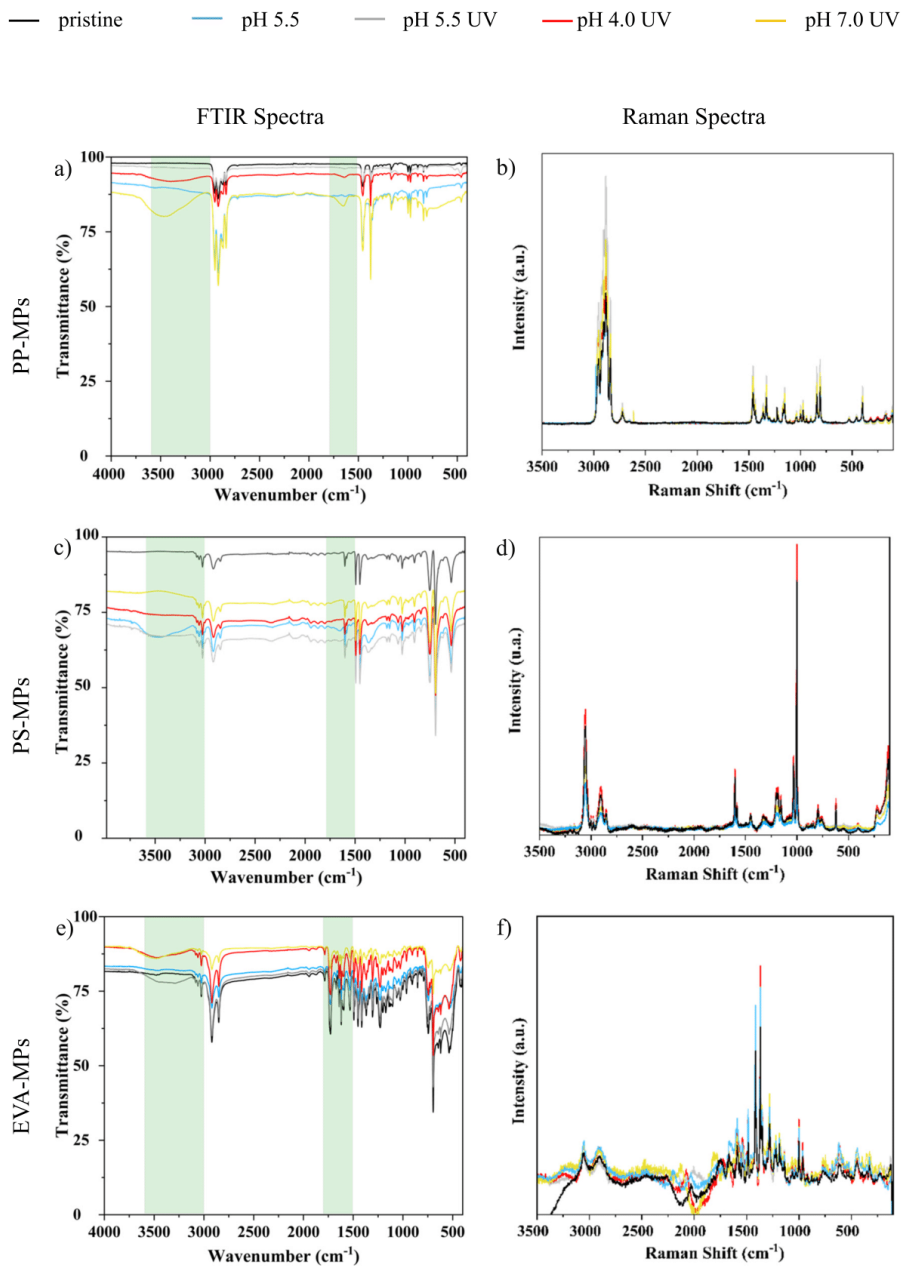


Fig. 2. Spectra of MPs under varying aging conditions in MPs-only systems. ATR-FTIR spectra (a, c, e) spanning the wavenumber range of 4000–400 cm^{-1} versus transmittance (%), with two distinct ranges highlighted in green (3600–3000 and 1800–1500 cm^{-1}), for PP-MPs, PS-MPs, and EVA-MPs. Raman spectra (b, d, f) covering a Raman shift range of 3500–100 cm^{-1} versus intensity are presented for PP-MPs, PS-MPs, and EVA-MPs, respectively.

Table 1
Water contact angles (θ, in degrees) of pristine and aged microplastics of polypropylene (PP-MPs), polystyrene (PS-MPs), and ethylene-vinyl acetate (EVA-MPS) in MP-only systems under various pH and UV exposure conditions. (n = 8).

	PP-MPs		PS-MPs		EVA-MPs	
	θ_{left}	θ_{right}	θ_{left}	θ_{right}	θ_{left}	θ_{right}
pristine	104.2 ± 8.8	102.4 ± 6.3	101.4 ± 9.2	102.6 ± 9.7	113.8 ± 8.5	115.9 ± 9.1
pH 5.5	89.6 ± 7.1	89.7 ± 6.9	88.5 ± 9.8	88.2 ± 11.8	109.3 ± 4.3	107.0 ± 4.4
pH 5.5 UV	98.5 ± 3.8	97.5 ± 5.8	100.4 ± 7.2	97.8 ± 7.4	102.3 ± 5.7	103.5 ± 2.5
pH 4.0 UV	94.3 ± 3.5	93.7 ± 3.2	94.8 ± 3.8	93.6 ± 5.7	110.0 ± 3.4	108.8 ± 4.7
pH 7.0 UV	99.8 ± 5.2	101.3 ± 5.2	103.2 ± 4.8	106.5 ± 2.0	109.8 ± 4.8	109.9 ± 5.9

of photoaging on MPs, elucidating alterations in both hydrophilicity and surface morphology, including surface oxidation, increased roughness, and the formation of microcracks. For instance, Gewert et al. (2018) observed noticeable yellowing and partial degradation of the polymer backbone after UV exposure. This phenomenon varies depending on the type of the polymer. In the case of PP, photooxidation accelerated by UV radiation results in the formation of carbonyl, hydroxyl, and alkenyl groups as well as the release of volatile compounds, such as acetone and acetaldehyde. Consequently, PP polymers experience increased brittleness, crosslinking, and deterioration in their mechanical properties. In the case of PS, photooxidation involves the absorption of light by the benzene ring, initiating a cascade of reactions leading to degradation. Oxygen pressure, additives, and surface modifications can alter the degradation pathways. The temperature and wavelength of radiation also affect the extent of degradation (Huang and Wang, 2023).

Aging processes not only promote the formation of smaller MPs, but they also influence their ability to interact with hydrophobic chemicals, due to increased surface area and the introduction of functional groups that facilitate additional sorption mechanisms. Guo et al. (2023) studied the coexistence of tetracycline with artificially photoaged powders of various polymers. Polybutylene adipate terephthalate (PBAT) and PS exhibited fragmentation and flaking, PP produced cracks, and PE exhibited distinct characteristics with UV and chemical aging. PBAT exhibited an increased adsorption capacity for tetracycline after chemical aging owing to its increased crystallinity (Guo et al., 2023). Moreover, the main driving forces for MP adsorption of hydrophobic chemical reagents are predominantly hydrophobic interactions (Fu et al., 2021; Chen et al., 2023; Jang et al., 2024; Li et al., 2024). However, Puckowski et al. (2021) highlighted that the sorption of MPs in distilled water is not solely dependent on the log K_{OW} values, as their structural characteristics indicate specific electrostatic interactions rather than solely hydrophobic interactions (Puckowski et al., 2021). This implies that van der Waals forces and other non-covalent interactions such as π-π interactions, hydrogen bonding, and electrostatic interactions can also contribute to the adsorption process (Fu et al., 2021; Yu et al., 2021; Li et al., 2024).

In our study, although the analyses revealed surface alterations, the experimental conditions may not have induced noticeable color changes, pores, or cracks on the MPs, enabling the sorption of TPhP molecules (size 1.086 nm (Wang et al., 2020c)). While hydrophobic interactions are pointed out as the primary driving force for the adsorption of hydrophobic chemical reagents onto MPs, a range of other forces and environmental factors can modulate this process. The adsorption capacity and the specific interactions involved can be influenced by various factors, including the type of MP, size the chemical nature of the adsorbate, environmental conditions such as pH, ionic strength, and temperature, as well as the presence of other substances like humic acid (Fu et al., 2021; Yu et al., 2021; Martinho et al., 2022; Chen et al., 2023; Jang et al., 2024; Li et al., 2024). This highlights the need for comprehensive understanding and further research in this field.

3.3. TPhP adsorption dynamics in simulated soil-MPs systems

The incorporation of MPs granules into the soil did not alter the equilibrium state after 48 h (Fig. 3 a, c and e); however, differences were evident in the adsorption capacities of the various soil-MPs subsystems when subjected to different aging conditions (Fig. 3 b, d and f). Fig. 4 illustrates the comparison of adsorption capacities between soil-only and soil-MP systems after reaching equilibrium, revealing that the presence of MPs enhances the adsorption capacity in the soil. At pH 5.5, the soil-only system exhibited a q_e value of 0.1609 $\mu g_{TPhP}/g_{adsorbent}$. However, q_e increased to 0.1966, 0.3962, and 0.3547 $\mu g_{TPhP}/g_{adsorbent}$ for the soil + PP-MPs, soil + PS-MPs, and soil + EVA-MPs systems, respectively. When UV radiation was applied at a pH of 5.5, the q_e of the soil-only system increased to 0.3586 $\mu g_{TPhP}/g_{adsorbent}$ (220 %), and to 0.3560, 0.4647, and 0.5681 $\mu g_{TPhP}/g_{adsorbent}$ for the soil + PP-MPs, soil + PS-MPs, and soil + EVA-MPs systems, respectively. By maintaining the UV radiation and decreasing the pH to 4.0, the q_e of the soil-only system was 0.2940 (183 %), which increased to 0.4436, 0.3383, and 0.3326 $\mu g_{TPhP}/g_{adsorbent}$ for the soil + PP-MPs, soil + PS-MPs, and soil + EVA-MPs systems, respectively. Furthermore, under pH 7.0 UV radiation, the q_e of the soil-only system was 0.2762 $\mu g_{TPhP}/g_{adsorbent}$ (172 %), and the q_e values of the soil + PP-MPs, soil + PS-MPs, and soil + EVA-MPs systems were 0.3962, 0.2776, and 0.3987 $\mu g_{TPhP}/g_{adsorbent}$, respectively. The data demonstrate that no individual MP polymer consistently surpasses the others under all conditions. The soil + PS-MP system displayed a greater value of q_e at a pH of 5.5, whereas the soil + EVA-MP system showed high q_e at pH 5.5, under UV radiation, and at pH 7.0 under UV radiation, and the soil + PP-MPs system exhibited high q_e at pH 4.0 under UV. The pH_{PZC} values for the systems were 5.7, for soil + PS-MPs, and 6.1 for soil + PP-MPs and soil + EVA-MPs (Fig. S2 b-d in the Supporting Information).

Examining the IR data (Fig. 5), the characteristic peaks of each polymer remained unchanged, and the alterations in the ATR-FTIR spectra were similar to those observed in the MP-only system, although they were more pronounced. Similarly, in the μ-Raman spectra, alterations in the shifts of the background intensities did not appear to have any detrimental effects under the tested conditions, with the polymer spectra remaining distinctly identifiable. Moreover, variations in the WCA were observed among the different types of MPs (Table 2 and Fig. S5 in Supporting Information), with variations in the hydrophobicity of PP- MPs under pH 5.5 (θ_{left} = 75.4° and θ_{right} = 76.6°), pH 4.0 with UV (θ_{left} = 85.6° and θ_{right}t = 87.3°) and under pH 7.0 with UV exposure (θ_{left} = 90.0° and θ_{right}t = 89.8°). Although changes in the MP surface morphology attributed to the formation of oxygen-containing surface functional groups were mainly induced by UV radiation, degradation induced by the pH of the media was also observed. This is consistent with the observations reported in the literature (Binda et al., 2023). However, we were unable to correlate the surface changes with the improvement in the TPhP adsorption. As hypothesized for MP-only systems, it is possible that the surface alterations were insufficient to promote adsorption. Additionally, considering that MPs represent only 5 % (w/w) of the total adsorbent, the amount of TPhP adsorbed onto MPs may be too small to yield measurable results. Photographs of pristine and aged MPs are presented in Fig. S6 in the Supporting Information. Although these images provide information about the physical appearance of MPs, they may not necessarily prove a connection between the surface features and adsorption behavior of TPhP, the

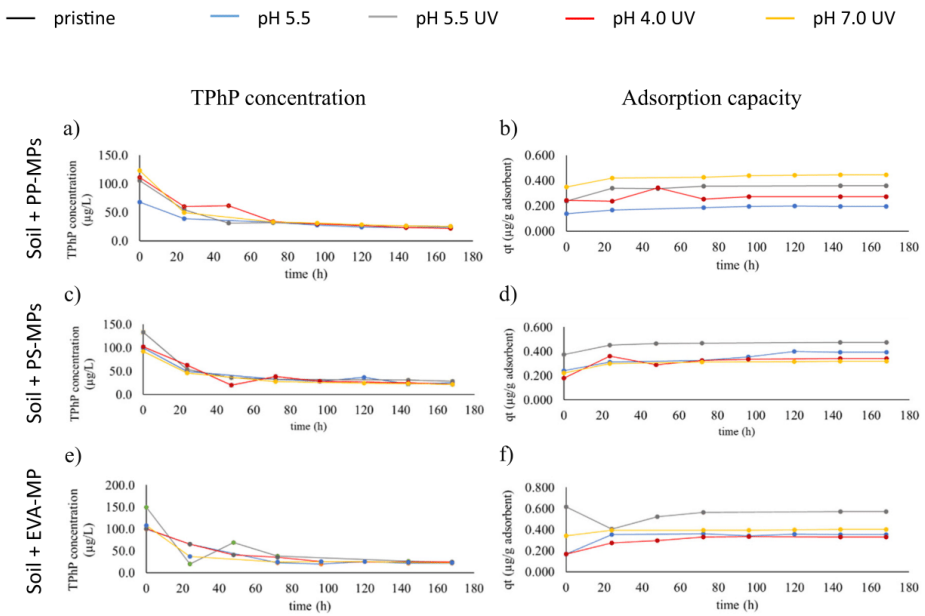


Fig. 3. Temporal variation in TPhP concentration (µg/L) over 168 h (a, c, e) and adsorption capacity (µg/$g_{adsorbent}$) of TPhP in soil-MP systems (b, d, f) for soil + PP-MPs, soil + PS-MPs, and soil + EVA-MPs.

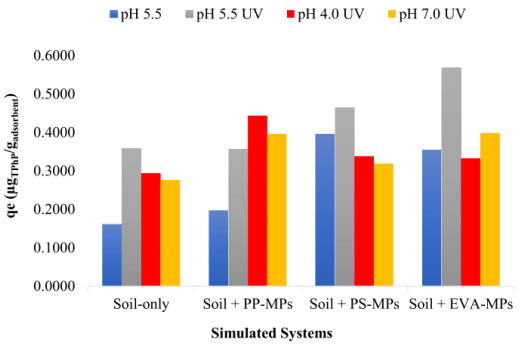


Fig. 4. Variation of equilibrium adsorption capacity (qe, µg$_{TPhP}$/g$_{adsorbent}$) across different systems of soil-only and soil-MPs subjected to varying aging conditions of pH and radiation.

targeted chemical.

While some studies in the literature have explored the co-occurrence of MPs and pesticides (Šunta et al., 2020) and pharmaceuticals (Hu et al., 2020; Wang et al., 2022) in soil, the variability in factors such as the shape, size, and degree of aging of MPs presents challenges for comparison. Nevertheless, further analysis of MP-contaminant interactions could provide valuable insights into the mechanisms governing MP fate and transport in natural systems. In our study, in addition to the influence of MPs on contaminant adsorption in the soil, their presence significantly affected soil dynamics. The size, shape, and polymer composition of MPs play a crucial role in the formation and stability of soil aggregates (Wang et al., 2020a; Lehmann et al., 2021; Liu et al., 2023).

Aggregates are vital to soil structure and are influenced by OM, which promotes soil agglomeration (Chen et al., 2022). The configuration of particles in aggregates forms pore networks, which are crucial for soil OC and other essential nutrient distributions (Ju et al., 2023). Studies have suggested that MPs that closely resemble soil particles in terms of shape and size tend to have a lower impact on soil stability (De Souza Machado et al., 2018; Ju et al., 2023). However, MPs, such as fibers and films, negatively affect aggregate stability regardless of their composition (Lehmann et al., 2021; Liang et al., 2021; Ju et al., 2023; Liu et al., 2023). In addition to their ability to alter aggregates, smaller MP generally possess a larger specific surface area, which provides more adsorption sites (Hu et al., 2023). Studies have found that 72 % of granule-shaped MPs are present in soil aggregates, but their aggregation depends on MP particle size distribution. During the breakdown of OM and MPs by microorganisms, specific soil aggregates may bind to MPs, leading to selective binding (Lehmann et al., 2021; Liu et al., 2023). Furthermore, soil containing MP particles larger than 1 mm demonstrated a higher degree of water repellence compared to soil without MP and soil with MP smaller than 1 mm (Shafea et al., 2023). This observation emphasizes that MPs can impact soil wettability and potentially hinder soil water infiltration owing to their hydrophobic properties (Cramer et al., 2023; Shafea et al., 2023). The particle size of EVA, PS, and PP MPs employed in our study were larger than those of the soil particles (< 2 mm); therefore, it is reasonable to suggest that the presence of MPs disrupt soil aggregates.

Our study yielded inconclusive findings regarding the cause of elevated q_e values in soils containing MPs. Whether this increase is due to alterations in the soil matrix or an increase in the OC content of the adsorbent material remains unclear. Additionally, environmental conditions such as pH and radiation influence the adsorption process of MPs. In summary, MPs have been demonstrated to influence the adsorption of pollutants in soil, with interactions affected by various factors, including MP characteristics, organic fraction of the soil, properties of pollutants, and aging factors. This study serves as a starting

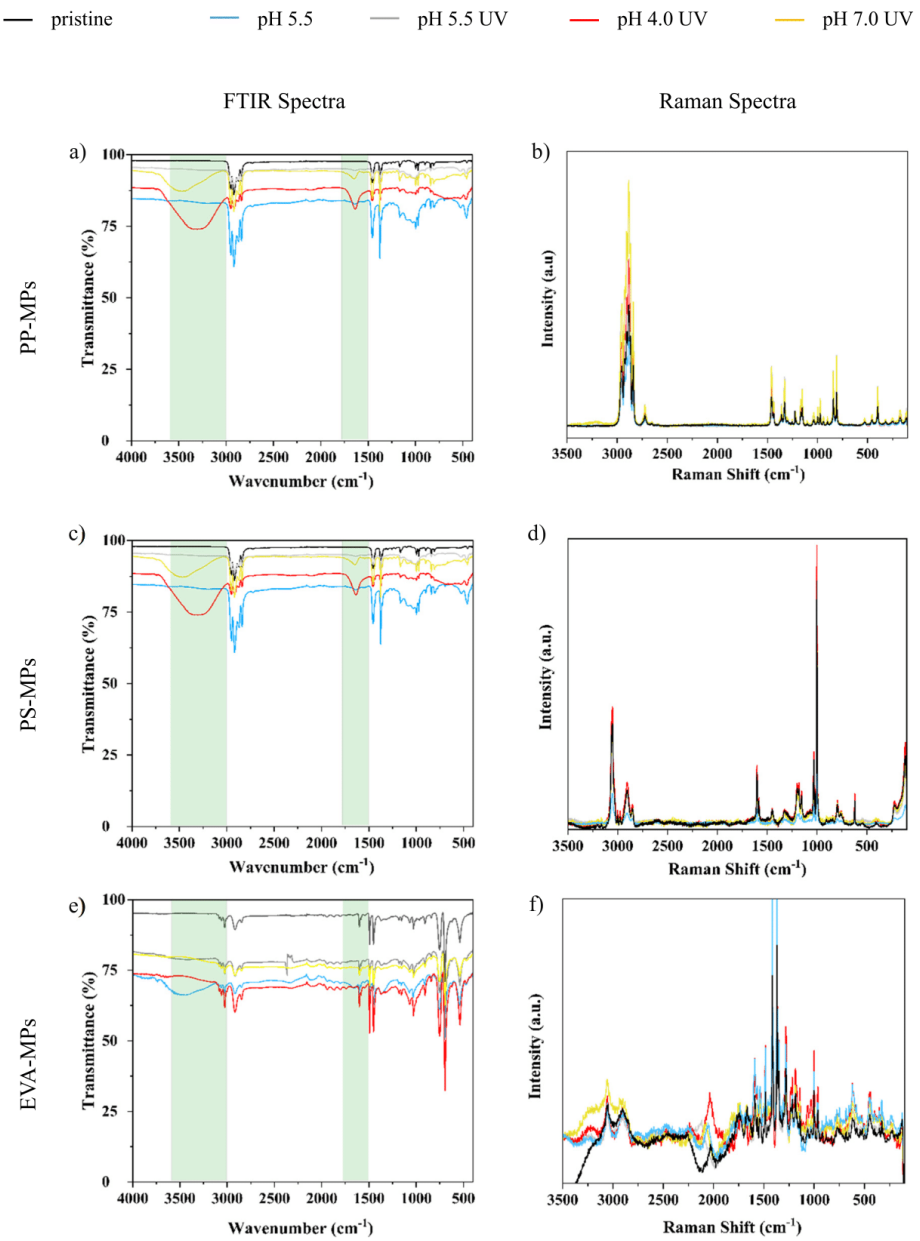


Fig. 5. ATR-FTIR and Raman spectra from soil-MP systems. ATR-FTIR spectra (a, c, e) spanning the wavenumber range of 4000–400 cm^{-1} versus transmittance (%), with two distinct ranges highlighted in green (3600–3000 and 1800–1500 cm^{-1}), for PP-MPs, PS-MPs, and EVA-MPs, respectively. Raman spectra (b, d, f) covering a Raman shift range of 3500–100 cm^{-1} versus intensity are presented for PP-MPs, PS-MPs, and EVA-MPs. respectively.

point for further exploration of the complex interactions resulting from the coexistence of MPs and pollutants in soil.

4. Conclusion

The presence of MPs in soil poses challenges in assessing their presence and impact, owing to their diverse characteristics, including particle morphology, chemical composition, and levels of degradation.

Table 2
Water contact angles (θ, in degrees) of pristine and aged microplastics of polypropylene (PP-MPs), polystyrene (PS-MPs), and ethylene-vinyl acetate (EVA-MPS) in soil-MP systems under various pH and UV exposure conditions. ($n = 8$).

	PP-MPs		PS-MPs		EVA-MPs	
	θ_{left}	θ_{right}	θ_{left}	θ_{right}	θ_{left}	θ_{right}
pristine	104.2 ± 8.8	102.4 ± 6.3	101.4 ± 9.2	102.6 ± 9.7	113.8 ± 8.5	115.9 ± 9.1
pH 5.5	75.4 ± 5.1	76.6 ± 4.9	100.1 ± 2.0	100.2 ± 2.8	110.0 ± 6.1	109.1 ± 5.8
pH 5.5 UV	96.1 ± 5.9	94.4 ± 6.7	94.3 ± 10.9	97.3 ± 11.5	106.3 ± 4.7	105.6 ± 4.8
pH 4.0 UV	85.6 ± 7.0	87.3 ± 3.1	89.4 ± 5.5	87.4 ± 4.5	107.9 ± 5.7	111.0 ± 8.1
pH 7.0 UV	90.0 ± 9.8	89.8 ± 9.6	97.7 ± 6.7	98.6 ± 6.6	113.5 ± 5.4	113.5 ± 5.0

This study explored the intricate interplay among TPhP sorption dynamics, soil properties, MP characteristics, and environmental conditions. It involved 32 subsystems, including blank controls, soil-only, MPs-only, and soil-MP systems, to investigate TPhP adsorption under different pH and UV radiation conditions, while maintaining temperature and humidity. Significant TPhP adsorption onto soil particles was observed in the soil-only system, influenced by OC content, pH, and UV radiation. In contrast, MP-only systems exhibited limited equilibrium, suggesting kinetic limitations. Incorporating MPs into the soil altered the TPhP adsorption, with varying equilibrium capacities observed for different MP polymers and aging conditions.

The presence of MPs makes it challenging to predict soil dynamics and contaminant behavior because their shape, size, and polymer composition affect aggregate formation and stability. Although the appearance of aged MPs may resemble that of pristine polymers, analysis of ATR-FTIR and μ-Raman spectra and WCA measurements provided evidence of photooxidation processes and changes in the surface hydrophobicity of aged MPs. Given the ubiquity of MPs and their related chemicals such as pesticides, pharmaceuticals, and heavy metals, it is crucial to not overlook the role of plastic additives in ecosystems. Studies focusing on the interactions between plastic additives and MPs are essential to understand the dynamics of environmental contamination. The findings of our study underscore the complexity of TPhP sorption in soil-MP environments and emphasize the importance of considering multiple factors, including those relevant to bioaccumulation, to understand the fate and transport of contaminants. Further research is needed to elucidate the degradation mechanisms of TPhP, the drivers of its sorption onto soil particles in the presence of MPs, and to assess their long-term implications.

Funding

Diana Rede thanks Fundação para a Ciência e Tecnologia and Ministério da Ciência, Tecnologia e Ensino Superior (FCT/MCTES) and European Social Fund (ESF) through NORTE 2020 (Programa Operacional Região Norte) for her PhD grant ref. SFRH/BD/147404/2019. This work received financial support from FCT/MCTES through project MTS/SAS/0077/2020 "Honey+: New reasons to care honey from the Natural Park of Montesinho: A bioindicator of environmental quality & its therapeutic potential.

CRediT authorship contribution statement

Diana Rede: Writing – original draft, Validation, Methodology, Investigation, Formal analysis. **Rui Vilarinho:** Software, Resources, Investigation, Formal analysis. **Joaquim Agostinho Moreira:** Software, Resources, Investigation, Formal analysis. **Cristina Delerue-Matos:** Supervision, Resources, Project administration, Investigation, Conceptualization. **Virgínia Cruz Fernandes:** Writing – review & editing, Visualization, Validation, Supervision, Methodology, Investigation, Funding acquisition, Conceptualization.

Declaration of competing interest

The authors declare that they have no known competing financial interests or personal relationships that could have appeared to influence the work reported in this paper.

Data availability

Data will be made available on request.

Acknowledgments

This work received support and help from FCT/MCTES (LA/P/0008/2020, doi: 10.54499/LA/P/0008/2020, UIDP/50006/2020, doi: 10.54499/UIDP/50006/2020 and UIDB/50006/2020, doi: 10.54499/UIDB/50006/2020), through national funds. The authors would also like to express their gratitude to the FCT for the support through the project PLASTOXIC 2022.15094.CBM (bilateral cooperation between Portugal and France under the 2023–2024 person program), and project number 49190WH (PHC PESSOA 2023).

Appendix A. Supplementary data

Supplementary data to this article can be found online at https://doi.org/10.1016/j.scitotenv.2024.173745.

References

Almond, J., Sugumaar, P., Wenzel, M.N., et al., 2020. Determination of the carbonyl index of polyethylene and polypropylene using specified area under band methodology with ATR-FTIR spectroscopy. E-Polymers 20, 369–381. https://doi.org/10.1515/epoly-2020-0041.

Andrade, J., Muniategui, S., 2019. A low-cost system to simulate environmental microplastic weathering. Mar. Pollut. Bull. 149, 110663 https://doi.org/10.1016/j.marpolbul.2019.110663.

Araujo, C.F., Nolasco, M.M., Ribeiro, A.M.P., Ribeiro-Claro, P.J.A., 2018. Identification of microplastics using Raman spectroscopy: latest developments and future prospects. Water Res. 142, 426–440. https://doi.org/10.1016/J.WATRES.2018.05.060.

Australian Government, 2023. Triphenyl phosphate and diphenyl phosphate: Evaluation statement [EVA00108].

Binda, G., Zanetti, G., Bellasi, A., et al., 2023. Physicochemical and biological ageing processes of (micro)plastics in the environment: a multi-tiered study on polyethylene. Environ. Sci. Pollut. Res. 30, 6298–6312. https://doi.org/10.1007/s11356-022-22599-4.

Björnsdotter, M.K., Romera-García, E., Borrull, J., et al., 2018. Presence of diphenyl phosphate and aryl-phosphate flame retardants in indoor dust from different microenvironments in Spain and the Netherlands and estimation of human exposure. Environ. Int. 112, 59–67. https://doi.org/10.1016/j.envint.2017.11.028.

Boots, B., Russell, C.W., Green, D.S., 2019. Effects of microplastics in soil ecosystems: above and below ground. Environ. Sci. Technol. 53, 11496–11506. https://doi.org/10.1021/acs.est.9b03304.

Campanale, C., Savino, I., Massarelli, C., Uricchio, V.F., 2023. Fourier transform infrared spectroscopy to assess the degree of alteration of artificially aged and environmentally weathered microplastics. Polymers 15. https://doi.org/10.3390/polym15040911.

Chen, M., Zhang, S., Liu, L., et al., 2022. Organic fertilization increased soil organic carbon stability and sequestration by improving aggregate stability and iron oxide transformation in saline-alkaline soil. Plant and Soil 474, 233–249. https://doi.org/10.1007/s11104-022-05326-3.

Chen, Z., Yang, J., Huang, D., et al., 2023. Adsorption behavior of aniline pollutant on polystyrene microplastics. Chemosphere 323, 138187. https://doi.org/10.1016/j.chemosphere.2023.138187.
Cheng, H., Luo, H., Hu, Y., Tao, S., 2020. Release kinetics as a key linkage between the occurrence of flame retardants in microplastics and their risk to the environment and ecosystem: a critical review. Water Res. 185, 116253 https://doi.org/10.1016/j.watres.2020.116253.
Chokwe, T.B., Okonkwo, J.O., 2019. Occurrence, distribution and ecological risk assessment of organophosphorus flame retardants and plasticizers in sediment samples along the Vaal River catchment, South Africa. Emerg. Contam. 5, 173–178. https://doi.org/10.1016/j.emcon.2019.05.003.
Cramer, A., Benard, P., Zarebanadkouki, M., et al., 2023. Microplastic induces soil water repellency and limits capillary flow. Vadose Zo J 22, 1–11. https://doi.org/10.1002/vzj2.20215.
Cristale, J., Álvarez-Martín, A., Rodríguez-Cruz, S., et al., 2017. Sorption and desorption of organophosphate esters with different hydrophobicity by soils. Environ. Sci. Pollut. Res. 24, 27870–27878. https://doi.org/10.1007/s11356-017-0360-0.
De Souza Machado, A.A., Lau, C.W., Till, J., et al., 2018. Impacts of microplastics on the soil biophysical environment. Environ. Sci. Technol. 52, 9656–9665. https://doi.org/10.1021/acs.est.8b02212.
Dong, X., Yang, X., Hua, S., et al., 2021. Unraveling the mechanisms for persulfate-based remediation of triphenyl phosphate-contaminated soils: complicated soil constituent effects on the formation and propagation of reactive oxygen species. Chem. Eng. J. 426, 130662 https://doi.org/10.1016/j.cej.2021.130662.
Doane, T.A., Silva, L.C.R., Horwarth, W.R., 2019. Exposure to Light Elicits a Spectrum of Chemical Changes in Soil. J. Geophys. Res. Earth Surf. https://doi.org/10.1029/2019JF005069.
Dong, X., Feng, R., Jiang, Y., et al., 2022. The impacts of temperature, soil-water ratio, and background multiplied inorganic anions on the degradation of organophosphorus flame retardants in soil by peroxydisulfate-based advanced oxidation processes. Process. Saf. Environ. Prot. 168, 422–433. https://doi.org/10.1016/j.psep.2022.09.059.
Du, Z., Zhang, Y., Wang, G., et al., 2016. TPhP exposure disturbs carbohydrate metabolism, lipid metabolism, and the DNA damage repair system in zebrafish liver. Sci. Rep. 6, 1–10. https://doi.org/10.1038/srep21827.
Fabian, C., Reimann, C., Fabian, K., et al., 2023. Spatial distribution of the pH of European agricultural and grazing land soil. Appl. Geochem. 48, 207–216. https://doi.org/10.1016/j.apgeochem.2014.07.017.
Feng, X., Hills, K.M., Simpson, A.J., et al., 2011. Organic geochemistry the role of biodegradation and photo-oxidation in the transformation of terrigenous organic matter. Org. Geochem. 42, 262–274. https://doi.org/10.1016/j.orggeochem.2011.01.002.
Fernandez-Gonzalez, V., Andrade-Garda, J.M., Lopez-Mahía, P., Muniategui-Lorenzo, S., 2021. Impact of weathering on the chemical identification of microplastics from usual packaging polymers in the marine environment. Anal. Chim. Acta 1142, 179–188. https://doi.org/10.1016/j.aca.2020.11.002.
Fu, L., Li, J., Wang, G., et al., 2021. Adsorption behavior of organic pollutants on microplastics. Ecotoxicol. Environ. Saf. 217, 112207 https://doi.org/10.1016/j.ecoenv.2021.112207.
Gewert, B., Plassmann, M.M., Macleod, M., 2015. Pathways for degradation of plastic polymers floating in the marine environment. Environ Sci Process Impacts 17, 1513–1521. https://doi.org/10.1039/c5em00207a.
Gewert, B., Plassmann, M., Sandblom, O., Macleod, M., 2018. Identification of chain scission products released to water by plastic exposed to ultraviolet light. Environ. Sci. Technol. Lett. 5, 272–276. https://doi.org/10.1021/acs.estlett.8b00119.
Guo, C., Wang, L., Lang, D., et al., 2023. UV and chemical aging alter the adsorption behavior of microplastics for tetracycline. Environ. Pollut. 318, 120859 https://doi.org/10.1016/j.envpol.2022.120859.
He, M., Lu, J., Wei, S., 2019. Organophosphate esters in biota, water, and air from an agricultural area of Chongqing, western China: Concentrations, composition profiles, partition and human exposure *. Environ. Pollut. 244, 388–397. https://doi.org/10.1016/j.envpol.2018.10.085.
Hiejima, Y., Kida, T., Takeda, K., et al., 2018. Microscopic structural changes during photodegradation of low-density polyethylene detected by Raman spectroscopy. Polym. Degrad. Stab. 150, 67–72. https://doi.org/10.1016/j.polymdegradstab.2018.02.010.
Hodson, M.E., Duffus-Hodson, C.A., Clark, A., et al., 2017. Plastic bag derived-microplastics as a vector for metal exposure in terrestrial invertebrates. Environ. Sci. Technol. 51, 4714–4721. https://doi.org/10.1021/acs.est.7b00635.
Horton, A.A., Walton, A., Spurgeon, D.J., et al., 2017. Microplastics in freshwater and terrestrial environments: evaluating the current understanding to identify the knowledge gaps and future research priorities. Sci. Total Environ. 586, 127–141. https://doi.org/10.1016/j.scitotenv.2017.01.190.
Hou, R., Luo, X., Liu, C., et al., 2019. Enhanced degradation of triphenyl phosphate (TPHP) in bioelectrochemical systems: kinetics, pathway and degradation mechanisms. Environ. Pollut. 254, 113040 https://doi.org/10.1016/j.envpol.2019.113040.
Hu, B., Li, Y., Jiang, L., et al., 2020. Influence of microplastics occurrence on the adsorption of 17β-estradiol in soil. J. Hazard. Mater. 400, 123325 https://doi.org/10.1016/j.jhazmat.2020.123325.
Hu, M., Huang, L., Wang, Y., et al., 2023. Insight into the effect of microplastics on the adsorption and degradation behavior of thiamethoxam in agricultural soils. Chemosphere 337, 139262. https://doi.org/10.1016/j.chemosphere.2023.139262.
Huang, Z., Wang, H., 2023. Study on the impact of photoaging on the generation of very small microplastics (MPs) and nanoplastics (NPs) and the wettability of plastic surface. Environ. Sci. Pollut. Res. 30, 92963–92982. https://doi.org/10.1007/s11356-023-29012-8.
Jang, M.H., Kim, T.K., Park, J.W., et al., 2024. Elucidating adsorption mechanisms of benzalkonium chlorides (BACs) on polypropylene and polyethylene terephthalate microplastics (MPs): effects of BACs alkyl chain length and MPs characteristics. J. Hazard. Mater. 468, 133765 https://doi.org/10.1016/j.jhazmat.2024.133765.
Ju, T., Yang, K., Chang, L., et al., 2023. Microplastics sequestered in the soil affect the turnover and stability of soil aggregates: a review. Sci. Total Environ. 904 https://doi.org/10.1016/j.scitotenv.2023.166776.
Kim, U.J., Oh, J.K., Kannan, K., 2017. Occurrence, removal, and environmental emission of organophosphate flame retardants/plasticizers in a wastewater treatment plant in New York State. Environ. Sci. Technol. 51, 7872–7880. https://doi.org/10.1021/acs.est.7b02035.
Kinigopoulou, V., Pashalidis, I., Kalderis, D., Anastopoulos, I., 2022. Microplastics as carriers of inorganic and organic contaminants in the environment: a review of recent progress. J. Mol. Liq. 350, 118580 https://doi.org/10.1016/j.molliq.2022.118580.
Kole, P.J., Löhr, A.J., Van Belleghem, F.G.A.J., Ragas, A.M.J., 2017. Wear and Tear of Tyres: A Stealthy Source of Microplastics in the Environment. Int. J. Environ. Res. Public Health 14, 1265. https://doi.org/10.3390/ijerph14101265.
Kwak, J. Il, An, Y., 2021. Microplastic digestion generates fragmented nanoplastics in soils and damages earthworm spermatogenesis and coelomocyte viability. J. Hazard. Mater. 402, 124034 https://doi.org/10.1016/j.jhazmat.2020.124034.
Lehmann, A., Leifheit, E.F., Gerdawischke, M., Rillig, M.C., 2021. Microplastics have shape- and polymer-dependent effects on soil aggregation and organic matter loss – an experimental and meta-analytical approach. Microplastics and Nanoplastics 1, 1–14. https://doi.org/10.1186/s43591-021-00007-x.
Li, C., Jiang, B., Guo, J., et al., 2022. Aging process of microplastics in the aquatic environments: aging pathway, characteristic change, compound effect, and environmentally persistent free radicals formation. Water 14, 3515. https://doi.org/10.3390/w14213515.
Li, L., Li, J., Yan, Y., et al., 2023. Removal of organophosphorus flame retardant by biochar-coated nZVI activating persulfate: synergistic mechanism of adsorption and catalytic degradation. Environ. Pollut. 331, 121880 https://doi.org/10.1016/j.envpol.2023.121880.
Li, X., Jiang, H., Zhu, L., et al., 2024. Adsorption interactions between typical microplastics and enrofloxacin: relevant contributions to the mechanism. Chemosphere 351, 141181. https://doi.org/10.1016/j.chemosphere.2024.141181.
Liang, Y., Lehmann, A., Yang, G., et al., 2021. Effects of microplastic fibers on soil aggregation and enzyme activities are organic matter dependent. Front. Environ. Sci. 9, 1–11. https://doi.org/10.3389/fenvs.2021.650155.
Liu, Y., Zhong, Y., Hu, C., et al., 2023. Distribution of microplastics in soil aggregates after film mulching. Soil Ecol. Lett. 5, 230171 https://doi.org/10.1007/s42832-023-0171-9.
Luo, H., Zhao, Y., Li, Y., et al., 2020. Aging of microplastics affects their surface properties, thermal decomposition, additives leaching and interactions in simulated fluids. Sci. Total Environ. 714, 136862 https://doi.org/10.1016/j.scitotenv.2020.136862.
Ma, Y., Xie, Z., Lohmann, R., et al., 2017. Organophosphate ester flame retardants and plasticizers in ocean sediments from the North Pacific to the Arctic Ocean. Environ. Sci. Technol. 51, 3809–3815. https://doi.org/10.1021/acs.est.7b00755.
Magnusson, B., Örnemark, U., 2014. Eurachem Guide: The Fitness for Purpose of Analytical Methods – A Laboratory Guide to Method Validation and Related Topics, 2nd edn.
Martinho, S.D., Martinho, S.D., Fernandes, V.C., et al., 2022. Study of the potential accumulation of the pesticide alpha-endosulfan by microplastics in water systems. Polymers 14, 3645. https://doi.org/10.3390/polym14173645.
Martinho, S.D., Fernandes, C., Figueiredo, S.A., Vilarinho, R., 2023. Laboratory Studies about Microplastic Aging and Its Effects on the Adsorption of Chlorpyrifos. Polymers 15, 3468. https://doi.org/10.3390/polym15163468.
Meeker, J.D., Stapleton, H.M., 2010. House Dust Concentrations of Organophosphate Flame Retardants in Relation to Hormone Levels and Semen Quality Parameters, 318–323. https://doi.org/10.1289/ehp.0901332.
Nantaba, F., Palm, W.U., Wasswa, J., et al., 2021. Temporal dynamics and ecotoxicological risk assessment of personal care products, phthalate ester plasticizers, and organophosphorus flame retardants in water from Lake Victoria, Uganda. Chemosphere 262, 127716. https://doi.org/10.1016/j.chemosphere.2020.127716.
OECD SIDS, 2002. Triphenyl Phosphate Cas N ° : 115-86-6.
Prendergast-Miller, M.T., Katsiamides, A., Abbass, M., et al., 2019. Polyester-derived micro fibre impacts on the soil-dwelling earthworm Lumbricus terrestris. Environ. Pollut. 251, 453–459. https://doi.org/10.1016/j.envpol.2019.05.037.
Puckowski, A., Cwięk, W., Mioduszewska, K., et al., 2021. Sorption of pharmaceuticals on the surface of microplastics. Chemosphere 263, 127976. https://doi.org/10.1016/j.chemosphere.2020.127976.
Rede, D., Delerue-Matos, C., Fernandes, V.C., 2023a. The microplastics iceberg: filling gaps in our understanding. Polymers (Basel) 15, 1–28. https://doi.org/10.3390/polym15163356.
Rede, D., Teixeira, I., Delerue, C., et al., 2023b. Assessing emerging and priority micropollutants in sewage sludge: environmental insights and analytical approaches. Environ. Sci. Pollut. Res. https://doi.org/10.1007/s11356-023-30963-1.
Robinson, S.A., Young, S.D., Brinovcar, C., et al., 2020. Ecotoxicity assessment and bioconcentration of a highly brominated organophosphate ester flame retardant in two amphibian species. Chemosphere 260, 127631. https://doi.org/10.1016/j.chemosphere.2020.127631.

Schefer, R.B., Armanious, A., Mitrano, D.M., 2023. Eco-Corona formation on plastics: adsorption of dissolved organic matter to pristine and photochemically weathered polymer surfaces. Environ. Sci. Technol. 57, 14707–14716. https://doi.org/10.1021/acs.est.3c04180.

Shafea, L., Felde, V.J.M.N.L., Woche, S.K., et al., 2023. Microplastics effects on wettability, pore sizes and saturated hydraulic conductivity of a loess topsoil. Geoderma 437, 116566. https://doi.org/10.1016/j.geoderma.2023.116566.

Song, Q., Feng, Y., Liu, G., Lv, W., 2019a. Degradation of the flame retardant triphenyl phosphate by ferrous ion-activated hydrogen peroxide and persulfate: kinetics, pathways, and mechanisms. Chem. Eng. J. 361, 929–936. https://doi.org/10.1016/j.cej.2018.12.140.

Song, Q., Feng, Y., Wang, Z., et al., 2019b. Degradation of triphenyl phosphate (TPhP) by CoFe2O4-activated peroxymonosulfate oxidation process: kinetics, pathways, and mechanisms. Sci. Total Environ. 681, 331–338. https://doi.org/10.1016/j.scitotenv.2019.05.105.

Song, Y., Cao, C., Qiu, R., et al., 2019c. Uptake and adverse effects of polyethylene terephthalate microplastics fibers on terrestrial snails (Achatina fulica) after soil exposure. Environ. Pollut. 250, 447–455. https://doi.org/10.1016/j.envpol.2019.04.066.

Sun, M., Yang, Y., Huang, M., et al., 2022. Adsorption behaviors and mechanisms of antibiotic norfloxacin on degradable and nondegradable microplastics. Sci. Total Environ. 807, 151042 https://doi.org/10.1016/j.scitotenv.2021.151042.

Šunta, U., Prosenc, F., Trebše, P., et al., 2020. Adsorption of acetamiprid, chlorantraniliprole and flubendiamide on different type of microplastics present in alluvial soil. Chemosphere 261, 127762. https://doi.org/10.1016/j.chemosphere.2020.127762.

Wang, G., Du, Z., Chen, H., et al., 2016. Tissue-specific accumulation, depuration, and transformation of triphenyl phosphate (TPHP) in adult zebrafish (danio rerio). Environ. Sci. Technol. 50, 13555–13564. https://doi.org/10.1021/acs.est.6b04697.

Wang, W., Deng, S., Li, D., et al., 2018a. Sorption behavior and mechanism of organophosphate flame retardants on activated carbons. Chem. Eng. J. 332, 286–292. https://doi.org/10.1016/j.cej.2017.09.085.

Wang, Y., Sun, H., Zhu, H., et al., 2018b. Occurrence and distribution of organophosphate flame retardants (OPFRs) in soil and outdoor settled dust from a multi-waste recycling area in China. Sci. Total Environ. 625, 1056–1064. https://doi.org/10.1016/j.scitotenv.2018.01.013.

Wang, F., Zhang, M., Sha, W., et al., 2020a. Sorption behavior and mechanisms of organic contaminants to nano and microplastics. Molecules 25, 1827. https://doi.org/10.3390/molecules25081827.

Wang, K., Zhang, Y., Zhong, Y., et al., 2020b. Flotation separation of polyethylene terephthalate from waste packaging plastics through ethylene glycol pretreatment assisted by sonication. Waste Manag. 105, 309–316. https://doi.org/10.1016/j.wasman.2020.02.021.

Wang, P., Li, D., Fan, X., et al., 2020c. Sorption and desorption behaviors of triphenyl phosphate (TPhP) and its degradation intermediates on aquatic sediments. J. Hazard. Mater. 385, 121574 https://doi.org/10.1016/j.jhazmat.2019.121574.

Wang, X., Liu, Q., Zhong, W., et al., 2020d. Estimating renal and hepatic clearance rates of organophosphate esters in humans: impacts of intrinsic metabolism and binding affinity with plasma proteins. Environ. Int. 134, 105321 https://doi.org/10.1016/j.envint.2019.105321.

Wang, K., Han, T., Chen, X., et al., 2022. Insights into behavior and mechanism of tetracycline adsorption on virgin and soil-exposed microplastics. J. Hazard. Mater. 440, 129770 https://doi.org/10.1016/j.jhazmat.2022.129770.

Ya, H., Jiang, B., Xing, Y., et al., 2021. Science of the total environment recent advances on ecological effects of microplastics on soil environment. Sci. Total Environ. 798, 149338 https://doi.org/10.1016/j.scitotenv.2021.149338.

Ya, H., Zhang, T., Xing, Y., et al., 2023. Co-existence of polyethylene microplastics and tetracycline on soil microbial community and ARGs. Chemosphere 335, 139082. https://doi.org/10.1016/j.chemosphere.2023.139082.

Yang, Y., Yin, H., Peng, H., et al., 2020. Biodegradation of triphenyl phosphate using an efficient bacterial consortium GYY: degradation characteristics, metabolic pathway and 16S rRNA genes analysis. Sci. Total Environ. 713, 136598 https://doi.org/10.1016/j.scitotenv.2020.136598.

Yu, Y., Mo, W.Y., Luukkonen, T., 2021. Adsorption behaviour and interaction of organic micropollutants with nano and microplastics – a review. Sci. Total Environ. 797, 149140 https://doi.org/10.1016/j.scitotenv.2021.149140.

Zhang, H., Wang, J., Zhou, B., et al., 2018. Enhanced adsorption of oxytetracycline to weathered microplastic polystyrene: kinetics, isotherms and influencing factors. Environ. Pollut. 243, 1550–1557. https://doi.org/10.1016/j.envpol.2018.09.122.

Zhang, Q., Wang, Y., Zhang, C., et al., 2022. A review of organophosphate esters in soil: Implications for the potential source, transfer, and transformation mechanism. Environ. Res. 204, 112122 https://doi.org/10.1016/j.envres.2021.112122.

Zhao, J., Zhang, H., Guan, D., et al., 2023. New insights into mechanism of emerging pollutant polybrominated diphenyl ether inhibiting sludge dark fermentation. Bioresour. Technol. 368, 128358 https://doi.org/10.1016/j.biortech.2022.128358.

Zheng, C., Feng, S., Wang, Q., 2016. Application of SPME-GC / MS to study the sorption of organophosphate esters on peat soil. Water Air Soil Pollut. https://doi.org/10.1007/s11270-016-2913-0.

Supporting Information

Investigating the Impact of Microplastics on Triphenyl Phosphate Adsorption in Soil: Insights into Environmental Factors and Soil Properties

Diana Rede[1,2], Rui Vilarinho[3,4], Joaquim Agostinho Moreira[3,4], Cristina Delerue-Matos[1], Virgínia Cruz Fernandes[1*]

[1]REQUIMTE/LAQV, Instituto Superior de Engenharia do Porto, Instituto Politécnico do Porto, Rua Dr. António Bernandino de Almeida 431, 4249-015 Porto, Portugal
[2]Departmento de Química e Bioquimica, Faculdade de Ciências, Universidade do Porto, Rua do Campo Alegre s/n, 4169– 007 Porto, Portugal
[3]Departmento de Física e Astronomia, Faculdade de Ciências, Universidade do Porto, Rua do Campo Alegre s/n, 4169– 007 Porto, Portugal
[4]IFIMUP—Instituto de Física dos Materiais Avançados, Nanotecnologia e Fotónica, Faculdade de Ciências, Universidade do Porto, Rua do Campo Alegre s/n, 4169– 007 Porto, Portugal

*vir@isep.ipp.pt

S.1 Materials and Methods

S.1.1 Microplastics characteristics

Table S1: Manufacturer-provided characteristics of pristine microplastics used in the study (GoodFellow 2024a, b, c). N.a. – not available on the technical sheets.

Polymer	Shape	Particle size (mm)	Color	Density (g cm^{-3})	Radiance resistance	Resistance to UV radiation	Resistance to alkalis	Resistance to diluted acids	Crystallinity
PP	Granule	5	Natural	N.a.	Fair	Poor	Good	Good-fair	Semi-crystalline
PS	Granule	3-5	Natural	1.050	Good	Poor	Good-fair	Good-fair	N.a.
EVA	Granule	3-5	Yellow	N.a.	N.a.	N.a.	N.a.	N.a.	N.a.

S.1.2 Determination of pH at the point of zero charge of soil-only and soil-MPs system

The pH_{PZC} was determined following the modified methodology introduced by MJ Fernandes et al. (2019), which was originally based on the method by Carabineiro et al. (2012). The adaptation included an extended agitation period of 24 hours. The mass and volume adjustments were also made to match the experimental conditions, which involved using 2 g of soil, 4 pieces of the 3 types of MPs, and 10 mL of deionized water for each test. This procedure was applied to soil-only, soil-PS, soil-PP, and soil-EVA. The initial pH values of the deionized water ranged from 2.0 to 12.0, and pH adjustments were achieved using NaOH or HCl solutions. After 24 hours of agitation, the final pH values were measured, and the pH_{PZC} value was determined as the plateau on the curve representing final pH versus initial pH (Carabineiro et al. 2012; Fernandes et al. 2019).

S.2 Results

S.2.1 TPhP adsorption dynamics in simulated soil-only systems

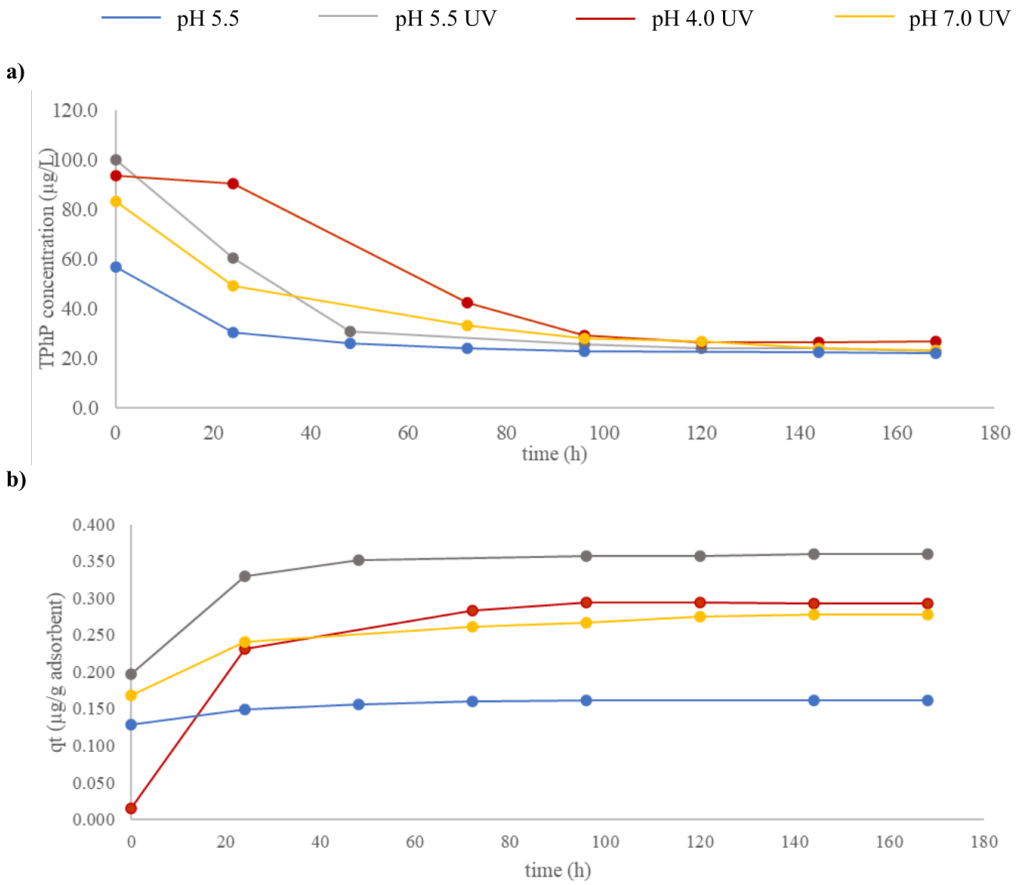


Fig. S1: a) Concentration of TPhP in soil-only systems over time, showing the temporal variation in TPhP concentration within the soil matrix; b) Adsorption capacity (qt) expressed as µg of TPhP per g of adsorbent in soil-only systems over time (t, h)

S.2.2 pH_{PZC} of soil-only and soil-MP systems

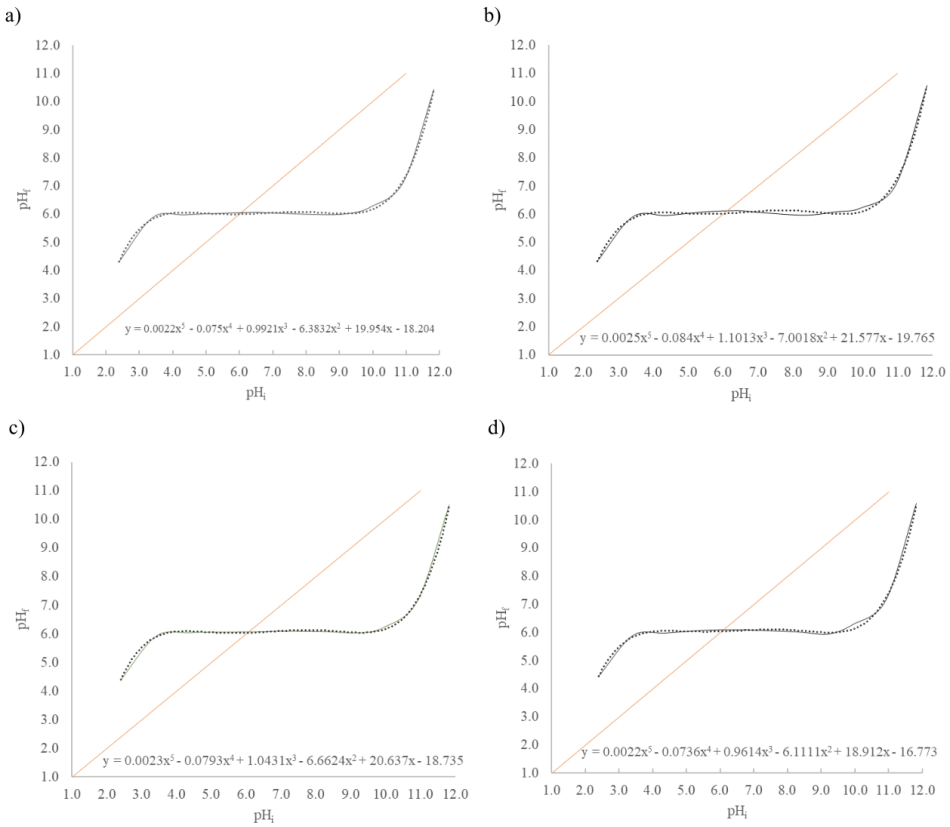


Fig. S2: pH at point zero charge for a) soil-only, b) soil + PP-MPs, c) soil + PS-MPs; and d) soil + EVA-MPs

S.2.3 TPhP adsorption dynamics in simulated MP-only systems

Table S2: Concentration of TPhP over time in MP-only systems subjected to pH 5.5 with UV radiation.

t (h)	C TPhP (µg/L)		
	PP- MPs	PP- MPs	EVA - MPs
0	120.9	128.3	114.0
24	115.6	112.5	99.3
48	96.2	105.1	76.8
72	108.5	93.6	70.6
144	88.9	100.3	59.1
168	89.8	78.8	70.6

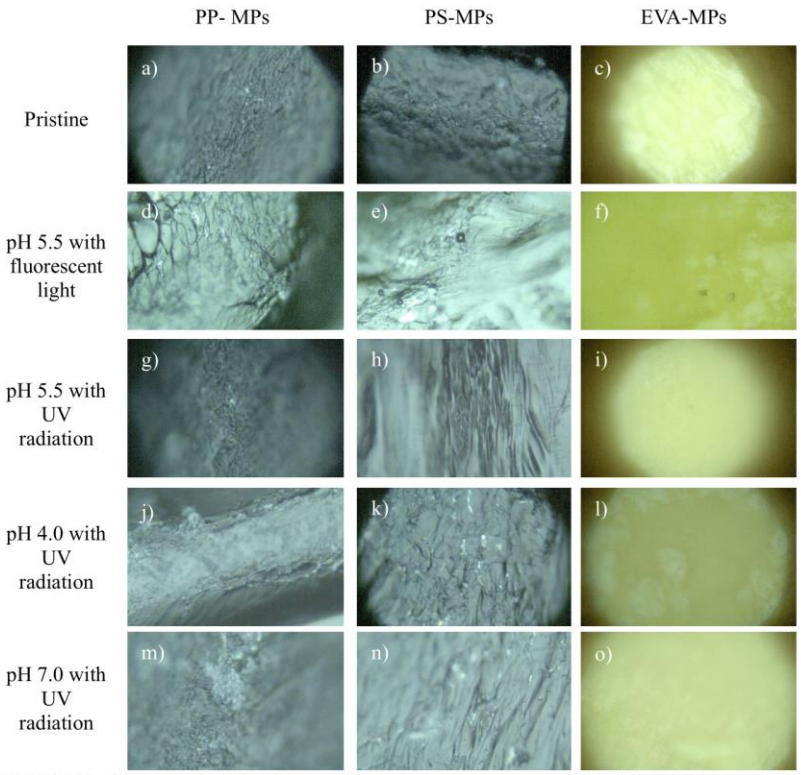


Fig. S3: Images of MPs from MP-only systems captured using a Leica DM2700 microscope equipped with a 50x objective lens. Each image corresponds to MPs subjected to different aging conditions in MPs-only systems: pristine (a-c); pH 5.5 with fluorescent light (d-f); pH 5.5 with UV radiation (g-i); pH 4.0 with UV radiation (j-l); and pH 7.0 with UV radiation (m-o). Column 1: PP- MPs; column 2: PS-MPs; column 3: EVA-MPs.

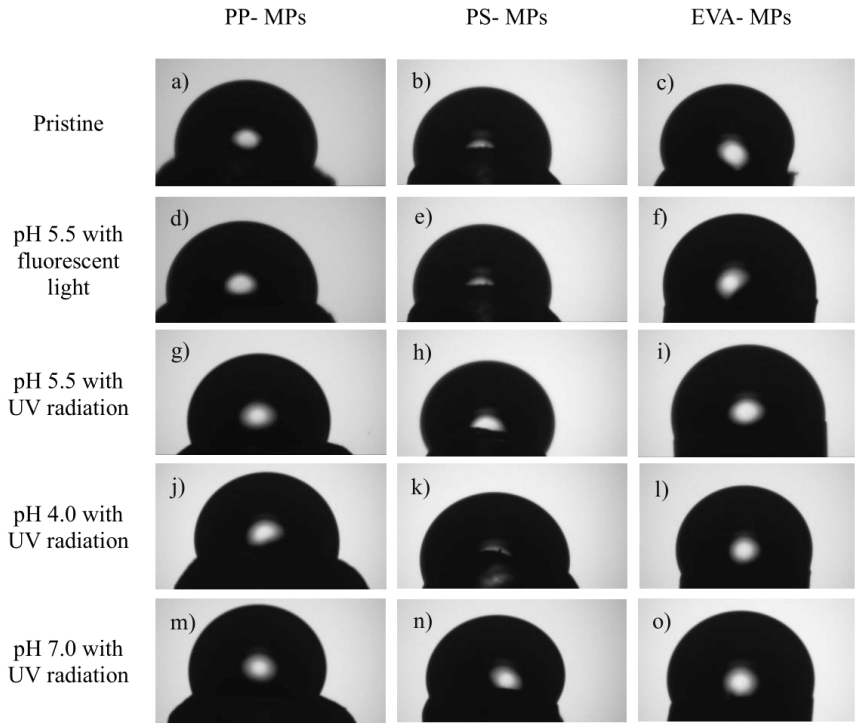


Fig. S4: Images of contact angles from MPs systems captured using a AFWCAMVM high-resolution. Each image corresponds to MPs subjected to different aging conditions in MPs-only systems: pristine (a-c); pH 5.5 with fluorescent light (d-f); pH 5.5 with UV radiation (g-i); pH 4.0 with UV radiation (j-l); and pH 7.0 with UV radiation (m-o). Column 1: PP- MPs; column 2: PS-MPs; column 3: EVA-MPs.

S.2.3 TPhP adsorption dynamics in simulated soil-MPs systems

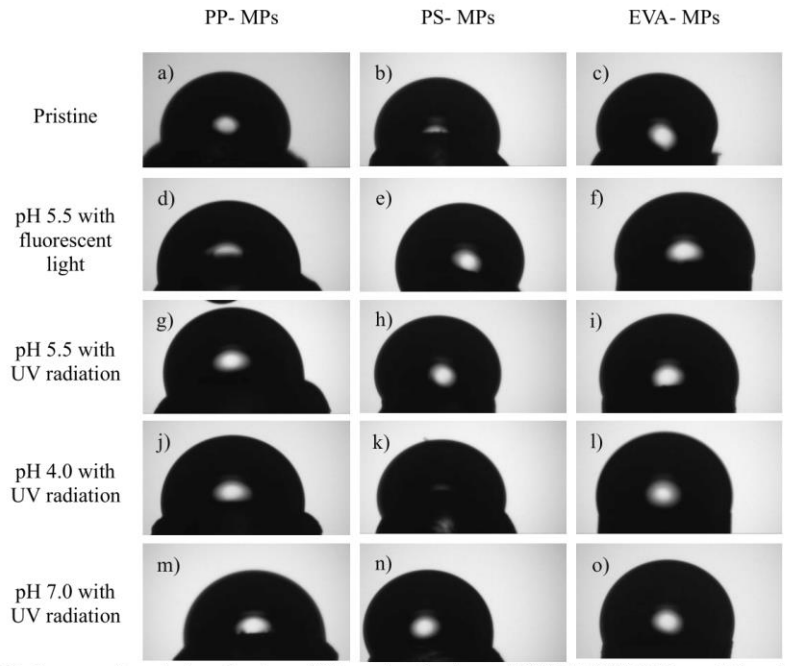


Fig. S5: Images of contact angles from MPs captured using a AFWCAMVM high-resolution. Each image corresponds to MPs subjected to different aging conditions in soil-MPs systems: pristine (a-c); pH 5.5 with fluorescent light (d-f); pH 5.5 with UV radiation (g-i); pH 4.0 with UV radiation (j-l); and pH 7.0 with UV radiation (m-o). Column 1: PP- MPs; column 2: PS-MPs; column 3: EVA-MPs

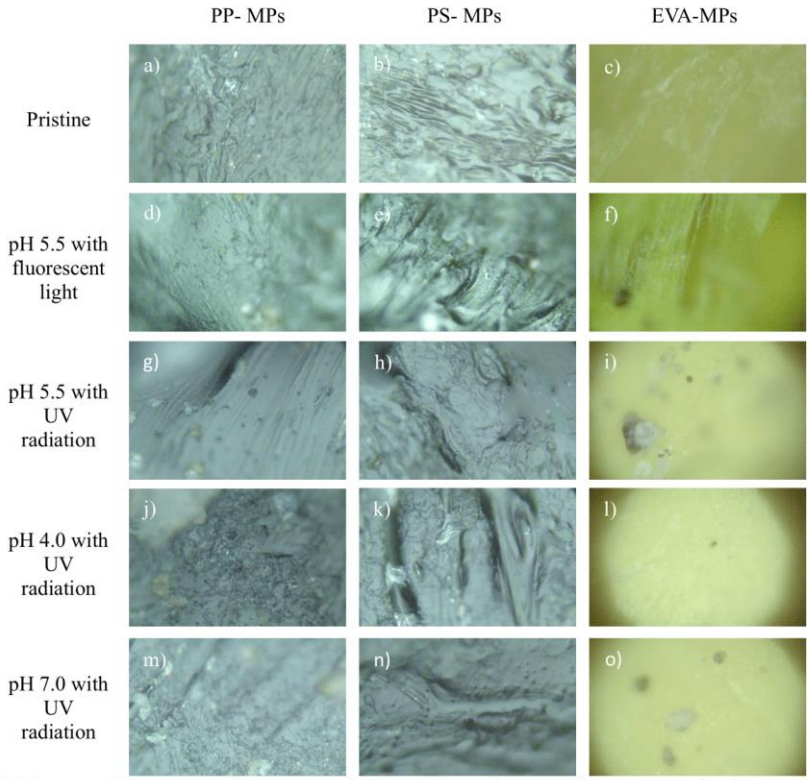


Fig. S6: Images of MPs from soil-MPs systems subjected to various conditions, captured using a Leica DM2700 microscope equipped with a 50x objective lens. Column 1: PP- MPs; column 2: PS-MPs; and column 3: EVA-MPs. a-c: pristine MPs; d-f: exposed MPs to pH 5.5 with fluorescent light; g-i: exposed MPs to pH 5.5 with UV radiation; j-l: exposed MPs to pH 4.0 with UV radiation; and m-o: exposed MPs to pH 7.0 with UV radiation. Note: Some images reveal soil fragments adhering to the surface of MPs, indicating potential interactions between microparticles and soil components during aging processes

References

Carabineiro SAC, Thavorn-amornsri T, Pereira MFR, et al (2012) Comparison between activated carbon , carbon xerogel and carbon nanotubes for the adsorption of the antibiotic ciprofloxacin. Catal Today 186:29–34. https://doi.org/10.1016/j.cattod.2011.08.020

Fernandes MJ, Moreira MM, Paíga P, et al (2019) Bioresource Technology Evaluation of the adsorption potential of biochars prepared from forest and agri-food wastes for the removal of fl uoxetine. Bioresour Technol 292:121973. https://doi.org/10.1016/j.biortech.2019.121973

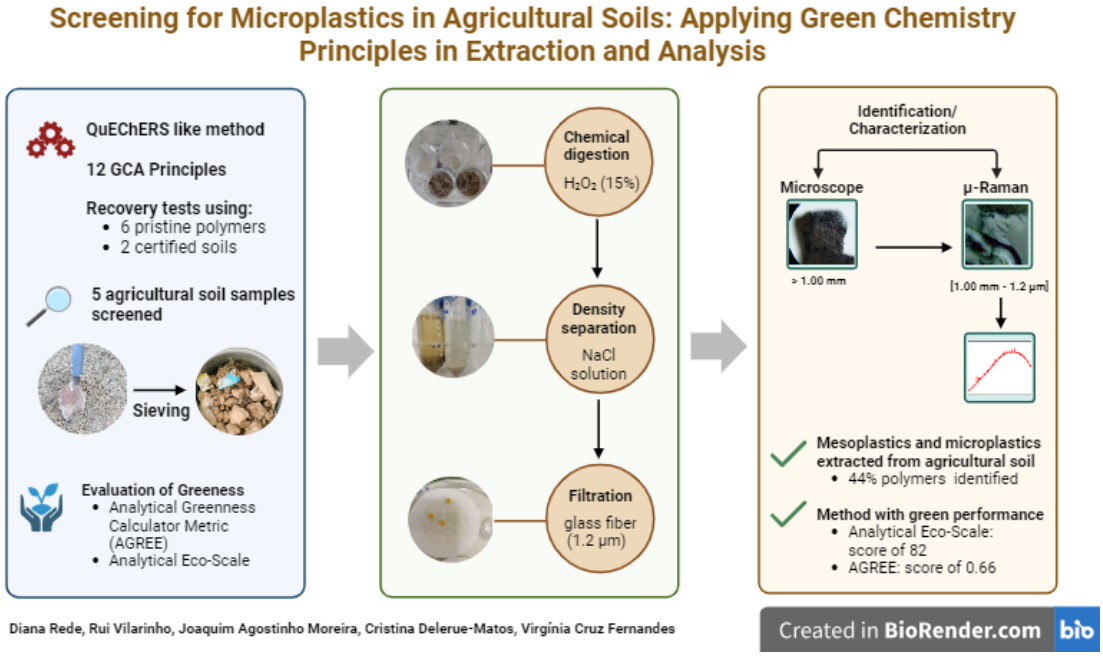
GoodFellow (2024a) Material Properties for Polypropylene. https://www.goodfellow.com/p/pp30-gl-000112/polypropylene-pp-granule. Accessed 5 Jan 1BC

GoodFellow (2024b) Material Properties for Polystyrene. https://www.goodfellow.com/p/st31-gl-000111/polystyrene-granule. Accessed 5 Jan 1BC

GoodFellow (2024c) Universal Masterbatch PEVA Granule 3-5 mm particle size EVA. https://www.goodfellow.com/p/et34-gl-000100/universal-masterbatch-peva-granule. Accessed 5 Jan 1BC

4. Extracting Microplastics from Soil

4.1. Screening for Microplastics in Agricultural Soils: Applying Green Chemistry Principles in Extraction and Analysis



Under Review, Manuscript No. *ENVPOL-D-24-06001*

Contribution Statement

The candidate contributed to the development and implementation of a method for extracting and identifying MPs in agricultural soils, with a focus on green chemistry principles. This involved collecting agricultural soil samples from various rural areas in Viseu, Northern Portugal. The candidate was involved in the conceptualization and development of the extraction methodology, conducting sample analysis and data processing, as well as drafting the original manuscript. Additionally, the candidate also drafted the original manuscript and participated in the review and editing stages. The graphical abstract and Figure 1 were created using BioRender.com.

Screening for Microplastics in Agricultural Soils: Applying Green Chemistry Principles in Extraction and Analysis

Diana Rede[1,2], Rui Vilarinho[3,4], Joaquim Agostinho Moreira[3,4], Luca Nizzetto[5,6], Cristina Delerue-Matos[1], Virgínia Cruz Fernandes[1]*

[1]REQUIMTE/LAQV, Instituto Superior de Engenharia do Porto, Instituto Politécnico do Porto, Rua Dr. António Bernardino de Almeida 431, 4249-015 Porto, Portugal

[2]Departamento de Química e Bioquímica, Faculdade de Ciências, Universidade do Porto, Rua do Campo Alegre s/n, 4169– 007 Porto, Portugal

[3]Departamento de Física e Astronomia, Faculdade de Ciências, Universidade do Porto, Rua do Campo Alegre s/n, 4169– 007 Porto, Portugal

[4]IFIMUP—Instituto de Física dos Materiais Avançados, Nanotecnologia e Fotónica, Faculdade de Ciências, Universidade do Porto, Rua do Campo Alegre s/n, 4169– 007 Porto, Portugal

[5]Norwegian Institute for Water Research (NIVA), Gaustadelléen 21, 0349, Oslo, Norway

[6]Research Centre for Toxic Compounds in the Environment (RECETOX), Faculty of Science, Masarik University, Kamenice 753/5, 625 00, Brno, Czech Republic

*vir@isep.ipp.pt

Highlights

- Recovery tests conducted with 6 pristine MPs and 2 certified soils.
- Chemical digestion with H_2O_2 and centrifugation to reduce interferent materials.
- Density separation repeated three times per sample, yielding three filters.
- Visual sorting of MPs with an inverted microscope and identification by µ-Raman.
- Method scored 0.66 on AGREE analysis, indicating green performance.

Abstract

In recent years, microplastic (MP) pollution has garnered significant attention owing to its ability to permeate various ecosystems, including soil. These particles can infiltrate the environment, either directly or through the degradation of larger plastic items. Despite growing concerns, standardized methods for quantification are still lacking. This study

aimed to screen for the presence of MPs in agricultural soils while incorporating green analytical principles in the methodology. Key components of this methodology, based on the principles of QuEChERS, include minimizing sample quantities, reagent consumption, and waste production without compromising the efficiency of extraction and analysis. Recovery tests using certified soils spiked with pristine MPs demonstrated high extraction efficacy, particularly for larger particles (3-5 mm). Spectroscopic analysis revealed slight alterations in the Raman spectra of MPs after extraction. Transitioning to agricultural soil analysis has revealed challenges, including spectral interferences. Nine mesoplastics were detected, predominantly polypropylene and polyethylene (PE), along with seven MPs, three identified as PE and the remainder as inconclusive, including one fiber. The evaluation of the method's sustainability using the Analytical Eco-Scale and Analytical GREEnness Metric Approach (AGREE) highlighted its greenness, demonstrating its potential as a responsible approach to MP analysis in soils. This study emphasized the need for refined methodologies and effective monitoring strategies to mitigate MP pollution in agricultural soils.

Keywords: Microplastics, soil, spectroscopic analysis, μ-Raman, Green Analytical Chemistry, AGREE metrics

1. Introduction

Microplastics, often referred to as MPs, are widely recognized as significant environmental pollutants. These tiny particles, measuring less than 5 mm in size, exhibit a diverse range of chemical compositions, physicochemical properties, shapes, and varying levels of aging (Dorau et al., 2023; Rede et al., 2023a). Some researchers have proposed further categorizing MPs into large and small MPs, although specific cutoffs are not universally agreed upon. For instance, some studies define small MPs as <300 μm (Nava et al., 2021; Niu et al., 2022) or 500 μm in size (Vermeiren et al., 2020), while others proposed MPs <1 mm in size (Fadare et al., 2023; Thomas et al., 2020). Numerous studies have detected MPs across different environments, including water bodies, sediments, soil, air, biota, and even in human consumables, showcasing their widespread impact (Chandrakanthan et al., 2024; EL Hayany et al., 2020; Phuong et al., 2018; Zhang et al., 2023). Despite a substantial increase in publication count from 21 to 2822 articles between 2011 and 2021 (Picó and Barceló, 2022), the research focus has primarily centered on aquatic environments and air, leaving soil monitoring comparatively understudied (Dorau et al., 2023; Henseler et al., 2019). This is concerning, given estimates suggesting that the presence of plastic in soil exceeds that in water by 4 to 23 times (Horton et al., 2017; Li et al., 2024), emphasizing the urgent need for enhanced

research and monitoring of MP pollution in the soil to understand its implications for ecosystem health (Selonen et al., 2021). MPs can enter soil through various pathways, including localized inputs like sewage sludge application or diffuse transport through wind and fluvial transport (Dorau et al., 2023; Horton et al., 2017).

Despite the increasing number of studies on MP pollution in soil, many analytical methods are adaptations from those designed for aquatic systems, potentially overlooking the complexities of soil matrices and presenting challenges in sample preparation and analysis (Dorau et al., 2023; Horton et al., 2017; Sobhani et al., 2019; Thomas et al., 2020). Soil, characterized by its diverse organic matter (OM) content ranging from 0.02% in desert soils to up to 100% in bog soils, poses unique analytical challenges due to its variable density (Li et al., 2019; Prosenc et al., 2021; Sobhani et al., 2019). Once MPs enter the soil, they integrate into the OM pool and interact with mineral particles, forming stable soil aggregates over time. This integration complicates the identification and quantification of MPs, especially isolating polymers from complex organic-rich soils (Li et al., 2019; Shafea et al., 2023). Additionally, weathered MPs tend to bind more strongly to soil aggregates. It is important to note that spiked samples, often used for validation, may not fully represent the diversity of MPs found in environmental samples (Li et al., 2019).

The analysis protocols for MPs lack harmonization, posing challenges in comparing and interpreting data across studies (Bellasi et al., 2021). This variation may arise from differences in MP used for validation, sample amount, reagents, sequence of steps, identification methods, and processing time (Li et al., 2024; Prosenc et al., 2021; Radford et al., 2021; Sobhani et al., 2019). Despite this lack of uniformity, studies typically follow a common structure involving pre-treatment to reduce OM, extraction methods, and identification techniques (Dorau et al., 2023; Pham et al., 2023). Frequent preparation of soil samples involves oven drying (60%), size fractionation, and removal of soil OM with hydrogen peroxide (H_2O_2, 76%). Most studies utilized density separation using a single salt solution (63%), two salt solutions (23%), or up to three salt solutions for a single study. Additionally, stereomicroscopy is commonly employed alone (70%) or in combination with Fourier-transform infrared spectroscopy (FTIR, 40%), attenuated total reflection FTIR (23%), or Raman spectroscopy (14%) to identify the polymer type in soil samples (Dorau et al., 2023).

The choice of analytical method depends on factors such as particle size, polymer composition, sample matrix, required confirmation level, interference removal techniques, and available technique/instrumentation in the laboratory (Picó and Barceló,

2021; Rani et al., 2023). However, the rapid development of new techniques poses obstacles to standardization (Rani et al., 2023). While various methods are available for MP analysis, not all are environmentally friendly, with insufficient attention given to safety, waste management, and energy consumption. For instance, chemical digestion and density separation, though widely used, present significant sustainability challenges due to their extensive use of hazardous chemicals (e.g. Fenton's reagent or zinc chloride), multiple analytical steps, high waste generation, and prolonged experimental durations, which may extend up to 10 days (Pham et al., 2023; Picó and Barceló, 2022, 2021).

The 2030 Agenda for Sustainable Development highlights the importance of balancing socioeconomic progress with environmental conservation and biodiversity enhancement (Picó and Barceló, 2021). In this context, the adoption of greener analytical methods becomes imperative. Green Analytical Chemistry (GAC) aims to enhance the safety of both humans and the environment by minimizing toxic reagents, reducing waste generation, and lowering energy consumption in analytical method design (Sajid and Justyna, 2022). The 12 principles of GAC (Gałuszka et al., 2013) ensure that methods meet these objectives without compromising efficiency, reproducibility, repeatability, or the ability to detect and identify target analytes (Picó and Barceló, 2022). Within GAC, various metrics such as the Green Analytical Procedure Index (GAPI), Life Cycle Assessment (LCA), Analytical GREEnness Metric Approach (AGREE), and Analytical Eco-scale can be applied to assess the environmental impact of analytical methods for detecting MPs and compare their greenness (Gałuszka et al., 2012; Pena-Pereira et al., 2020; Picó and Barceló, 2022; Sajid and Justyna, 2022).

The objective of this study was to screen for the presence of MPs in samples from agricultural soils using established methods in the field of MPs, including OM digestion, density separation, and vibrational spectroscopy, while incorporating the principles of GAC. To accomplish this goal, we drew inspiration from the QuEChERS approach, known for its acronym representing Quick, Easy, Cheap, Effective, Rugged, and Safe. Widely recognized for its efficacy in extracting organic pollutants from environmental matrices, the QuEChERS method is valued for its simplicity, speed, and cost-effectiveness (Rede et al., 2023b). Our extraction methodology was tailored to achieve rapid, user-friendly, cost-effective, and environmentally friendly extraction, addressing the specific challenges associated with MPs analysis in soil. In this study, we examined two types of certified soils (sand and sandy loam) and six types of pristine MPs with varied characteristics, including size, morphology, and polymer type (polystyrene (PS), polypropylene (PP), ethylene vinyl acetate (EVA), low-density polyethylene (LDPE),

polyamide 6 (PA 6), and tire wear particles (TWP)). The recovery percentage of MPs was calculated, and any potential damage induced by the extraction process was assessed using micro-Raman spectroscopy (μ-Raman). Subsequently, the developed method was applied to five samples of agricultural soil sourced from the Viseu Region of Portugal. To our knowledge, this study represents the first effort to screen agricultural soils in this region while critically evaluating method analytical performance and level of greenness.

2. Materials and Methods

2.1 Reagents and Materials

Deionized water with a resistance of 15.8 MΩ cm was obtained using an Elix® Essential Water Purification System that featured a Progard® TS2 cartridge and a Vent Filter MPK01 for the storage tank, which was supplied by Merck Millipore based in Darmstadt, Germany. Sodium chloride (NaCl), table grade, was obtained from a local supermarket, while hydrogen peroxide 30% (H_2O_2) was sourced from CARLO ERBA Reagents GmbH (Emmendingen, Germany) and butanol from Honeywell (Seelze, Germany). Pristine MPs were purchased from Goodfellow Cambridge, Ltd. (Huntingdon, UK), and included LDPE white powder (<300 μm), PA 6 white powder (15-20 μm), EVA yellow granules (3-5 mm), PS colorless granules (3-5 mm), and PP colorless granules (5 mm). TWP black powder (<180 μm) was produced by Genan (Denmark) from mixed end-of-life passenger car tires and was further processed at the Norwegian Institute for Water Research (NIVA) (Selonen et al., 2021). Two standard soils were used: the Lufa 2.2 sandy loam sourced from LUFA Speyer (Speyer, Germany), and sand supplied by MIBAL - Minas de Barqueiros S.A. (Apúlia, Portugal). Glass microfibers MFV3 with a diameter of 47 mm and 1.2 μm pore size were provided by Filter-Lab® (Barcelona, Spain). Test sieves with mesh sizes of 5.00 mm, 1.00 mm, 100 μm, and 40 μm, each with a diameter of 100 mm, were from Retsch™ (Retsch, Milling Sieving Assisting, Hann, Germany).

2.2 Sampling site

Agricultural soil samples, designated as A through E, were collected from various rural locations in Viseu, Northern Portugal. Soil A was obtained from an olive grove, Soil B from blueberry cultivation, and Soil C from a vineyard. These sampling sites (A-C) were located outside nearby residential areas. Soil D and E were collected from the same backyard, but before and after ploughing, respectively. Given the location of this site, we anticipated the possibility of MP contamination from both residential and road-related sources, as evidenced by the visible presence of mesoplastic debris. These five soils were selected to reflect a wide array of agricultural land use and management practices,

as well as distinct geological characteristics present in rural settings, offering a nuanced perspective on soil dynamics across varied landscapes.

A composite sample was obtained from each sampling location, with soil collected at five random points that were spaced approximately 2 m apart. At each of these five points, a subsample was collected from a depth of 5 cm using a stainless-steel shovel and mixed with soil from the other points in a pre-cleaned glass bottle, resulting in a total of approximately 1 kg of composite sample after removing any large visible debris of plants and woody materials or stones. Visible suspects of mesoplastics were kept for identification. The samples were then stored at room temperature for further analysis. The method for OM determination is presented in Supplementary Information.

2.3 Laboratory Precautions and Sample Control

Concerns regarding minimizing contamination are well documented in the literature, although a formal protocol remains elusive. Drawing on the proposals of several studies aimed at preventing background contamination (Braun et al., 2021; Fadare et al., 2023; Harley-Nyang et al., 2022; Li et al., 2021; Nuelle et al., 2014; Worek et al., 2022), a series of measures was implemented. These measures include the avoidance of plastic materials whenever possible, and the utilization of glassware washed with deionized water and acetone. Following preparation, the glassware was stored and covered with either aluminium foil or lids to prevent airborne contamination. Moreover, both deionized water and NaCl solutions were filtered using glass microfiber filters with a pore size of 1.2 µm. The experiments were carried out in a fume hood (Braun et al., 2021; Harley-Nyang et al., 2022), cotton lab coats were worn and gloves avoided when possible. Samples were covered with aluminum foil until the next analytical step when necessary. Procedural blanks and control tests were performed in triplicate.

2.4 Recovery tests of pristine microplastics from certified soils

Recognizing the absence of standardized approaches and the multitude of proposed protocols, we chose to utilize density separation with centrifugation coupled with µ-Raman spectroscopy. Our methodology was inspired by the QuEChERS approach and integrates insights gathered from prior research, along with practical solutions derived from our preliminary testing. The challenges we encountered in our preliminary tests, including settling time, disturbance of settled material with filtration, and material loss, have also been noted by other authors (Coppock et al., 2017; Li et al., 2024; Nakajima et al., 2019; Thomas et al., 2020).

In the recovery tests, the two certified soils were individually spiked with concentrations of 1%, 2%, and 5% (w/w) of each of the six MPs, following a method mostly based on Prosenc et al. (2021), with specific modifications tailored to this study. Five grams of spiked soil sample were placed into a 50 mL glass beaker, where 10 mL of H_2O_2 (15%) was added to reduce OM. After allowing the mixture to stand for 15 minutes, it was subjected to a 3-hour water bath at 40 °C. To prevent contamination, the beakers were covered with aluminium foil, and butanol drops were added as needed to minimize foam formation (Li et al., 2019). At this stage, the final OM content was determined in a subsample. The sample was transferred to a 50 mL centrifuge tube, and 25 mL of NaCl solution (1.2 g cm^{-3}) was added. The sample was mixed for 30 seconds to facilitate disaggregation between soil and MP particles using a vortex shaker (Heidolph Instruments GmbH & Co., Schwaback, Germany). Subsequently, the mixture underwent centrifugation at 4500 rpm for 30 minutes (Heraus Magafuge 16 R centrifuge, ThermoFisher Scientific, Germany). The supernatant was filtered using a vacuum system unit (Sartorius, Goettingen, Germany) and a pre-weighed fiberglass filter with a pore size of 1.2 µm. The material retained on the filter was washed with 50 mL of deionized water to remove salt residues. Density separation was repeated three times, yielding three filters per sample. The filters were dried at 40 °C overnight (Corradini et al., 2021; Pfeiffer and Fischer, 2020). Between samples, the filtration apparatus was rinsed with deionised water and acetone.

For particles between 3-5 mm, the polymer recovery rate was calculated as the number of extracted particles over the number of added particles (Li et al., 2024; Savino et al., 2022), expressed as a percentage. For particles between 15-300 µm, the filters were weighed, and the recovery rates were calculated similarly, but using weight instead of particle number. Additionally, tests using only MPs were conducted to assess their integrity after the extraction process. Soils without MPs were prepared as controls to evaluate the non-plastic material transferred to the filter during extraction. A procedure blank conducted to assess any protocol-related contamination.

Micro-Raman analysis enabled the assessment of potential damage to the pristine MPs used in spiking and confirmed the efficacy of the extraction method for MPs < 1 mm. Spectra were recorded using an InVia™ Qontor® confocal Raman spectrometer (Renishaw, United Kingdom), coupled with a Leica DM2700 microscope (Ernst Leitz GmbH, Germany), and controlled by WiRE™ 5.2 software (Renishaw Inc., United Kingdom). A 50x objective was used to focus the laser beam on each measured target. The diffraction grating density had 1800 lines per mm, the spectra were collected from 100 to 3500 cm^{-1}, using a 633 nm He-Ne laser as the excitation light source, with a

maximum power of 100 mW adjusted for each target. Integration time was 10 or 30 seconds, the number of accumulations was 3, and the spectral resolution exceeded 2 cm^{-1}. Spectra were pre-processed (cosmic ray removal, signal smoothing, baseline correction, and normalization) (Araujo et al., 2018) using OriginPro, Version 2024 (OriginLab Corporation, Northampton, MA, USA). Additionally, spectral interference from the filter was investigated. Each filter of blank and control underwent µ-Raman analysis at ten random points using a helicoidal pattern. Figure 1 provides a visual summary of the experimental protocol described in the text.

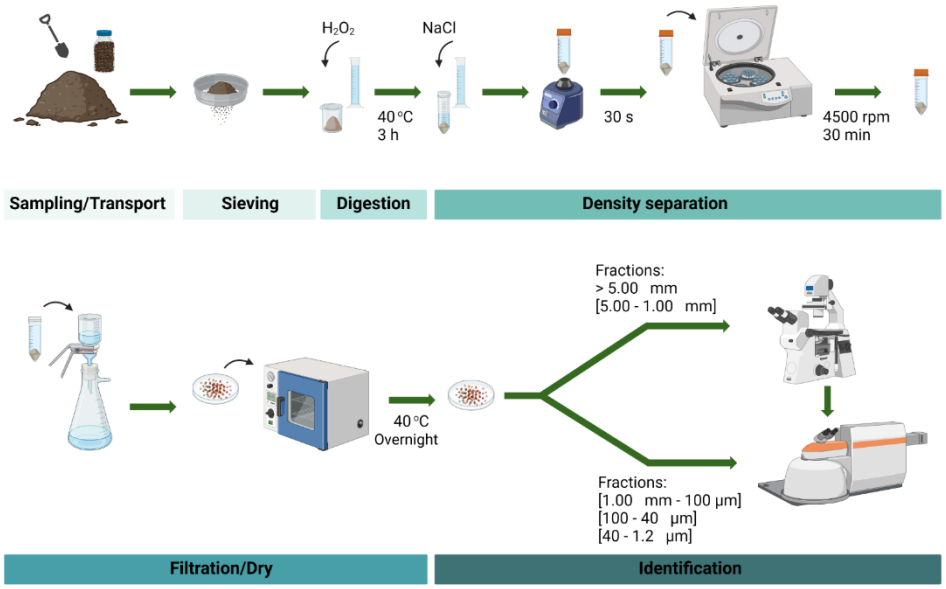


Figure 1. Overview of the experimental steps for microplastic extraction from agricultural soil samples. Created with BioRender.com.

2.5 Application of the extraction procedure on agricultural soil samples

In the application of the extraction procedure to the agricultural soil samples, the five soil samples underwent an initial drying process at 40 °C for 48 hours (Dorau et al., 2023; Thomas et al., 2020). After drying, the samples were sieved using a sieve shaker AS 200 Basic Retsch with a column containing four test sieves (5.00 mm, 1.00 mm, 100 µm, and 40 µm). Each fraction below 5.00 mm then underwent the extraction procedure outlined in section 2.4.1, with replicates conducted for every sub-sample. The resulting filters were collected in Petri dishes and stored for further analysis.

For fractions > 5.00 mm and [5.00-1.00 mm], suspected mesoplastics and MPs were visually inspected using a Nikon Eclipse MA100 inverted microscope at up to 10x magnification. This microscope, manufactured by Nikon Metrology NV, is equipped with a Nikon Digital Sight camera and the NIS-Elements imaging software. For MPs, this pre-screening involved transferring suspects to Petri dishes. Identification criteria included the absence of cellular or organic structures, the presence of fibers displaying uniform thickness and 3-dimensional bending, and particles with consistent and homogeneous color, classified as black-gray, yellow-orange, white-transparent, red-pink, or blue-green, with considerations for instances of bleaching, biofouling, or weathering which could alter appearance. Shapes were further categorized as fiber, primary MPs (pellet, granule), or secondary MPs (fragment, film) (Abbasi et al., 2021; Chandrakanthan et al., 2024). Visually detected suspects of meso- and MPs, along with filters, were then subjected to µ-Raman analysis, using the same operational conditions as described in section 2.4. For filters, a helical pattern was adopted, with ten randomly selected points examined for each filter. The PublicSpectra database, accessible at https://publicspectra.com, was used to conduct polymer identification and matching after pre-processing the spectra. A score of 70% or higher was considered a positive identification, whereas scores between 60% and 70% required user interpretation. Anything below 60% was classified as inconclusive (Markic et al., 2023).

2.6 Evaluation of the greenness of analytical methodology

The sustainability of the method of the method was evaluated using two methodologies: the Analytical Eco-Scale and AGREE (Gałuszka et al., 2012; Pena-Pereira et al., 2020). The Analytical Eco-Scale approach considers an ideal analysis on criteria such as the use of non-hazardous reagents, energy consumption of less than 0.1 kWh per sample, and zero waste production. Each unmet criterion results in point deductions ranging from 5 to 20, depending on the severity of the non-compliance. A score of 100 is assigned to the ideal approach, with penalty points deducted as analytical parameters deviate from this optimal state. Methods scoring above 75 are considered excellent in green analysis, those above 50 are deemed acceptable, and those below 50 are considered inadequate (Gałuszka et al., 2012). On the other hand, the AGREE approach is based on 12 principles for GAC. These principles include reducing solvent use, minimizing waste, and utilizing sustainable reagents. Method scores were determined using the AGREE: Analytical Greenness Calculator, which is available for free at https://mostwiedzy.pl/en/wojciech-wojnowski,174235-1/AGREE (Pena-Pereira et al., 2020). This tool assigns scores from 0 to 1 for each principle, with deductions of up to 0.2 points for each principle that is not met. The average score determining the

greenness level of the method, and a colour scale (red-yellow-green) is used to visually represent how well each principle is reflected in the methodology (Pena-Pereira et al., 2020; Sousa et al., 2023). All 12 GAC principles were considered equally important, so default weights were assigned to each criterion (Pham et al., 2023).

3. Results and Discussion

3.1 Recovery tests of pristine microplastics from certified soils

To assess the efficacy of MP extraction from certified soils, procedure blanks were used to prevent contamination, confirmed by the absence of plastic fragments or fibers in the filters. In terms of material transfer during extraction, analysis indicated a higher yield of extracted material during the initial extraction, with subsequent extractions showing relatively consistent levels (Figure 1S in Supplementary Information). In sandy soil, the extracted masses varied between 0.070 g and 0.033 g, while in Lufa 2.2 soil, they ranged from 0.090 g to 0.040 g, primarily comprising non-plastic substances such as mineral material in sandy soil and mineral and woody material in the case of Lufa 2.2 soil. Although the literature provides limited information on the amount of non-plastic material from soil that passes to the filter during the extraction process, we can still compare our filters with the images provided in some papers (Fadare et al., 2023; Maes et al., 2017).

In an effort to address the difficulty of isolating MPs from environmental samples while minimizing the impact of non-plastic materials, our study used chemical digestion (15% H_2O_2 at 40 °C in a water bath) to reduce OM (Chandrakanthan et al., 2024; Li et al., 2024; Worek et al., 2022), followed by centrifugation (Grause et al., 2022; Phuong et al., 2018; Prosenc et al., 2021) to remove natural mineral particles such as quartz whit a density of 2.6 g cm^{-3} (Piehl et al., 2018). To determine the endpoint of the chemical digestion process, the absence of bubbling and a visible color change in Lufa 2.2 soil, which has a higher OM content of 3.8%, was monitored (Dorau et al., 2023; Papuga et al., 2022). Additionally, sandy soil with an OM content of 0.6% was tested, and no reactivity was observed within the designated timeframe, establishing it as a benchmark for soil environmental samples. Consequently, a reduction in OM content of 53% for Lufa 2.2 and 79% for sandy soil was achieved, reflecting the differences between initial and final measurements.

Hydrogen peroxide is commonly used to eliminate soil OM until no carbon dioxide is released or a light-colored suspension is obtained (Papuga et al., 2022). This reagent breaks down rapidly via disproportionation, with only a small proportion (10%) being converted into hydroxyl radicals. However, its decay is slower in soils with low OM content (Petigara et al., 2002). The treatment with H_2O_2 can modify soil properties by

degrading inorganic compounds and forming new minerals, thus altering the content of Al_2O_3 and Fe_2O_3 and affecting particle size. Despite its potential for altering soil composition, this process may be time-consuming, although heat application can accelerate the reduction in OM (Papuga et al., 2022). Reductions in OM content have been shown to impact pristine MPs, influencing their quantity, size, shape, and chemical composition (Sridhar et al., 2022). Factors such as polymer composition, exposure duration, sample matrix, and applied chemical treatments can significantly influence degradation levels (Hurley et al., 2018; Pfeiffer and Fischer, 2020; Pfohl et al., 2021; Schrank et al., 2022).

Moreover, existing research on weathered MPs emphasizes the importance of avoiding temperatures exceeding 40 °C, as they can adversely affect the physical and structural properties of MPs through processes like glass transition, melting, or degradation (Dorau et al., 2023; Prata et al., 2020; Savino et al., 2022). Therefore, to effectively screen for MPs in soil samples, it is crucial to preserve the synthetic polymers while reducing naturally occurring particles (Enders et al., 2020; Schrank et al., 2022). Given the limited understanding of the effects of digestion processes on weathered MPs, we adopted a conservative approach, drawing inspiration from methods proposed for soil, road dust, sludge, and marine snow (Sujathan et al., 2017; Worek et al., 2022; Zhao et al., 2017). The potential alterations induced by the process on the pristine MPs were examined following the methodology proposed by Enders et al. (2017). No changes in color were observed, but alterations in the µ-Raman spectra were observed for all MPs (Figure 2S in the Supporting Information). Higher peak intensities were observed for PP, PS, and TWP MPs, while LDPE and PA 6 MPs showed higher fluorescence and weaker peaks. For EVA MPs, the results were inconclusive because the fluorescence and noise were already high in the pristine spectrum, which is attributed to the yellow color. Despite these alterations, all polymer types could still be recognized due to their distinct spectral characteristics. Consequently, the disintegration level was classified as L1, indicating initial visually recognizable changes in color and surface morphology (Enders et al., 2017). Therefore, the digestion conditions were maintained.

Recovery tests were conducted to assess the feasibility of the entire process, considering the potential presence of non-plastic materials on the filters, which could complicate MP identification (Mushtak et al., 2024). The results of the recovery tests showed that particles measuring 3-5 mm, composed of PP, PS, and EVA, achieved 100% recovery rates in both soil types in a single extraction, except for Lufa 2.2 spiked with 5% EVA-MPs, which exhibited a slightly lower recovery rate of 91.0%. Repeating the extraction process for this set of MPs was considered unnecessary due to all

recoveries being above 90%. The unrecovered EVA-MPs, identified by their yellow color and size, were easily removed using tweezers, although the purpose of this study was to evaluate the extraction process without additional intervention. Furthermore, during the study, a distinct behavior of EVA was observed, which differed from the typical density reported of 0.9 g cm^{-3}. This was accompanied by a unique movement within the solution. The EVA-MPs used in this study exhibited porosities or irregularities in their structures, which likely resulted from the pellet manufacturing process. This may have contributed to the observed behavior by affecting the density and buoyancy characteristics of the material. In contrast, the PS-MPs and PP-MPs, which were visually identified as nurdles, displayed buoyancy behavior that was more consistent with their reported densities (1.05-1.06 g cm^{-3} for PS and 0.85-0.94 g cm^{-3} for PP (Okoffo et al., 2021)). Figure 2 presents images from the extraction of this MP group.

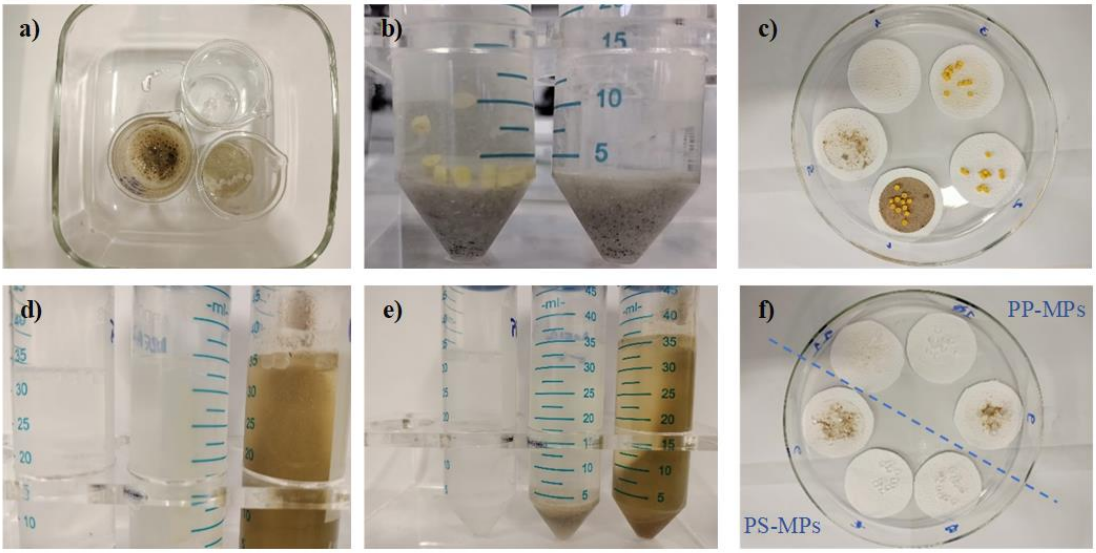


Figure 2. a) Samples prior to digestion, taken 15 minutes before the process; b) EVA-MP after centrifugation; c) EVA-MPs after filtration; d) PS-MPs after centrifugation; e) PP-MPs after centrifugation; f) PS-MPs and PP-MPs after filtration. Photographs captured using an OPPO Reno 8 Lite smartphone.

The recovery rates for particles sized 15-300 µm (including TWP, LDPE, and PA 6) relied on mass rather than the number of particles and are significantly influenced by two key factors: the varying presence of undesired soil material transferred to the filter and the pervasive challenge posed by surface tension. Surface tension causes numerous particles to disperse along the edge of the liquid level and adhere to the glass during static settlement time, resulting in transfer losses (Li et al., 2024). Moreover, Gang Li et al. (2024) observed that fine soil particles persisted with MPs even after extended flotation periods of up to 24 hours, highlighting the difficulty in effectively separating all particles by suspension alone. Consequently, recovery percentages may be misleading,

particularly when considering the visible soil material on filters. Despite these challenges, vibrational spectroscopy confirmed the presence of MPs in all filters. However, multiple extractions were necessary to improve yield, significantly extending analysis times (Table 1). This limitation was also identified by Schrank et al. (2022), who noted that extraction validation based solely on gravimetry might not accurately represent smaller MPs. The Supplementary Information includes photographs of filters from the 5% spiking tests, providing additional insights into particle distribution on the filters to complement the quantitative data from the recovery tests, as well as μ-Raman images of TWP, LDPE, and PA 6 (Figures 3S-6S).

Table 1. Cumulative recovery percentages of TWP, LDPE, and PA 6 in sandy soil and Lufa 2.2 soil at various polymer concentrations.

Polymer	Concentration (% v/v)	Cumulative recovery (%)	
		Sandy soil	Lufa 2.2 soil
TWP (0.86 g cm^{-3})	1	117	87.4
	2	100	103
	5	86.9	112
LDPE (0.91-0.94 g cm^{-3})	1	80.2	127
	2	102	90.1
	5	125	130
PA 6 (1.12-1.14 g cm^{-3})	1	69.3	106
	2	87.9	72.2
	5	123.1	86.2

When evaluating recovery tests with pristine polymers, it is crucial to consider the dissimilarities in their interactions with environmental matrix components, such as soil and water, compared to environmentally aged MPs, which are typically aggregated in the soil matrix (Li et al., 2019). Generally, pristine polymers retain uniform sizes and shapes, while environmental MPs may not behave similarly due to the presence of contaminants, weathering processes, and altered physical and chemical properties. As a result, recovery and identification results may be impacted, leading to an overly optimistic assessment of the effectiveness of the methods used.

3.2 Extraction and identification of MPs in agricultural soil

Five agricultural soil samples, labelled A to E, were screened for the presence of MPs. The examination of the soil samples was enhanced by introducing an additional pre-treatment step involving sieving (Käppler et al., 2016; Watteau et al., 2018). This

refinement in the extraction procedure facilitated the removal of large debris such as wood, plants, and rocks from the soil samples, and it ensured that the MPs were separated into consistent fractions for µ-Raman analysis (Dorau et al., 2023). Despite the Guidance on monitoring of marine litter in European Seas (Käppler et al., 2016) size classes of 5.00-1.00 mm and 1.00 mm-20 µm, the latter was subdivided into 1.00 mm-100 µm, 100-40 µm, and 40-1.2 µm (with the lower limit defined by the filter pore size (Thomas et al., 2020)). Table 2 details the fractions generated during sieving and the methods used to identify suspected particles. Fractions larger than 5.00 mm underwent visual inspection, with suspected mesoplastics collected in Petri dishes for further analysis using photomicroscopy and µ-Raman spectroscopy. The remaining fractions were subjected to the extraction protocol to isolate MPs, resulting in 102 filters. During the extraction process, the mass of material transferred to the filter varied depending on soil texture and between replicas of the same sample. Generally, the quantity of material transferred for filters decreases as the size of the fractions decreases. Furthermore, upon repeated extractions, the filters tended to become progressively cleaner, as observed in the recovery tests (refer to Figure 7S and 8S in Supplementary Information). Additionally, the OM content for each sample was as follows: A = 4.7%, B = 3.7%, C = 2.1%, D = 4.5%, and E = 5.1%.

Table 2. Fractions, soil samples, and methods of polymer identification.

Fractions	**Soil Samples**					**Sorting and Identification of Suspected Polymers**
> 5.00 mm	A	B	C	D	E	Visual sorting of mesoplastics, photomicroscopy using an inverted microscope, µ-Raman spectroscopy
[5.00-1.00 mm]	A	B	C	D	E	Visual sorting of MPs using an inverted microscope, µ-Raman spectroscopy
[1.00 mm-100 µm]	A	B	C	D	E	µ-Raman spectroscopy
[100-40 µm]	A	-	C	D	E	µ-Raman spectroscopy
[40-1.2 µm]	A	-	C	-	E	µ-Raman spectroscopy

Measuring each trapped particle is a time-consuming and labor-intensive process, particularly for larger sample sets including smaller particle sizes (Maes et al., 2017). This process can take several hours to days for spectroscopic measurements on filters with a 47 mm diameter, even with mapping (Xu et al., 2019). Additionally, the entire analytical process, from sample preparation to identification/quantification, can last up to 100 hours for a single environmental sample, making it unfeasible to automate the process for multiple samples (Rhee et al., 2024). The complexity of establishing the required extent of investigation for reproducible and representative results across the

entire filter area adds further challenges. Different approaches are often used to select a subset of the sample, such as randomly selecting a specific area of the filter or using a percentage/number of particles on the filter or mathematical models (Huppertsberg and Knepper, 2020; Li et al., 2024; Nava et al., 2021).

To identify MPs, we used two different approaches. For the [5.00-1.00 mm] fraction, we used optical microscopy to screen ten suspected MPs before conducting µ-Raman analysis. For the remaining fractions (72 filters), we examined ten random points on each filter in a helicoidal pattern, acknowledging the possibility of underestimating the number of MPs. The obtained spectra were pre-processed and compared with PublicSpectra library for identification. We also observed visible and collectable particles in the [1.00 mm-100 µm] range, but from our perspective, using the same screening approach as for the [5.00-1.00 mm] fraction could result in losing smaller particles. Moreover, the [1.00 mm-100 µm] fraction presented topped particles from buoyant OM and minerals, which interfered with identification.

Mesoplastics suspects were identified in samples D and E, obtained from the same soil but collected before and after tillage, respectively. Regarding the identification of these suspects, a variety of mesoplastics exhibiting diverse shapes, hues, and polymer compositions were discovered. Sample D contained three mesoplastics, including 7 films, 1 fragment, and 1 fiber. Sample E showed a higher prevalence of mesoplastics, with a total of 6 particles detected. The identified polymer compositions were predominantly polypropylene (33%) and polyethylene-based (11%), while the remaining 56% could not be conclusively determined. These included a white-transparent fiber, a yellow-orange film, a black-gray fragment, and a white-transparent and yellow-orange film. For further details, please refer to Table 1S and Fig. 9S in the Supplementary Information.

Regarding the analysis of suspects of MPs, a total of 35 black fragments were detected and analyzed across subsamples C ([5.00-1.00 mm], [1.00 mm-100 µm]), D ([1.00 mm-100 µm], [40-1.2 µm]), and E ([5.00-1.00 mm], [40-1.2 µm]). These fragments, varying in quantity among each sample (C=4, D=11, and F=22), showed a correlation with ketjen black when compared via the PublicSpectra library. This observation aligns with the prevalence of carbonaceous materials in nature. However, caution is warranted, as studies suggest that black carbon, commonly used in rubber products and thermoplastics such as tires, may be underestimated in MP counts due to spectral similarities (Lenz et al. 2015; Rødland et al. 2023). This is particularly relevant for samples D and E, which are from a backyard near roads, supporting the expectation of uncovering TWP in these

environments. Additionally, the remaining fragments and fibers were detected in samples C, D, and E, with their presence in samples D and E being predictable due to the presence of mesoplastics in these samples (Table 3).

Table 3. Analysis of microparticles in soil Samples C, D, and E, showing characteristics and polymer compositions, including number of particles, shape, colour, polymer type, and distribution in 5 g of subsamples.

Sample	Fraction	Replica, Extraction	No. particles	Shape	Color	PublicSpectra Identification (score %)
C	[5.00-1.00 mm]	1, 2	1	secondary MP	red-pink	Inconclusive (51.53%, EPDM rubber)
D	[5.00-1.00 mm]	1, 1	1	fiber	white-transparent	Inconclusive (15.17%, acetylsalicylic acid)
E	[5.00-1.00 mm]	1, 1	1	secondary MP	white-transparent	PE-based (95.58%, poly(ethylene-co-1-butene))
		2, 2	2	secondary MP	white-transparent	PE-based (95.58%, poly(ethylene-co-1-butene))
				secondary MP	white-transparent	PE-based (94.32%, poly(ethylene-co-1-butene))
		2, 3	1	secondary MP	white-transparent	Inconclusive
	[40-1.2 µm]	1, 3	1	secondary MP	blue-green	Inconclusive (29.47%, poly(m-phenylene terephthalamide)

The detected MPs were categorized as secondary MPs, constituting approximately 86% of the total particles. White-transparent was the most common color, accounting for approximately 71% of all particles. The most prevalent polymer detected, consistent with recent findings, was PE, attributed to its high global production (Boughattas et al., 2021; Chandrakanthan et al., 2024; Khan et al., 2023). However, 57% of the particles had inconclusive polymer identifications, including a red-pink fragment, a white-transparent fiber, a blue-green fragment, and a white transparent fragment. This complexity emphasizes the challenges of MP analysis in environmental samples and is consistent with previous observations (Chandrakanthan et al., 2024; Kim et al., 2021). In Figure 3, images, and spectra of identified MPs are presented. Images of non-identified MPs can

be consulted in the Supplementary Information (Figure 10S). The images revealed evidence of adherent or trapped soil particulates, consistent with the findings of Abbasi et al. (2021).

Distinguishing polymeric from non-polymeric particles based on spectral data alone requires careful consideration, especially for aged MPs (Huppertsberg and Knepper, 2020). Weathering processes, such as UV radiation, biodegradation, physical abrasion, and chemical oxidation, have the potential to alter the surfaces of MP particles making them unidentifiable using μ-Raman (Chandrakanthan et al., 2024; Dong et al., 2020; Lenz et al., 2015). These differences may result in incorrect identification of specific MPs, as changes in peak intensities and the emergence of new oxidative functional groups due to weathering processes can occur. Various alterations have been reported, including the weakening of stretching vibrations in the 2800–3000 cm^{-1} range and the appearance of a broad, strong band at 2100–2200 cm^{-1} (Dong et al., 2020; Luo et al., 2020; Martinho et al., 2023; Nava et al., 2021). Additionally, the presence of additives like colorants and plasticizers in plastic products can make it challenging to interpret Raman signatures accurately. These substances may emit fluorescence signals, leading to spectral distortion and a lower signal-to-noise ratio in the spectra of MPs (Liu et al., 2023; Nava et al., 2021). Fluorescence emissions can be stronger than Raman scattering, especially for red and yellow-colored MPs (Lenz et al., 2015).

To obtain high-quality spectra from individual particles within a reasonable timeframe, optimizing analysis conditions, such as exposure time and laser power, is crucial to avoid interferences and particle damage (Huppertsberg and Knepper, 2020). In our study, we utilized a 633 nm laser wavelength for Raman spectroscopy measuring different spots on each particle and limiting laser power to 10% to prevent damage and unwanted chemical reactions. Furthermore, separating MPs smaller than 1 mm, particularly buoyant materials such as PE and PP, from complex environmental matrices is a significant challenge (Fadare et al., 2023; Prosenc et al., 2021). Despite proper pretreatment, eliminating all organic material is difficult, and fluorescence can still occur in organic-rich samples (Nava et al., 2021). To mitigate the adverse effects of OM coating that produces overlapping spectral information (Dorau et al., 2023), we employed a digestion method using 15% H_2O_2. This approach aimed to reduce OM interference while preserving the integrity of synthetic polymers, based on the results of recovery tests conducted with pristine polymers. Additionally, H_2O_2 treatment facilitates the degradation of soil OM, but its effectiveness is influenced by various factors such as soil composition and OM content (Papuga et al., 2022).

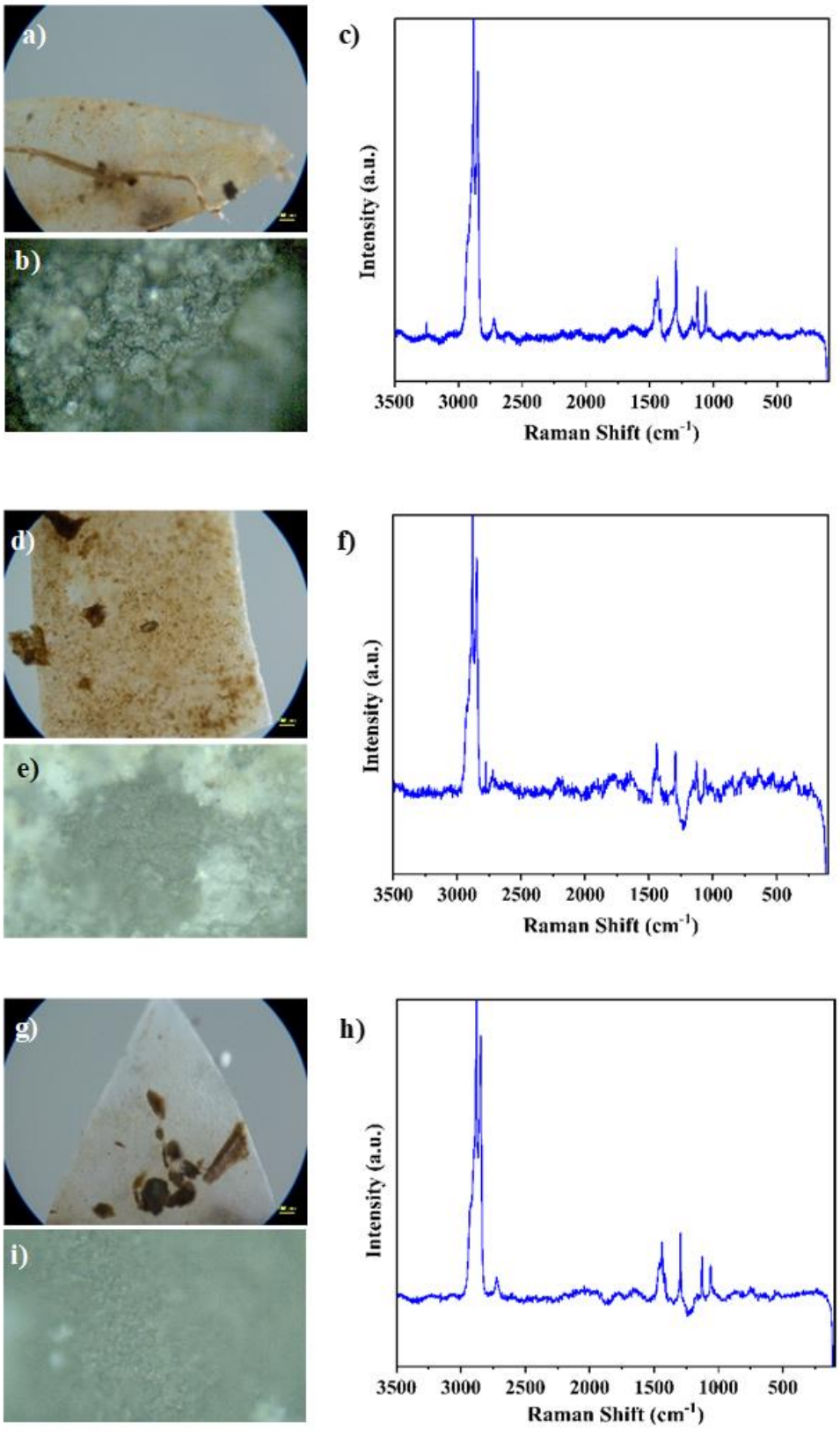


Figure 3. Images and Raman spectra of the MP identified as poly(ethylene-co-1-butene) in sample E. a), b), and c) White-transparent fragment from replica 1, repetition 1 (score 95.58%): microscope image, µ-Raman image, and spectrum, respectively. d), e), and f) White-transparent fragment from replica 2, repetition 2 (score 95.58%): microscope image, µ-Raman image, and spectrum, respectively. g), h), and j) White-transparent fragment from replica 2, repetition 3 (score 94.32%): microscope image, µ-Raman image, and spectrum, respectively.

Comparing abundance data across different regions in soil MP research presents a significant challenge due to variations in protocol approaches. These differences encompass sample size, pre-treatment methodologies, the number and size of fractions, as well as the techniques employed for identification (Boughattas et al., 2021; Grause et al., 2022; Kononov et al., 2022; Prosenc et al., 2021; Rani et al., 2023). For instance, the study conducted by Abbasi et al. (2021) investigated the distribution of MPs in the soil of Kavir and Lut Deserts in Iran. Soil samples weighing 300 g each were treated with $ZnCl_2$ solution to extract MPs. Suspects were visually identified by spectroscopy microscope, characterized by using a μ-Raman spectrometer (laser of 785 nm and a Raman shift of 400−1800 cm^{-1}) and a scanning electron microscope. The results revealed that the distribution of MPs was uneven, with no detected particles in some areas and up to 25 particles per 300 g in others. The most common color of MPs was white-transparent, and over 93% of the identified MPs were fibers, whereas fragments and films comprised the remaining particles. The study also found that the distribution of MPs varied significantly based on size, with more particles present in the finest size fraction (≤ 100 μm) than in the coarsest fraction (≥ 1.00 mm) (Abbasi et al., 2021). In addition, Chandrakanthan et al. (2024) examined soil samples collected from Phoenix, Arizona in 2005 and 2015. Each 60 g sample was treated with NaI solution and analyzed for MP content using μ-Raman spectroscopy (laser of 532 nm and a Raman shift of 50−3800 cm^{-1}). The study revealed variations in the presence of unidentified MPs across sites, with an average of 54% in 2015 and 67% in 2005. Moreover, the analysis identified diverse polymers such as PS, PVC, PA, and PP, but PE emerged as the predominant polymer, constituting 75% of the identified MPs across all sites (Chandrakanthan et al., 2024).

The heterogeneity within soil samples poses a challenge when upscaling from small sample masses, typically in the range of a few grams, to larger quantities such as one kilogram. This discrepancy can lead to the generation of unrealistic values, thereby impairing the comparability of results (Dorau et al., 2023), especially in cases where studies rely only on visual identification for particle number estimation. In our study, we detected the presence of MPs in three samples. Although the most common way to present results in soil analysis is in particles per kilogram, we chose not to do so. This decision was made because it remains unclear whether false negatives result from the absence of MPs in the sample or from inherent limitations in our experimental setup. Premature upscaling of units can lead to biased conclusions.

3.3 Evaluation of the greenness of analytical methodology

The sustainability of the method was evaluated using two methodologies: the Analytical Eco-Scale approach and the AGREE analysis method. In the Analytical Eco-Scale assessment, the method received a score of 82, classifying it as an excellent green analysis. This high score is likely attributed to the minimization of materials, such as the reduced amount of sample (5 g), volumes of H_2O_2 (10 mL) and NaCl (75 mL), resulting in approximately 100 mL of waste per sample collected for proper treatment. Additionally, the energy consumption was established as ≤0.1 kWh per sample based on the energy consumed by the µ-Raman spectrometer.

The results obtained with AGREE coincide with those obtained using the Analytical Eco-Scale. In the AGREE analysis, the method received a score of 0.66, indicating that it can be considered to have green performance. The lowest scores were assigned to principles 3 and 4, followed by principles 1, 8, and 10, respectively. Principles 3 and 4 concern offline sampling and analytical device positioning, respectively, while principle 8 is related to the number of analytes that can be determined in a single run. We set this value to six, corresponding to the polymers used in the recovery test. However, any polymer with a density lower than 1.2 g cm^{-3} is a potential target for analysis. Principle 10 pertains to the use of bio-based reagents. The remaining principles scored higher than 0.8, and are depicted in green, indicating that the method was miniaturized and required a small sample size, semi-automatic sample preparation, no derivatization step, moderate waste generation, and minimal involvement of toxic reagents. These evaluation results are presented in Fig. 4.

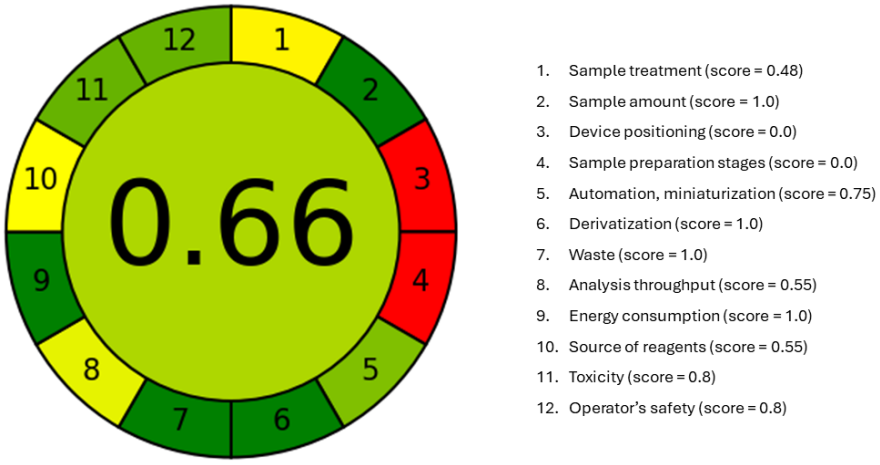


Figure 4. Results of AGREE analysis for the method. Scores range from 0.0 (red) to 1.0 (dark green), with higher scores indicating more desirable outcomes. The score for each principle is provided in parentheses.

An extensive assessment of the techniques applied to soil samples utilizing AGREE resulted in scores spanning from 0.29 to 0.8 (Pham et al., 2023). This variability may be because the determination of MPs in environmental samples is relatively recent, many methods are still in their initial stages, and there is a recognized global lack of harmonization. Numerous problems in efficiency and implementation are yet to be solved, showing that greenness is still a pending subject in the analysis of MPs (Picó and Barceló, 2021). At least two studies (Pham et al., 2023; Picó and Barceló, 2021) have shown that chemical oxidation and/or density separation methods are the least sustainable methods for isolating MPs. Moreover, while microscopy and spectroscopy methods are considered green due to their low energy usage (<0.1 kWh per sample), they often require extensive pretreatment to remove interfering organic and biological materials, thus lowering the method's overall sustainability. Therefore, in our assessment, it was more accurate to consider the total energy consumption of each sample.

4. Comments and possible variations of the method

Polymer Standardization: As it is not feasible to conduct recovery tests with all polymers, we suggest adopting a standardized set of polymers based on their ubiquitous distribution in the soil. PET, PS, PVC, PP, and PS, referred to as the "common five" suggested by Dorau et al. (2023), could be used to perform recovery tests. This could facilitate performance comparisons across methods and promote greater harmonization.

Pre-treatment and Extraction: To further refine the MP separation process, we propose adding a mesh with 500 µm openings to effectively subdivide the smaller fraction and minimize the presence of interferents. Additionally, optimizing the method by reducing the OM content should be considered while ensuring the integrity of weathered MPs (Savino et al., 2022) in each soil sample and the feasibility of the process. While NaCl solution (1.2 g cm^{-3}) is commonly used for extraction due to its cost-effectiveness and non-toxic properties (Bellasi et al., 2021), it may lead to underestimation of denser and widespread MPs such as PVC. This is particularly significant given the wide range of polymer densities, spanning from 0.9 to 1.6 g cm^{-3} (Enders et al., 2020; Picó and Barceló, 2021) for approximately 5800 polymers. Nonetheless, it remains applicable in studies with limited resources and poor waste treatment procedures. An alternative, non-toxic option is $KHCO_3$ solution (1.4 g cm^{-3}) (Mushtak et al., 2024; Picó and Barceló, 2021). However, with the goal of reducing the number of filters and optimizing the extraction of MPs, it would be beneficial to invest in a sequential extraction method using different salt solutions. This requires additional investigation in our future studies. Moreover,

introducing GAC Principles in the method design is essential in a rapidly evolving field with a lack of harmonization. The implementation of GAC metrics is crucial to evaluate the greenness of the method (Picó and Barceló, 2022).

Detection: Micro-Raman spectroscopy is considered a green technique and is a useful tool for contamination surveys, providing information on MP size, color, shape, composition, and degradation level. Bench-top µ-Raman spectrometers can be operated by non-experts to analyze chemical data using advanced spectral library software. However, the absence of libraries for weathered MPs makes identification challenging, and results in high rates of inconclusive outcomes. Mapping analysis also presents difficulties owing to reduced peak intensities in weathered MPs, requiring careful peak selection for integration (Lenz et al., 2015). Despite these challenges, promising techniques such as Coherent Anti-Stokes Raman Scattering (CARS) microspectroscopy require minimal sample preparation and may overcome degradation issues associated with chemical digestion (Sobhani et al., 2019). Another prominent approach is scanning electron microscope (SEM) combined with surface-enhanced Raman spectroscopy (SERS), which improves the precision of identifying and analyzing small-sized MPs in soil (Li et al., 2024). Additionally, our extraction method can be combined with other environmentally friendly detection techniques like fluorescence microscopy, µ-FTIR, FTIR imaging and Raman imaging. However, further investigation is needed in future studies to explore these possibilities fully.

Conclusion

This study aimed to address the challenge of quantifying MPs in soil, incorporating GAC principles such as reducing sample quantities, reagents, and waste. MP extraction efficacy was evaluated through recovery tests using certified soils spiked with pristine MPs of two size categories: 3-5 mm and 15-300 µm. Hydrogen peroxide was used to reduce OM, followed by centrifugation to remove natural mineral particles. The method excelled in extracting larger MPs, with 100% recovery for PP, PS, and EVA particles, except for 91% recovery for 5% EVA-MPs in Lufa 2.2 soil. Repeated extractions enhanced recovery efficiency for smaller MPs. Despite effective OM removal, slight alterations in the Raman spectra of pristine MPs were noted. In agricultural soils, nine mesoplastics were identified, consisting of three PP, one PE, and seven additional MPs, with three of them identified as PE and the remainder inconclusive, including two fibers. The greenness of the method was evaluated using Analytical Eco-Scale and AGREE metrics, which highlighted its sustainability. Challenges in transitioning to environmental

sample analysis include altered interactions between MPs and soil particles, non-polymeric material interference on filters, and differing spectral fingerprints of weathered MPs. Future research should focus on developing digestion methods for aged and environmental MPs exploring density separation approaches and creating a library for weathered MPs. This pioneering study in Portugal sheds light on MP pollution in agricultural soils, urging further investigation for effective monitoring strategies, enabling robust actions to combat plastic pollution.

Funding

Diana Rede acknowledges the Fundação para a Ciência e Tecnologia/Ministério da Ciência, Tecnologia e Ensino Superior (FCT/MCTES) and the European Social Fund (ESF) through NORTE 2020 (Programa Operacional Região Norte) for her PhD grant reference SFRH/BD/147404/2019. This work also received financial support from FCT/MCTES through project MTS/SAS/0077/2020 titled "Honey+: New reasons to care for honey from the Natural Park of Montesinho: A bioindicator of environmental quality & its therapeutic potential.

Acknowledgments

The authors acknowledge the financial support from national funds of Portugal, specifically provided by the FCT/MCTES, through projects UIDB/50006/2020, UIDP/50006/2020, and LA/P/0008/2020. They also express appreciation to the FCT for funding the PLASTOXIC project (2022.15094.CBM) and project number 49190WH (PHC PESSOA 2023), which facilitated bilateral cooperation between Portugal and France under the 2023–2024 person program.

Author contributions

Diana Rede contributed to conceptualization, methodology development, and sample analysis, and was involved in the writing of the original draft as well as the review and editing stages. Rui Vilarinho and Joaquim Agostinho Moreira provided access to micro-Raman spectrometer and training on its use. Luca Nizzetto contributed to resources and investigation. Cristina Delerue-Matos provided supervision, managed resources, review and acquired funding. Virgínia Cruz Fernandes provided supervision, contributed to conceptualization and methodology development, participated in the review and editing stages of the writing process. All authors read and approved the final manuscript.

References

Abbasi, S., Turner, A., Hoseini, M., Amiri, H., 2021. Microplastics in the Lut and Kavir Deserts, Iran. Environ. Sci. Technol. 55, 5993–6000.

https://doi.org/10.1021/acs.est.1c00615

Araujo, C.F., Nolasco, M.M., Ribeiro, A.M.P., Ribeiro-Claro, P.J.A., 2018. Identification of microplastics using Raman spectroscopy: Latest developments and future prospects. Water Res. 142, 426–440. https://doi.org/10.1016/J.WATRES.2018.05.060

Bellasi, A., Binda, G., Pozzi, A., Boldrocchi, G., Bettinetti, R., 2021. The extraction of microplastics from sediments: An overview of existing methods and the proposal of a new and green alternative. Chemosphere 278, 130357. https://doi.org/10.1016/j.chemosphere.2021.130357

Boughattas, I., Hattab, S., Zitouni, N., Mkhinini, M., Missawi, O., 2021. Assessing the presence of microplastic particles in Tunisian agriculture soils and their potential toxicity effects using Eisenia andrei as bioindicator. Sci. Total Environ. 796, 148959. https://doi.org/10.1016/j.scitotenv.2021.148959

Braun, M., Mail, M., Heyse, R., Amelung, W., 2021. Plastic in compost: Prevalence and potential input into agricultural and horticultural soils. Sci. Total Environ. 760, 143335. https://doi.org/10.1016/j.scitotenv.2020.143335

Chandrakanthan, K., Fraser, M.P., Herckes, P., 2024. Microplastics are ubiquitous and increasing in soil of a sprawling urban area, Phoenix (Arizona). Sci. Total Environ. 906, 167617. https://doi.org/10.1016/j.scitotenv.2023.167617

Coppock, R.L., Cole, M., Lindeque, P.K., Queirós, A.M., Galloway, T.S., 2017. A small-scale, portable method for extracting microplastics from marine sediments. Environ. Pollut. 230, 829–837. https://doi.org/10.1016/j.envpol.2017.07.017

Corradini, F., Casado, F., Leiva, V., Huerta-Lwanga, E., Geissen, V., 2021. Microplastics occurrence and frequency in soils under different land uses on a regional scale. Sci. Total Environ. 752, 141917. https://doi.org/10.1016/j.scitotenv.2020.141917

Dong, M., Zhang, Q., Xing, X., Chen, W., She, Z., Luo, Z., 2020. Raman spectra and surface changes of microplastics weathered under natural environments. Sci. Total Environ. 739, 139990. https://doi.org/10.1016/j.scitotenv.2020.139990

Dong, Y., Gao, M., Song, Z., Qiu, W., 2020. Microplastic particles increase arsenic toxicity to rice seedlings. Environ. Pollut. 259, 113892. https://doi.org/10.1016/j.envpol.2019.113892

Dorau, K., Hoppe, M., Rückamp, D., Köser, J., Scheeder, G., Scholz, K., 2023. Status quo of operation procedures for soil sampling to analyze microplastics. Microplastics and Nanoplastics. https://doi.org/10.1186/s43591-023-00063-5

EL Hayany, B., EL Fels, L., Quénéa, K., Dignac, M.F., Rumpel, C., Gupta, V.K., Hafidi, M., 2020. Microplastics from lagooning sludge to composts as revealed by fluorescent staining- image analysis, Raman spectroscopy and pyrolysis-GC/MS. J.

Environ. Manage. 275. https://doi.org/10.1016/j.jenvman.2020.111249

Enders, K., Lenz, R., Beer, S., Stedmon, C.A., 2017. Extraction of microplastic from biota: Recommended acidic digestion destroys common plastic polymers. ICES J. Mar. Sci. 74, 326–331. https://doi.org/10.1093/icesjms/fsw173

Enders, K., Lenz, R., Ivar do Sul, J.A., Tagg, A.S., Labrenz, M., 2020. When every particle matters: A QuEChERS approach to extract microplastics from environmental samples. MethodsX 7, 100784. https://doi.org/10.1016/j.mex.2020.100784

Fadare, O.O., Martin, L., Lascelles, N., Myers, J.T., Kaiser, K., Xu, W., Conkle, J.L., 2023. Binary solvent extraction of microplastics from a complex environmental matrix. Limnol. Oceanogr. Methods 21, 414–420. https://doi.org/10.1002/lom3.10554

Gałuszka, A., Konieczka, P., Migaszewski, Z.M., 2012. Analytical Eco-Scale for assessing the greenness of analytical procedures 37, 61–72. https://doi.org/10.1016/j.trac.2012.03.013

Gałuszka, A., Migaszewski, Z., Jacek Namiesnik, 2013. The 12 principles of green analytical chemistry and the SIGNIFICANCE mnemonic of green analytical practices. Trends Anal. Chem. 50, 78–84. https://doi.org/10.1016/j.trac.2013.04.010

Grause, G., Kuniyasu, Y., Chien, M., Inoue, C., 2022. Separation of microplastic from soil by centrifugation and its application to agricultural soil. Chemosphere 288, 132654. https://doi.org/10.1016/j.chemosphere.2021.132654

Harley-Nyang, D., Memon, F.A., Jones, N., Galloway, T., 2022. Investigation and analysis of microplastics in sewage sludge and biosolids: A case study from one wastewater treatment works in the UK. Sci. Total Environ. 823, 153735. https://doi.org/10.1016/j.scitotenv.2022.153735

Henseler, M., Brandes, E., Kreins, P., 2019. Microplastics in agricultural soils: a new challenge not only for agro-environmental policy?, in: 172nd EAAE Seminar ‘Agricultural Policy for the Environment or Environmental Policy for Agriculture?‘. pp. 1–16.

Horton, A.A., Walton, A., Spurgeon, D.J., Lahive, E., Svendsen, C., 2017. Microplastics in freshwater and terrestrial environments: Evaluating the current understanding to identify the knowledge gaps and future research priorities. Sci. Total Environ. 586, 127–141. https://doi.org/10.1016/j.scitotenv.2017.01.190

Huppertsberg, S., Knepper, T.P.P., 2020. Validation of an FT-IR microscopy method for the determination of microplastic particles in surface waters. MethodsX 7, 100874. https://doi.org/10.1016/j.mex.2020.100874

Hurley, R.R., Lusher, A.L., Olsen, M., Nizzetto, L., 2018. Validation of a Method for Extracting Microplastics from Complex, Organic-Rich, Environmental Matrices. Environ. Sci. Technol. 52, 7409–7417. https://doi.org/10.1021/acs.est.8b01517

Käppler, A., Fischer, D., Oberbeckmann, S., Schernewski, G., Labrenz, M., Eichhorn, K.J., Voit, B., 2016. Analysis of environmental microplastics by vibrational microspectroscopy: FTIR, Raman or both? Anal. Bioanal. Chem. 408, 8377–8391. https://doi.org/10.1007/s00216-016-9956-3

Khan, M.A., Huang, Q., Khan, S., Wang, Q., Huang, J., 2023. Abundance , spatial distribution , and characteristics of microplastics in agricultural soils and their relationship with contributing factors 328. https://doi.org/10.1016/j.jenvman.2022.117006

Kim, S.K., Kim, J.S., Lee, H., Lee, H.J., 2021. Abundance and characteristics of microplastics in soils with different agricultural practices: Importance of sources with internal origin and environmental fate. J. Hazard. Mater. 403, 123997. https://doi.org/10.1016/j.jhazmat.2020.123997

Kononov, A., Hishida, M., Suzuki, K., Harada, N., 2022. Microplastic Extraction from Agricultural Soils Using Canola Oil and Unsaturated Sodium Chloride Solution and Evaluation by Incineration Method. Soil Syst. 6, 1–11. https://doi.org/https://doi.org/10.3390/soilsystems6020054

Lenz, R., Enders, K., Stedmon, C.A., Mackenzie, D.M.A., Gissel, T., 2015. A critical assessment of visual identi fi cation of marine microplastic using Raman spectroscopy for analysis improvement. Mar. Pollut. Bull. 100, 82–91. https://doi.org/10.1016/j.marpolbul.2015.09.026

Li, G., Pei, Z., Li, Y., Yang, R., Wang, P., Liang, Y., 2024. A high-precision , effective method for extraction and identification of small-sized microplastics from soil. Talanta 272, 125802. https://doi.org/10.1016/j.talanta.2024.125802

Li, Q., Wu, J., Zhao, X., Gu, X., Ji, R., 2019. Separation and identification of microplastics from soil and sewage sludge. Environ. Pollut. 254, 113076. https://doi.org/10.1016/j.envpol.2019.113076

Li, Q., Zeng, A., Jiang, X., Gu, X., 2021. Are microplastics correlated to phthalates in facility agriculture soil? J. Hazard. Mater. 412, 125164. https://doi.org/10.1016/j.jhazmat.2021.125164

Liu, Y., Hu, J., Lin, L., Yang, B., Huang, M., Chang, M., Huang, X., Dai, Z., 2023. Overcoming the fl uorescent interference during Raman spectroscopy detection of microplastics. Sci. Total Environ. 897, 165333. https://doi.org/10.1016/j.scitotenv.2023.165333

Maes, T., Jessop, R., Wellner, N., Haupt, K., Mayes, A.G., 2017. A rapid-screening

approach to detect and quantify microplastics based on fluorescent tagging with Nile Red 1–10. https://doi.org/10.1038/srep44501

Markic, A., Bridson, J.H., Morton, P., Hersey, L., Budi, A., Maes, T., Bowen, M., 2023. Microplastic pollution in the intertidal and subtidal sediments of Vava ' u , Tonga 186. https://doi.org/10.1016/j.marpolbul.2022.114451

Martinho, S.D., Fernandes, C., Figueiredo, S.A., Vilarinho, R., 2023. Laboratory Studies about Microplastic Aging and Its Effects on the Adsorption of Chlorpyrifos. Polymers (Basel). 15, 1–21. https://doi.org/https://doi.org/10.3390/polym15163468

Mushtak, F., Prakash, J., Singh, S., 2024. Micro and Nano Engineering Microplastics in complex soil matrix : Recovery , identification and removal using micro nano techniques. Micro Nano Eng. 22, 100237. https://doi.org/10.1016/j.mne.2023.100237

Nakajima, R., Lindsay, D.J., Tsuchiya, M., Matsui, R., Kitahashi, T., Fujikura, K., Fukushima, T., 2019. A small, stainless-steel sieve optimized for laboratory beaker-based extraction of microplastics from environmental samples. MethodsX 6, 1677–1682. https://doi.org/10.1016/j.mex.2019.07.012

Nava, V., Frezzotti, M.L., Leoni, B., 2021. Raman Spectroscopy for the Analysis of Microplastics in Aquatic Systems 75. https://doi.org/10.1177/00037028211043119

Niu, J., Gao, B., Wu, W., Peng, W., Xu, D., 2022. Occurrence, stability and source identification of small size microplastics in the Jiayan reservoir, China. Sci. Total Environ. 807, 150832. https://doi.org/10.1016/j.scitotenv.2021.150832

Nuelle, M.-T., Dekiff, J.H., Remy, D., Fries, E., 2014. A new analytical approach for monitoring microplastics in marine sediments. Environ. Pollut. 184, 161–169. https://doi.org/10.1016/j.envpol.2013.07.027

Okoffo, E.D., O'Brien, S., Ribeiro, F., Burrows, S.D., Toapanta, T., Rauert, C., O'Brien, J.W., Tscharke, B.J., Wang, X., Thomas, K. V., 2021. Plastic particles in soil: State of the knowledge on sources, occurrence and distribution, analytical methods and ecological impacts. Environ. Sci. Process. Impacts 23, 240–274. https://doi.org/10.1039/d0em00312c

Papuga, K., Kaszubkiewicz, J., Kawałko, D., Kreimeyer, M., 2022. Effect of Organic Matter Removal by Hydrogen Peroxide on the Determination of Soil Particle Size Distribution Using the Dynamometer Method. Agriculture 12, 2–14. https://doi.org/https://doi.org/10.3390/agriculture12020226

Pena-Pereira, F., Wojnowski, W., Tobiszewski, M., 2020. AGREE—Analytical GREEnness Metric Approach and Software. Anal. Chem. 92, 10076–10082. https://doi.org/10.1021/acs.analchem.0c01887

Petigara, B.R., Blough, N. V., Mignery, A.C., 2002. Mechanisms of Hydrogen Peroxide

Decomposition in Soils. Environ. Sci. Technol. 36, 639–645.

Pfeiffer, F., Fischer, E.K., 2020. Various Digestion Protocols Within Microplastic Sample Processing — Evaluating the Resistance of Different Synthetic Polymers and the Efficiency of Biogenic Organic Matter Destruction 8, 1–9. https://doi.org/10.3389/fenvs.2020.572424

Pfohl, P., Roth, C., Meyer, L., Heinemeyer, U., Gruendling, T., Lang, C., Nestle, N., Hofmann, T., Wohlleben, W., Jessl, S., 2021. Microplastic extraction protocols can impact the polymer structure. Microplastics and Nanoplastics 1, 1–13. https://doi.org/https://doi.org/10.1186/s43591-021-00009-9

Pham, D.T., Park, H.J., Mohamed, D.F.M.S., Kim, P.G., Tarafdar, A., Kwon, J.H., 2023. Greenness of analytical methods for isolation and identification of microplastics in environmental and food samples - A critical review. TrAC - Trends Anal. Chem. 167, 117263. https://doi.org/10.1016/j.trac.2023.117263

Phuong, N.N., Poirier, L., Lagarde, F., Kamari, A., Zalouk-Vergnoux, A., 2018. Microplastic abundance and characteristics in French Atlantic coastal sediments using a new extraction method. Environ. Pollut. 243, 228–237. https://doi.org/10.1016/j.envpol.2018.08.032

Picó, Y., Barceló, D., 2022. Micro(Nano)plastic analysis: a green and sustainable perspective. J. Hazard. Mater. Adv. 6. https://doi.org/10.1016/j.hazadv.2022.100058

Picó, Y., Barceló, D., 2021. Analysis of microplastics and nanoplastics: How green are the methodologies used? Curr. Opin. Green Sustain. Chem. 31, 100503. https://doi.org/10.1016/j.cogsc.2021.100503

Piehl, S., Leibner, A., Löder, M.G.J., Dris, R., Bogner, C., Laforsch, C., 2018. Identification and quantification of macro- and microplastics on an agricultural farmland. Sci. Rep. 8, 17950. https://doi.org/10.1038/s41598-018-36172-y

Prata, J.C., Reis, V., Paço, A., Martins, P., Cruz, A., Costa, J.P., Duarte, A.C., Rocha-santos, T., 2020. Effects of spatial and seasonal factors on the characteristics and carbonyl index of (micro) plastics in a sandy beach in Aveiro , Portugal. Sci. Total Environ. 709, 135892. https://doi.org/10.1016/j.scitotenv.2019.135892

Prosenc, F., Leban, P., Šunta, U., 2021. Extraction and Identification of a Wide Range of Microplastic Polymers in Soil and Compost. Polymers (Basel). 13, 2–16. https://doi.org/https://doi.org/10.3390/ polym13234069

Radford, F., Zapata-Restrepo, L.M., Horton, A.A., Hudson, M.D., Shaw, P.J., Williams, I.D., 2021. Developing a systematic method for extraction of microplastics in soils. Anal. Methods 13, 1695–1705. https://doi.org/10.1039/d0ay02086a

Rani, M., Ducoli, S., Depero, L.E., Prica, M., Tubi´c, A., Ademovic, Z., Morrison, L.,

Federici, S., 2023. Complex Environmental Matrices. Molecules 28, 1–37. https://doi.org/https://doi.org/10.3390/molecules28155710

Rede, D., Delerue-Matos, C., Fernandes, V.C., 2023a. The Microplastics Iceberg: Filling Gaps in Our Understanding. Polymers (Basel). 15, 1–28. https://doi.org/10.3390/polym15163356

Rede, D., Teixeira, I., Delerue, C., Virgínia, M., Fernandes, C., 2023b. Assessing emerging and priority micropollutants in sewage sludge : environmental insights and analytical approaches. Environ. Sci. Pollut. Res. https://doi.org/10.1007/s11356-023-30963-1

Rede, D., Vilarinho, R., Moreira, J.A., Delerue-Matos, C., Fernandes, V.C., 2024. Investigating the impact of microplastics on triphenyl phosphate adsorption in soil: Insights into environmental factors and soil properties. Sci. Total Environ. 944, 173745. https://doi.org/10.1016/j.scitotenv.2024.173745

Rhee, H., Jeong, S., Lee, H., Gyu, M., Sik, D., 2024. Rapid detection and identification of microplastics from nonchemically treated soil with CARS microspectroscopy ☆. Environ. Pollut. 342, 123080. https://doi.org/10.1016/j.envpol.2023.123080

Sajid, M., Justyna, P., 2022. Green analytical chemistry metrics : A review. Talanta 238. https://doi.org/10.1016/j.talanta.2021.123046

Savino, I., Campanale, C., Trotti, P., Massarelli, C., Corriero, G., Uricchio, V.F., 2022. Effects and Impacts of Different Oxidative Digestion Treatments on Virgin and Aged Microplastic Particles. Polymers (Basel). 14, 1–21. https://doi.org/https://doi.org/10.3390/ polym14101958

Schrank, I., Möller, J.N., Imhof, H.K., Hauenstein, O., Zielke, F., Agarwal, S., Löder, M.G.J., Greiner, A., Laforsch, C., 2022. Microplastic sample puri fi cation methods - Assessing detrimental effects of puri fi cation procedures on speci fi c plastic types. Sci. Total Environ. 833. https://doi.org/10.1016/j.scitotenv.2022.154824

Selonen, S., Dolar, A., Jemec Kokalj, A., Sackey, L.N.A., Skalar, T., Cruz Fernandes, V., Rede, D., Delerue-Matos, C., Hurley, R., Nizzetto, L., van Gestel, C.A.M., 2021. Exploring the impacts of microplastics and associated chemicals in the terrestrial environment – Exposure of soil invertebrates to tire particles. Environ. Res. 201, 111495. https://doi.org/10.1016/j.envres.2021.111495

Shafea, L., Felde, V.J.M.N.L., Woche, S.K., Bachmann, J., Peth, S., 2023. Microplastics effects on wettability, pore sizes and saturated hydraulic conductivity of a loess topsoil. Geoderma 437. https://doi.org/10.1016/j.geoderma.2023.116566

Sobhani, Z., Amin, A., Naidu, R., Megharaj, M., Fang, C., 2019. Analytica Chimica Acta Identi fi cation and visualisation of microplastics by Raman mapping 1077, 191–199. https://doi.org/10.1016/j.aca.2019.05.021

Sousa, S., Paíga, P., Pestana, D., Faria, G., Delerue-Matos, C., Ramalhosa, M.J., Calhau, C., Domingues, V.F., 2023. Optimization of a simple, effective, and greener methodology for polycyclic aromatic hydrocarbon extraction from human adipose tissue. Anal. Methods 15, 1722–1733. https://doi.org/10.1039/d2ay02075k

Sridhar, A., Kannan, D., Kapoor, A., Prabhakar, S., 2022. Chemosphere Extraction and detection methods of microplastics in food and marine systems : A critical review MS. Chemosphere 286, 131653. https://doi.org/10.1016/j.chemosphere.2021.131653

Sujathan, S., Kniggendorf, A.K., Kumar, A., Roth, B., Rosenwinkel, K.H., Nogueira, R., 2017. Heat and Bleach: A Cost-Efficient Method for Extracting Microplastics from Return Activated Sludge. Arch. Environ. Contam. Toxicol. 73, 641–648. https://doi.org/10.1007/s00244-017-0415-8

Thomas, D., Schütze, B., Heinze, W.M., Steinmetz, Z., 2020. Sample preparation techniques for the analysis of microplastics in soil—a review. Sustain. 12, 1–28. https://doi.org/10.3390/su12219074

Vermeiren, P., Muñoz, C., Ikejima, K., 2020. Microplastic identification and quantification from organic rich sediments: A validated laboratory protocol. Environ. Pollut. 262. https://doi.org/10.1016/j.envpol.2020.114298

Watteau, F., Dignac, M.F., Bouchard, A., Revallier, A., Houot, S., 2018. Microplastic Detection in Soil Amended With Municipal Solid Waste Composts as Revealed by Transmission Electronic Microscopy and Pyrolysis/GC/MS. Front. Sustain. Food Syst. 2. https://doi.org/10.3389/fsufs.2018.00081

Worek, J., Badura, X., Białas, A., Chwiej, J., Kawoń, K., Styszko, K., 2022. Pollution from Transport: Detection of Tyre Particles in Environmental Samples. Energies 15, 1–15. https://doi.org/10.3390/en15082816

Xu, J., Thomas, K. V, Luo, Z., Gowen, A.A., 2019. Raman imaging for microplastics analysis : State of the art , challenges and prospects. Trends Anal. Chem. 119, 115629. https://doi.org/10.1016/j.trac.2019.115629

Zhang, Q., Liu, L., Jiang, Y., Zhang, Y., Fan, Y., Rao, W., Qian, X., 2023. Microplastics in infant milk powder. Environ. Pollut. 323, 121225. https://doi.org/10.1016/j.envpol.2023.121225

Zhao, S., Danley, M., Ward, J.E., Mincer, T.J., 2017. An approach for extraction, characterization and quantitation of microplastic in natural marine snow using Raman microscopy. Anal. Methods 9, 1470–1478. https://doi.org/10.1039/C6AY02302A

Supporting Information

Screening for Microplastics in Agricultural Soils: Applying Green Chemistry Principles in Extraction and Analysis

Diana Rede[1,2], Rui Vilarinho[3,4], Joaquim Agostinho Moreira[3,4], Luca Nizzetto[5,6], Cristina Delerue-Matos[1], Virgínia Cruz Fernandes[1]*

[1]REQUIMTE/LAQV, Instituto Superior de Engenharia do Porto, Instituto Politécnico do Porto, Rua Dr. António Bernardino de Almeida 431, 4249-015 Porto, Portugal

[2]Departamento de Química e Bioquímica, Faculdade de Ciências, Universidade do Porto, Rua do Campo Alegre s/n, 4169– 007 Porto, Portugal

[3]Departamento de Física e Astronomia, Faculdade de Ciências, Universidade do Porto, Rua do Campo Alegre s/n, 4169– 007 Porto, Portugal

[4]IFIMUP—Instituto de Física dos Materiais Avançados, Nanotecnologia e Fotónica, Faculdade de Ciências, Universidade do Porto, Rua do Campo Alegre s/n, 4169– 007 Porto, Portugal

[5]Norwegian Institute for Water Research (NIVA), Gaustadelléen 21, 0349, Oslo, Norway

[6]Research Centre for Toxic Compounds in the Environment (RECETOX), Faculty of Science, Masarik University, Kamenice 753/5, 625 00, Brno, Czech Republic

*vir@isep.ipp.pt

S.1 Materials and Methods

S.1.1 Determination of soil organic matter content

Soil organic matter (OM) was assessed using the Loss-on-Ignition method described by Al-Selwi and Joshi (2015). Approximately 10 g of each certified soil sample was oven-dried overnight at 105 °C to remove water content. Then, 5 g of each sample underwent heating in a muffle furnace at 550 °C for 4 hours (Al-Selwi and Joshi 2015). Agricultural soil samples were initially sieved to a particle size of 5 mm. Subsequently, they were crushed using a mortar, following the same procedure as for the certified soil samples. The OM content was calculated using the equation:

$$OM\ (\%) = \frac{dry\ weight_{105} - dry\ weight_{505}}{dry\ weight_{105}} \times 100 \qquad \text{Eq. 1S}$$

S.2 Results

S.2.1 Recovery tests of pristine microplastics from certified soils

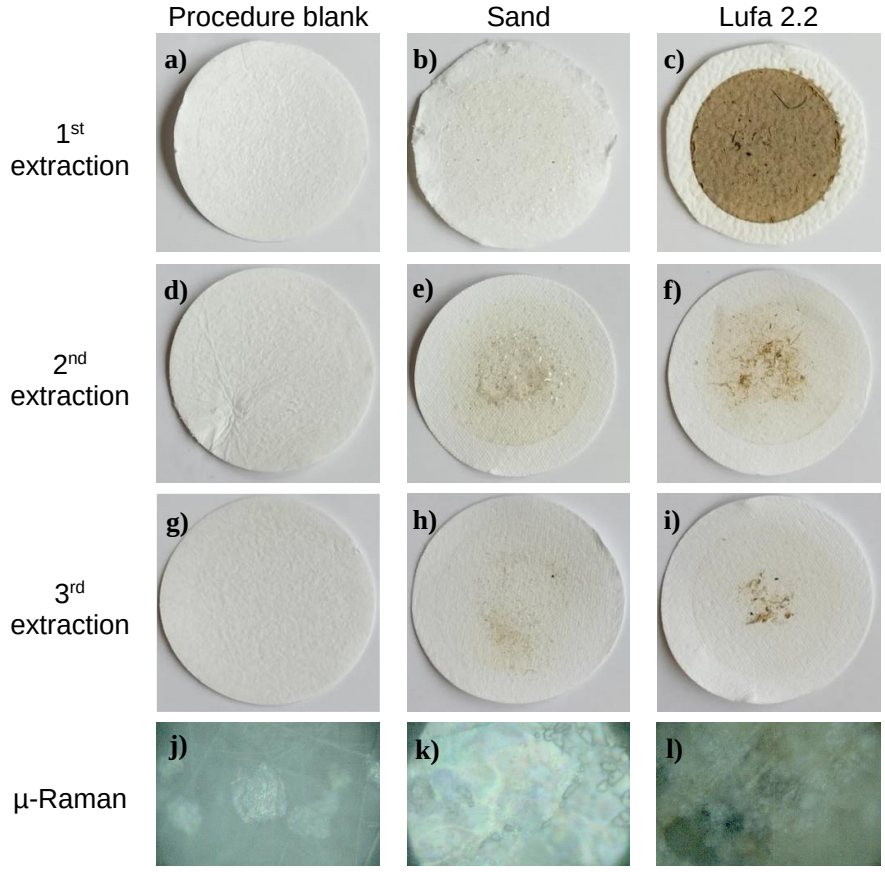


Figure 1S. a-i) Images of the filters obtained in three extractions for procedure blank, sandy soil, and Lufa 2.2 soil captured using an OPPO Reno8 Lite smartphone; j-l) µ-Raman images for blank, sandy soil, and Lufa 2.2 soil captured using a Leica DM2700 microscope with a 50x objective.

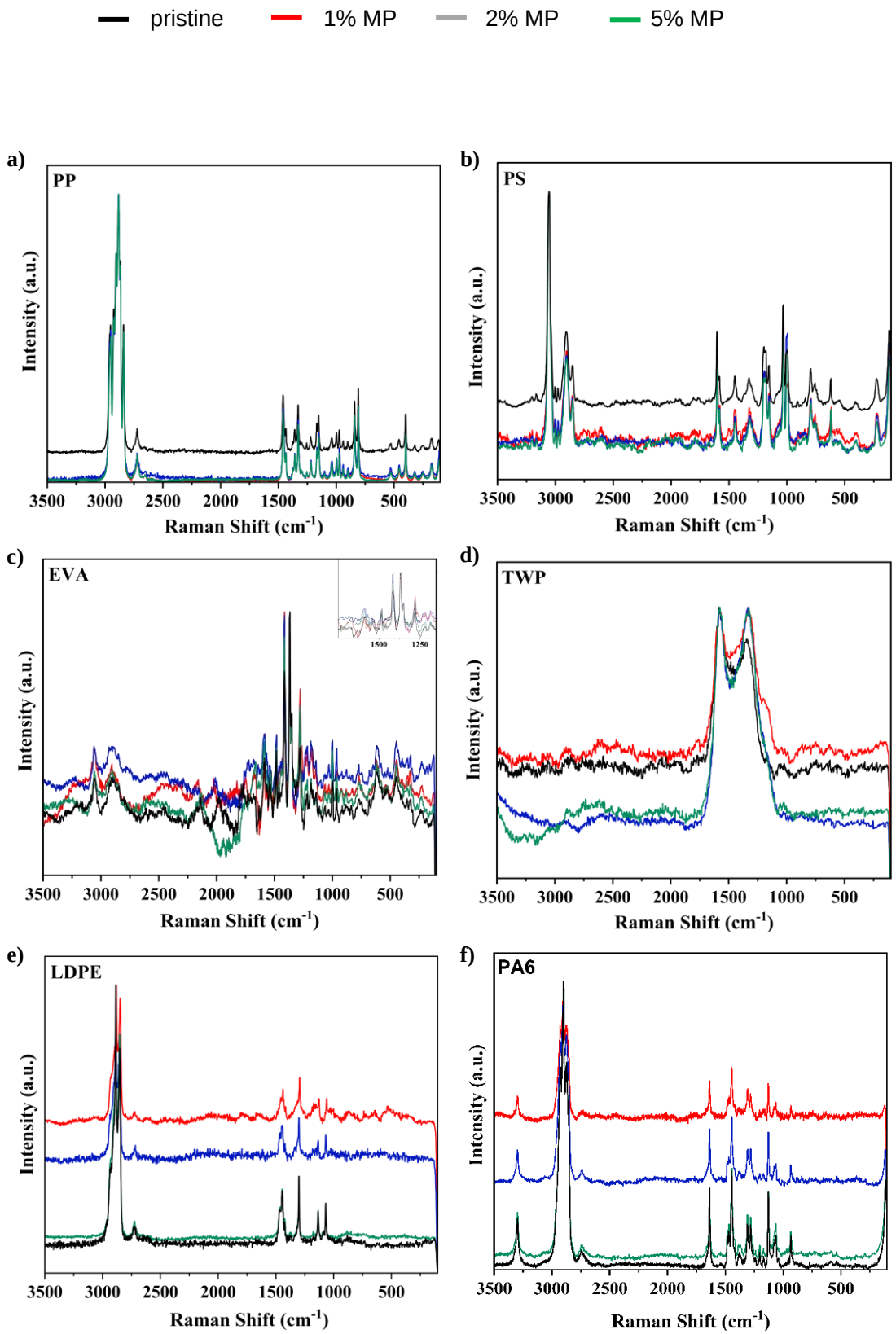


Figure 2S. Normalized Raman spectra obtained for digestion degradation tests for spikes containing 1, 2 and 5% of MP. a) PP-MPs, b) PS-MPs, c) EVA-MPs, d) TWP-MPs, e) LDPE-MPs, and f) PA 6-MPs. Spectra collected from 100 to 3500 cm^{-1}, using 633 nm He-Ne laser as the excitation light source.

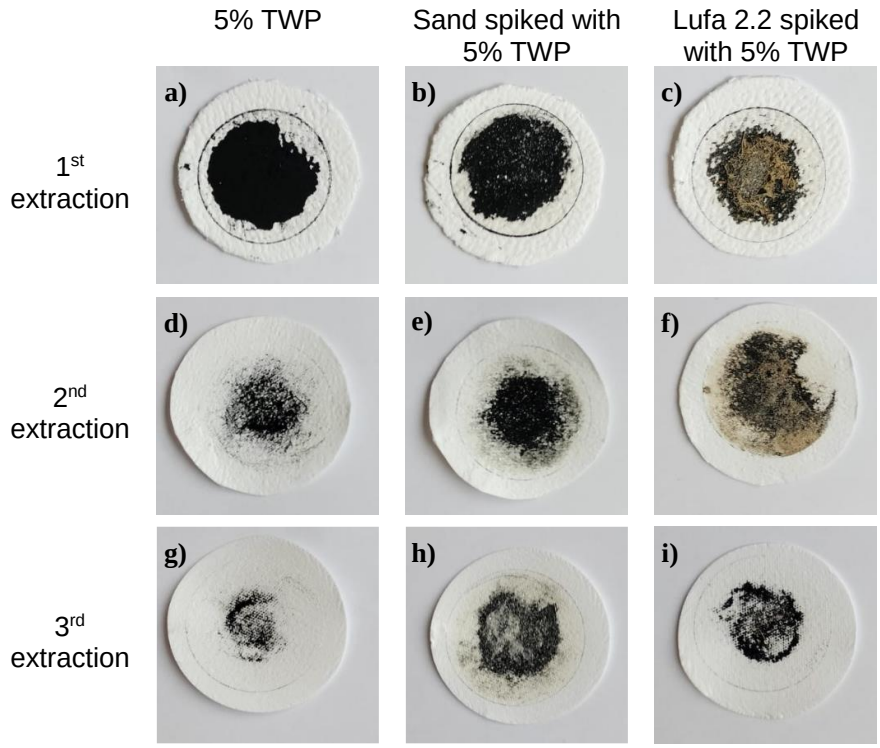


Figure 3S. Images of the filters obtained in three extractions for spikes containing 5% TWP, referring to: a), d) and g) digestion degradation tests; b), e) and h) recovery tests with sandy soil; c), f) and j) recovery tests with Lufa 2.2 soil. The images were captured using an OPPO Reno8 Lite smartphone.

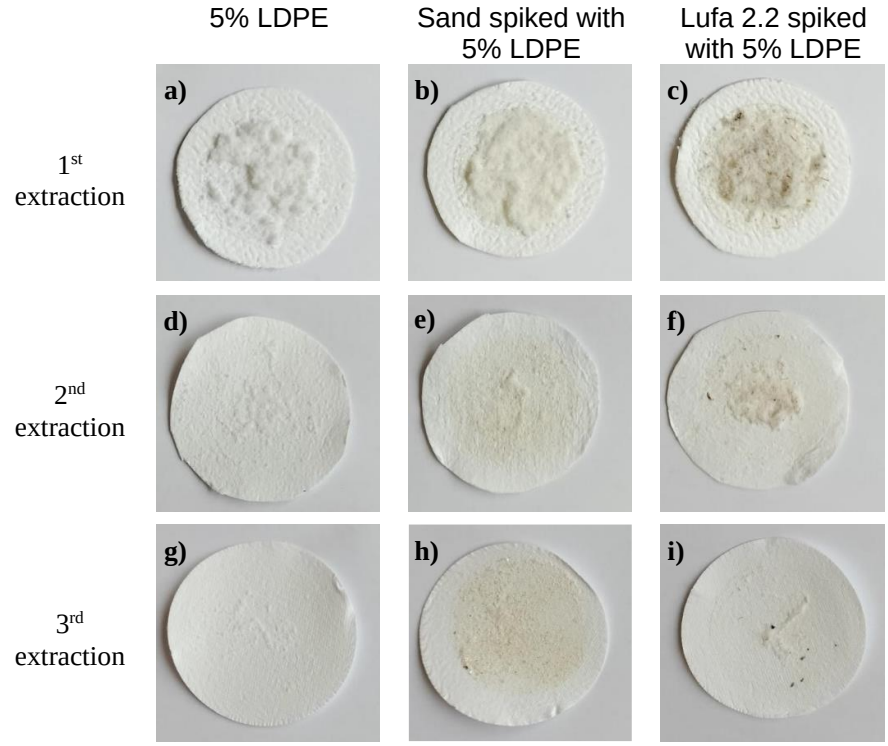


Figure 4S. Images of the filters obtained in three extractions for spikes containing 5% LDPE, referring to: a), d) and g) digestion degradation tests; b), e) and h) recovery tests with sandy soil; c), f) and j) recovery tests with Lufa 2.2 soil. The images were captured using an OPPO Reno8 Lite smartphone.

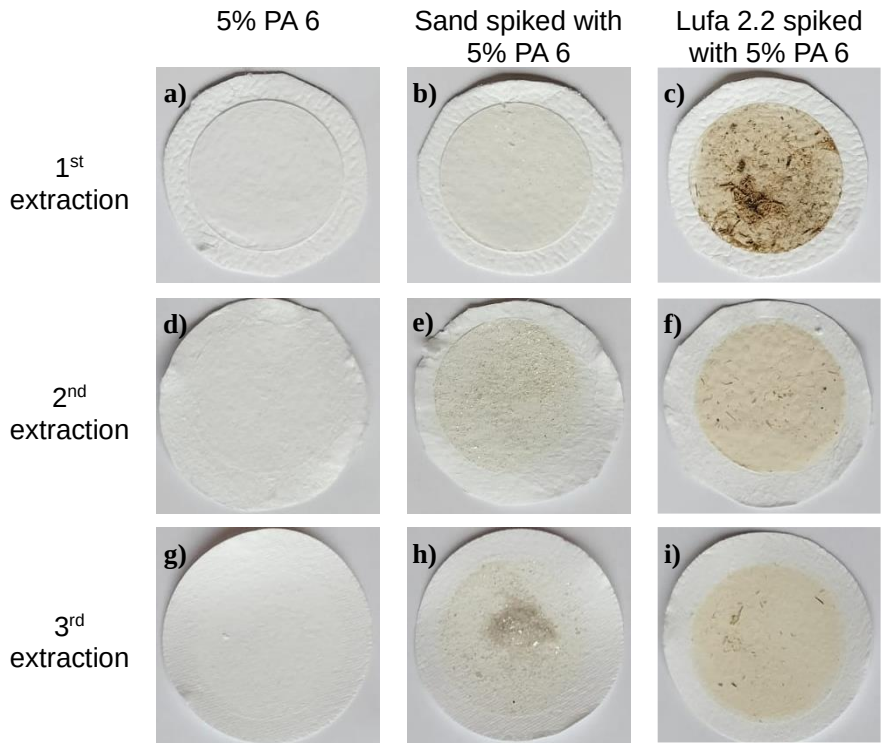


Figure 5S. Images of the filters obtained in three extractions for spikes containing 5% PA 6, referring to: a), d) and g) digestion degradation tests; b), e) and h) recovery tests with sandy soil; c), f) and j) recovery tests with Lufa 2.2 soil. The images were captured using an OPPO Reno8 Lite smartphone.

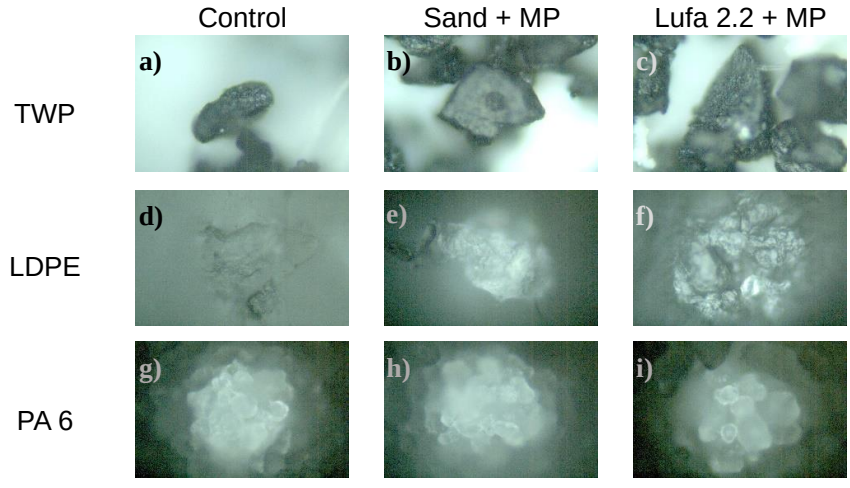


Figure 6S. µ-Raman images of TWP-MPs, LDPE-MPs and PA 6-MPs, captured using a Leica DM2700 microscope with a 50x objective. a) digestion degradation tests for TWP 1%, 1st extraction; b) Sand + TWP 1%, 3rd extraction; c) Lufa 2.2 soil + TWP 1%, 1st extraction; d) digestion degradation tests for LDPE 1%, 1st extraction; e) Sand + LDPE 2%, 3rd extraction; f) Lufa 2.2 soil + LDPE; g) digestion degradation tests for PA 6 2%, 3rd extraction; h) Sand + PA 6 2%, 2nd extraction; and i) Lufa 2.2 soil + PA 6 2%, 2nd extraction.

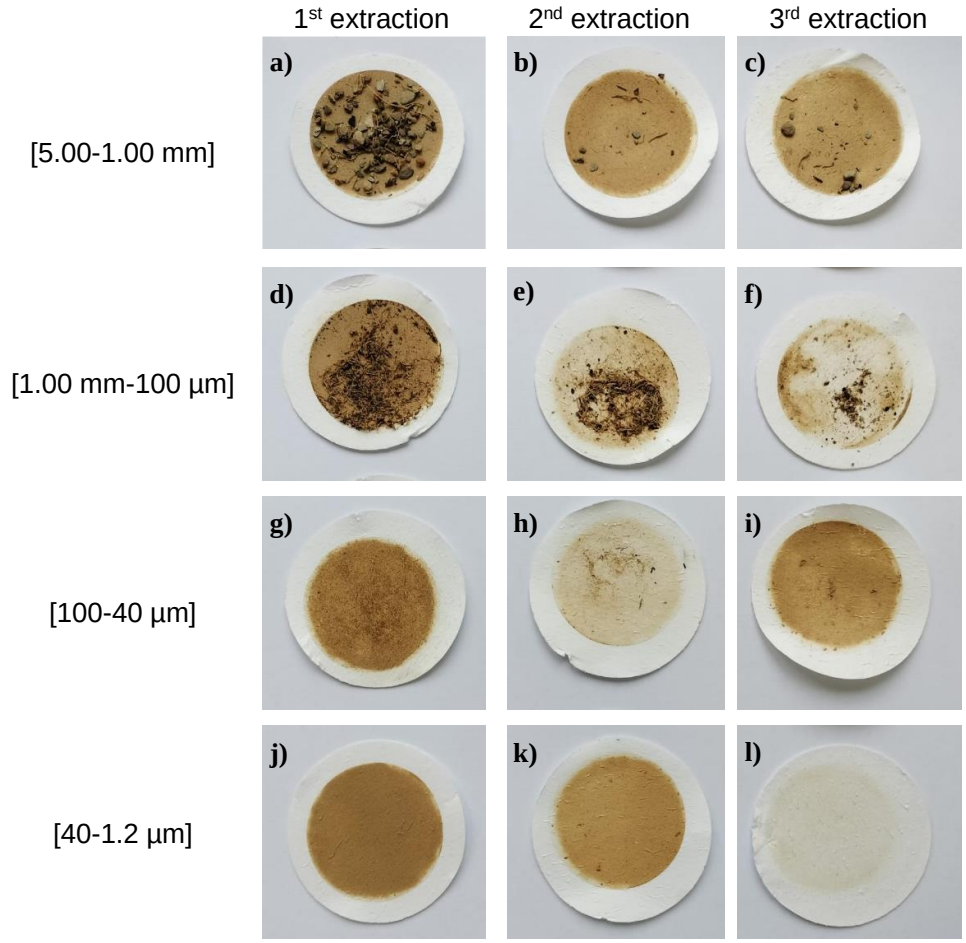


Figure 7S. Images of the filters obtained in three extractions for each fraction of Sample A. The images were captured using an OPPO Reno8 Lite smartphone.

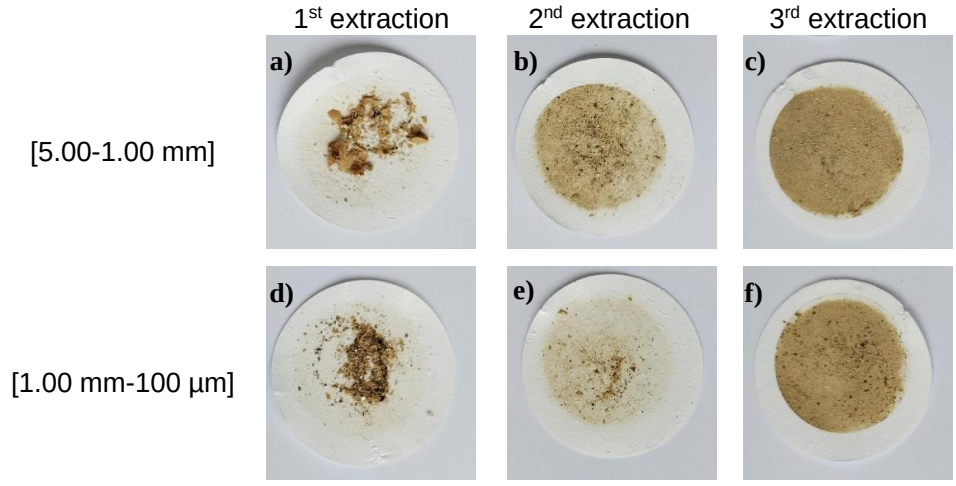
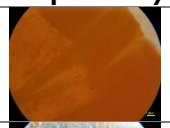
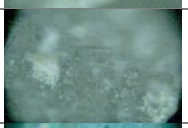
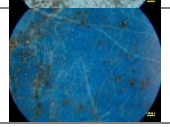
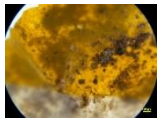
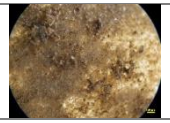
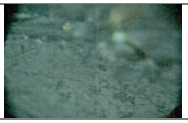


Figure 8S. Images of the filters obtained in three extractions for each fraction of Sample B. The images were captured using an OPPO Reno8 Lite smartphone.

Table 1S. Analysis of mesoplastics extracted from samples D and E, showing characteristics and polymer compositions, including number of particles, shape, color, polymer type, and images obtained with a microscope and µ-Raman.

Sample	No. Fragments	Shape	Color	PublicSpectra Score (%)	Polymer	Microscope image (5x ampliation)	µ-Raman image (50x ampliation)
D	1	film	yellow-orange	19.6	Inconclusive (melamine formaldehyde resin)		
	1	fragment	black-gray	1.01	Inconclusive (melamine formaldehyde resin)		
	1	fiber	white-transparent	-	Inconclusive		
E	6	film	white-transparent	62.77	Inconclusive (poly(cyclohexanedimethylene terephthalate))		
		film	blue-green yellow-orange	87.6	PP		
		film	yellow-orange white-transparent	52.68	Inconclusive (PVC)		
		film	white-transparent	90.23	PE-based (poly(ethylene-co-1-butene))		

	film	white-transparent	98.41	PP-based (propylene-ethylene block copolymer)		
	film	white-transparent	89.07	PP		

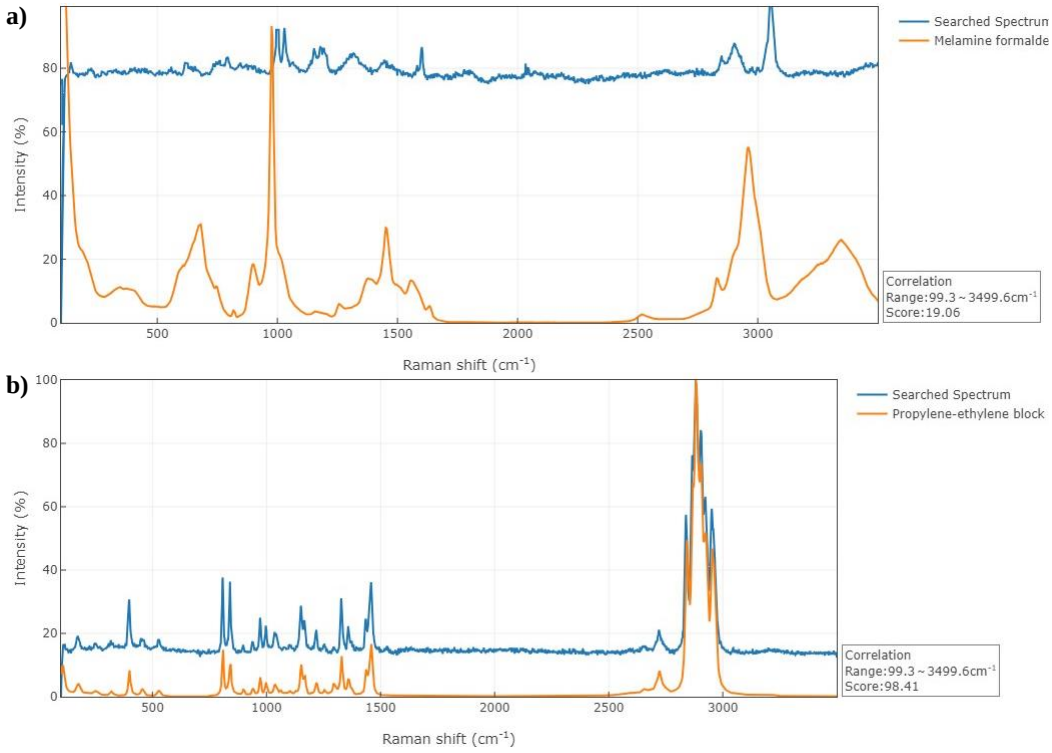


Figure 9S. Output of PublicSpectra for two mesoplastics in samples D and E. a) Yellow-orange film in sample D with inconclusive identification. b) White-transparent film in sample E identified as PP-based, specified as propylene-ethylene block copolymer.

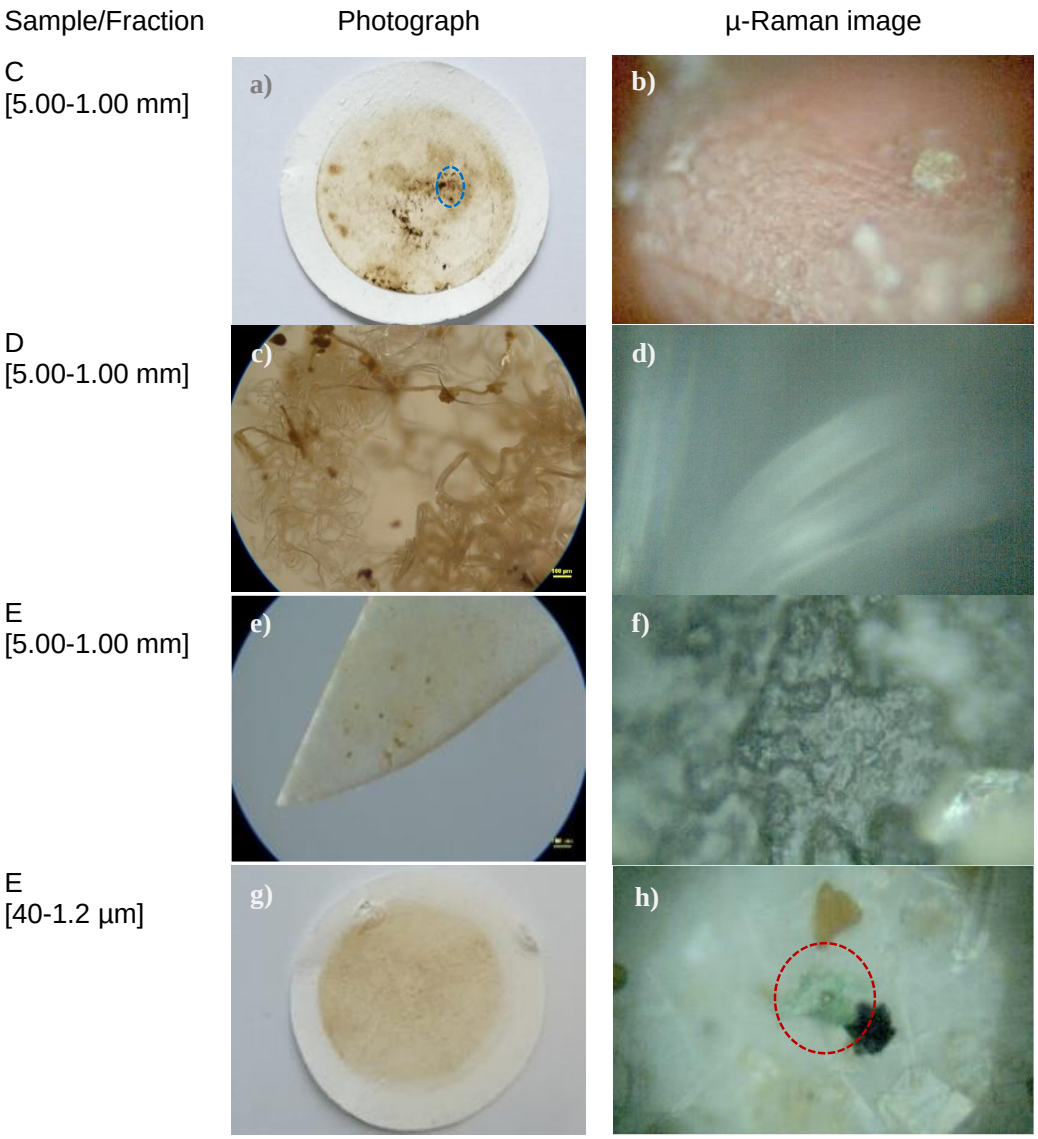


Figure 10S. Images of non-identified suspects in samples D and E. a) and b) red-pink fragment in sample D; c) and d) white-transparent fiber in sample D; e) and f) white-transparent fragment in sample E [5.00-1.00 mm]; g) and h) blue-green fragment in sample E [40-1.2 μm]. Images a) and g) were captured with OPPO Reno8 Lite smartphone, while c) and e) were collected with an inverted microscope at 5x ampliation.

References

Al-Selwi A, Joshi M (2015) Source Rock Evaluation using Total Organic Carbon (TOC) and the Loss- On-Ignition (LOI) Techniques. Oil Gas Res 1:1–5. https://doi.org/10.4172/2472-0518.1000105.

Conclusions and Final Remarks

MPs have become widespread in the environment, reaching even remote areas such as the Arctic and the Alps. They pose harm to wildlife by causing physical damage to their digestive systems and potentially facilitating the adsorption of harmful chemicals. Human exposure to MPs and their related chemicals occurs daily, starting from infancy; however, the long-term effects are still unclear. Soil plays a pivotal role as a pathway for human exposure to MPs. These particles can settle onto the soil through various means, including atmospheric deposition, runoff from polluted areas, and the application of SS or agricultural amendments, among others. Once in the soil, MPs can become incorporated into the soil matrix through natural processes such as erosion and biological activity.

This highlights the need for comprehensive research to understand how MPs interact with soil ecosystems and their potential impact on human health and environmental integrity. The primary focus of this thesis was to explore the key factors affecting the presence of MPs and related contaminants in the soil. This thesis provides an analytical scientific overview addressing the gaps in the understanding of MPs by investigating their possible sources, distribution, concentrations, and interactions with other pollutants in the soil environment. By advancing the knowledge of MPs and their environmental behavior, this study aimed to contribute to the development of standardized protocols for assessing MP contamination and raise public awareness to encourage governmental action.

SS, a possible source of soil contamination, was analyzed for emerging and priority micropollutants. The study developed a method based on QuEChERS extraction with dispersive solid phase extraction (d-SPE) clean-up, coupled with chromatographic techniques. The coexistence of MPs (3-5 mm) with a flame retardant found in the SS was evaluated. Gas chromatography was used to assess the concentration of the flame retardant over time, while alterations in polymer surface and composition were examined using ATR-FTIR and micro-Raman spectroscopy, as well as water contact angle measurements. An extraction method incorporating green chemistry principles for separating MPs in agricultural soil and identification via micro-Raman spectroscopy was developed.

SS presents a significant risk of soil contamination, owing to its complex composition and the presence of chemical pollutants. An analytical method was developed to simultaneously extract and analyze 42 target analytes from SS samples, achieving recoveries ranging from 59.5% to 117%, with limits of detection between 0.00700 and 0.271 µg g^{-1}. The concentrations of the detected analytes ranged from below the limit of

quantification to 26.8 μg g^{-1} dry weight, including persistent organic pollutants like α-endosulfan and organophosphorus flame retardants such as TPhP. The Sewage Sludge Directive (86/278/EEC of 12 June 1986), implemented in the European Union for over 36 years, regulates the application of SS to soil. However, emerging pollutants such as organophosphate ester flame retardants or even MPs were not included, highlighting the need for updated protocols and comprehensive strategies to address these contaminants and protect soil health. Furthermore, with the European Green Deal promoting a shift to a circular economy, the application of SS may increase, potentially amplifying concerns regarding environmental pollution and underscoring the need for expanded legislative coverage. Future research could explore the presence of MPs in SS samples and evaluate their ecotoxicological impacts following sludge application to soils.

Additionally, this thesis explored the coexistence of pollutants, focusing on the dynamics of TPhP adsorption in simulated soil, MPs, and soil-MPs systems under diverse experimental conditions. The study revealed that TPhP adsorption capacity increased under ultraviolet radiation and acidic conditions in simulated soil. However, the presence of MPs in soil altered the adsorption dynamics of TPhP, leading to varied equilibrium capacities depending on the type of MP polymer and aging conditions investigated. Overall, continued research is necessary to better understand the sorption/desorption dynamics of polymers in soils and SS. The recently opened 2024 LRI grant call for projects on “Mechanistic understanding of sorption/desorption of polymers in environmental media” funded by Cefic (European Chemical Industry Council) and LRI (Long-range Research Initiatives) highlights the significance of ongoing research in this field.

Furthermore, the thesis also focused on extracting and identifying MPs in agricultural soils, integrating green analytical chemistry (GAC) principles to minimize reagent use and waste generation during the extraction methodology. Recovery tests using spiked soils and pristine MPs of various polymers and sizes (15 μm - 5mm) demonstrated efficient retrieval of larger MPs, while smaller MPs required multiple extraction cycles. The methodology successfully identified 50% of meso- and MPs in soil samples, with sustainability evaluated using Analytical Eco-Scale and AGREE metrics. However, challenges in transitioning to environmental sample analysis were identified, including altered interactions between MPs and soil particles, interference from non-polymeric materials on filters, and variability in spectral characteristics of weathered MPs. Future research directions include developing digestion methods tailored for aged MPs, investigating density separation techniques, establishing a comprehensive library for

weathered MPs, and conducting ecotoxicological studies to assess the impacts of MPs on soil organisms and ecosystems. Moreover, capitalizing on science and technology research networks such as COST Action PRIORITY (European Cooperation in Science and Technology), which fosters collaboration among researchers in the field of MPs, is crucial for advancing standardized protocols and promoting international cooperation.

In summary, this thesis addresses a pressing environmental issue with practical implications that can and should inform the regulatory authorities in terms of policies and procedures. This study contributes to the understanding of these complex challenges by exploring the widespread presence and potential effects of MPs and plastic-related chemicals in soil. The development of new analytical methods, with a focus on standardization and GAC principles, reflects a commitment to sustainable research. Further investigation into both MPs and plastic additives such as flame retardants and other plastic-related chemicals is crucial for guiding effective environmental policies. Finally, this study contributes with valuable insights to address MP pollution, promote healthier ecosystems and communities, and support the goals of the 2030 Agenda for Sustainable Development.